SYSTEMIC AND LOCAL REGULATION OF ANGIOGENESIS, AND OTHER ADAPTATIONS, IN RESPONSE TO HYPOXIA

By

EMILY MARGARET KEWLEY

A thesis submitted to
The University of Birmingham
For the degree of
DOCTOR OF PHILOSOPHY
March 2009

Department of Physiology
Division of Cardiovascular Sciences
The university of Birmingham
Birmingham, UK

ABSTRACT

Changes in oxygen levels, due to the environment or disease initiates a plethora of acute and chronic responses in the body to enable optimal physiological adaptation to overcome impaired oxygen delivery. Homeostatic regulation mechanisms in the cardiovascular and respiratory systems rapidly act to maintain oxygen supply to sustain normal metabolism; prolonged exposure to a low oxygen tension initiates changes in gene expression. In control of many of these responses is a transcription factor (hypoxia-inducible factor, HIF). Among other responses it induces changes in erythropoiesis, glycolysis and angiogenesis. This study primarily aimed to elucidate the conditions of hypoxia, local or systemic, which would initiate capillary growth in different tissues, and determine whether manipulation of the pathway (by HIF stabilisation) would enhance this response. A systemic response to hypoxia led to increased capillarity in the heart and diaphragm, and in both the local and systemic models changes in vascularity varied with degree of hypoxia, though manipulation of the HIF pathway had no effect. HIF upregulation under conditions of normoxia with muscle overload, also failed to show effects of manipulation of the HIF pathway. Therefore, ablation of individual enzymes controlling levels of HIF was utilised. A number of genes associated with angiogenesis and protein remodelling were upregulated, as seen with gene arrays, though histological evidence for the former was poor, suggesting a delay in gene expression and translation into downstream effects. We examined whether changes in plasma EPO expression were predictive of sickness upon ascent to altitude, and whether leukocytes could be used as a circulating indicator of HIF-mediated gene expression. EPO was enhanced in all subjects following exposure to hypoxia, and it may be one marker for AMS, but individual variation in gene responses to hypoxia suggests leukocytes may not be a viable indicator of the circulating systemic response to hypoxia. This study emphasises the complexity of the HIF pathway, highlighting the multitude of its effects both on a molecular and physiological level.

ACKNOWLEDGEMENTS

I would firstly like to would like to acknowledge and extend my gratitude to Dr Stuart Egginton, for his continual support, guidance and patience throughout the last three years, which has made the completion of this project possible.

Thanks to Professor Chris Pugh and members of the lab at the Henry Wellcome Building for Molecular Physiology in Oxford, for their continual patience and help during my time there. I also wish to thank Jennifer Marshall, Phillip Antczak, Kai Toellner, Clare Ray and Ian Ricketts in Birmingham, and Helen Lockstone in Oxford, along with members of the Angiogenesis Research Group and Department of Physiology for their significant contribution in helping me to achieve this thesis.

The Birmingham Medical Research Expeditionary Society has provided immeasurable support and encouragement, along with some extremely memorable expeditions. Thank you also to Professor Ian Maclennan for his support, intellectual and financial input, Ian Chesner for funding the high altitude research, and Professor Damian Bailey for the use of the hypoxic chamber for the high altitude study.

Thank you to the Rowbotham Request for funding this work, and to Alison Kewley and George Rodway for their help in final editing.

Finally, I wish to thank the rest of my family for their continued support and faith in me, throughout.

FIGURES

TABLES

APPENDICIES

REFERENCES

ABBREVIATIONS

ALD-A	aldalase-A
AMS	acute mountain sickness
Ang-2	angiopoitein-2
BM	basement membrane
C:F	capillary to fibre ratio
CAIX	carbonic anhydrase IX
CBP	CREB binding protein
CD	capillary density
CO	cardiac output
COPD	chronic obstructive pulmonary disease
DMOG	dimethyloxalyglycine
EC	endothelial cell
ECM	extracellular matrix
EDL	extensor digitorum longus
EPC	endothelial progenitor cell
EPO	erythropoietin
ES	enrichment score
ESQ-C	environmental symptoms questionnaire
FA	femoral artery
FC	fold change
FDR	false discovery rate
FIH	factor inhibiting HIF
Flk-1	fms-like tyrosine kinase III (aka KDR)
Flt-1	fms-like tyrosine kinase receptor I
HACE	high altitude cerebral oedema
HAPE	high altitude pulmonary oedema

HB	haemoglobin
HCT	haematocrit
HIF	hypoxia inducible factor
HMOX-1	haemoxygenase
HRE	hypoxic response element
HVR	hypoxic ventilatory response
IHC	immunohistochemistry
iNOS	inducible nitric oxide synthase
K/O	knockout
LL	lake louise scoring system
MFA	mean fibre area
MMP	matrix metalloproteinase
NFkB	nuclear factor kB
O_2	oxygen
ODD	oxygen-dependent degradation domain
PAD	peripheral arterial occlusive disease
PHD	prolyl hydroxylase
PO_2	partial pressure of oxygen
PVD	peripheral vascular disease
RBCC	red blood cell concentrate
RM	relative mass
ROS	reactive oxygen species
SOL	soleus
TA	tibialis anterior
VEGF	vascular endothelial growth factor
VHL	von Hippel Lindau complex
WBC	white blood cell
WT	wildtype

1 General Introduction

1.1 Hypoxia

1.1.1 Systemic hypoxia

The fall in PO_2 associated with ascent to altitude or impaired oxygen uptake due to disease lowers the alveolar and arterial O_2 tension, causing hypoxia defence and compensatory mechanisms to become activated by a variety of O_2-sensing and signal transduction pathways. These occur both on an acute and chronic timescale, enabling immediate and acclimatory adjustments to the low O_2 availability (Fig 1.1).

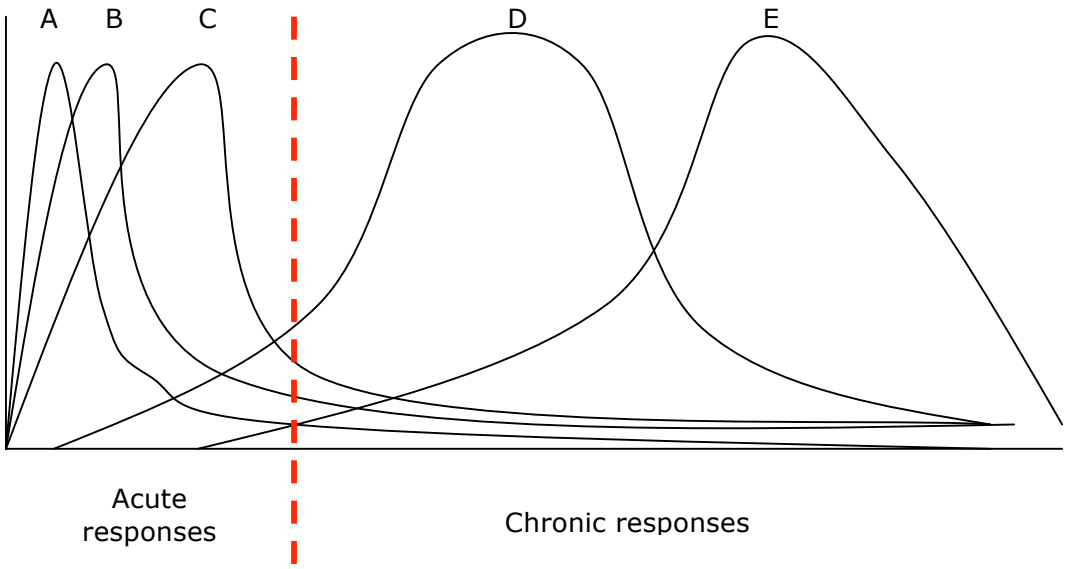

Figure 1.1 Illustration of acute and chronic responses to hypoxia. A: ventilatory changes, B: changes in pH, C: fluid shift, D: EPO response, E: angiogenesis

1.1.1.1 Acute responses

The carotid body O_2 sensors initiate the primary responses and an enormous increase in ventilation occurs, known as the hypoxic ventilatory response (HVR), which protects the alveolar PO_2 against decreasing inspired values (West, 1990). The PO_2 at sea level is about 160mmHg but on the summit of Mount Everest (8848m) is less than 30mmHg (West, 1982) reducing at a rate equivalent to a drop of approximately 2.5% in the air O_2 for every 1000m increase in altitude (Julian, 2007). The increase in ventilation occurs within seconds, reaching full intensity within minutes, and a ventilatory acclimatisation occurs after continuous exposure over days (Lahiri *et al.* 2000). Resting ventilation can increase up to 4 times at extreme altitude (greater than 6000m) (West, 1982). Hyperventilation lowers arterial PCO_2 causing respiratory alkalosis and a left shift in the haemoglobin–O_2 dissociation curve, decreasing the ventilatory drive. This causes an increase in the affinity of Hb for O_2, increasing O_2 uploading by the pulmonary capillaries (West, 1990). These ventilatory changes are closely followed by an increase in cardiac output (CO), ensuring that organs of higher priority receive a larger proportion of the blood flow compared to organs that can function sufficiently on a low blood flow, a phenomenon known as 'blood flow steal'.

Subsequently, the pulmonary vasculature O_2 sensors initiate regulation of the hypoxic pulmonary vasoconstrictor response, increasing pulmonary vascular resistance by 30-500% (Mougdil *et al.* 2005) and resulting in improved ventilation–perfusion matching. This vasoconstriction is mediated by K^+ channel opening (Lee *et al.* 1998), and enables increased efficiency of O_2 delivery by diverting flow to the better-aerated parts of the lungs. A fluid shift also occurs on exposure to hypoxia, from the intravascular space to the interstitial and intracellular spaces, resulting in haemoconcentration (Berglund *et al.* 2002).

Low O_2 delivery to cells induces a multitude of effects on a molecular level which take effect on both an acute and chronic timescales. The precise way in which O_2 levels are sensed is still an area of controversy, though it is postulated that the O_2 sensors are

two-domain haem-based proteins: some are haemokinases, others are flavohaemoproteins (Bunn and Poyton, 1996). O_2 is thought to bind to these and be converted into a reactive O_2 intermediate which then serves as a signaling molecule (Zhu *et al.* 2007; Coceani, 2000). Mitochondrial O_2 consumption is required for ATP generation and cell survival is threatened when cells are deprived of O_2. Mitochondria are also thought to function as O_2-sensors and release reactive O_2 species (ROS) to the cytoplasm from the electron transport chain: the primary site of ROS production during hypoxia appears to be complex III (Simon, 2006; Guzy and Schumacher, 2006). Mitochondria are thought crucial for signaling hypoxic HIF-α stabilisation, the transcription factor involved in regulation of a host of genes involved in acclimatisation and adaptation to systemic hypoxia.

1.1.1.2 Chronic responses

Chronic hypoxic pulmonary vasoconstriction induces right ventricle hypertrophy as the heart works harder to overcome the increased pulmonary artery resistance. This hypertophy may arise due to a combination of both pressure and volume-overload, the former resulting from an increased CO, and the latter due to the increased blood volume, mediated acutely by the splenic release of red blood cells (RBCs) (Kuwahira *et al.* 1999) and over a chronic timescale by EPO production. The latter is a well-known characteristic of acclimatisation to hypoxia, first reported by Viault in 1890 (Smith *et al.* 2008). It is released mainly from interstitial fibroblasts in the kidneys of the adult (Chavez *et al.* 2006). EPO is under control of the transcription factor HIF (Pugh *et al*. 1991), and as HIF is thought to be one of the main O_2 sensors under hypoxia (above), it provides a direct link between changing O_2 levels and EPO synthesis and release.

EPO is thus responsible for enhancing the O_2-carrying capacity of the blood by increasing the production of RBC, causing polycythaemia. Erythropoietin (EPO) production can be increased within hours of exposure to hypoxia (Eckhardt *et al.* 1989), though erythropoietic effects can take much longer to become evident, from weeks

(Barcroft *et al.* 1923) to months (Reynafarje *et al.* 1959), depending on the environmental conditions and additional external stress (e.g. exercise).

Angiogenesis, the growth of new vessels from an existing network, is a further chronic adaptation to systemic hypoxia, increasing blood flow in deprived areas and thus enhancing O_2 delivery (see 1.4). It can occur due to a variety of factors such as mechanical strain and metabolic stress. Despite vasoconstriction occurring in the lungs, the rest of the body undergoes systemic vasodilatation, mediated in part by adenosine release from tissues (Kobayashi *et al.* 2000), resulting, in one circumstance, in a modification of skeletal muscle blood flow. The importance of capillary supply in maintaining the aerobic function of muscles is well-known, though there are many discrepancies in the literature. Prolonged exposure to hypoxia causes a reduction in muscle mass, due to anorexia and energy deficits associated with adaptation to the lowered PO_2, and this results in a lowered fibre size (Mathieu-Costello, 2001). However, this was not originally taken into account on observation of an increase in the capillarity of skeletal muscle, hence there actually was no change, only a reduction in fibre size which subsequently increased the recorded capillary density (CD). Several confounding factors can explain differences in the contrasting data from different studies, with some eliciting an angiogenic response in different muscles under chronic hypoxia, and others failing to show. This level of hypoxia, alterations in dietary intake, animal growth (fibre cross-sectional area increases linearly with body weight) and the lethargy following exposure to a lowered PO_2 (Mathieu-Costello, 2001), as well as regional variations in muscle composition (Deveci *et al.* 2001) may all be responsible for discrepancies in the data.

The oxidative capacity of skeletal muscle varies depending on the composition of muscle fibres (Table 1.1): the extensor digitorum longus (EDL) in the hindlimb is composed of mixed muscle fibres, with a characteristically low proportion of mitochondria and a decreased capillary density when compared with an oxidative fibre type, such as those composing another hindlimb skeletal muscle, the soleus. The features of these

skeletal muscles consequently result in differential changes under hypoxaemia: a number of studies have failed to show an increase in capillarity with systemic hypoxaemia in phasic muscles such as the EDL, though have shown significant increases in muscle with predominantly oxidative fibres such as the soleus (Deveci *et al*. 2001). Furthermore, controversy surrounds the phenomenon of changes in the proportion of fibre-types under hypoxia: an enhanced population of fast-twitch glycolytic fibres have been reported in adult rats (SIllau and Banchero, 1977), although proportions of fibre-types have been shown unchanged in human skeletal muscle with altitude adaptation (Green *et al.* 1989).

	FIBRE TYPES		
Characteristic	**Type IIB Fast-twitch**	**Type IIA Fast-Twitch**	**Type I Slow-twitch**
Colour	white	White/red	Red
Capillary density	low	intermediate	high
Mitochondrial volume	low	intermediate	high
Glycolytic capacity	high	medium	high
Oxidative capacity	low	medium	High
Fatigue resistance	low	high	high

Table 1.1 Representation of muscle fibre types (taken from McArdle, W., Katch, F and Katch, V)

1.1.3 Local hypoxia

Local hypoxia or ischaemia occurs when the O_2 supply to a region of tissue is limited or stopped, resulting in a metabolic error signal: a mismatch in the supply and/or demand to or from a tissue caused e.g. by a pathological state such as human peripheral arterial occlusive disease (PAD), which occurs subsequent to obstruction of large arteries, e.g. in the leg. The reduction in blood flow causes a chronic deficiency of O_2 supply to the surrounding tissues and subsequent changes in the metabolic and oxidative state of the tissue. Angiogenesis is initiated *via* activation of HIF and a host of its downstream factors, which are subsequently involved in endothelial migration and proliferation, extracellular proteolysis, endothelial differentiation (capillary tube formation), and vascular wall remodelling (Buschmann & Schaper, 1999) (see 1.4). It is an important

mechanism of restoring blood flow following limb ischaemia (to increase O_2 tissue transport), allowing for an increase in enzymatic activity which supports adaptation to the low O_2.

1.1.3.1 Ischaemia-reperfusion injury

Skeletal muscle ischaemia-reperfusion injury is a frequent occurrence following obstruction of blood flow in the femoral artery, when blood flow returns to the tissue after a period of absence. Restoration of the circulation results in inflammation and oxidative damage through the induction of oxidative stress, rather than restoration of normal function. One study followed the injury and recovery of mouse hindlimb tissue using MRI scanning, and illustrated how a time period of 21 days permitted a full recovery (Heemskerk *et al.* 2007).

1.1.3.2 Inflammation following ischaemia

Muscle regeneration is characterised by three distinct phases: necrosis of the muscle fibres, activation of inflammatory cells and an increase in permeability of the cells. This is followed by activation of the muscle repair process and partial recovery of the muscle fibres. Inflammation of the hindlimb following ligation is a well-studied phemonena as it has been shown that leukocyte infiltration following ischaemia is an important trigger for ischaemia-induced angiogenesis due to the subsequent angiogenic cytokines that are released (Egami *et al.* 2006). However, there is controversy surrounding this issue as it has also been shown that limitation of the blood supply to the skeletal muscles does not necessarily lead to inflammation, based on staining for macrophage infiltration (Brown *et al.* 2003).

As mentioned, a single transcription factor is in control of many of the described processes and acts as a master regulator in governing the response to hypoxia on a molecular level, subsequently aiding adaptation of the body to the lowered O_2 in the surrounding environment. This transcription factor is known as hypoxia inducible factor

(HIF-1α), important in the upregulation of glycolysis under chronic hypoxia, the initiation of erythropoiesis, and the remodelling of the existent vasculature, among many other processes.

1.2 Hypoxia inducible factor (HIF)

1.2.1 HIF activity and regulation

HIF controls the hypoxic expression of a wide range of genes (Table 1.2) involved in angiogenesis, glycolysis, erythropoiesis, iron metabolism, apoptosis and metastasis, among many others (William *et al.* 2004), and was first identified as a complex that binds to the hypoxia responsive enhancer element (HRE) in nuclear extracts of cells exposed to low O_2 tension. It is known to control at least 70 genes on a transcriptional level (Semenza, 2004), 40 of which have been identified either by activating or repressing their expression (Semenza, 2002). HIF-1 is a heterodimeric protein complex consisting of an α and β subunit and is of the Per-Arnt-Sim (PAS) family of basic helix-loop-helix proteins (Cummins and Taylor, 2005). The HIF-1β subunit is constitutively expressed whereas the HIF-1α subunit is tightly regulated by the availability of cellular O_2. There are a number of HIF isoforms: HIF-1α is the most ubiquitously expressed and is recognised as a key factor in hypoxic signalling (Bardos and Ashcrost, 2005). HIF-2α has similar regulatory activities to HIF-1α but is only expressed in specific cells (Appelhoff *et al.* 2004). HIF-1α and HIF-2α share only 48% identity: HIF-1α-null mice exhibit mid-gestation lethality and severe blood vessel defects, and despite HIF-2α-null mice exhibiting similar defects, they do sometimes survive post-natally (Uchida *et al.* (2004).

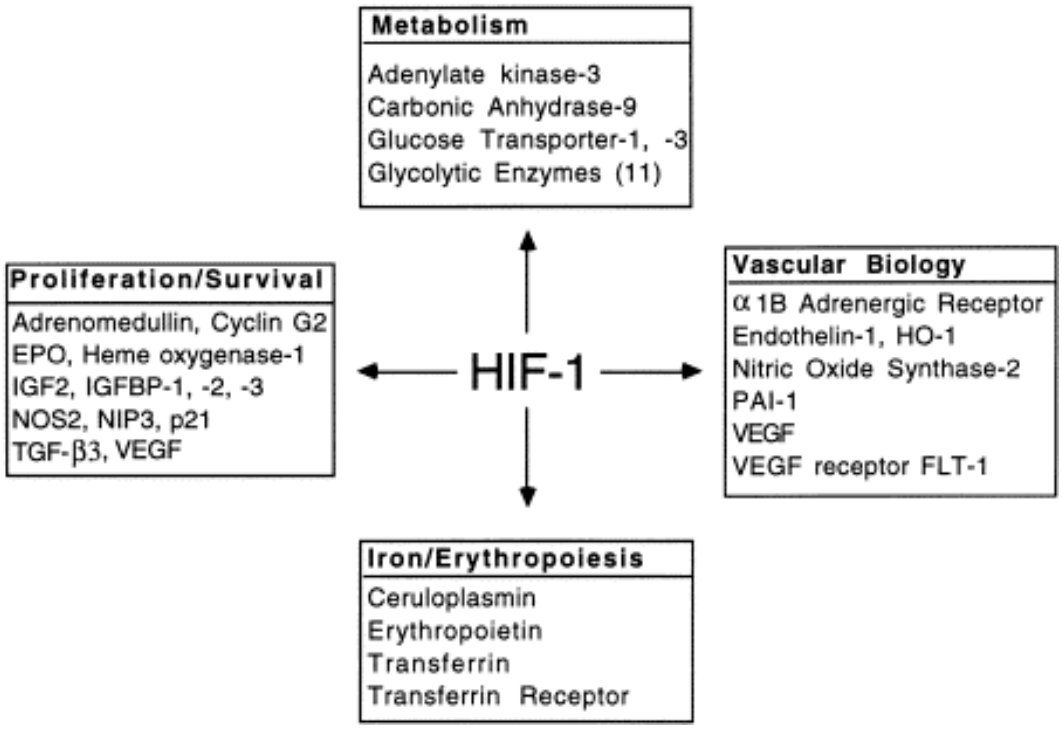

Figure 1.2 Genes controlled by HIF-1 (From Semenza *et al.* 2001)

HIF-1α chains have a domain structure with different parts of the molecule fulfilling different functions. The amino terminal part is involved in DNA binding and dimerisation. The carboxy-terminal half contains two regions termed the N-terminal (N-TAD) and the C-terminal (C-TAD) transactivation domains (Bardos and Ashcrost, 2005) (Fig 1.2). These mediate interactions with coactivators such as CREB binding protein (CBP), p300 Ref-1, Jab-1, SCR-1 and TIF2 (Semenza, 2004): p300 and CBP are homologous transcription adapters. These co-activators form a DNA-binding complex with HIF-1α under hypoxic conditions, causing subsequent induction of one of the many hypoxia-responsive genes (Bardos and Ashcrost, 2005), although dimerisation of the two HIF subunits is mandatory for this DNA-binding and transactivation activity under hypoxic conditions. Under normoxic conditions, HIF-1α is very unstable and is degraded quickly,

having a half-life of less than five minutes (Semenza, 2004), but accumulates rapidly in hypoxia.

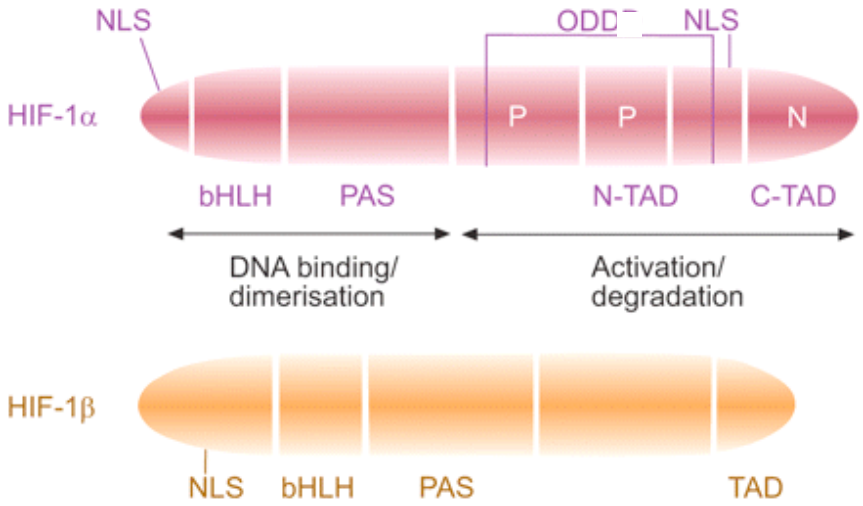

Figure 1.3 Structure of HIF-1 subunits (Taken from Berchner-Pfannschmidt *et al.* 2008)

The negative regulation of HIF-1α is acheived *via* modification of the O_2-dependent degradation domain (ODD) within the HIF protein (Cummins and Taylor, 2005) (Fig 1.3) by members of the 2-oxo-glutarate-dependent dioxygenase superfamily; the prolyl hydroxylases (PHDs). Three PHD isoforms have been identified (PHD 1-3) though the relative importance of each in regulating HIF activity is an area of current research. The amino-terminal half of HIF-1α consists of basic helix-loop-helix (bHLH) and Per-ARNT-Sim homology (PAS) domains. The carboxy-terminal half contains the transactivation domains (TAD-N and TAD-C) (Fig. 1.3). The proline residues 402 and 564 of the α subunit undergo hydroxylation by the PHDs. The residues share the sequence LXXLAP and are converted to 4-hydroxyproline. This is required for the interaction of HIF-1α with the von Hippel-Lindau tumour-suppressor protein (VHL), which is the recognition component of an E3 ubiquitin-protein ligase that targets HIF-1α for proteasomal degradation and polyubiquitylation (William *et al.* 2004) (Fig. 1.4). The hydroxylation

process requires O_2, iron and 2-oxoglutarate for activity (Harris, 2002). HIF is also under negative regulation in normoxia by factor-inhibiting HIF (FIH) which hydroxylates Asn803 within the C-terminal transactivation domain (Tan *et al.* 2007). During hypoxia, the hydroxylation system is inhibited allowing HIF protein to become transcriptionally activated and switch on downstream genes. The PHDs are targeted by proteasomal degradation by Siah1a and Siah2 (E3 ligases), and the level of regulation determines the amount of HIF-1α activation (Nakayama *et al.* 2004). Activation of HIF-1α is now known to occur under both hypoxic and non-hypoxic conditions (Semenza, 2002).

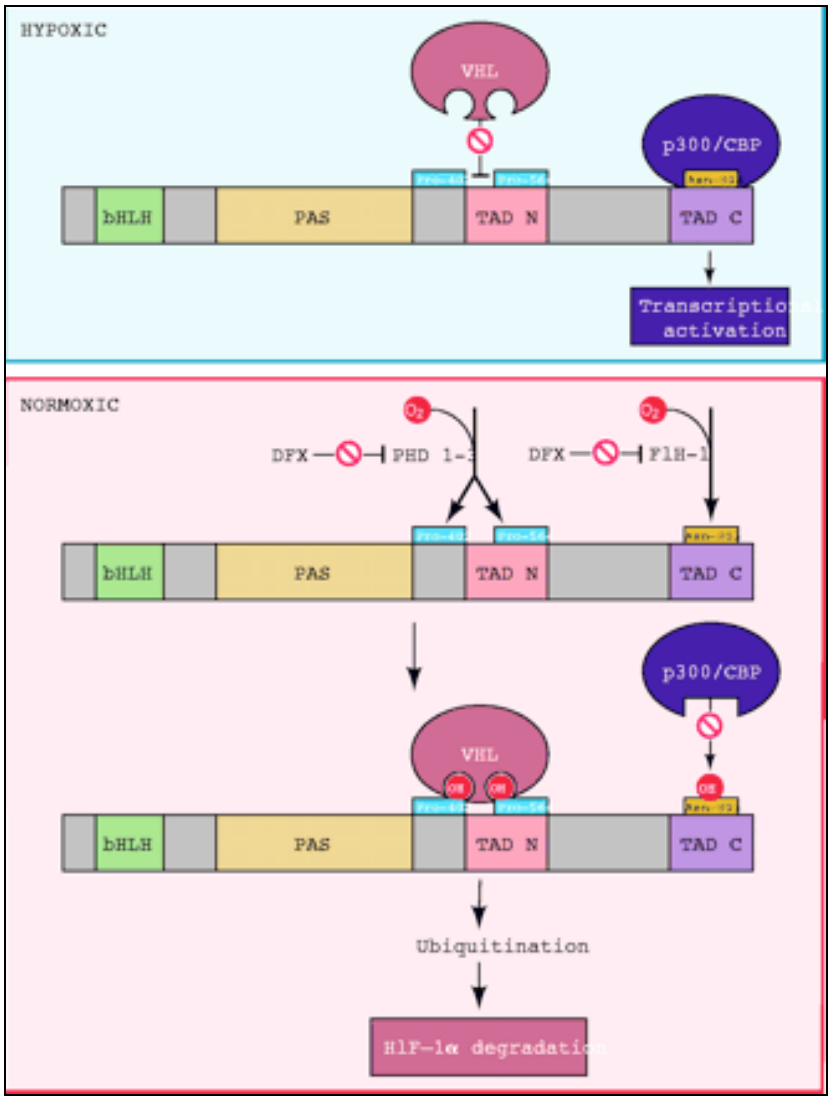

Figure 1.4 Oxygen sensing as demonstrated by the hydroxylation of HIF-1α (From Semenza, 2004)

1.2.2 HIF-mediated responses to systemic hypoxia: adapatation to high altitude

An array of HIF-mediated genes are involved in the systemic response to hypoxia which aid acclimatisation to the lowered PO_2. Many of these genes are multi-functional and play important roles not only in the erythropoietic, glycolytic and metabolic adaptations to whole-body deprivation of O_2, but are involved in blood vessel adaptation, angiogenesis (see 1.3) under both chronic systemic and local hypoxia. The role EPO plays under chronic systemic hypoxia has already been discussed, it being a major factor in enabling the body to increase its O_2-carrying capacity under these conditions. The necessity for HIF in pulmonary and systemic responses to chronic hypoxia has been demonstrated using HIF1$\alpha^{+/-}$ mice (HIF1-$\alpha^{-/-}$ mice are embryonically lethal, Carmeliet *et al.* 1998), further illustrating that HIF is crucial for normal development). These studies have shown that polycythaemia was significantly impaired in HIF-1$\alpha^{+/-}$ mice compared to wildtype, inline with studies confirming that HIF is in regulation of EPO under hypoxia (Yu *et al.* 1999). Furthermore, partial HIF-1α deficiency had significant effects on the response of the pulmonary vasculature to chronic hypoxia whereas in the normal response, HIF-1$\alpha^{+/-}$ mice showed no reduction in voltage-gated K^+ channel activity in pulmonary arteriolar smooth muscle cells.

HIF-regulated genes occur under differing functional categories. An example of a gene involved in metabolic adaptations to hypoxia is Aldolase-A, an enzyme responsible for catalysing one of the adol reactions involved in glycolyis, thus being responsible for an increase in ATP production. Vascular adaptations such as vasodilatation are largely influenced by nitric oxide (NO) which is produced from arginine by inducible nitric oxide synthase (iNOS), the latter of which is targeted for upregulation by VEGF under normoxic conditions (Kroll and Waltenberger, 1998). iNOS is important in the inflammatory response under hypoxia. Many HIF-regulated genes exhibit inter-dependent relationships that are enhanced under normoxic and hypoxic conditions. A significant number of these relationships involve VEGF, a multi-tasking cytokine involved in

stimulating differentiation, survival migration, proliferation, and vascular permeability (Zachary, 2003), thus being important in the angiogenic response to hypoxia. One of its receptors, Flt-1 (VEGFR-1), is expressed on the surface of ECs and negatively modulates blood vessel formation and endothelial cell proliferation during embryonic development (Roberts *et al.* 2004). Flk-1 (VEGFR-2), also expressed on ECs, is thought to be negatively regulated by Flt-1 (Rahimi *et al.* 2000). VEGF and sFLT are thought to play a potential role in regulating permeability of blood vessels which may subsequently lead to high altitude cerebral oedema (HACE) or pulmonary oedema (HAPE) at high altitude, though there is a significant degree of controversy surrounding this, with some studies suggesting that an increased amount of free VEGF is associated with the effects of acute mountain sickness (AMS) (Tissot van Patot *et al.* 2005), with others showing no evidence (Pavlicek *et al*. 2000).

Haemoxygenase (HMOX-1), is also upregulated by HIF and is known to have anti-inflammatory, anti-apoptotic and anti-proliferative effects. It is also thought to regulate the synthesis and activity of VEGF, resulting in a positive feedback loop (Bussolati and Mason, 2006). Transforming growth factor β (TGF-β) is a multifunctional peptide that controls proliferation, differentiation and other functions in many cell types, and also stimulates VEGF production under hypoxia (Nakagawa *et al*. 2004). Taken together, these genes, when upregulated, provide a sufficient representation of activation of the HIF-system.

1.3 Angiogenesis

1.3.1 Background

Angiogenesis was first used to describe new blood vessel growth by John Hunter in 1787 after he discovered that interrupting the blood flow in stag antlers resulted in newly formed blood vessels to carry the existent blood flow, and that gunshot wounds only

healed if there was an adequate blood supply (Greenberg and Jin, 2004). Angiogenesis is observed to be a compensatory response to prolonged imbalances between the perfusion capabilities of the blood vessels and the metabolic requirements of the tissue cells (Adair *et al.* 1995). It likely occurs at the venular end of capillaries and involves remodelling of the vasculature (Hudlicka 1991).

There are three described processes of neovascularisation. The formation of new blood vessels starts during embryonic development and is known as 'vasculogenesis', a process whereby angioblasts (endothelial cell precursors) migrate to discrete locations, differentiate into blood islands, proliferate within a previously avascular tissue and then coalesce to form a primitive capillary plexuses (Risau, 1997). It is at this time that the vessel fate is decided. The endothelial cells (ECs) have an exceptional plasticity (Carmeliet, 2003). The second form of vascularisation is angiogenesis, the process whereby this primitive network formed by vasculogenesis is developed and remodelled into a mature network (Hudlicka *et al.* 1992). These vessels act to increase the surface area to volume ratio, decreasing the distance for O_2 diffusion, thus optimising the speed at which O_2 is available for use. The third form of vascularisation occurs as the circulation commences, and is known as arteriogenesis: the formation of new arterioles and venules, which occurs by investing capillaries with vascular smooth muscle. This process is necessary to cope with the increased blood flow and to maintain haemodynamic stability. A natural system of pre-existing arteries is also present that can bypass sites of arterial occlusion by forming collateral bridges between arterial networks. These vessels can extensively increase their lumen diameter to increase blood flow and perfusion to occluded areas, resulting in fully functional and structurally normal arteries (Buschmann and Schaper, 1999).

1.3.2 The history of angiogenesis

Factors known to be important for blood vessel growth have been a matter of controversy for a long time. Landerer (cited by Marchant, 1901) talked about the

importance of mechanical factors connected with changes in blood flow, evidential from the formation of sprouts in areas of least resistance in the vascular bed (Hudlicka and Tyler, 1986). Similarly, Thoma (1893, 1911) described a combination of velocity of flow and/or pressure and growth of the surrounding tissue and resulting wall stress resulted in the formation of vascular sprouts, as studied in chick embryos. Clark and Clark (1932) were highly influential in establishing the field of vascular biology. Their initial experiments involved placing glass-windowed chambers in the rabbit ear, allowing them to make exquisite drawings of the branching patterns of the blood vessels that entered the wound. Several scientists, including Loeb in 1893, have shown that metabolic factors are extremely important in eliciting an angiogenic response. Adair *et al.* (1995) proposed that O_2 was an important factor controlling the growth of blood vessels. They found that decreased oxygenation caused the tissue to become hypoxic and this initiated a variety of signals that then lead to the growth of new blood vessels. A negative feedback loop was suggested, so that when an adequate amount of O_2 had been provided, further development of the vasculature was attenuated. In the early 1970s, Judah Folkman proposed that angiogenesis and tumour growth might go hand in hand, and he subsequently demonstrated that tumour growth was halted if the tumour was deprived of a blood supply (Folkman, 2002). Experiments done by Krogh in 1919 were the first to show that angiogenesis is controlled by metabolic regulation (Pugh and Ratcliffe, 2003).

1.3.3 Types of Angiogenesis

The endothelium is usually quiescent in healthy adults with only 0.01% of ECs undergoing division (Carmeliet, 2003). Angiogenesis is only switched on under specific conditions. Physiological angiogenesis is activated during embryogenesis and in the female reproductive system, for example. Pathological vascular remodelling is found in tumour growth, atherosclerosis and diabetes, as prime examples. There are thought to be major differences between the blood vessels associated with tumours and those

associated with physiological angiogenesis with the former being described as more leaky and less well organised compared to the normal vasculature (Liekens *et al.* 2001).

1.3.3.1 Sprouting angiogenesis

There are three described mechanisms of angiogenic growth, the main difference being the mode of stimulation for the production of new vessels. The classical form of angiogenesis is sprouting angiogenesis which occurs when a stimulus from the abluminal side of the vessel, for example muscle overload (extirpation), initiates the release of cytokines and growth factors from skeletal muscle. Proteolytic degradation of the extracellular matrix (ECM) occurs following an increase in the permeability or integrity of the basement membrane (BM), a barrier made of structural proteins that provides support to the capillaries (see 1.3.4 for more detail). Disruption of the BM allows the growth and migration of the EC into new vessel architecture (Haas *et al.* 2000). The BM breakdown is mediated by MMPs activated by vascular endothelial growth factor (VEGF) and new blood vessel growth then occurs via EC migration and differentiation. The growth of tumour vessels occurs by this form of angiogenesis (Folkman, 1971).

1.3.3.2 Splitting angiogenesis

Splitting angiogenesis can also occur due to a luminal-triggered stimulus, for example an increase in blood flow, increasing shear stress and upregulating nitric oxide (NO) production. There are two forms of splitting angiogenesis: intussusception occurs when a single capillary splits into two capillaries from within by the formation of a longitudinal divide on the luminal side of the capillary (Prior *et al.* 2004), and involves abluminal activation of mural cells such as fibroblasts. The other form of splitting angiogenesis occurs whereby endothelial cells, as opposed to interstitial cells, send filopodial processes into the capillary lumen which then join and form a separate branch, and this subsequently propogates down the capillary (Zhou *et al.* 1998).

The main difference between the described mechanisms is that sprouting

angiogenesis requires BM and extracellular matrix degradation, allowing migration and proliferation of ECs, and thus the development of the sprouting tube. Work done by Egginton *et al.* (2001) supports the notion that BM degradation is not a pre-requisite for splitting capillary growth.

1.3.4 Mechanisms of blood vessel growth

The sprouting growth of new capillaries is initiated via degradation of the BM underlying the ECs and this requires the cooperation of the plasminogen activator protease system (PA) and the matrix metalloproteinases (MMPs) (Conway *et al.* 2001), alongside a wide range of growth factors (Table 1.3, Fig 1.4). MMPs play a critical role in breaking down the BM of the vessel and the ECM via release of ECM-bound growth factors. The increased vascular permeability due to a combination of VEGF and the MMPs enables extravasation of plasma proteins that lay down a provisional scaffold for migrating cells (Carmeliet, 2003). This also results in the release of other growth factors involved in stimulating angiogenesis and up-regulating VEGF mRNA expression, including insulin-like growth factor-1 (IGF-1), transforming growth factor β (TGF-β), platelet-derived-growth-factor (PDGF) and basic fibroblast growth factor (bFGF), among others. PDGF is produced by a variety of cell types, and targets a range of cells including capillary cells, ECs and vascular smooth muscle, initiating the establishment of paracrine and autocrine loops for EC activation and proliferation (Dunn *et al.* 2000).

The formation of properly patterned and structurally stable microvascular networks requires the coordinated recruitment of pericytes to microvessels (Ponce and Price, 2003) and it has been suggested that pericytes lead capillary sprouts into tissues. Pericytes are known as mural cells, involved in the formation of vasculature, and have the ability to differentiate into fibroblasts, smooth muscle cells or macrophages. They have been shown to exist at the early stage of the angiogenesis and to induce proliferation of the endothelium, guiding migration and sprouting *via* VEGF-A secretion (Morikawa and Ezaki, 2005).

Steps in angiogenesis	Stimulatory factors	Inhibitory factors
Vasodilatation	Nitric oxide synthases	
Increased vascular permeability	VEGF (Flt-1, Kdr)	Ang-1 (Tie-2)
Extravasation of plasma proteins	VEGF	Ang-1 (Tie-2)
Endothelial sprouting	Ang-2 Tie 2 VEGF (Flk-1)	
Degradation of extracellular matrix	MMPs & TIMPs (tissue inhibitors) Collagen prolyl-4-hydroxylase	PAI-1
Liberation of growth factors	uPA receptor	Thrombospondin-1 PAI-1
Endothelial cell proliferation & migration	VEGF, Ang 1&2, FGFs, PDGF	
Pericyte and smooth muscle recruitment	PDGF	
Endothelial assembly and lumen acquisition	VEGF, Ang-1 (Tie-2) Integrins	Thrombospondin
Stablilisation of nascent vessels	PAI-1	
Maintenance of differentiation and remodelling	Ang-1 (Tie-2)	Ang-2 (Tie-2)

Table 1.2 Summary of the molecular basis underlying new blood vessel growth (Receptors are indicated in brackets) (From Pugh and Ratcliffe, 2003).

A number of factors contribute to the dissociation and movement of ECs through the matrix. The Tie-2 receptor is a signalling system involved in vessel maintenance, growth and stabilisation. Tie-2 is a membrane bound receptor tyrosine kinase that binds angiopoietins 1 and 2 (Ang1 and Ang2). To enable ECs to dissociate from each other, competitive inhibition of Tie-2 by Ang2 occurs, initiating the loosening of matrix contacts and support cell interactions, thus allowing access for the above-mentioned growth factors and other angiogenic inducers (Hanahan, 1997). Redistribution of intercellular adhesion molecules (platelet endothelial cell adhesion molecule (PECAM-1) and vascular endothelial (VE)-cadherin) also contributes to the dissociation of ECs from their neighbouring cells, causing them to undertake mitosis, and, due to loss of contact inhibition, start migrating throughout the matrix. Proteinases also expose new epitopes in ECM proteins that induce migration, along with a matrix of fibronectin and fibrin, and another group of adhesion molecules called the integrins ($\alpha_v\beta_3$ and $\alpha_v\beta_5$) (Eliceiri and

Cheresh, 1999). These all assist in guiding the ECs towards their objective sites (Carmeliet, 2003).

During the migration of the ECs to distant sites, there is a complex interplay and redundancy between VEGF, bFGF and angiopoietins. Via phosphorylation of Tie2, Ang1 stimulates interactions between pericytes and ECs and induces sprouting of new capillaries (Conway *et al.* 2001), solidifying and stabilising a newly formed blood vessel. Initial breakages in the BM are repaired quickly as an intact BM was found around many EC sprouts (Egginton *et al.* 2001).

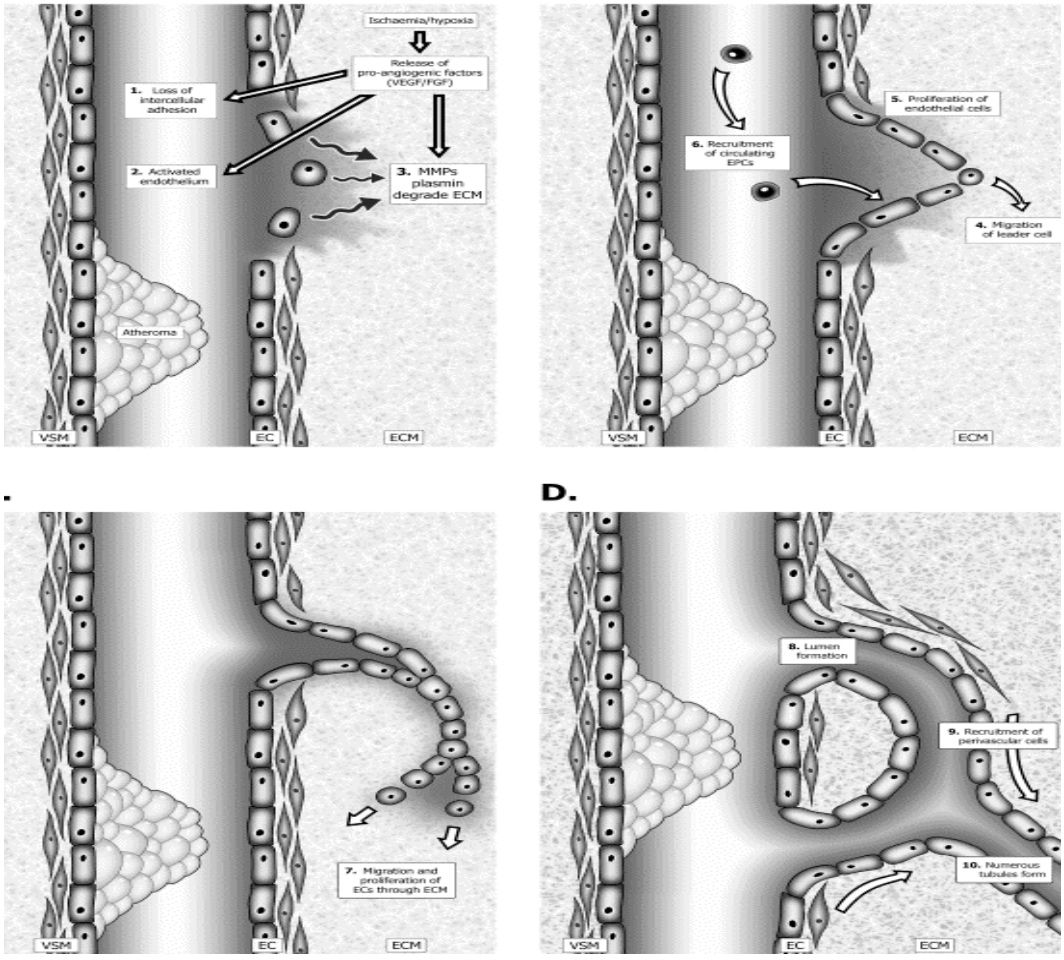

Figure 1.5 Mechanisms of blood vessel growth *via* BM degradation, EC migration, differentiation and reformation into tubes that form new capillaries (Taken from Collinson and Donnelly, 2004)

1.3.5 Angiogenic stimuli

A number of factors are responsible for the initiation of angiogenesis, and the nature of the stimulus determines the morphological characteristics that ensue. There is a very fine balance between pro- and anti-angiogenic factors, and disruption of this balance provides the driving force for the development of new vessels (Fig 1.5).

1.3.5.1 Metabolic and mechanical factors

Metabolic factors are also responsible for the formation of new blood. It is uncertain as to which type of angiogenesis is initiated by hypoxia, though it is possible that polycythaemia, caused by an increase in RBCs under hypoxia, could increase shear stress and initiate angiogenesis *via* luminal splitting (Deveci *et al.* 2002).

Mechanical factors influencing angiogenesis include the increase in blood flow (leading to increased shear stress) that follows the initiation of exercise, cyclical wall tension in response to pulsatile blood pressure, and the strain imposed by muscle fibres if they increase in size (for example with exercise, training or imposed by conditions of overload). Functional overload, due to the alteration in load bearing, is induced in the remaining muscle. The disruption of the abluminal environment caused by stretch and conditions required for the increase in muscle mass, a phenomenon commonly observed, stimulates the sprouting form of angiogenesis (Zhou *et al.* 1998). This extended network of capillaries is responsible for maintaining blood flow and O_2 supplies to enable new protein synthesis for the elongation of muscle fibres (Goldspink *et al.* 1991).

Any alterations in stretch or shear induce transformational changes in the blood vessel wall. These changes are sensed by ECs and transmitted *via* stretch-activated ion channels (Lansman *et al.* 1987) to the cytoskeleton, which subsequently initiates changes in gene expression, altering the proliferation and survival of cells. Several genes which initiate angiogenesis are upregulated, including MMP-2 and VEGF, both of which are involved in the breakdown of vessels, the starting point for the initiation of new vessel growth (Egginton *et al.* 1998). Until recently, HIF expression was thought to

only be important under hypoxic conditions, but it is now known to be upregulated under non-hypoxic conditions such as stretch: Williams *et al.* (2006b) showed that HIF-1α was upregulated under both conditions of shear and stretch-induced angiogenesis. Subsequently, Milkiewicz *et al.* (2007) showed that both HIF-1α and HIF-2α, on a protein and mRNA level, play a core role in stretch-induced angiogenesis.

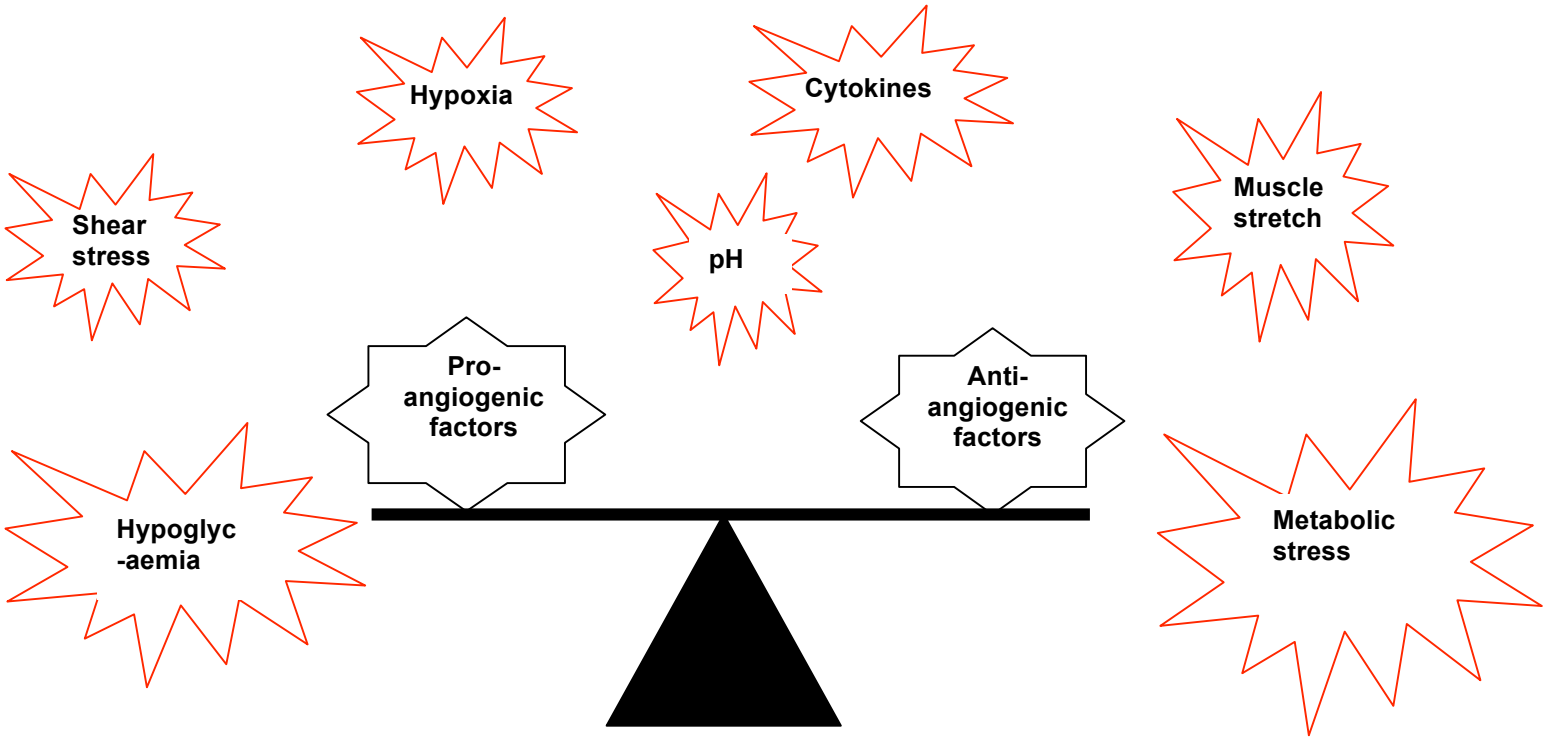

Figure 1.6 The angiogenic balance: a fine balance exists between pro and anti-angiogenic factors with a wide range of stimuli affecting the outcome.

1.4.7 Angiogenesis and disease

Angiogenesis was originally only implicated in the development of cancer, arthritis and psoriasis. However, an increasing amount of research has been centered around understanding the molecular basis of this phenomenon, and it has become evident that excessive, insufficient or abnormal angiogenesis contributes to the pathogenesis of many other disorders. Table 1.3 shows a range of diseases where angiogenesis is implicated as a major factor.

ORGAN	**DISEASE**
Numerous organs	Cancer (activation of oncogenes; loss of tumour suppressors); autoimmune disorders (activation leucocytes)
Blood vessels	Vascular malformations (tie2 mutation); DiGeorge syndrome (low VEGF and neuropilin-1 expression)
Adipose tissue	Obesity
Skin	Psoriasis, warts, allergic dermatitis, scar keloids, blistering disease, Kaposi sarcoma in AIDS patients
Eye	Persistent hyperplastic vitreous syndrome (loss of ang-2 or VEGF164); diabetic retinopathy; retinopathy of prematurity
Lung	Primary pulmonary hypertension, asthma, nasal polyps
Intestines	Inflammatory bowel and periodontal disease, peritoneal adhesions
Reproductive system	Endometriosis, uterine bleeding, ovarian cysts
Bone, joints	Arthritis, synovitis, osteomyelitis

Table 1.3 Disease characterised or caused by abnormal or excessive angiogenesis (From Carmeliet, 2003)

Hypoxia plays a role in initiating many of the above-mentioned diseases. One disease where hypoxia-stimulated angiogenesis plays an important role is in PAD, whereby the build up of an atherosclerotic plaque in the arteries supplying the heart such as the

femoral artery (FA), causes disease of the blood vessels, and the loss of blood flow to the immediate tissue initiates remodelling of the vasculature (angiogenesis).

1.4.8 Therapeutic angiogenesis

A current challenge for therapeutic angiogenesis is to find the most efficient method of targeting ischaemic areas in need of revascularisation. There have been a wide range of trials, including administration of growth factors such as VEGF and FGF. Gene therapy is an extremely attractive form of gene administration, with differing administration routes: viral and non-viral. Non-viral gene therapy is limited by a low transfection efficiency and low transgene expression (Bobek *et al.* 2006). Viral vectors are a more attractive alternative as there are a range of possible vectors and the transfection efficiency is higher than with non-viral transmission. Problems with gene therapy in humans arise due to the limited tissue diffusion of the vector and the greater volume of tissue present in humans, when compared to the animal models from which the methods were derived.

Aside from gene therapy as an external method of manipulating blood vessel growth, the use of chemicals to manipulate molecular pathways involved in the angiogenic cascade are widely being trialled. One of these is dimethyloxalylglycine (DMOG), a PHD and FIH inhibitor which upregulates HIF activity. It has been shown to upregulate HIF-1α and downstream angiogenesis in a model of femoral artery ischaemia (Milkiewicz *et al.* 2005), and thus shows potential for use in mitigating the effects of chronic ischaemia.

1.5 Hypothesis and aims

Aim 1: To elucidate the conditions of systemic hypoxia required to manipulate the HIF-regulated genomic response in different mouse tissues, and in parallel to study the same host of genes in human leucocytes alongside the plasma EPO response to hypoxia.

Objective 1: This was achieved by exposing mice to a stimulus of 10% hypoxia for 2 wks, and a two-phase study in humans consisting of an acute exposure to 4600m (~12%) and a chronic exposure to 4392m.

Hypotheses: (1) Human leucocytes may be used as a viable circulating indicator of the systemic response to hypoxia, and (2) EPO may be used to determine the erythropoietic response and susceptibility to acute mountain sickness (AMS).

Aim 2: To evaluate the levels of local or systemic, hypoxic or non-hypoxic stress required to initiate angiogenesis, and to evaluate whether chemical manipulation of HIF-1α stability would enhance these responses.

Objective 2: This was investigated using (1) a model of femoral artery ligation in the mouse to study the effects of local hypoxia (ischaemia) with and without the addition of DMOG, and (2) mice were exposed to 10% and 12% hypoxia for 1, 2 and 4 wks to study the effects of systemic hypoxia.

Hypotheses: (1) Chemically manipulating availability of HIF-1α *via* inhibition of the PHDs (with DMOG) would enhance angiogenesis and help to restore blood flow to the ischaemic muscle, (2) A similar effect of enhancing angiogenesis to that previously shown in a model of local hypoxia, would be seen in an array of tissues when the proximate signal is systemic.

Aim 3: To elucidate whether the same HIF-1α-mediated pathways were operating under conditions of stretch-induced angiogenesis as seen under hypoxia.

Objectives 3: DMOG was administered to mice subjected to unilateral extirpation.

Hypothesis: If HIF-regulated stretch-induced angiogenesis is operating *via* the same pathway as under local hypoxia, DMOG should also enhance capillary growth under normoxic conditions.

Aim 4: To establish relationships between genomic and functional responses in skeletal muscle following genetic manipulation of molecular pathways leading to HIF-1α stability.
Objective 4: This was achieved using PHD1 and PHD3 knockout mice and the established model of unilateral extirpation, using gene arrays to evaluate the genetic response.
Hypothesis: The PHDs working non-redundantly, and a differential gene response should be seen following specific PHD ablation.

Chapter 2

METHODS

2 Methods

All experiments were performed in accordance with the Home Office Animals (Scientific Procedures) Act, 1986. The Home Office license holder is Dr. Stuart Egginton and the number is 40/2872, and my personal license number is 40/8197. All experiments and surgery, with the exception of the following, were conducted in the Department of Physiology in Birmingham: Western Blotting (Chapter 3), Gene array and analysis (Chapter 6) (Wellcome Laboratories, University of Oxford), Chapter 3 and 8, RT-PCR (IBR, Department of Immunology, University of Birmingham), Chapter 8 – Phase I in the University of Glamorgan, Phase II in Chile.

2.1 Dimethyloxalylglycine

Dimethyloxaloylglycine (DMOG) is a cell penetrant oxoglutarate analogue which inhibits all enzymes of the oxoglutarate-dependent dioxygenase class, including collagen prolyl hydroxylases, PHD 1–3 and FIH, thus inducing stabilisation of both HIF-1α and HIF-2α proteins. This subsequently allows downstream gene expression, promoting capillary growth. Its development as a regulator of HIF came following the characterisation of the PHDs (Mole *et al*. 2003). The direct effect of DMOG is inhibition of enzyme activity: it is hydrolysed in cells to NOG which sits in the active site in place of 2OG, stopping the enzyme from turning over. There is no direct effect on the level of PHD protein concentration but an increase in HIF protein is seen.

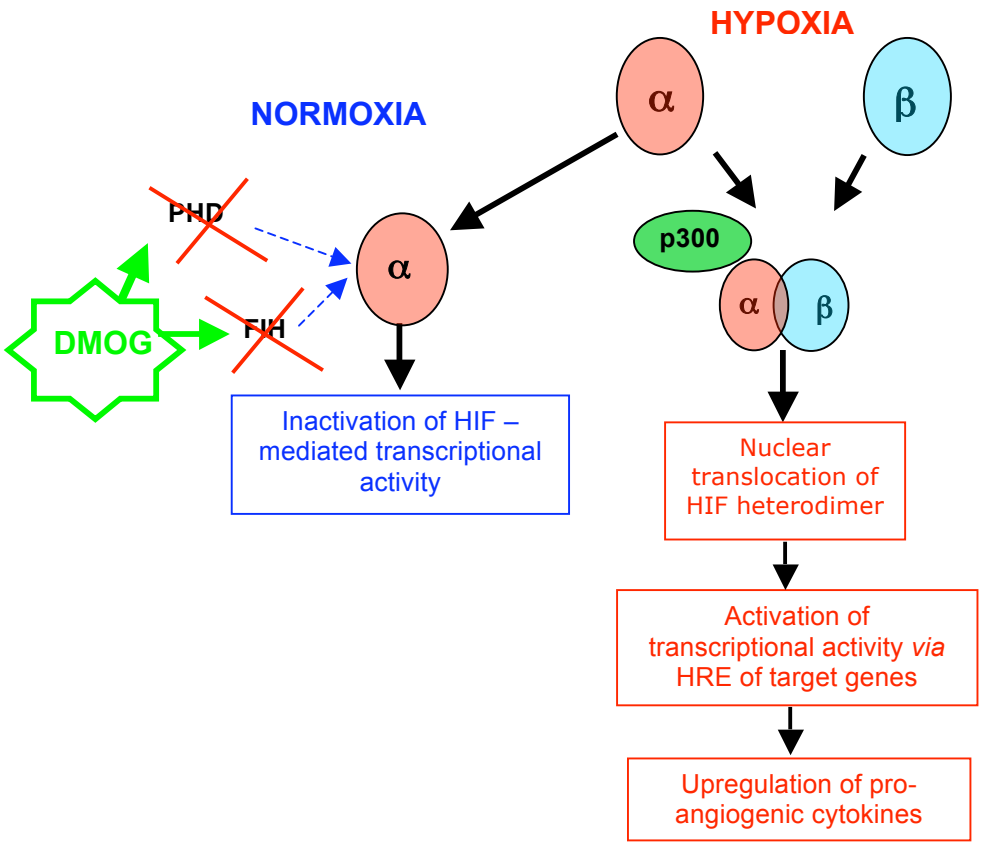

Figure 2.1 Illustration of how DMOG interacts with HIF under hypoxia

2.1.1 Protocol

DMOG (Frontier Scientific Europe Ltd-D1070) was administered *via* i.p injection to the C57Bl6/J strain of mouse, at a concentration of 16mg.ml^{-1} in saline, at a dose of 0.5ml every other day.

2.1.2 Product research and development

Initial experiments conducted using DMOG from Frontier Scientific failed to produce any observable changes in the capillary supply in the EDL muscle resulting from the femoral artery ligation, as expected from previous studies (Milikiewicz *et al.* 2005). A detailed analysis was carried out in collaboration with the chemistry laboratory in Oxford to determine the similarity of the chemical to a previous batch used (Milkiewicz *et al.* 2005) which was synthesised in Oxford. Mass spectrometry (MS) and nuclear magnetic

resonance (NMR) imaging were both employed and were carried out by Benedikt Kessler (Wellcome Centre for Molecular Biology in Oxford) and Chris Schofield (University of Oxford, Department of Chemistry). MS identifies the chemical composition of a compound or sample on the basis of the mass-to-charge ratio of charged particles. It involves fragmentation of the molecule and identification of the corresponding spectra that are produced that relate to the compounds mass and charge (Gross, 2004). NMR involves resonance of protons to pulsed radiation in a magnetic field. The protons on the molecule spin depending on the group present on the compound, and the protons shift differently depending on the environment, producing a series of peaks on a graph (Hornak, 1997).

A slight difference in the molecular makeup of the DMOG from Frontier Scientific was found compared to the DMOG used previously in studies (Fig. 2.2, 2.3). The FS DMOG was not as pure as the original batch and although this may have no effect, it could disrupt the function of the DMOG. To try and overcome this problem, a new batch of DMOG was synthesised at the original source and used in subsequent experiments.

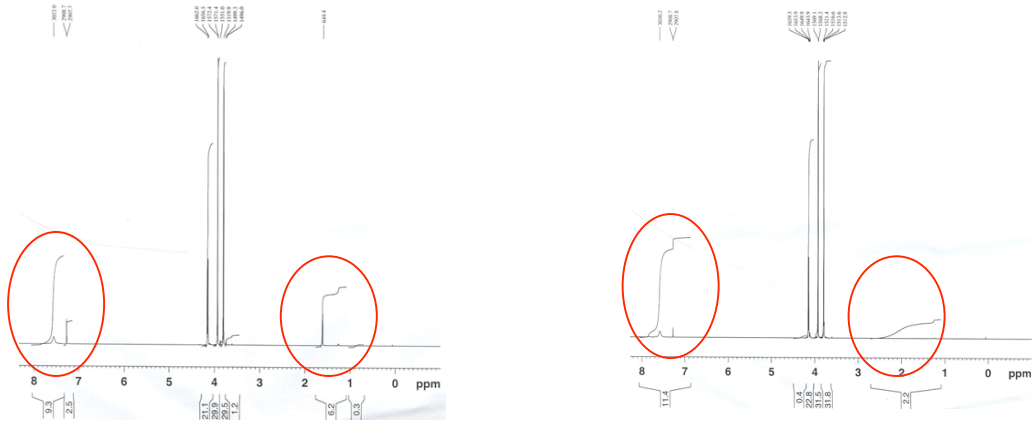

Oxford Frontier

Figure. 2.2 A comparison of DMOG, using NMR, synthesised in Oxford and a commercial source. Circles demonstrate the different peaks obtained. Both spectra show a small amount of monoester of DMOG with an additional NH proton at 7.8 ppm and only one methoxy group (OCH3) of methyl ester at the region around 4 ppm. Despite the fact that both spectra show about 95% presence of DMOG, the 'Oxford' batch has been deemed to have a less noisy spectra and is therefore cleaner

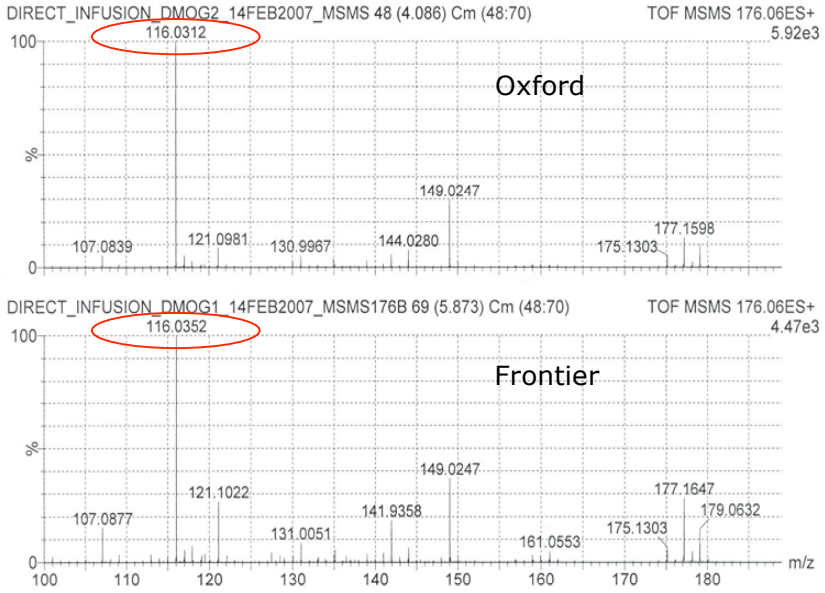

Figure 2.3 Values obtained for the 'DMOG peak' in mass spectrometry

2.2 Skeletal muscle sampling

Following cervical dislocation at the end of experiments, skeletal muscle was removed from the hindlimb of the mouse (Fig 2.4). The main tissue studied was the *extensor digitorum longus* (EDL) which is a pennate muscle that inserts into the middle and distal phalanges of the lateral four digits of the hindlimb. Its action is the extension of the toes and ankle and is important for stability. The EDL has a mixed fibre type composition (Zierath and Wallberg-Henriksson, 2002) and thus gives a good representation of response to both the hypoxic and non-hypoxic conditions in these experiments. In the extirpation experiments, it was necessary to study the EDL as it is the synergist muscle to the TA muscle which is removed.

The soleus was also studied in some of the experiments. It is a powerful muscle in the back part of the lower leg and is involved in walking and is very important in posture when standing. It is mainly composed of slow twitch oxidative muscle fibres (Hirofujl *et al.* 1992).

Only muscle from the affected limb was sampled and not that from the contralateral muscle. It has been shown (Williams, unpublished) that as a consequence of surgery on the ipsilateral limb, the contralateral limb undergoes some physiological changes to compensate for the intervention on the ipsilateral limb. Because of this, physiological readings from the affected limb are compared to untreated control animals. All this tissue sampling was performed in Birmingham.

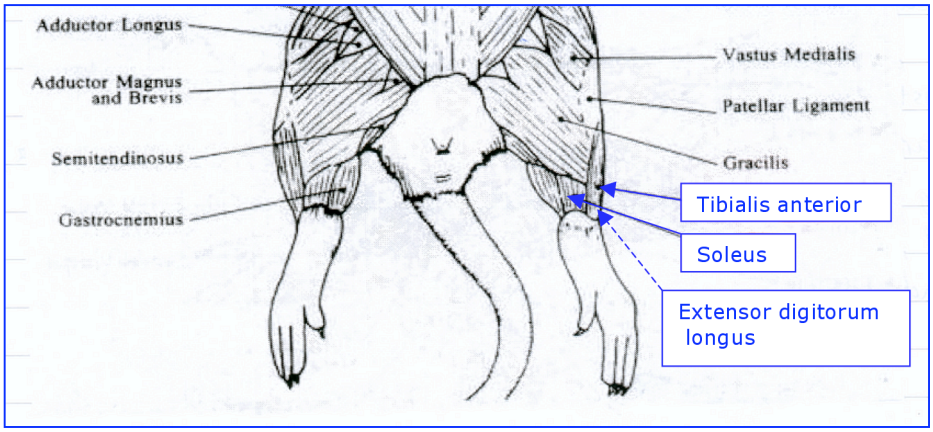

Figure 2.4 Location of muscles used for sampling tissue (Cook, 1965)

2.2.1 Procedure

An incision was made along the upper side of the hindlimb on top of the location of the TA. The tendon of the TA was identified and lifted up using a fine pair of forceps before being cut at the base. A small amount of tension was placed on the TA and it was then carefully pulled upwards and separated by blunt dissection from the remaining muscles, before being cut at the top from underneath using a scalpel blade. This left the EDL exposed and the same procedure was repeated. The soleus rests around the back of the hindlimb and can be identified by the red colour of the muscle, indicative of its oxidative capacity and attachment to skin above the ankle.

2.3 Freezing tissue and cryosectioning

Correct timing and efficiency of freezing the desired tissue is required to ensure freezing damage does not prevail. Liquid nitrogen has a low specific heat capacity and thus the tissue is not frozen directly with it. Due to the formation of an insulating layer of gas, ice crystals would form. Instead, isopentane, cooled using liquid nitrogen, is a wetting agent used to freeze the muscle.

2.3.1 Freezing tissue

The desired tissue was placed on a cork disk with a pin stuck in the middle to maintain the correct orientation and coated with OCT (tissue tek, 4583) compound. The tissue was then lined up against the pin to ascertain correct orientation, and dropped into cold isopentane. Isopentane was cooled to its freezing point by liquid nitrogen. The appropriate temperature was determined visually by an increase in viscosity and cloudiness. After 30 s, the cork was removed from the isopentane and the pin taken out. The discs were stored in liquid nitrogen before transfer to the -80°C freezer.

2.3.2 Cryosectioning

Before sectioning, the tissue was removed from storage in liquid nitrogen and stuck onto a metal chuck. The microtome (at -20±3°C) was used to finely section the tissue at a thickness of 10µm and the section was then picked up on a glass slide. The slide was then left to sit at room temperature (RT) for 30 min to dry and ensure adequate binding. Slides were stored at -20°C or used immediately for staining.

2.4 Immunohistochemical staining and capillary counting

2.4.1 Lectin staining

Lectins are sugar-binding proteins which are highly specific for different sugar moieties. Here, the fluorochrome conjugates, while mainly binding to the galactose residues

present in the glycocalyx lining the blood vessels, also faintly stains the sarcolemma of the muscle fibres which makes analysis of the capillary to fibre ratio easier.

2.4.1.1 Protocol

Sections were air dried for 30 min on removal from the freezer and encircled with a wax pen. Sections were fixed in acetone and left to evaporate. Fluorescein labelled *Griffonia simplicifolia* Lectin I (GSL I, BSL I) (Vector, FL-1101) was used at a concentration of 5µg.ml^{-1} in 10mM phosphate buffered saline (PBS) (Sigma Aldrich, P5368). PBS was used in combination with $CaCl_2$ (1Mm $CaCl_2$ in 10Mm PBS), 500µl per slide. Slides were left for 1 h at RT out of direct light and subsequently rinsed 3 x 5 min washes with PBS, with a final rinse in distilled water.

2.4.2 VEGF triple stain

4',6-diamidino-2-phenylindole (DAPI) (Invitrogen, MP01036) is a fluorescent nuclear stain, excited by ultraviolet light and shows strong blue fluorescence when bound to DNA. Co-localisation of VEGF-A by immunostaining with lectin and DAPI staining enables a comparison of those capillaries which are actively undergoing angiogenesis with those that are not. Angiogenesis induces an increase in the number of endothelial cells and nuclei associated with them, thus by studying the proportion of DAPI and lectin stained cells, a measure of cellularity can be obtained, and the proportion of lectin-stained vessels that are VEGF positive, an indication of widespread or local angiogenic activation.

2.4.2.1 Solutions

0.5% PBS-Tween

Primary antibody dilution buffer

1% bovine serum albumin (BSA, Sigma Aldrich, 05491) in 0.5% PBS-Tween (0.5% tween in 10mM PBS) (Tween: Sigma Aldrich, P5927)

Secondary antibody dilution buffer

1.5% normal goat serum (NGS) (SantaCruz Biotechnology, sc-2043) + 1%BSA in PBS-Tween.

HEPES solution + Ca^{2+}

1mM $CaCl_2$ solution in 10mM HEPES solution

2.4.2.2 Protocol

Sections were air dried for 30 min prior to staining and then fixed in pre-cooled acetone for 10 min. Slides were washed 3x for 5 min. in PBS and 1x 5 min. in PBS-Tween. The slides were dried and the sections circled using a wax pen. The primary antibody (VEGF 147^{A20}: targets VEGF-A, Santa Cruz sc-152) was diluted to a concentration of 1:100 in primary antibody dilution buffer, and the slides were incubated for 1 h at RT. Slides were then washed 3x for 5 min in 0.5% PBS-tween. The secondary antibody (Alexafluor-488 goat anti-rabbit: Invitrogen A11034) was diluted down in secondary antibody dilution buffer (0.01M PBS, 0.5% Tween, as described) to a concentration of 1:250, and the slides incubated for 1 hour at RT. The slides were then washed 2x for 5 min in PBS-Tween and 2x 5 min in PBS. 500µl of lectin (prepared as in 1.6.1.1) was then applied to each slide and left at RT for 1 hour. Slides were washed 3x for 5 min. in PBS and 1x in distilled water. 1-2 drops of Vectashield with DAPI (1.5 $\mu g.ml^{-1}$: Vector labs, H-1200) was added to each slide to stain nuclei, followed by a cover slip, taking care to make sure no air bubbles were present. The slides were then visualised using a fluorescent microscope.

2.4.3 Capillary and fibre counting

2.4.3.1 Lectin stain

Capillaries were visualised using a fluorescent microscope (Zeiss Axioskop 2 plus with the AxioVision programme 4.4). One section of each piece of tissue was photographed at a

magnification of x20 using the FITC filter with an excitation filter boundary of 490/20nm (center wavelength/width of band) and an emission filter boundary of 528/38nm. 4 photographs were taken to cover both the lateral and medial sections of the tissue to ensure that the naturally occurring variation in the number of capillaries due to fibre type (oxidative or glycolytic) were accounted for when counting. Using Adobe Photoshop®, images could be digitally enhanced to aid accuracy of visualising the capillaries and fibres. A sampling grid of 18x13 squares was randomly placed onto the image, and the number of capillaries and fibres within that area recorded. Any capillaries or fibres lying on the top and right sides of the sampling square were included in the count. Any lying or touching the bottom and left sides of the square were excluded (Egginton, 1990). The capillary density and fibre size were calculated from the estimation of the number of capillaries and fibres with this area of 93 600μm^2, as determined by calibration with a graticule.

2.4.3.2 VEGF/lectin/DAPI triple stain

Capillaries were visualised (above) and the number of lectin stained capillaries recorded. VEGF positive capillaries were visualised with an excitation filter boundary of 555/28nm and an emission filter boundary of 617/73nm. The DAPI staining was visualised using an excitation filter boundary of 360/40nm and an emission filter boundary of 457/50nm. Digital photos were obtained by multidimensional acquisition to record each channel as elements of a single image. The proportion of lectin stained capillaries that were VEGF positive was determined, and the number of lectin stained capillaries that were lectin and DAPI positive was recorded. The number of capillaries that had been stained with DAPI (shown by fluorescent blue staining) divided by the number of lectin stained capillaries is proportional to the cellularity of the vessel, and the proportion of lectin and VEGF, along with lectin and DAPI compared to lectin alone give an estimation of those capillaries actively undergoing angiogenesis.

2.5 RNA extraction

The purification of RNA from samples is used as a starting point for further analyses such as RT-PCR and gene arrays. Qiagen and Trizol are both well described methods used to extract the RNA from cells and tissues. To establish which would give the higher yield of RNA, an extraction was carried out using both. They gave similar yields though the Qiagen kit was used as it was more time efficient.

2.5.1.1 Tissue homogenisation

Glass homogenisers were placed in an oven at 200°C for 3 h to inactivate RNAses. The worktop and all instruments involved were cleaned using RNAse zap. The muscle to be used was wrapped in a small piece of foil and placed on a frozen metal block in a polystyrene box surrounded by liquid nitrogen. The muscle was then crushed with a pestle and the powder transferred to the glass homogeniser on ice. It was then homogenised and the Qiagen RNeasy kit (Qiagen, Crawley, UK) used to extract the RNA using Appendix C from the handbook. Eluted RNA was stored at -20°C.

2.5.1.2 Cell homogenisation

To remove adherent GC-1 cells (originating from mouse testicles and used as a positive control for PHD1) from the petri dish, all DMEM (Invitrogen, 31885-023) was removed with a pipette and 600µl of buffer RLT (RNA lysis tissue buffer)+ β-mercaptoethanol (Qiagen kit) was added. After ensuring adequate spreading, the dish was checked under the microscope to determine if all the cells were in solution. GC-1 cells were scraped off the plate and transferred into an Eppendorf and spun at 17,900g for 5 min. Subsequently, the protocol was then followed for RNA extraction from animal cells, from the Qiagen RNeasy protocol. Eluted RNA was stored at -20°C.

2.5.2 Determination of RNA purity

It is important to determine the purity of the RNA before further use, and this was determined *via* two methods. RNA denaturing gel electrophoresis and the nanodrop was used for assurance of purity, and the latter to also determine the concentration of the RNA. Intact total RNA run on a denaturing gel will have sharp 28S and 18S rRNA bands. The 28S rRNA band should be approximately twice as intense as the 18S rRNA band. This 2:1 ratio (28S:18S) is a good indication that the RNA is intact. Partially degraded RNA will have a smeared appearance, will lack the sharp rRNA bands, or will not exhibit a 2:1 ratio. The nanodrop is a full-spectrum spectrophotometer used to quantify nucleic acids, proteins, fluorescent dyes and other compounds. It requires 2µl of sample for determination and produces spectra as shown by the red line in Fig. 2.5. If the sample is pure it will have a 260/280nm value of above 2. Any spectra that give different values from this indicate impurity in the sample.

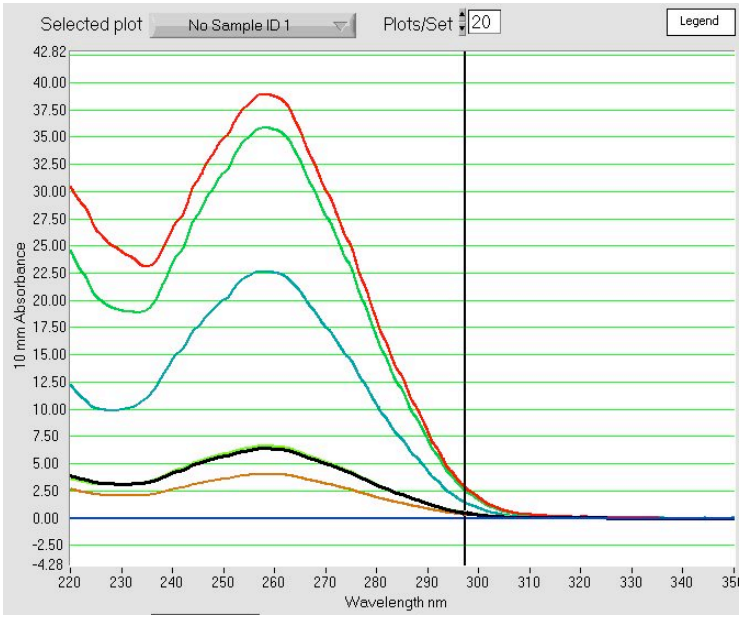

Figure 2.5 An example of spectra produced by the nanodrop in a collection of pure samples, all with a 260/280nm ratio >=2

2.5.2.1 RNA electrophoresis gel solutions

Gel loading buffer II – denaturing agarose, A 1-2X solution

95% Formamide (Fisher Scientific, BP227-100), 18mM EDTA (5.3g EDTA, Sigma Aldrich, 431788), 0.025% SDS (Fisher Scientific, BP166-100), Xylene Cyanol, and Bromophenol Blue (Sigma Aldrich G526).

10X MOPS (1L) (autoclave and store in the dark at 4°C)

41.8 g MOPS (Embi-Tec 1020) in 700 ml of sterile DEPC-treated H_2O. Adjust the pH to 7.0 with 2 M NaOH. Add 20 ml of DEPC-treated 1 M sodium acetate to 20 ml of DEPC-treated 0.5 M EDTA (pH 8.0). Adjust the volume to 1 litre with DEPC-treated H_2O.

2.5.2.2 Protocol

Gel preparation (1%)

2g of agarose was heated in 144ml water until dissolved, then cooled to 60°C. 20ml of 10X MOPS running buffer and 36ml 37% formaldehyde (Sigma Aldrich, 252549) was added. The plastic gel holder was taped along both ends, the gel was poured and the comb inserted. It was left to set for 20 min.

Sample preparation

Ethidium bromide was added to sample loading buffer at a final concentration of $10\mu g.ml^{-1}$. The loading buffer was then added to the RNA sample at a ratio of 1:1. This was heated at 65°C for 5 min.

Assembling the gel

The tape was removed from the ends of the gel holder and assembled in the tank. 800ml of 1x MOPS running buffer was added to cover the gel and the comb was removed. Samples were loaded onto the gel and it was run at 60V until bromophenol

bands were 2cm into gel, then the voltage was increased to 80V. This was run until 2/3 length of the gel. The gel was then visualised with a UV transilluminator (UVP®).

2.6 Real-Time RT-PCR and cDNA synthesis

Real time reverse-transcription-polymerase chain reaction (RT-PCR) is a very sensitive RNA quantification assay that involves two steps. Firstly, the complementary DNA (cDNA) is made from mRNA *via* reverse transcription. This cDNA is then used as a template for the polymerase chain reaction (PCR), whereby the gene of interest is amplified until there are millions of copies. DNA is much more stable than RNA so is a useful starting point for RT-PCR.

2.6.1 Synthesis of cDNA

RNA was extracted using the Qiagen RNeasy kit and eluted in water. 10µl of RNA was added to 1µl of oligo-dN6 (3µg.µl^{-1}) (Roche, 13819820) and denatured for 10 min at 70°C. This was shock cooled on ice and subsequently reverse transcribed using 9µl of the following mix: 0.5µl H_20, 4µl 5X first strand buffer (Invitrogen, P/N Y00147), 2µl 0.1M DTT (Invitrogen, P/N Y02321), 1µl dNTP (10Mm) (Promega, diluted to 10mM from 100mM stock provided), 0.5µl RNAse Inhibitor (RNAguard, Pharmacia, ~40 U.µl^{-1}), 1µl M-MLV (Gibco) (1µl.µg^{-1} RNA, stock 200 U.µl^{-1}). The sample was heated for 1 h < 42°C (41°C, block control and heated lid in Hybaid PCR machine) and then for 10 min to 90°C to inactivate RT. The sample was diluted with 80µl RNAse free water and stored at 4°C (-20°C for longer periods).

2.6.2 RT-PCR

RT-PCR is a very sensitive technique for mRNA detection and quantification. It involves the amplification and quantification of a specific DNA molecule. The quantitative data is collected at the point in which every sample is in the exponential phase of amplification. RT-PCR is the most sensitive method for the detection of low abundance mRNAs

compared to the two other commonly used techniques for quantifying mRNA levels, Northern blot analysis and RNase protection assay, and can be used to determine the amount of RNA present in a single cell. Of the range of probes that are available, Taqman probes are used here. These are oligonucleotides with a fluorescent reporter dye attached to the 5' end and a quencher dye attached to the 3' end. The probes are designed so that they hybridise to the internal region of the PCR product. The fluorescent increase with each cycle is proportional to the amount of probe cleavage that occurs every time the template is replicated (Fig. 2.6).

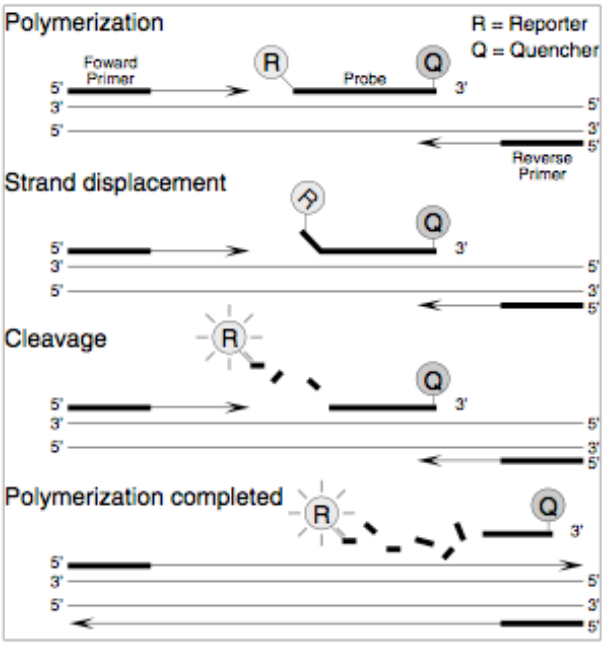

Figure 2 5′–3′ Nuclease Activity of the DNA Polymerase System

Figure 2.6 The Taqman system. DNA polymerase cleaves the TaqMan probe during the PCR. There is a reporter dye at the 5 ′end of the probe and a quencher dye at the 3 ′end. Cleavage results in increased fluorescence of the reporter (TaqMan Gene Expression Assays, Applied Biosystems)

The fluorescent signal can be directly measured using a laser and charged coupled device (CCD) camera, enabling real time detection of cDNA amplification (Fig. 2.7).

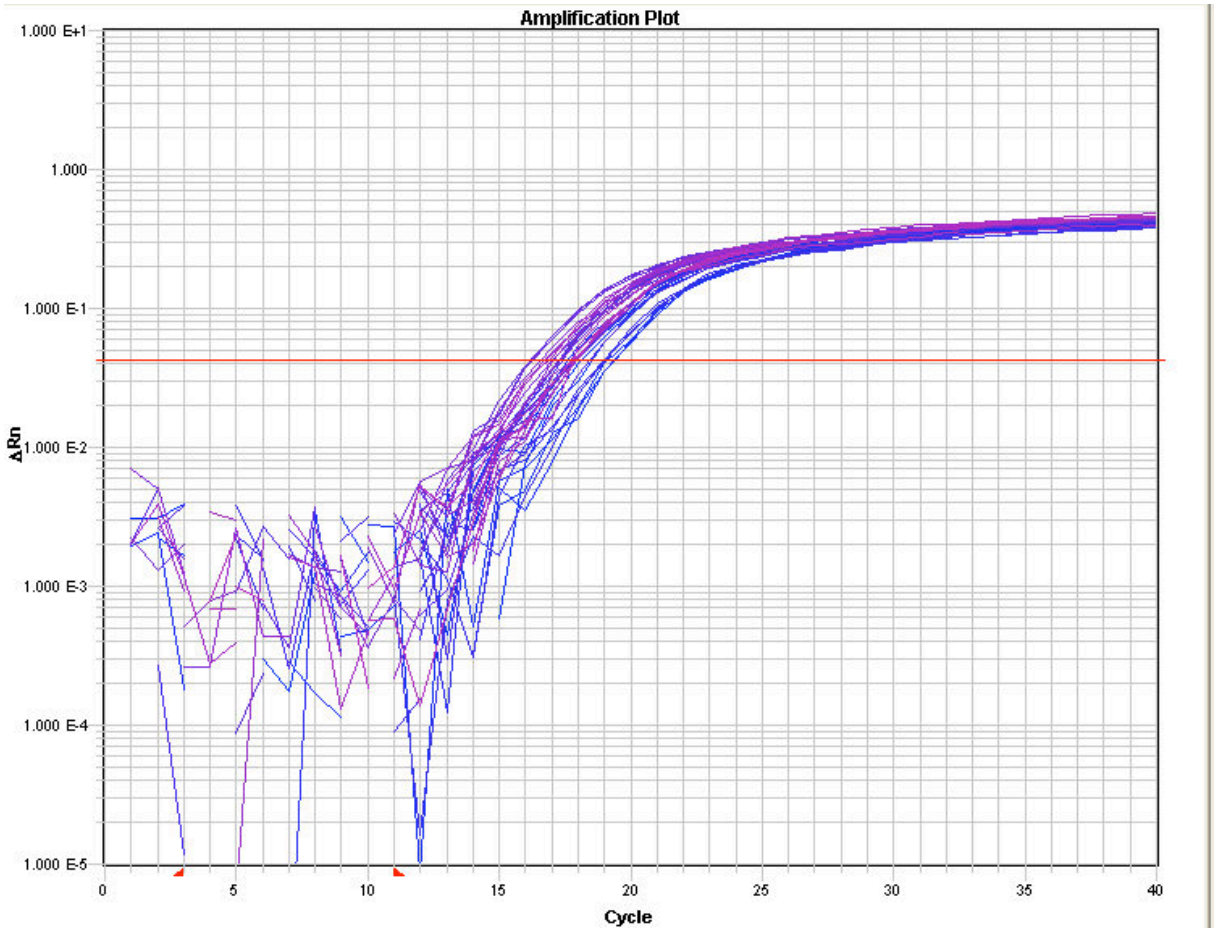

Figure 2.7 Illustration of the fluorescent signal yielded by β-actin from the cDNA of human WBCs. The cycle number is logged on the x-xis and the CT value is recorded on the y-axis.

2.6.2 Testing primers and probes

RT-PCR is typically referenced to an internal control gene. Currently, at least nine housekeeping genes (HK) are well described for the normalisation of expression signals (Stürzenbaum SR, Kille P. 2001.) β2- microglobulin (MWG, Germany: Forward: 5'-CATACGCCTGCAGAGTTAAGCA-3', Reverse: 5'-ATCACATGTCTCGATCCCAGTAGA-3', Probe: 5'-CAGTATGGCCGAGCCCAAGACCG-3' bound of CalFluor560 and Black Hole Quencher 1.) was used for the mouse gene RT-PCR (CHPT 3.2.2.1) and β-actin and 18S rRNA (small subunit of the two ribosomal subunits) were used for different human genes of interest (G of I) (CHPT 7.2.1.3). These were all pre-optimised control probes. In order to determine whether the primers and probes could be used in a multiplex array,

i.e. with both the HK gene and G of I in the same well, a plate was set up with a series of dilutions to determine cross reactivity. Positive and negative control samples were run in this array, as opposed to the actual samples.

For the study described in 3.2.2.1, mouse spleen was used as the positive control, as levels of G of I were significant in all organs as determined from genecard (www.genecard.com). For the human study (CHPT 7), WBCs were extracted from normoxic human whole blood and used as the positive control for HIF1α, ALD-A, VEGF and HMOX-1. Human umbilical vein endothelial cells (HUVEC) were used as a positive control for iNOS expression, nasal polyps were used as a positive for Flt-1 and Flk-1, and a series of renal cancer cell lines were used as positive and negative controls for CAIX (Cancer Institute, Birmingham).

A spreadsheet was used to calculate volumes of reagents and the 384-well plate was designed (Table 2.1) with samples in triplicate. Analysis was carried out using Microsoft Excel.

	1 2 3	**5 6 7**	**9 10 11**
A	1:1 HK gene	1:1 G of I	1:1 HK gene + G of I
C	1:3 HK gene	1:3 G of I	1:3 HK gene + G of I
E	1:9 HK gene	1:9 G of I	1:9 HK gene + G of I
G	1:27 HK gene	1:27 G of I	1:27 HK gene + G of I
I	1:81 HK gene	1:81 G of I	1:81 HK gene + G of I
K	1:243 HK gene	1:243 G of I	1:243 HK gene + G of I
M	1:729 HK gene	1:729 G of I	1:729 HK gene + G of I
O	NTC HK gene	NTC G of I	NTC HK gene + G of I

Table 2.1 Plate design for testing primers and probes

2.6.3 Using RT-PCR with the genes of interest

Relative quantification of specific cDNA species to β-actin/18S rRNA message was carried out in a multiplex PCR on the ABI 7900 real time PCR machine (Applied Biosystems,

Warrington, UK). Desired volumes of reagents required were calculated from a prepared spreadsheet of previously chraracterised optimal conditions. The RT-PCR was performed in 384 well plates with a total volume of 6µl per well (5µl buffer and 1µl cDNA) in triplicates, with ABI PCR 2X Master mix (Roche, 58003365-01). The primers and probes to amplify up the G of I were TaqMan Gene Expression Assays (Applied Biosystems), and were used according to the manufacturers instructions. These were at a concentration of 20x with the primer being at 18µM and the probe at 5µM.

Mouse G of I (CHPT 3) were amplified in multiplex with mouse β2-microglobulin as the HK gene control. The forward primer was CATACGCCTGCAGAGTTAAGCA (conc 60µM), the reverse was ATCACATGTCTCGATCCCAGTAGA (conc 80µM) (MWG Biotech) and this had a Yakima-Yellow Black Hole Quencher 1 labelled probe (CAGTATGGCCGAGCCCAAGACCG (conc 175µM) (Eurogentec). The human G of I (CHPT 7.2.1.2) were amplified in multiplex using β-actin or 18S rRNA. β-actin was amplified using the forward primer CCTGGCACCCAGCACAAT (conc 20µM), the reverse primer GCCGATCCACACGGAGTACT (conc 70µM), and a VIC TAMRA quencher labelled probe (ATCAAGATCATTGCTCCTCCTGAGCGC (conc 100µM)). 18S rRNA was amplified using the forward primer GCCGCTAGAGGTGAAATTCTTG, the reverse primer CATTCTTGGCAAATGCTTTCG, and a Yakima-Yellow Dark quencher labelled probe (CCGGCGCAAGACGGACCAGA), all at a concentration of 500µM. RT-PCR cycling was performed as follows: 2 min. at 50°C, 10 min at 95°C, and then 44 cycles of 15s at 95°C (melting) and 1 min at 62°C (annealing/extending).

Thresholds within the logarithmic phase of the PCR for G of I transcripts and the HK gene were set and the cycle number at which the threshold was reached (Ct) was determined. Ct for the HK gene was subtracted from the Ct for G of I. The relative amount was calculated as $2^{-\Delta Ct}$.

2.7 ELISA methodology

An enzyme-linked immunosorbent assay is a technique used to detect the presence of an antibody or antigen present in a sample. All samples were run in duplicate. The underlying principle of the kits used here employ the use of the specific monoclonal antibody being pre-coated onto the microplate. The samples were then pipetted onto the plate and any protein present binds to the antibody. After washing away excess substance, an enzyme-linked specific monoclonal antibody was added to the wells and left. Following a further wash, a substrate solution was added which reacts to change colour depending on the amount of substrate present. The intensity of colour was then measured in proportion to the amount of the protein that initially bound to the antibody, using a microplate reader at 450nm, and the sample values were then read off a standard curve. The substrate in all 3 kits used in these studies was horseradish peroxidase (conjugate) and the colour reagents used (substrate solution) were a combination of hydrogen peroxidase and tetramethylbenzidine (TMB) (ELISA kits from R&D systems, see specific chapters).

2.8 Western Blot

2.8.1 Controls

Western blotting was used to determine protein expression levels under systemic hypoxia in the heart and EDL muscle. PHD2 and HIF-2α were visualised on the membrane, but visualising HIF-1α, PHD1 and PHD3 was not possible. A variety of antibodies were utilised (Table 2.2), along with using a large gel to try and detect HIF-1α as this had previously been successful with a different species, but without success. Changing the time used for transfer, the surrounding conditions and the loading volume of proteins was also tried without success. A western blot for the detection of GLUT-1, a downstream gene of HIF-1α, was also attempted without success. A variety of positive controls were tested with these antibodies. For HIF-1α, thyroid hormone-responsive rat

pituitary tumor (GC) cells ± DMOG. For HIF-2α: liver treated with carbon monoxide and without, PC12 cells (a cancer cell line derived from a pheochromocytoma of the rat adrenal medulla). For PHD1: PHD1 knockout and wild-type testis, PHD1 knockout and wild-type mouse heart, 293T extract transfected with PHD1, radiolabeled proteins were produced by IVTT (Promega) utilizing [35S]methionine and plasmids encoding the cDNA. For PHD3: spa-tagged cells (tandem affinity tag - two tags and calmodulin binding peptide separated by aTEV protease cleavage site.), PHD3 knockout and wild-type mouse heart, radioactive (hot) IVTTs.

Protein	**1° Antibodies tested**	**Concentration**
HIF-1α	NB100-479 (novus)	1:1000
	HIF-1α H-206 (Santa Cruz Biotechnology)	1:1000
	PM14 (Oxford in-house antibody)	1:1000
PHD1	NB100-310 (novus)	1:1000
	Anti-sense sera against rat PHD1 (Oxford in-house antibody - YFJK)	1:250
	Polyclonal unpurified antibody (Oxford in-house antibody)	1:250
PHD3	NB100-139 (novus)	1:2000
	NB100-303 (novus)	1:2000
GLUT-1	652-206 (abcam)	1:1000

Table 2.2 Different primary antibodies used to detect hypoxically regulated proteins

2.8.2 Solutions

Urea/SDS

120mM Tris-HCl (Sigma Aldrich, T5941) pH 6.8, 4% SDS (Sigma Aldrich L3771), 4M Urea (Sigma Aldrich, UO631), 20% glycerol (Sigma Aldrich, G8773)

0.5M Tris-HCl/0.45% SDS (pH 6.8) (see supplier as above)

1.5M Tris-HCl/0.45%SDS (pH 8.8) (see supplier as above)

2x Sample buffer (some suppliers as above)

4% SDS, 20% glycerol, 10% 2-mercaptoethanol (Sigma Aldrich M7154), 0.004% bromophenol blue (Sigma Aldrich, 114391), 0.125M Tris HCl. pH 6.8.

1x running buffer

25mM Tris base, 192Mm Glycine (Sigma Aldrich G8898), 0.1% SDS

Make up to 1L with ddH_2O

1x Blotting Transfer Buffer

25mM Tris base, 0.2M glycine, 20% methanol (Sigma-Aldrich, 179337)

make up to 1L with ddH_2O, do not adjust pH.

Coomassie stain

50% methanol, 10% acetic acid (Sigma-Aldrich, 314641), 0.1% 1g/L brilliant blue (Sigma Aldrich B6529), 40% ddH_2O

Coomassie destain

50% methanol, 10% acetic acid, 40% ddH_20,

Ponceau stain

0.1%w/v ponceau (Fisher Scientific BP103-10) in 5% v/v acetic acid

2.8.3 Urea/SDS method of total protein extraction

2.8.3.1 Tissue homogenisation

Urea/SDS buffer was added to each Eppendorf (150µl for EDL, 300µl for heart) and cooled on dry ice with the pestle and mortar. A small amount of liquid nitrogen was transferred into the mortar, the tissue ground into a fine powder and quickly transferred to the prepared tube. Tissue was homogenised with an electrical homogeniser for 3 x 10s. The solution was centrifuged for 10 min at RT at 17,900g. The supernatant was removed and re-spun for 1 min at RT. The supernatant was again removed and vortexed gently and briefly before being stored at -80°C.

2.8.3.2 Protein assay

A set of BSA dilutions of 0.1, 0.2, 0.4, 0.8, 1.6, 3.2 and 6.4µg/µl was constructed from an initial stock of 6.4µg/µl^{-1}. The protein concentration was determined using the Biorad Assay kit (Biorad, 500-0121). 5µl of samples and BSA were added to a 96 well plate in duplicates. 160µl reagent B was added to each well, followed by 20µl reagent A' (Reagent A: 1ml A + 10µl S - Biorad). This was left at RT for 15 mins and the absorbance measured at A650. A standard curve was constructed and the protein concentration calculated.

2.8.4 Western Blotting Protocol

2.8.4.1 Gel Preparation

Gels were made according to the percentage required (Table 2.3 and 2.4): 10% for PHD2 and 6% for HIF-2α. The lower percentage gel separates the larger proteins whereas the larger percentage gels separate the smaller proteins (Table 2.5). Glass plates were assembled according to the manufacturers instructions and filled up to 1cm from the bottom of the comb with resolving gel, adding the TEMED (Sigma Aldrich, T92810) and APS (Sigma Aldrich, A3678) to the solution last. This was overlaid with butanol/H_20 (2ml

for a thick gel, 1ml for a thin gel) and left for 20 min to set. Plates were tipped to one side to remove the butanol/H_2O layer, absorbing excess liquid with filter paper. The stacking gel was poured in to the top of the glass plates and the comb inserted, this being left to polymerise for 20 min. When set, the glass plates were assembled in the electrophoresis chamber (see manufacturers instructions) and 1x running buffer carefully poured into the cell to a level ensuring both electrodes were submerged. A 1ml pipette was used to eject running buffer and clear each well.

	6%	10%
Tris/HCL/SDS pH 8.8 (ml)	2.5	2.5
Acrylamide (37.5/1) (ml)	2.0	3.3
ddH_20 (ml)	5.45	4.16
TEMED (µl)	9	9
10% APS (µl)	42	42

Table 2.3 Recipe for the resolving gel

Tris/HCL/SDS pH 6.8 (ml)	1.25
Acrylamide (30/0.8) (ml)	0.65
ddH_20 (ml)	3.05
TEMED (µl)	6
10% APS (µl)	31

Table 2.4 Recipe for the 1 thick stacking gel

Percentage of acrylamide	Range of protein separation
5%	57-212kDa
7.5%	36-94kDa
10%	16-68kDa
12%	13-50kDa
15%	12-43kDa

Table 2.5 Gel percentage separation guide for protein samples

2.8.4.2 Sample preparation

Each sample was spun down before use. 10µl rainbow marker (Biorad Precision Plus protein standards 161-0374) was loaded in lane 1. The protein sample was heated at 95°C for 5 min then put on ice for 5 min, before being vortexed and spun for a final time. 50µg of protein/well diluted in 2x sample buffer was loaded, as calculated from the protein assay. The gel was run at a constant current of 40mA for around 1 h

2.8.4.3 Blotting Transfer

3 pieces of filter paper and 1 piece of Hybond-ECL polyvinyl difluoride (PVDF, Amersham, RPN1416LFP) were cut to gel size. The transfer blotting solution was made up and the fibre pads soaked in it, after washing them thoroughly in ddH_2O. The membrane was washed with methanol, rinsed 2 times with ddH_2O and finally soaked in transfer buffer. The gel plates were removed from the holder and separated. The resolving gel was cut away with a scalpel and the staking gel placed onto 1 piece of filter paper (already soaked in transfer buffer) lying on top of one fibre pad and the black side of the blotting cassette. The membrane was carefully placed on top of the gel, making sure there were no bubbles underneath. The remaining 2 pieces of filter paper were soaked and placed on top of the membrane. Any air bubbles were removed by rolling a falcon tube over the top before placing the final fibre pad on top. The cassette was closed and placed into the blotting tank, with the clear side of the cassette facing the red side of the holder in the

tank. Tank was filled with 1x blotting transfer buffer (pre-cooled) and an ice pack and run at 100V for 1 h or 20V overnight (at 4°C).

2.8.4.4 Immuno-detection

The membrane was removed from the cassette minimised in size with a scalpel. Non-specific binding was blocked by immersing in 5% milk solution (made up in 0.5%PBS-tween) for 1 h (or overnight at 4°C). The membrane was then incubated with the primary antibody diluted in PBS-tween with a 2% milk solution for 1 h at RT (or overnight at 4°C). This was then washed 3 x 5 mins in PBS-tween before being incubated with the secondary antibody diluted in PBS-tween with a 2% milk solution for 1 h at RT (or overnight at 4°C). The membrane was washed 3 x 5 mins in PBS-tween.

1ml solution A was mixed with 25µl solution B (chemiluminescence reagents, Amersham, Biosciences, RPN2109). The membrane was dried and placed onto a clear sheet with the solution on top, and a second piece of clear sheet on top. This was left for 5 min, excess liquid drained off, the membrane sealed in a plastic wrap and developed using the gel doc software on the computer. Densitometry was used to quantify the bands using a house-keeping gene such as β-tubulin.

2.8.4.5 Stripping membranes

The membrane may be stripped of bound antibodies and re-probed several times. The membrane was submerged in stripping buffer (Pierce, 46430) and incubated for 30 min at 50°C. Then wash 3 x 20 min at RT.

2.8.4.6 Coomassie staining

This stain was used to determine visually if the amount of protein loaded in each lane was equal. Membrane was immersed in the stain for 2 min with agitation. Excess liquid was poured off and rinsed with destain solution 3 times. On the final wash with destain, the membrane was microwaved for 1 min.

2.8.4.7 Ponceau stain

This is a reversible stain to determine whether the protein transfer has taken place. The ponceau stain was added to the membrane and it agitated for 2 min. It was destained with tap water.

2.9 Cell and Tissue culture

Cell culture was necessary in order to obtain enough PC12 cells (rat adrenal medulla pheochromocytoma cells) for use as a positive control in western blots.

2.9.1 Cell culture

50ml of fetal bovine serum (FBS Invitrogen-Gibco, 10091-130) was added to DMEM. 5ml of L-Glutamine (Invitrogen-Gibco, 25030164) and 5ml penicillin (Invitrogen-Gibco,15140163) was added to this and it was mixed well. Cells were thawed by immersion in a water bath. They were added to 50ml of DMEM-Hi media (Invitrogen-Gibco, 21063045) and spun for 5 mins at 110g. The cells were subsequently transferred into a flask and into the incubator.

2.9.2 Tissue Culture

The DMEM was poured out of the petri dish and wash 2x with 1xPBS (Sigma Aldrich). The petri dish was tilted onto one side to drain the remaining liquid, and any excess was removed with a pipette. 150µl buffer (SDS/urea) was added and a spreader used to distribute it around the dish. This was then transferred to an Eppendorf and vortexed for 30 secs to break the stickiness. The solution was spun for 1 min to dissipate the foam then heated at 95°C for 5 min. Finally, it was vortexed hard for 1 min and spun for a further 5 min.

2.10 Statistical Analyses

Statistics are described in text and associated legends. Statistics used in this thesis include ANOVA and Fishers or Dunnetts post hoc test, where appropriate, paired t-test, and the Mann Whitney U-test.

Chapter 3

SYSTEMIC HYPOXIA

3.1 Introduction

A low PO_2 in the air caused by ascent to high altitude, or impaired O_2 uptake due to the presence of disease causes hypoxaemia in humans (or low O_2 delivery to tissues and cells). One of the primary responses to low blood PO_2 occurs at the chemoreceptors which stimulate an increase in breathing, and this is closely followed by an increase in CO from the heart, an obligate aerobic organ. The pulmonary artery vasoconstricts, increasing O_2 delivery to well-ventilated areas of the lungs and inducing right ventricle hypertrophy. Peripheral parts of the body undergo systemic vasodilatation, mediated in part by adenosine. A similar qualitative response is assumed to occur in mice, although details may vary, for example scale-dependent changes will exist, influencing the diffusion distance for O_2, among others.

Of the three described mechanisms of angiogenic growth, splitting angiogenesis is thought to be important in hypoxia-mediated capillary growth. It has been postulated that the increase in the haematocrit (polycythaemia) could increase shear stress, initiating angiogenesis *via* the luminal side of the vessel (Deveci *et al*. 2002).

On a molecular level, HIF regulates the expression of 70 known genes on a transcriptional level (Semeza, 2004) (CHPT 1 Fig 1.1), which are responsible for aiding adaptation to the lowered availability of O_2. Although there is evidence for hypoxic induction of HIF-α mRNA levels in some cell types (Wang et al. 1995b), the predominant modes of HIF-α regulation occur post-translationally (Stolze *et al.* 2006). Under hypoxic conditions, the hydroxylation of HIF is inhibited by prolyl hydroxylases (PHD) 1-3 and factor-inhibiting HIF (FIH), allowing the α and β subunits of the protein to form a heterodimer which then translocates to the nucleus. Here it activates downstream genes by binding to the hypoxia response element (HRE) located within their promoter region.

It has been shown that PHD2 is the key O_2 sensor under hypoxic conditions (Berchner-Pfannschmidt *et al.* 2008) and is the most abundant PHD in the cell cytoplasm during normoxia. Qutub *et al.* (2007) proposed that three autocrine feedback loops determine intracellular HIF-1α levels under chronic hypoxia: PHD2, succinate (a product of HIF-1α hydroxylation by PHD2) and HIF-1α feedback, ultimately resulting in a reduction of HIF-1α availability after a period of hours, allowing the system to adapt to the hypoxia (Fig 3.1).

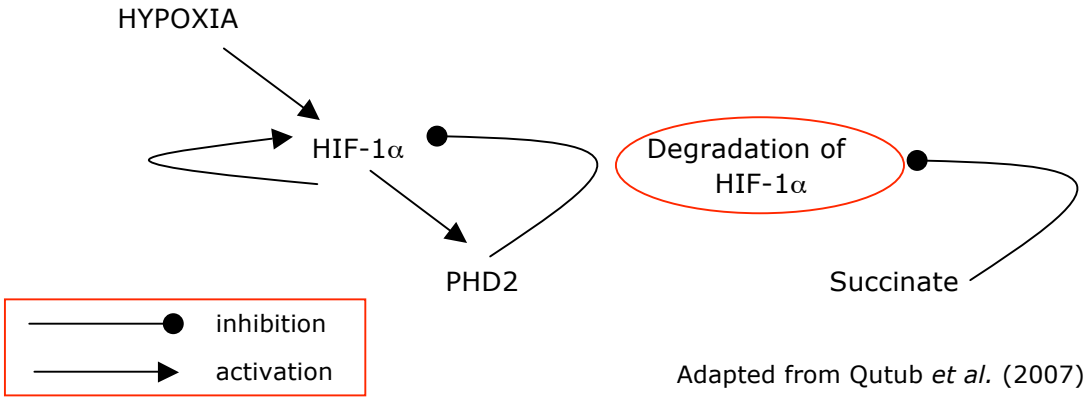

Adapted from Qutub *et al.* (2007)

Figure 3.1 Three autocrine loops determine HIF-1α expression in chronic hypoxia

A multitude of genes regulated by HIF are involved in both in the general adaptation to hypoxia, and the initiation of angiogenesis (described in CHPT 1.2.2). Many of these HIF-regulated genes exhibit inter-dependent relationships that are enhanced under normoxic and hypoxic conditions (Fig. 3.2). Taken together, these genes provide a representation of activation of pathways involved in angiogenesis, and adaptation to systemic hypoxia.

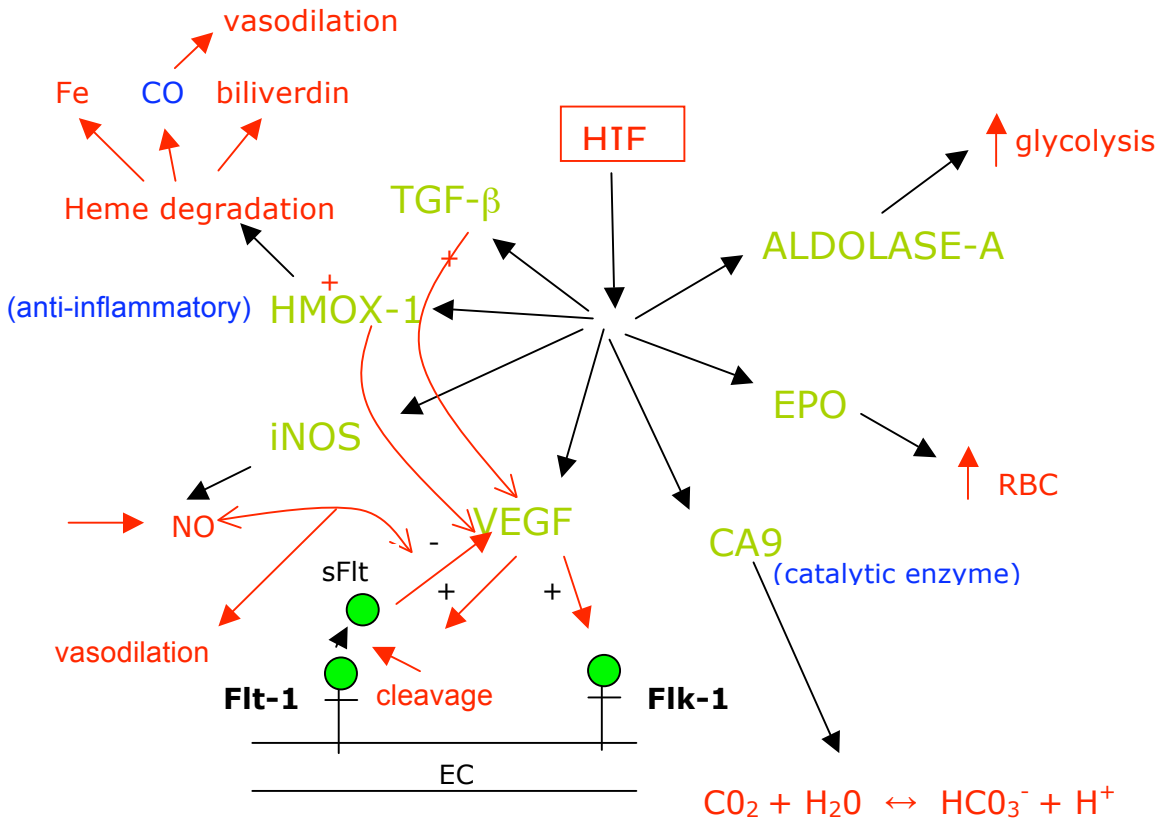

Figure 3.2 Representation of a selection of factors upregulated by HIF under hypoxia

Experiments were conducted to determine whether a hypoxic stimulus of either 10% or 12% O_2 was sufficient to induce an angiogenic response in the hindlimb, heart and diaphragm of the C57Bl6/J mouse, and whether chemical manipulation of the availability of HIF-1α using DMOG would enhance the expected angiogenic repsonse. DMOG is a cell penetrant oxoglutarate analogue which inhibits PHD 1–3 and factor inhibiting HIF (FIH), thereby increasing cellular levels of HIF protein. In response to local hypoxia (ischaemia), HIF-signalling may be enhanced by preventing its *in situ* degradation, using DMOG (Milkiewicz *et al*. 2004). Thus, we investigated whether a similar mechanism operates when the proximate stimulus is systemic hypoxaemia. Furthermore, the HIF-

regulated gene response to systemic hypoxia was studied along a time course to determine whether a common response was elicited in a variety of tissues, and furthermore to establish whether circulating leukocytes could be used as a minimally invasive marker of cellular hypoxia for use in a study of systemic hypoxia in humans (CHPT 7).

3.2 Methods

The dose of DMOG used in this study (also in CHPT 4 and 5) was based upon previous literature that had studied DMOG *in vivo* (Milkiewicz *et al*. 2004), and *in vitro* (Jaakkola *et al*. 2001). DMOG has been reported to stabilise HIF-1α at concentrations of >500 μM (Zhou *et al*. 2006), but dose-toxicity curves show that concentrations >1000μM caused disintegration of lung explants (Groenman *et al*. 2007).

3.2.1 Study design: 10%/12% normobaric hypoxia

Experiments were performed on groups of C57Bl6/J mice (n=12 in each experimental group), exposed to 12% normobaric hypoxia (a standard stimulus used widely in the literature, e.g. Mian and Marshall, 1996) with CO_2 scrubbing (carbon sequestration). Half of each group received DMOG (8mg.0.5mL^{-1} saline) (CHPT 2.1) *via* i.p. injection every other day, with the initial injection 2 days before exposure to hypoxia for 7, 14 and 28 d at 12% O_2 (5% CO_2 and 95% N_2). At the end of each experimental period, the mice were sacrificed *via* cervical dislocation, their body mass determined, and tissue samples taken: the heart was removed and total mass obtained. The atria were dissected and the right ventricle carefully isolated and weighed. The diaphragm was removed, along with the EDL and SOL muscles from the hindlimb. The tissue was stored in different ways for subsequent analysis (CHPT 2.3). The study was subsequently repeated at 10% O_2 for 14 d (initiated at 12%, then gradually reduced to 10% by the third day).

3.2.1.1 Tissue processing

Tissues were taken (CHPT 2.2) and stored at -80°C after being snap-frozen on corks in isopentane cooled in liquid nitrogen (CHPT 2.3), or directly snap-frozen in Eppendorf tubes in liquid nitrogen. Tissue was sectioned and stained (CHPT 2.3) and capillary and fibre numbers (C:F) counted as described in CHPT 2.4, using lectin staining. The number of capillaries actively undergoing angiogenesis was estimated using the lectin/VEGF/DAPI

triple stain (CHPT 2.4.2) in the diaphragm, soleus and EDL. Western blots were used as a semi-quantitative method of examining changing protein levels within the heart and EDL muscles.

3.2.1.2 Western blotting

This method was used to study the presence of HIF-2α and PHD2 in the heart and skeletal muscle of mice under differing hypoxic conditions. Attempts to study HIF-1α, PHD1 and PHD3 were unsuccessful, possibly due to technical difficulties associated with cross-species antibody reactivity. Two methods of protein extraction were attempted: total protein and nuclear extraction methods. Similar yields were produced, and the total protein extraction method chosen as it was less labour intensive. Methods are described in CHPT 2.8.

HIF-2α was detected using an in-house antibody (Oxford), PM-9. 100µg of protein was run on a thick (1.5mm) 6% gel and the membrane probed with a polyclonal primary antibody concentration of 1:1000 and a secondary antibody concentration of 1:2000. PHD2 was detected using an in-house polyclonal primary antibody (Oxford) at a concentration of 1:3000 and the secondary antibody at a concentration of 1:2000 (Rabbit Igs HRP, Dakocytomation, P0399). 50µg of protein was loaded onto a 10% gel. The PHD2 membrane was stripped and re-probed with monoclonal β-tubulin (primary antibody concentration 1:2000, secondary 1:2000) so that levels of protein could be normalised using densitometry.

3.2.2 Study design: 10% hypoxia

Experiments were performed on groups of C57Bl6/J mice (n=6 in each experimental group). Groups were exposed to 10% hypoxia for 3, 6 12, 24, 72 h and 1 week. At the end of the designated period, the mice were anaesthetised with 10mL.kg^{-1} ketamine/xylazine (ketamine: 0.1mg.kg^{-1}, xylazine: 0.01mg.kg^{-1}) and a blood sample

taken *via* the inferior vena cava (~0.8mL) to obtain a plasma sample and leukocytes for RNA extraction (CHPT 2.5). Mice were then sacrificed *via* cervical dislocation and tissue samples taken. The heart, liver, kidney, bone marrow, EDL and soleus were all removed and snap frozen in liquid nitrogen before being stored at -80°C.

3.2.2.1 Blood and tissue collection and processing

Blood was collected in a heparinised 1mL syringe. A mid-line incision was made and the intestines and liver retracted with forceps. The needle was bent at a right angle and inserted in an orientation parallel to the vein. Blood was spun for 20 min at 2700g and the plasma removed, aliquoted and snap-frozen in liquid nitrogen. It was analysed using an ELISA for mouse EPO (MEP00, R&D Systems). The pellet was resuspended in 0.16M NH_4Cl (cell lysis solution) and left for 10 min. This was spun for 5 min at 2700g, the supernatant removed and 1.5mL of sterile 1X PBS (see CHPT 2 for more details) added. The solution was resuspended with a pipette to dissolve then re-spun for 5 min at 2700g. This step was repeated, followed by a final 5 min spin at 2700g. The supernatant was removed and the leukocyte pellet frozen in liquid nitrogen. All organs were washed with PBS before being snap frozen in liquid nitrogen. Samples were stored at -80°C.

For extraction of the bone marrow, the mouse was splayed on a platform and fixed with needles, and the skin removed from both legs to expose the leg bones (femur, tibia and fibula) and muscle. Each leg was pulled at an angle to dislocate the hip from the pelvis. Bones were separated and the foot removed at the ankle joint. Incisions were made at the top and bottom of each bone, after removing any remaining bone and tissue, to expose the red bone marrow. Approximately 2 mL magnesium-free PBS was flushed through the bore of each bone and collected into a 15mL Falcon tube until bones appeared white in colour. The solution was aspirated with a 25 gauge needle and left for 5 min until debris settled. The solution was spun at 200g for 5 min (Hettich Zentrifugen EBA 12R), the supernatant removed and the pellet snap-frozen in liquid nitrogen.

3.2.2.2 RNA extraction and RT-PCR

RNA was extracted using the Qiagen RNeasy kit (CHPT 2.5) and gene expression studied using RT-PCR (CHPT 2.6). The following genes were studied, using TaqMan Gene Expression Assays (Applied Biosystems): HIF-1α (Mm00468869_m1), EPO (Mm00433126_m1), VEGF-A (Mm00437304_m1), Flk-1 (Mm00440099_m1), Flt-1 (Mm01210866_m1), CAIX (Mm00519870_m1), HMOX-1 (Mm00516004_m1), iNOS (Mm00440485_m1), TGF-β (Mm03024053_m1) and Ald-A (Mm00833172_g1).

3.3 Results

3.3.1 The effect of systemic hypoxia at 10% and 12% for 1, 2 and 4 weeks

3.3.1.1 Body mass changes

A significant 4-5% decrease in body mass was observed over the first 2 days in mice exposed to 12% hypoxia for 1, 2 and 4 wks (Fig. 3.3). After this time, the mass steadily increased to above the starting value by the end of the experimental period as mice regained their appetite and started to consume fluid again. Mice exposed to 10% hypoxia also experienced a significant decrease in body mass over 5 d, with those not receiving DMOG showing a more pronounced and significant loss compared to those receiving DMOG (Appendix A.1.2). After this time period, both groups increased mass steadily and by day 7 were back to around initial body mass. The mean starting weight ± SEM was 26.1 ± 0.262g. Refer to A.1.1 for mean mass ± SEM at 12% and A.1.2 for mean mass ± SEM at 10%. Statistical analyses were performed by ANOVA and Fishers post-hoc test was used.

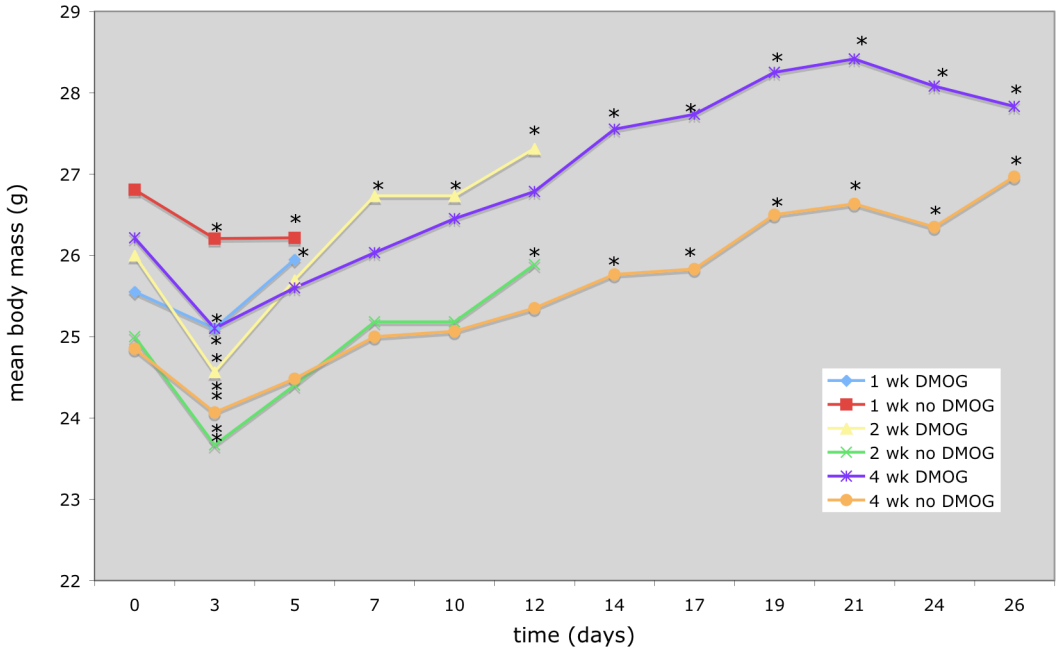

Figure 3.3 Change in body mass over time at 12% hypoxia (n=6-12 per group, *= $P<0.05$, 0 d vs days after hypoxic stimulus)

3.3.1.2 Effects of hypoxia on cardiac tissue and diaphragm

The relative total heart mass was significantly increased in all animals exposed to 10% and 12% hypoxia at 2 wks compared to control values (Table 3.1). By 4 wks, the body mass had increased beyond starting point so the effect of cardiac hypertrophy was no longer evident. See Appendix A.1.3 for right ventricle mass.

Experiment		Body mass (g)	M_H (g)	RM_H (%)
Control	(n=6)	26.0 ± 2.10	0.112 ± 0.006	0.43 ± 0.01
Control D	(n=6)	25.9 ± 1.01	0.115 ± 0.005	0.40 ± 0.01
1 wk D_{12}	(n=6)	25.1 ± 0.17	0.123 ± 0.003	0.48 ± 0.03
1 wk no D_{12}	(n=6)	25.9 ± 0.34	0.123 ± 0.002	0.50 ± 0.01
2 wk D_{10}	(n=12)	24.2 ± 0.24	0.144 ± 0.004 §	0.59 ± 0.02 §
2 wk D_{12}	(n=12)	24.7 ± 0.37	0.141 ± 0.010 §	0.54 ± 0.03 §
2 wk no D_{10}	(n=12)	26.0 ± 0.52	0.134 ± 0.004 §	0.54 ± 0.02 §
2 wk no D_{12}	(n=12)	27.3 ± 0.61	0.156 ± 0.009 §	0.61 ± 0.03 §
4 wk D_{12}	(n=6)	26.0 ± 0.52	0.122 ± 0.003	0.44 ± 0.01
4 wk no D_{12}	(n=6)	27.3 ± 0.61	0.100 ± 0.003	0.37 ± 0.02

Abbreviations: D_{10} = DMOG + 10% hypoxia, D_{12} = DMOG + 12% hypoxia, no D_{10} = hypoxia 10%, no D_{12} = hypoxia 12%, M_H = total heart weight, RM_H = relative heart weight, § = $P<0.05$ vs. control using ANOVA statistical analyses with Dunnetts post-hoc test. Mean ± standard error the mean (SEM), 'n' as stated in Table.

Table 3.1. Heart mass (g) and relative heart mass for experimental groups under hypoxia

There was no significant change in the capillary density (CD) in any region of the heart at 12% hypoxia (Table 3.2), though a significant increase in CD was found in the subepicardium and right ventricle in the hearts of mice exposed to 10% hypoxia (Fig 3.4).

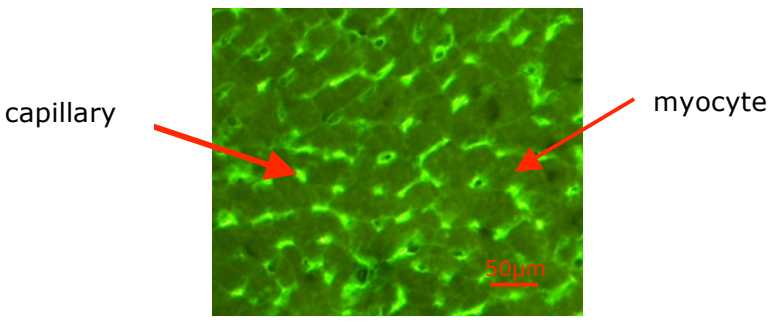

Figure 3.4 Illustration of lectin immunohistochemical staining in the subepicardium of the heart

Experiment		Subendocardium	Subepicardium	Right ventricle
Control	(n=6)	2477 ± 90	2274 ± 143	2099 ± 132
Control D	(n=6)	2564 ± 120	2321 ± 116	2085 ± 109
1 wk D_{12}	(n=6)	2498 ± 75	2812 ± 132	2168 ± 121
1 wk no D_{12}	(n=6)	2568 ± 123	2956 ± 124	2298 ± 143
2 wk D_{10}	(n=12)	2796 ± 125	3201 ± 107 §	2783 ± 52 §
2 wk D_{12}	(n=12)	2470 ± 299	2521 ± 318	2489 ± 255
2 wk no D_{10}	(n=12)	3104 ± 271	3113 ± 178 §	2819 ± 76 §
2 wk no D_{12}	(n=12)	2677 ± 324	2503 ± 685	2489 ± 674
4 wk D_{12}	(n=6)	2766 ± 152	2612 ± 211	2451 ± 98
4 wk no D_{12}	(n=6)	2745 ± 124	2549 ± 157	2844 ± 129

Abbreviations: D_{10} = DMOG + 10% hypoxia, D_{12} = DMOG + 12% hypoxia, no D_{10} = hypoxia 10%, no D_{12} = hypoxia 12%, § = $P<0.05$ vs. control. Mean ± S.E.M, 'n' as stated in Table

Table 3.2. Capillary density (cap.mm^{-2}) for heart in control and hypoxic animals ± DMOG at 10% and 12% hypoxia

There was a significant increase in the capillary to fibre ratio (C:F) of the diaphragm in mice exposed to 10% hypoxia compared to control animals, though not in those exposed to 12% (Table 3.3). There was also a significant rise in the capillary density (CD) of mice at 10% hypoxia with DMOG compared to those at 10% without DMOG.

Experiment	**C:F**	**CD** (cap.mm^{-2})	**MFA** (μm^2)
Control (n=6)	1.37 ± 0.06	1807 ± 190	775 ± 65
Control D (n=6)	1.36 ± 0.05	1856 ± 141	874 ± 58
2 wk no D_{10} (n=6)	1.41 ± 0.06 §	1591 ± 87	901 ± 67
2 wk D_{10} (n=6)	1.66 ± 0.052 §	2158 ± 123 *	808 ± 62
2 wk no D_{12} (n=12)	1.49 ± 0.08	1772 ± 87	848 ± 41
2 wk D_{12} (n=12)	1.42 ±0.03	1704 ± 103	854 ± 76

Abbreviations: D_{10} = DMOG + 10% hypoxia, D_{12} = DMOG + 12% hypoxia, no D_{10} = hypoxia 10%, no D_{12} = hypoxia 12%, § = P<0.05 vs. control. * = P<0.05 D_{10} *vs. no* D_{10}. Mean ± S.E.M. CD = capillary density, C:F = capillary to fibre ratio, MFA = mean fibre area, 'n' as stated in table.

Table 3.3. C:F and CD for control and hypoxic diaphragm ± DMOG at 10% and 12% hypoxia (2 wks)

3.3.1.3 Effects of hypoxia on hindlimb skeletal muscles

3.3.1.3.1 Lectin staining for changes in C:F, CD and MFA

There were no significant changes in the C:F (Fig. 3.5) of the extensor digitorum longus (EDL) in any of the experimental groups (Table 3.4). With the control EDL mass at 9.1 ± 0.4mg, the largest significant increase in EDL mass was seen in mice at 10% hypoxia without DMOG for 2 weeks.

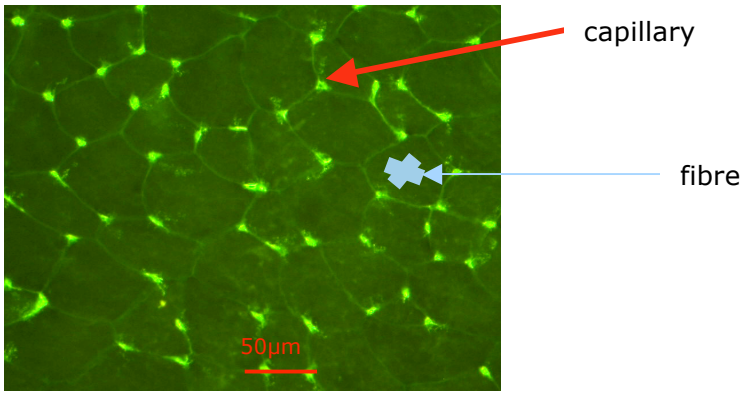

Figure 3.5 Lectin staining in the EDL muscle

Experiment	**C:F**	**CD** (cap.mm^{-2})	**MFA** (μm^2)	**RM$_{EDL}$ (%)**
Control (n=6)	1.26 ± 0.02	885 ± 67	1521 ±102	0.03 ± 0.002
Control DMOG (n=6)	1.19 ± 0.01	937 ± 118	1063 ± 86	0.03 ± 0.003
1 wk no D_{12} (n=6)	1.29 ± 0.07	833 ± 32	1755 ± 59	0.03 ± 0.009
1 wk D_{12} (n=6)	1.29 ± 0.05	803 ± 68	1678 ± 150	0.04 ± 0.001
2 wk no D_{10} (n=12)	1.29 ± 0.04	1055 ± 74	1266 ± 111	0.08 ± 0.003§
2 wk D_{10} (n=12)	1.29 ± 0.04	1157 ± 113	1154 ± 77	0.04 ± 0.005
2 wk no D_{12} (n=12)	1.35 ± 0.03	834 ± 40	1629 ± 56	0.04 ± 0.001
2 wk D_{12} (n=12)	1.37 ± 0.03	889 ± 39	1628 ± 92	0.04 ± 0.008
4 wk no D_{12} (n=6)	1.27 ± 0.01	821 ± 52	1510 ± 74	0.04 ± 0.004
4 wk D_{12} (n=6)	1.21 ± 0.04	887 ± 71	1462 ± 93	0.04 ± 0.002

Abbreviations: D_{10} = DMOG hypoxia 10%, D_{12} = DMOG hypoxia 12%, no D_{10} = hypoxia 10%, no D_{12} = hypoxia 12%, Mean ± S.E.M. CD = capillary density, C:F = capillary to fibre ratio, MFA = mean fibre area, mean ± SEM, § = $P<0.05$ as determined by ANOVA with Dunnetts post-hoc test, 'n' as stated in table

Table 3.4 Capillarity (C:F, CD), mean fibre area (MFA), relative EDL and body mass for all experimental groups subjected to systemic hypoxia

A significant increase in C:F values was observed in the soleus muscle for mice exposed to 10% hypoxia with DMOG when compared to control values (Table 3.5). There was a significant 1.3 fold increase in MFA when compared with control, in the soleus at 12% hypoxia.

Experiment	**C:F**	**CD** (mm^{-2})	**MFA** (μm^2)
Control (n=10)	1.52 ± 0.06	1229 ± 87	1272 ± 123
2 wk no D_{10} (n=6)	1.56 ± 0.05	1098 ± 96	1378 ± 95
2 wk D_{10} (n=6)	1.72 ± 0.10§	1475 ± 69	1180 ± 34
2 wk no D_{12} (n=12)	1.41 ± 0.07	984 ± 61 §	1452 ± 71
2 wk D_{12} (n=12)	1.49 ± 0.08	916 ± 31 §	1660 ± 104 §

Abbreviations: D_{10} = DMOG hypoxia 10%, D_{12} = DMOG hypoxia 12%, no D_{10} = hypoxia 10%, no D_{12} = hypoxia 12%, § = $P<0.05$ vs. control. Mean ± S.E.M. CD = capillary density, C:F = capillary to fibre ratio, MFA = mean fibre area, mean ± SEM

Table 3.5. Capillarity and mean fibre area for soleus under 10% and 12% hypoxia ± DMOG (2 wk)

3.3.1.3.2 VEGF staining

Table 3.6 illustrates a 13% increase in VEGF stained capillaries in the diaphragm after exposure to 10% hypoxia for 2 wks, alongside a 45% increase in the EDL and a 21% increase in the soleus. All of these were significant, determined using a paired t-test. Fig. 3.6 illustrates immunohistochemical staining: the red stain of the VEGF is difficult to see when combined with lectin and DAPI so is shown alone here. VEGF 'hotspots', identified as those stained significantly brighter than others, can clearly be seen. However, multi-acquisitional processing with the microscope enables efficient counting of capillaries with multiple staining.

Tissue	VEGF/LECTIN	DAPI/lectin
Control diaphragm	0.38 ± 0.02	1.02 ± 0.05
Diaphragm 10% hypoxia	0.43 ± 0.08§	1.10 ± 0.03§
Control EDL	0.25 ± 0.07	1.16 ± 0.03
EDL 10% hypoxia	0.38 ± 0.02§	1.09 ± 0.08§
Control soleus	0.34 ± 0.01	1.13 ± 0.03
Soleus 10% hypoxia	0.41 ± 0.02§	1.08 ± 0.07§

Table 3.6 Ratios for VEGF/lectin and DAPI/lectin staining in control diaphragm, EDL and soleus and at 10% hypoxia (mean of n = 4 ±SEM) § $P<0.05$, contol *vs.* 10% hypoxia as determined using a paired t-test.

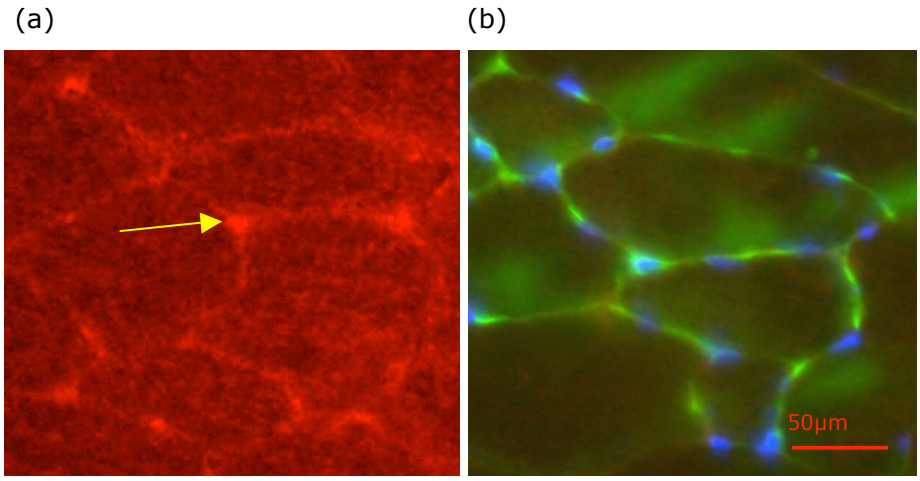

Figure 3.6 (a) Ilustration of the VEGF, and (b) DAPI and lectin immunohistochemical stain. The yellow arrow on (a) marks a VEGF positive capillary, a 'hotspot', as defined in the text above. Lectin staining for the presence of a capillary is shown in (b) with a green fluorescence, and DAPI stains blue

3.3.1.4 Changes at the protein level

It has been documented that the level of HIF protein decreases fairly rapidly following an upregulation by hypoxia (Stroka *et al*. 2001). Problems faced when trying to study the levels of HIF-1α and HIF-2α initiated a study designed to test whether detection of these proteins at 2 wks of hypoxia might not be possible. Mice were put in the hypoxic

chamber at 6% O_2 to elicit a maximal response, and tissue samples were taken from the heart and EDL after 1 and 6 h. Despite numerous attempts, using different primary antibodies, loading different amounts of protein onto the gel and using a different sized gel, detection of HIF-1α was not possible. However, HIF-2α protein, with 48% sequence homology to HIF-1α, was clearly visible both in normoxic and hypoxic heart tissue (Fig. 3.7).

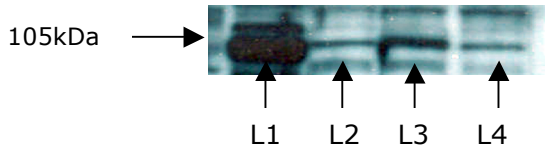

Figure 3.7 Western blot of HIF-2α. Lane 1: positive control (PC12 rat liver cells), lane 2: normoxic heart tissue, lane 3: heart tissue after 1 hour at 6% hypoxia, lane 4: heart tissue after 6 h at 6% hypoxia

An increase of 40% from control values in HIF-2α protein occurs following 1 h at 6% hypoxia, as determined by densitometry, subsequently decreasing by 15% after 6 h. This suggests that detection of the protein at 2 wks may not be possible due to the extremely low levels present, explaining why detection in any of the above mentioned experiments was not possible. PHD2 however, was shown to be present in the heart, EDL and soleus (Fig. 3.8).

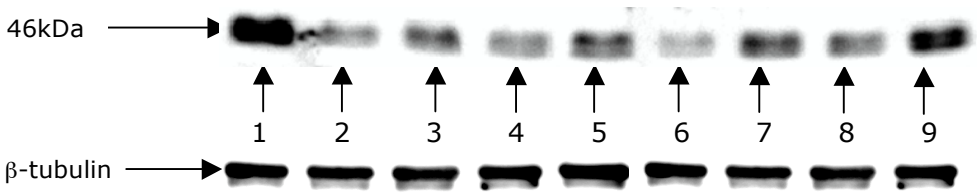

Figure 3.8 Western analysis of PHD2 in the hindlimb after 2 wks at 10% hypoxia using the gel imaging machine (UVP®), showing protein bands. Lane 1 is WT heart, lane 2 was control EDL, lane 3 EDL at 6% hypoxia after 1 hour, lane 4 EDL at 6% hypoxia after 6 h, lane 5 EDL at 10% hypoxia with no DMOG 2 wks, lane 6 EDL 10% hypoxia with DMOG 2 wks, lane 7 soleus control, lane 8 soleus 10% hypoxia with DMOG, lane 9 soleus 10% hypoxia.

Densitometry analysis (using β-tubulin as the reference protein) for the EDL from 3 mice (run twice on separate gels) was carried out using ImageJ (image analysis programme). The mean intensity of the protein band was measured and revealed the following fold

increases in PHD2 protein levels when compared to the control EDL, all values normalised to β-tubulin: EDL at 6% hypoxia, 1 h: 2x (mean±SEM, intensity of band = 105±3.4 compared control at 52.66±2.4), 6 h: 1.5x (mean intensity of 79.1±3.2), EDL at 10% hypoxia, 2 wks no DMOG: 2.3x (mean intensity of 122±4.9), EDL at 10% hypoxia, 2 wks DMOG: 0.57x (30.1±1.4). All of the changes under hypoxia for 1 and 6 h were significant when determined with ANOVA. Analysis of the soleus revealed a under 10% hypoxia with DMOG showed a slight decrease in expression of 0.7x, though a 2.6-fold increase (mean intensity of 215.2±4.9 when compared to control value of 82.8±5.2) when hypoxia alone was used, compared to control tissue, significantly increased when determined with ANOVA.

3.3.2 The effect of systemic hypoxia at 10% on gene expression and plasma EPO.

3.3.2.1 Changes in tissue specific mRNA expression under 10% hypoxia

The mRNA expression of 10 different genes was studied along 7 different time points: 0, 3, 6, 12, 24, 72 h and 1 wk (Fig. 3.9 - 3.18). Average CT illustrating gene expression is expressed along the y axis and time is in h along the x axis. Curves have been fitted by eye. *=P<0.05 when compared to control animals at time point 1, determined by Mann-Whitney U-tests.

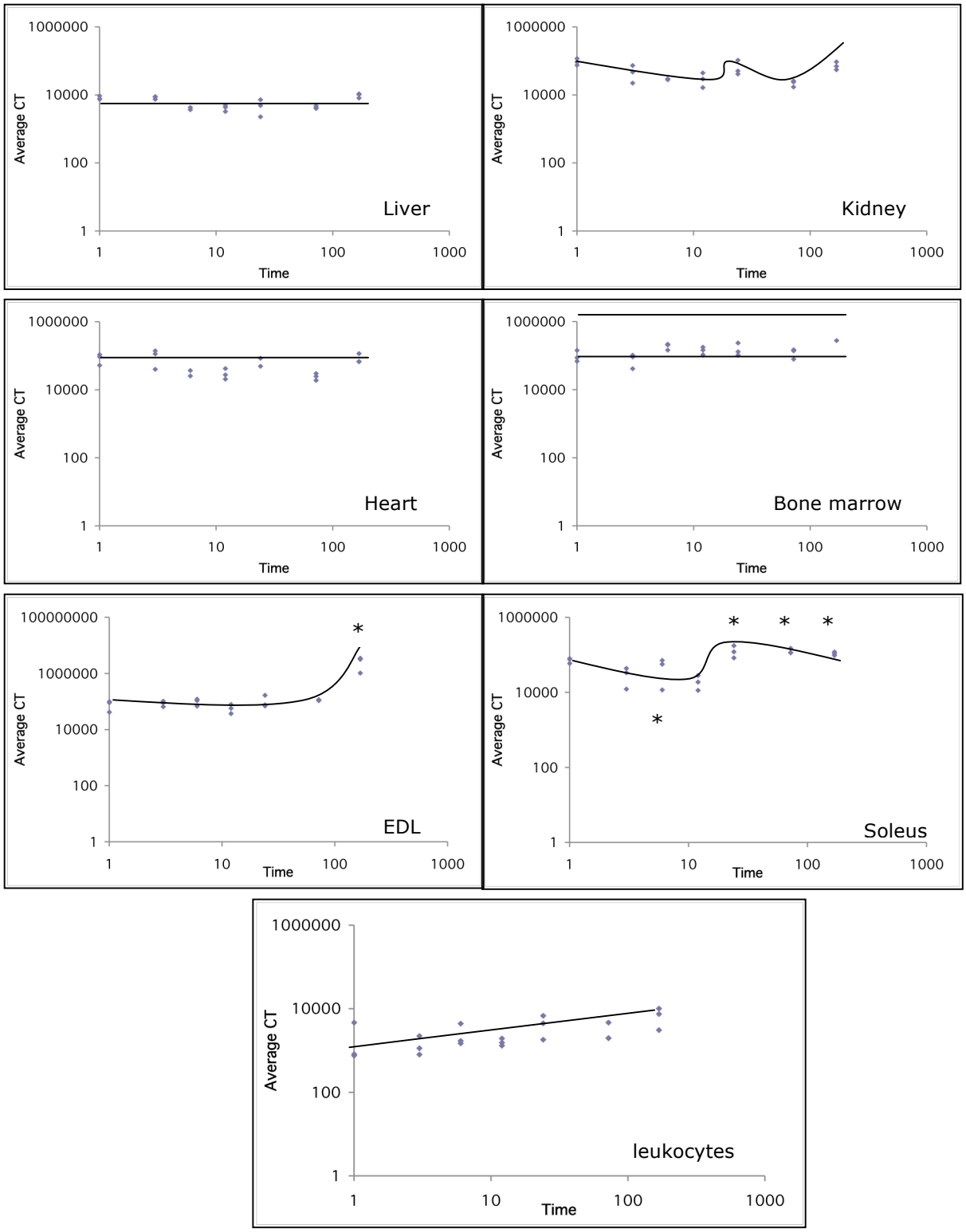

Figure 3.9 Average CT values showing HIF1α gene expression following QRT-PCR of mouse tissue from the liver, kidney, heart, bone marrow, EDL, soleus, and leukocytes after 0, 3, 6, 12, 24, 72 h and 1wk at 12% hypoxia

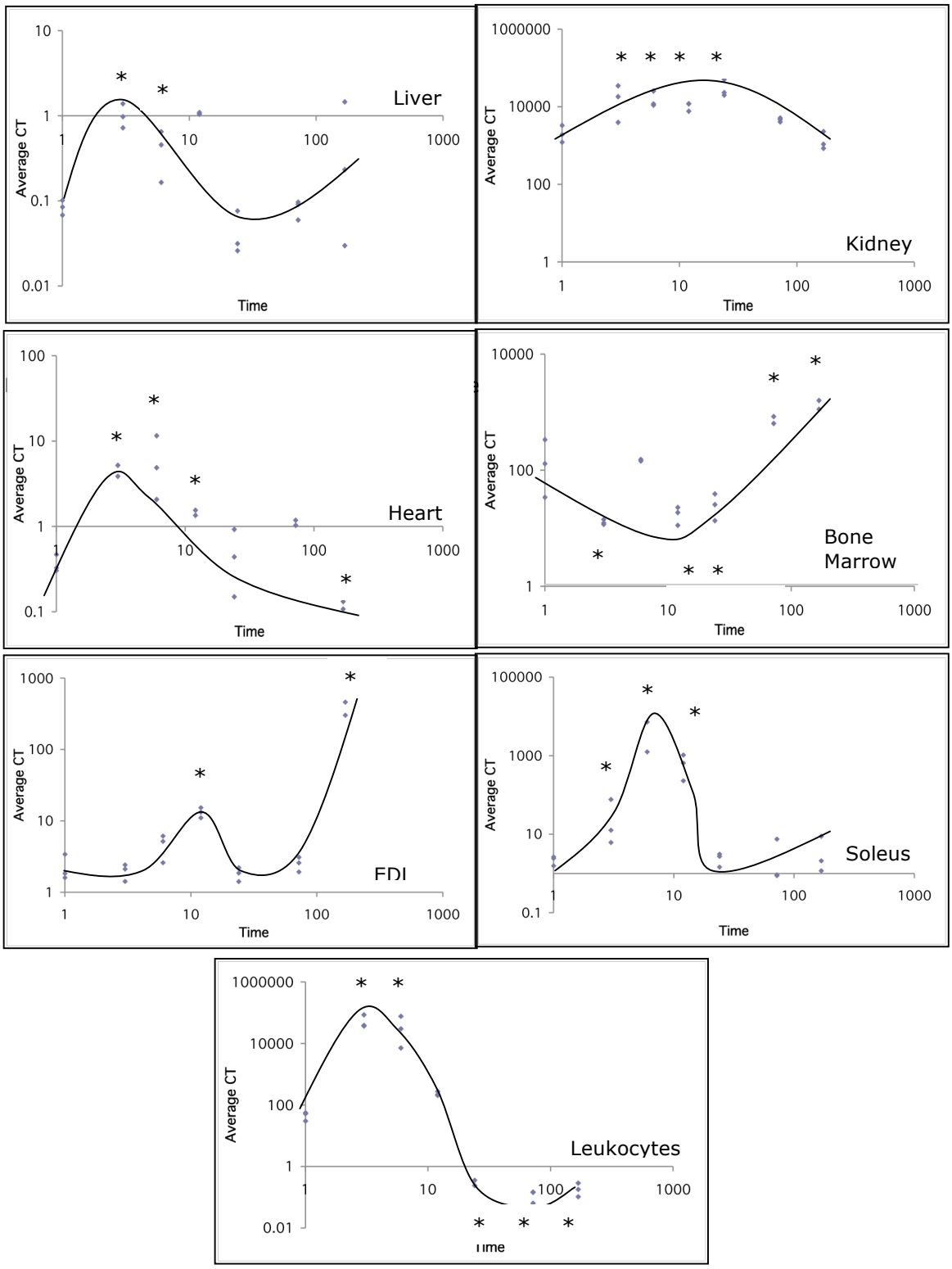

Figure 3.10 Average CT values showing EPO gene expression following QRT-PCR of mouse tissue from the liver, kidney, heart, bone marrow, EDL, soleus, and leukocytes after 0, 3, 6, 12, 24, 72 h and 1wk at 12% hypoxia (n=3)

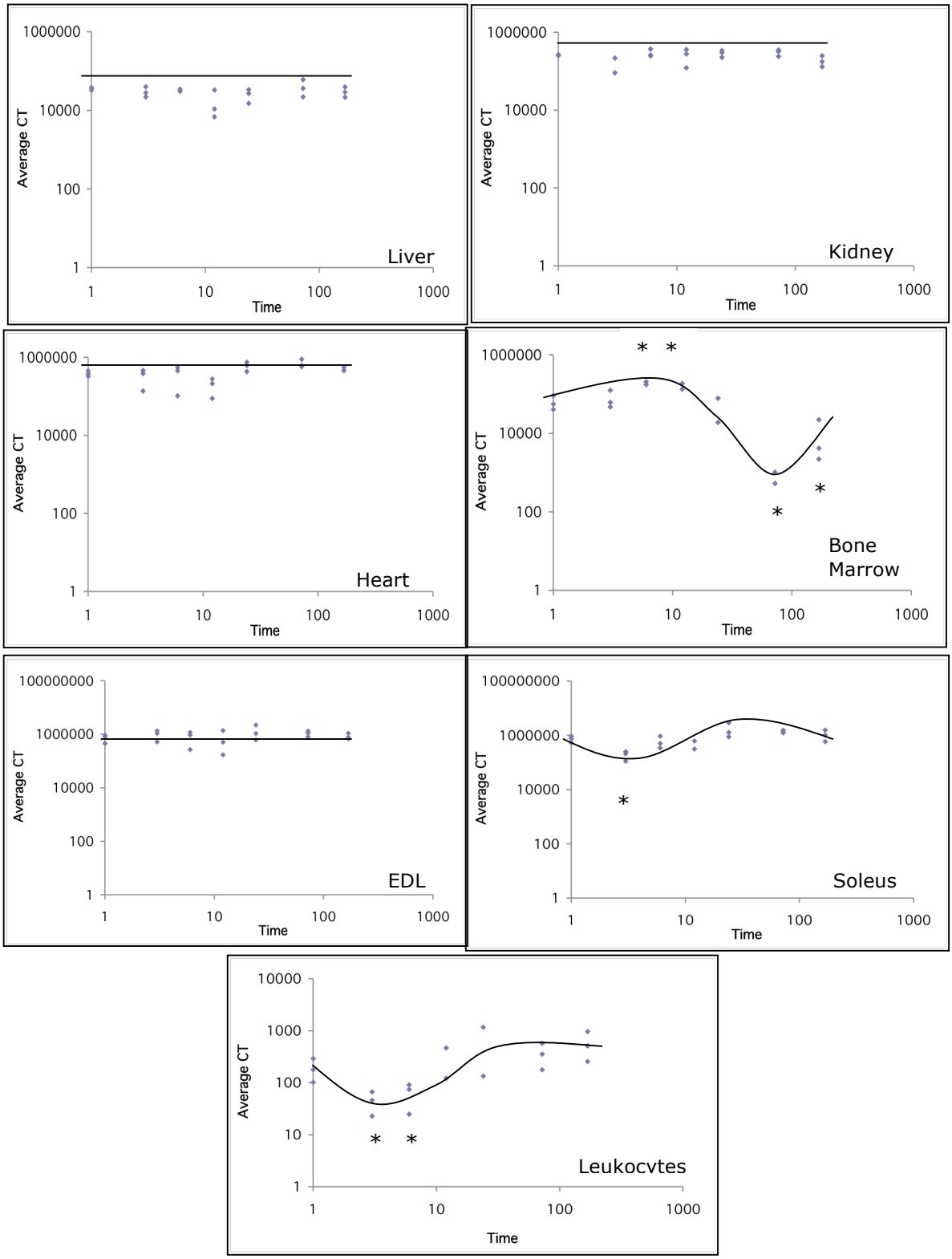

Figure 3.11 Average CT values showing VEGF gene expression following QRT-PCR of mouse tissue from the liver, kidney, heart, bone marrow, EDL, soleus, and leukocytes after 0, 3, 6, 12, 24, 72 h and 1wk at 12% hypoxia (n=3)

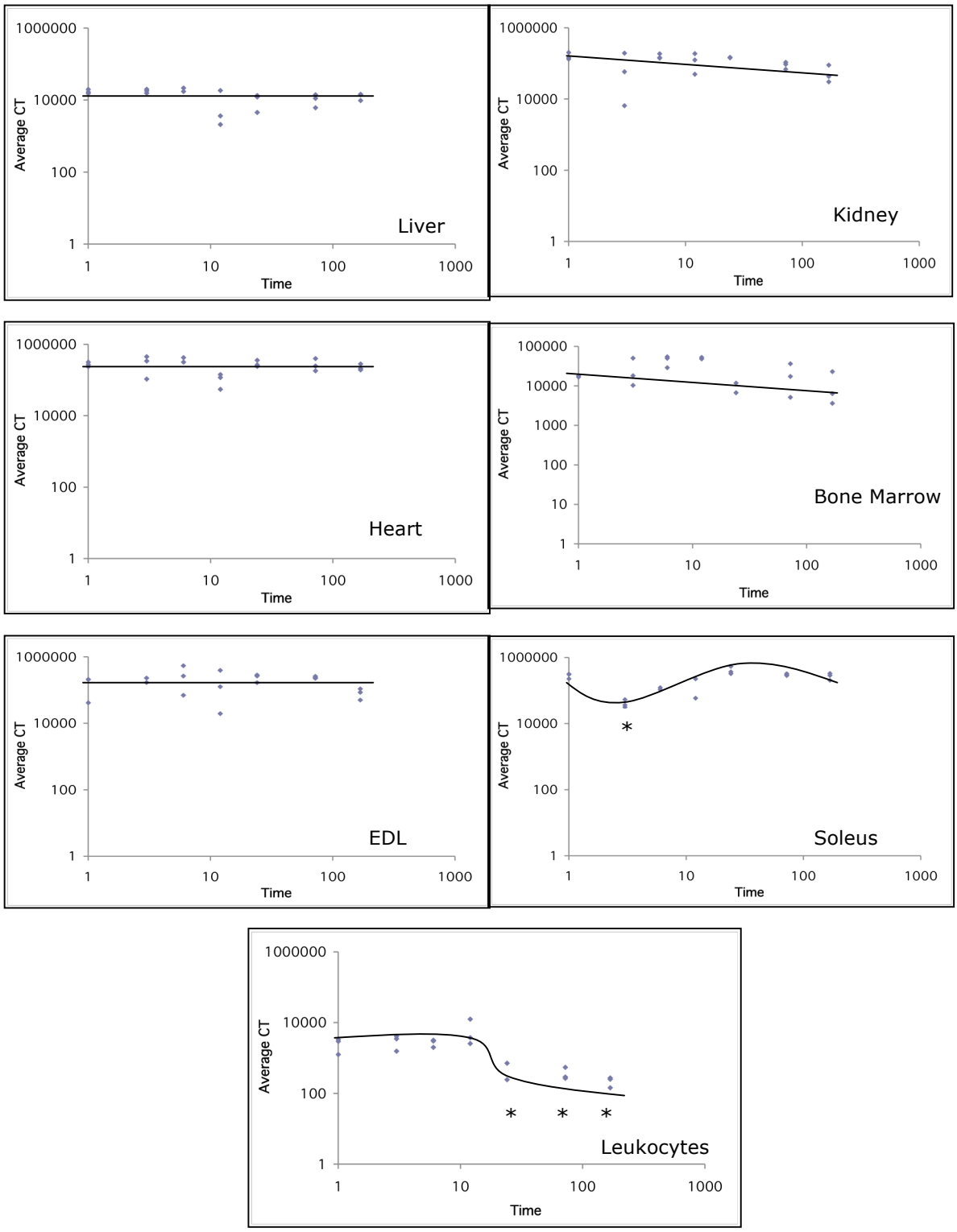

Figure 3.12 Average CT values showing Flk-1 gene expression following QRT-PCR of mouse tissue from the liver, kidney, heart, bone marrow, EDL, soleus, and leukocytes after 0, 3, 6, 12, 24, 72 h and 1wk at 12% hypoxia (n=3)

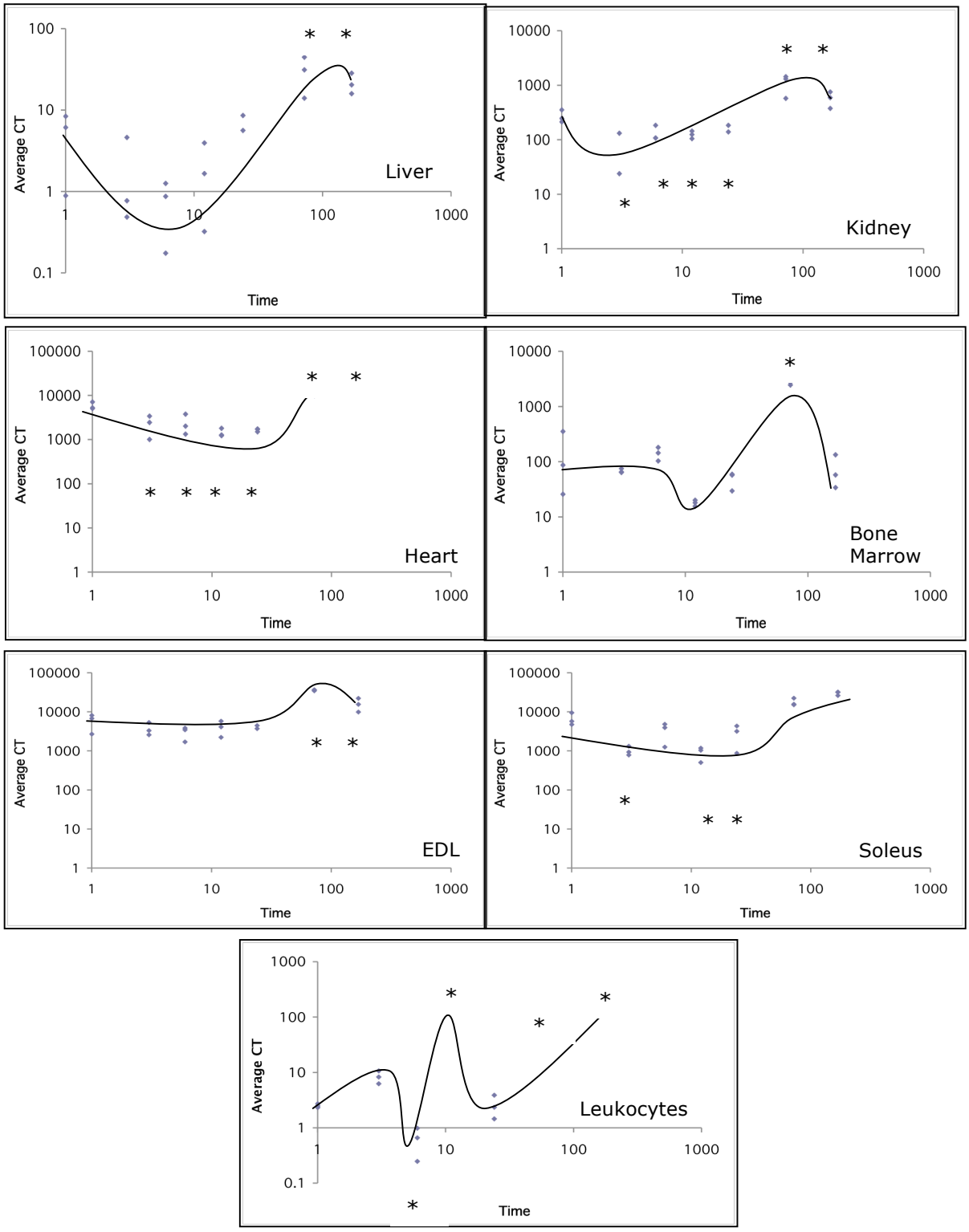

Figure 3.13 Average CT values showing iNOS gene expression following QRT-PCR of mouse tissue from the liver, kidney, heart, bone marrow, EDL, soleus, and leukocytes after 0, 3, 6, 12, 24, 72 h and 1wk at 12% hypoxia (n=3)

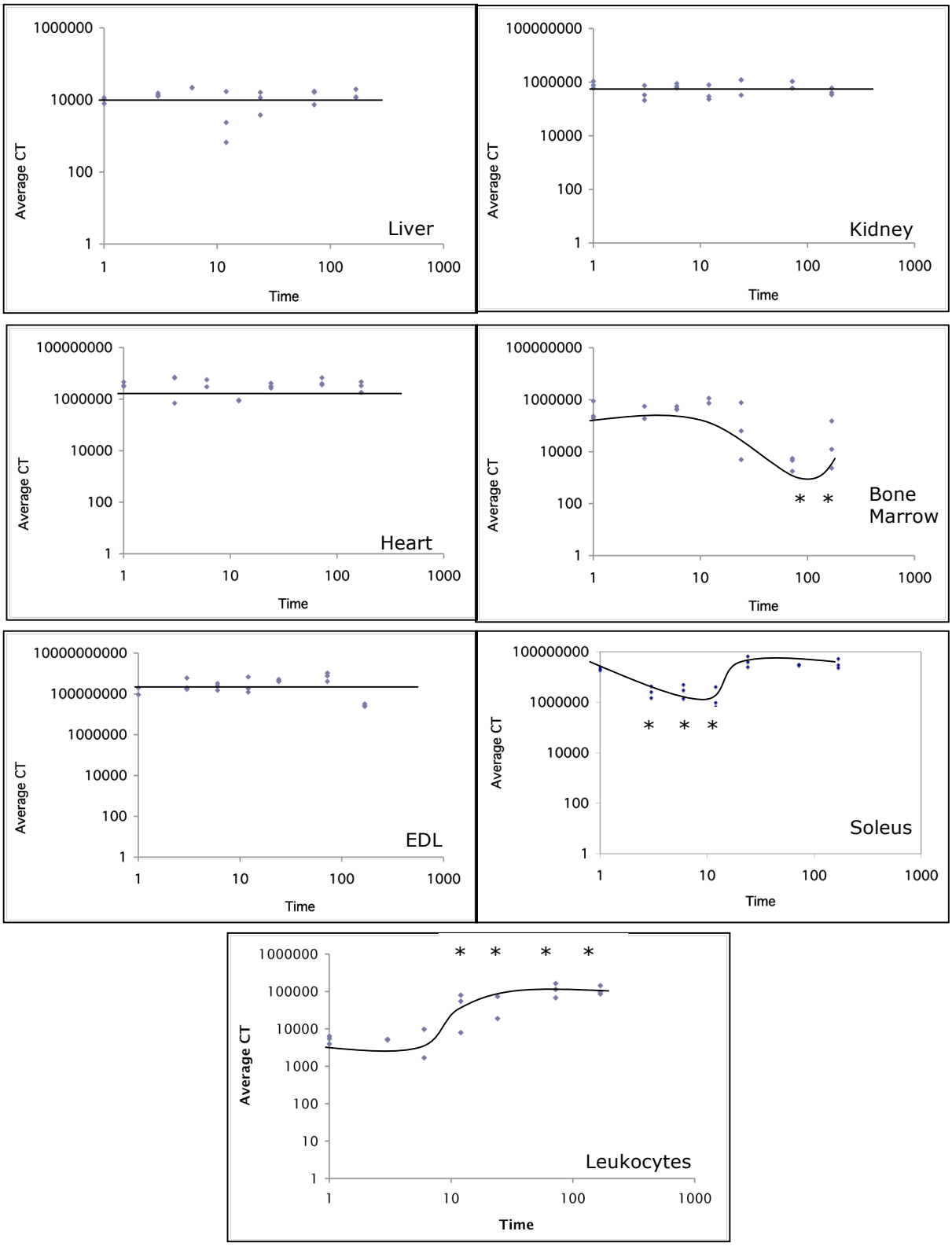

Figure 3.14 Average CT values showing aldolase-A gene expression following QRT-PCR of mouse tissue from the liver, kidney, heart, bone marrow, EDL, soleus, and leukocytes after 0, 3, 6, 12, 24, 72 h and 1wk at 12% hypoxia (n=3)

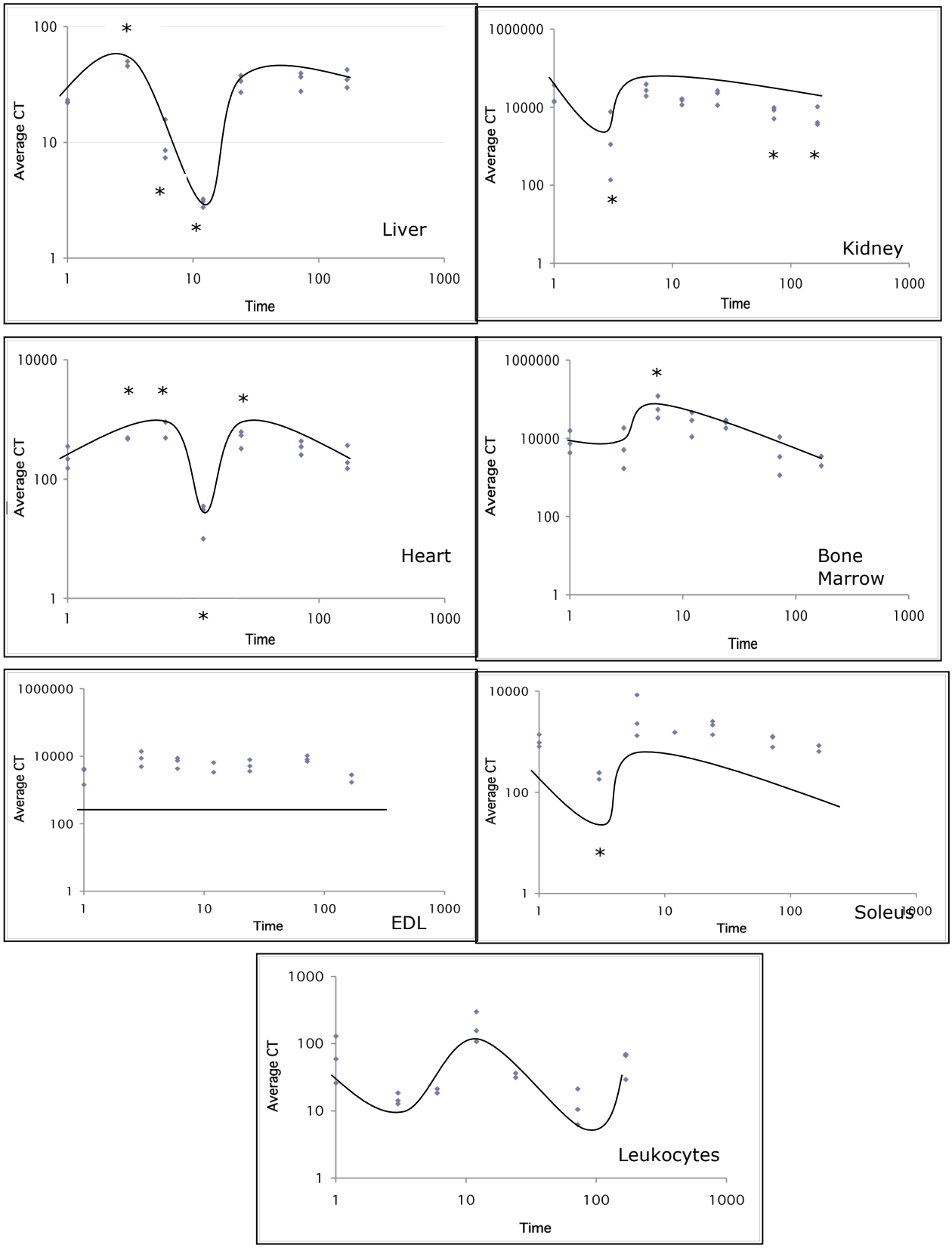

Figure 3.15 Average CT values showing CAIX gene expression following QRT-PCR of mouse tissue from the liver, kidney, heart, bone marrow, EDL, soleus, and leukocytes after 0, 3, 6, 12, 24, 72 h and 1wk at 12% hypoxia (n=3)

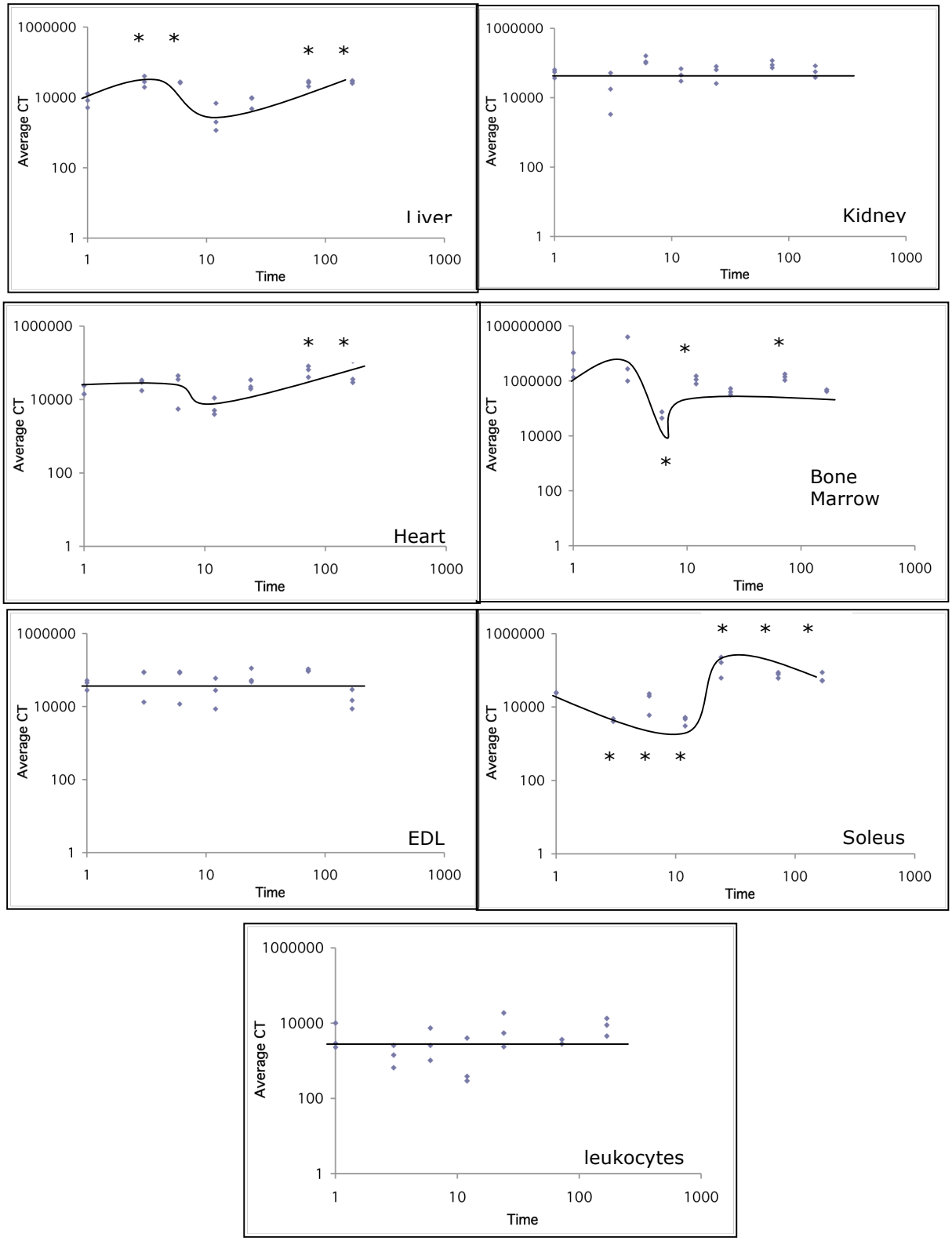

Figure 3.16 Average CT values showing HMOX gene expression following QRT-PCR of mouse tissue from the liver, kidney, heart, bone marrow, EDL, soleus, and leukocytes after 0, 3, 6, 12, 24, 72 h and 1wk at 12% hypoxia (n=3)

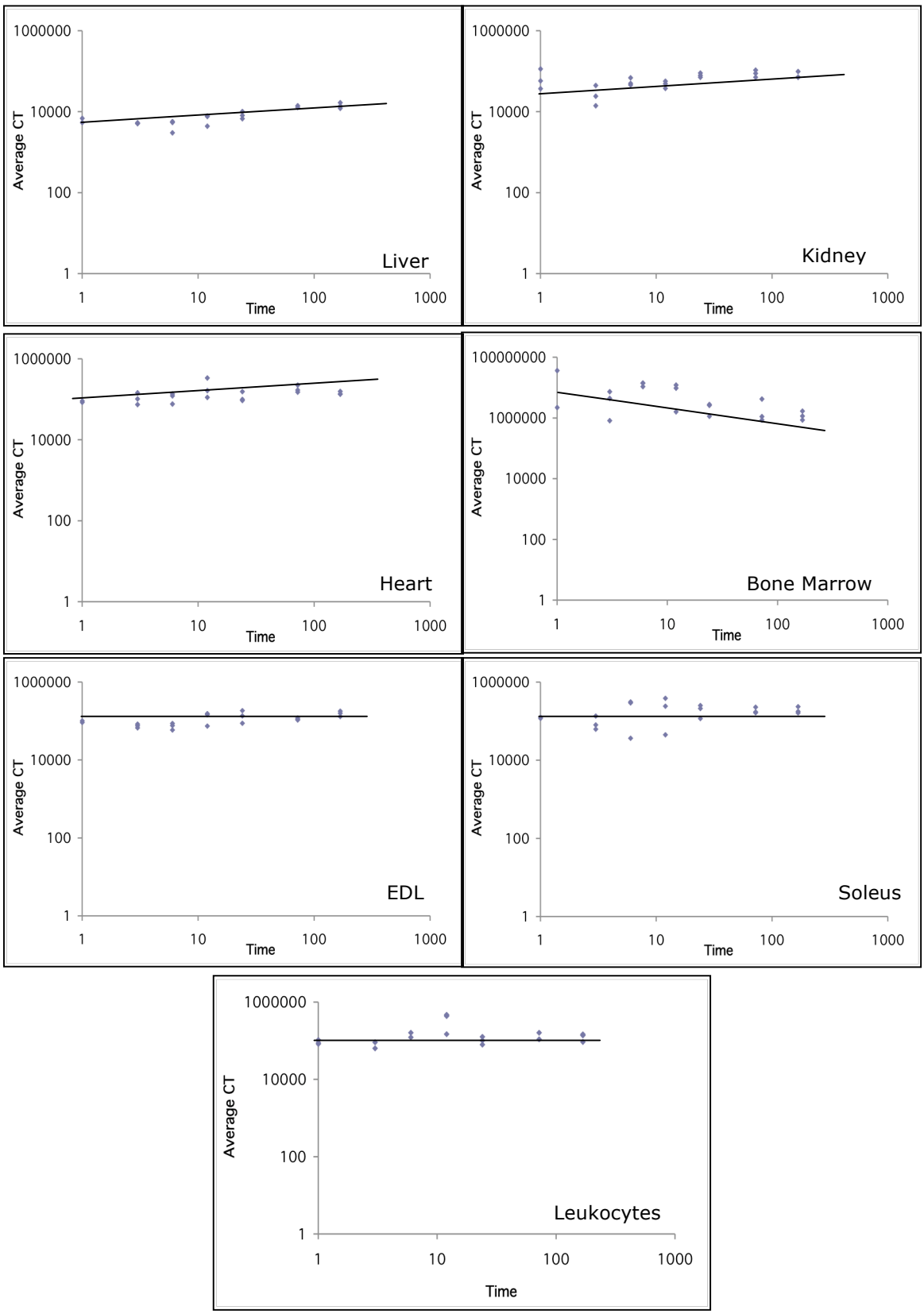

Figure 3.17 Average CT values showing TGF-β gene expression following QRT-PCR of mouse tissue from the liver, kidney, heart, bone marrow, EDL, soleus, and leukocytes after 0, 3, 6, 12, 24, 72 h and 1wk at 12% hypoxia (n=3)

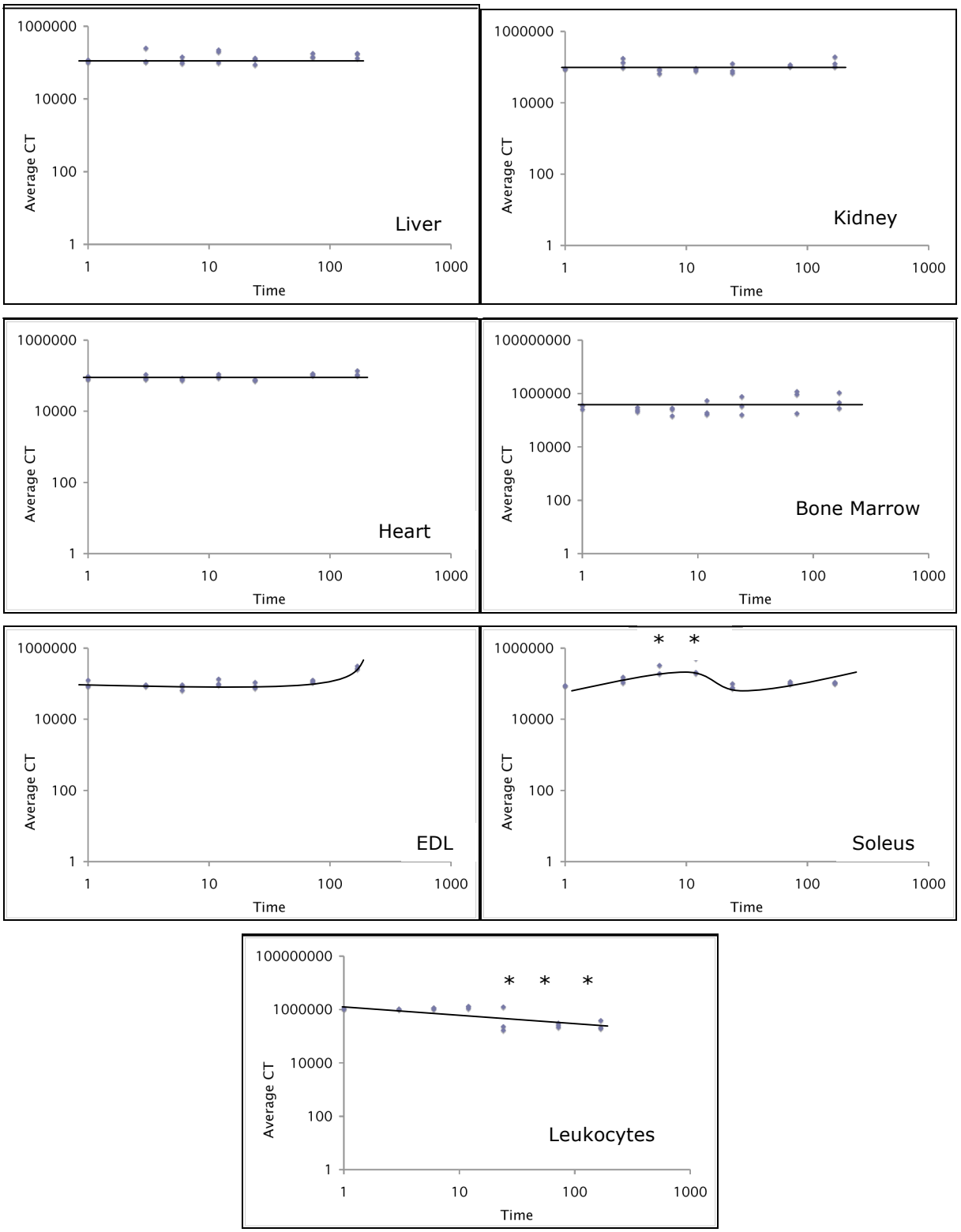

Figure 3.18 Average CT values showing Flt-1 gene expression following QRT-PCR of mouse tissue from the liver, kidney, heart, bone marrow, EDL, soleus, and leukocytes after 0, 3, 6, 12, 24, 72 h and 1wk at 12% hypoxia (n=3)

3.3.2.2 General tissue responses to 10% systemic hypoxia

Table 3.7 illustrates the overall tissue response to hypoxia for each gene studied, indicating whether there was a significant change in gene expression at any time point either in a negative or positive direction. EPO and iNOS mRNA were the only two genes showing both positive and negative changes in all seven tissues.

	VEGF	Flk-1	Flt-1	HIF	EPO	iNOS	ALD-A	CAIX	HMOX-1	TGF-β
Liver	×	×	×	×	✓	✓	×	✓	✓	×
Kidney	×	×	×	✓	✓	✓	×	✓	×	×
Heart	×	×	×	×	✓	✓	×	✓	✓	×
Bone marrow	✓	×	×	×	✓	✓	✓	✓	✓	×
EDL	×	×	×	✓	✓	✓	×	×	×	×
Soleus	✓	✓	✓	✓	✓	✓	×	✓	✓	×
Leukocytes	✓	✓	×	×	✓	✓	✓	✓	×	×

Table 3.7 Summary of significant changes observed in gene expression with individual tissues (Mann-Whitney U-tests). ✓ = significant changes observed, $P<0.05$, × = no statistical significance

3.3.2.3 Tissue-specific mRNA responses

3.3.2.3.1 HIF-1α

No discernable changes were seen across the tissue, with the exception of the EDL where a significant increase from control values was seen at 1 wk only, and the soleus which showed a significant decrease in gene expression at 12 h, followed by a significant upregulation from 24 h to 1 week.

3.3.2.3.2 EPO

Different tissues showed differing basal levels of gene expression, though all responded to the hypoxic stimulus in either a positive or negative direction. The liver, heart, soleus and leukocytes all exhibited a similar pattern, with an initial significant increase in gene expression, followed by a return to baseline values or below, by the 12 or 24 h time point. However, the fold-changes seen in each tissue were noticeably different. By 3 h, the liver had shown a 9.5-fold change, the heart a 13-fold change, the leukocytes an 800-fold change and the soleus a 4000-fold change.

The kidney had significantly raised EPO mRNA expression levels by 3 h, before showing a drop in expression to basal levels at 72 h. The BM showed an initial significant decrease in gene expression until 72 h, and the EDL experienced a significant rise by 12 h, followed by a decrease back to baseline values and then a greater than 100-fold change at 1 wk. The transcription of EPO mRNA in the kidney mirrors the initial protein response seen in the plasma (Fig. 3.18), where the highest levels were seen at 3 h.

3.3.2.3.3 VEGF

Changes in gene expression remained unremarkable in all tissues with the exception of the BM where a significant decrease in gene expression was observed at 72 h, and the leukocytes which showed a significant decrease followed by return to baseline values by

12 h. Basal levels in all tissues were within 100-fold of each other, with the exception of the leukocytes where expression levels were substantially lower.

3.3.2.3.4 Flk-1

No outstanding changes were seen other than a significant lowering of gene expression from 24 h onwards in leukocytes, and an initial decrease in expression in the soleus before return to baseline values. Lack of changes in expression correlated with unchanging levels of VEGF mRNA.

3.3.2.3.5 Flt-1

Significant changes were seen in the soleus only, with an increase in gene expression at 12 h. In correlation with Flk-1, the soleus was the only tissue where changing levels are seen, albeit reciprocal.

3.3.2.3.6 iNOS

All tissues experienced significant changes in expression, demonstrated mostly by a decrease in expression followed by a significant increase. A late response was common among all tissues, though with a wide range of basal values. The EDL was the least responsive tissue, a characteristic also observed in a variety of other genes, with a late yet significant increase at 1 wk.

3.3.2.3.7 ALD-A

Unchanged expression levels were seen in all but the BM, which experienced a significant lowering of expression at 72 h, the soleus which showed an initial decrease in expression at 3 h followed by a return to baseline levels by 24 h and the leukocytes which showed significantly raised expression levels from 12 h on.

3.3.2.3.8 Carbonic Andydrase IX (CAIX)

With the exception of the EDL, which experienced no change, gene expression was variable amongst tissues with the liver and heart showing a similar dip in expression at 12 h, though absolute levels of expression differed, as seen with other genes.

3.3.2.3.9 HMOX-1

The liver, heart, and BM exhibited a similar pattern of expression, with an initial increase then a slight dip, followed by rising levels until the final time point. The soleus showed a significant decrease at 6h followed by a significant increase at 24 h. Changes in the remaining tissues were unremarkable.

3.3.2.3.10 TGF-β

No changes in gene expression were seen across any tissue at any time point.

3.3.2.4 Plasma EPO expression under hypoxia

Plasma EPO levels increased rapidly by 3 h, and fell thereafter (Fig. 3.19). Protein levels at 3, 6, 12 and 24 h were all significantly raised compared to control values.

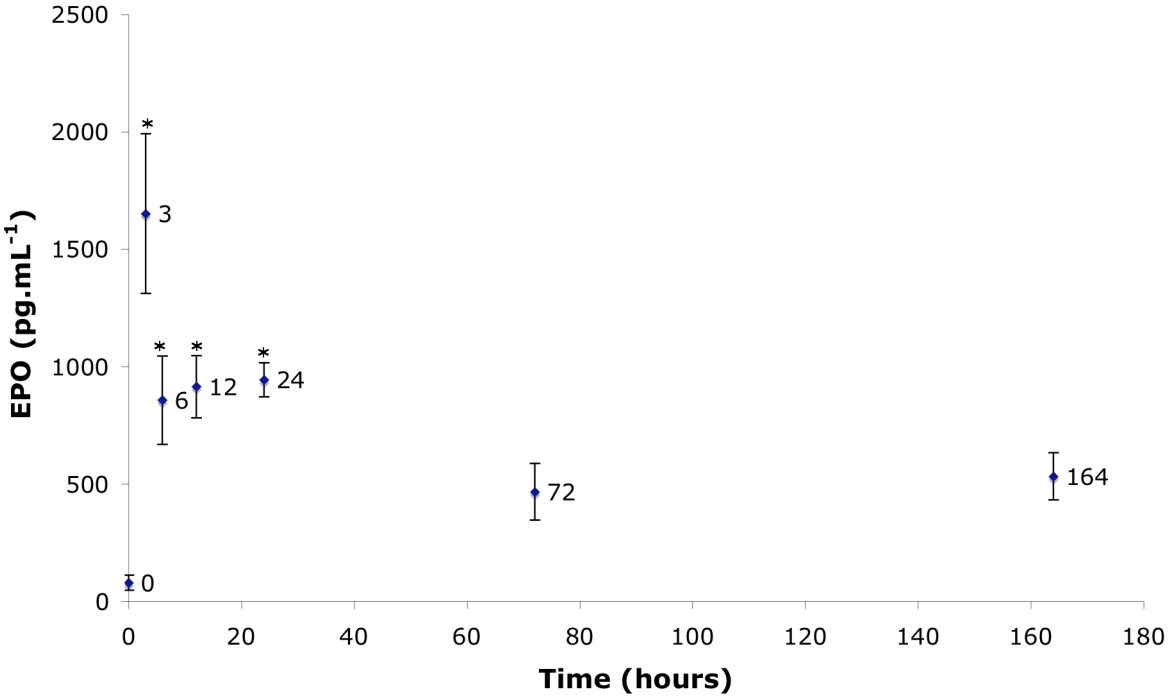

Figure 3.19 Plasma EPO levels as shown at control (0), 3, 6, 12, 24, 72 h and 1 wk at 10% O_2. (* = *P* <0.005) as determined using ANOVA with Fishers post-hoc test. (n=3 per group)

3.4 Discussion

This study was designed to determine whether a stimulus of 10% or 12% hypoxia was sufficient to induce angiogenic growth in the heart, diaphragm and hindlimb muscles of the C57Bl6/J mouse, and whether chemically manipulating the stability of HIF using DMOG could further enhance this response. In response to local hypoxia (tissue ischaemia) it has previously been demonstrated that HIF-signalling may be enhanced by preventing its *in situ* degradation using DMOG (Milkiewicz *et al*. 2004). This study therefore addressed the question of whether a similar pathway was operating under systemic hypoxaemia. The study also aimed to determine the response of a range of HIF-regulated genes under systemic hypoxia, over a defined time course, and to determine whether circulating leukocytes could be used as a suitable indicator of gene expression under these conditions.

3.4.1 Physiological effects

3.4.1.1 Changes in body mass

All animals showed an initial decrease in body mass (over the first 3 d at 12% and 5 d at 10%) followed by an increase as they began to acclimatise to the hypoxic environment. Animals were studied whilst in the hypoxic chamber and shown to be extremely lethargic compared to normoxic animals, both in the light and the dark. This hypokinetic state was probably in response to an inability to increase O_2 supply sufficiently to match tissue O_2 demand. This rapid loss in body mass may have been due to dehydration and hypophagia because, as shown, body mass rapidly returned to starting point and beyond when the appetite had returned, on acclimatisation. The subsequent increase in body mass from these time points reflects the initiation of chronic responses to sustained hypoxia to aid acclimatisation, such as the upregulation of genes controlled by HIF-1, for example EPO (increased RBC production), glucose-transporters GLUT1 and 3 (increasing glucose transport and therefore metabolism), and VEGF (angiogenesis).

3.4.1.2 Mechanical stretch effects in the heart and diaphragm

3.4.1.2.1 Cardiac hypertrophy

Hypoxia at both 10% and 12% O_2 for 2 wks was an adequate stimulus to cause cardiac hypertrophy, a response enabling the heart to maintain a normal stroke volume despite an increased afterload (Morgan and Baker, 1991). The pulmonary arteries are extremely sensitive to changing O_2 levels and immediately contract on detection of a lowered O_2 (Julian, 2007). In response to the increased resistance in the vessel, primarily the right ventricle, and to a lesser degree the left, undergo physiologic hypertrophy. Pressure-overload induced hypertrophy involves multiplication of the number of contractile muscle units resulting from an increased protein synthesis (Matsuo *et al.* 1998). This results in an increased wall thickness and concentric hypertophy, athough the heart does not enlarge *per se* (Grossman *et al.* 1975).

Volume-overload induced hypertrophy may also play a role: hypoxia causes an increase in the volume of circulating blood. Splenic contraction is responsible for the initial rise in haematocrit, due to sympathetic stimulation as a response to low PO_2 in the blood (Kuwahira *et al.* 1999). In the longer term, this increased O_2-carrying capacity is supplemented by erythropoietin (EPO) which is released from the kidney cells and causes an increase in the production of RBCs. Klausen *et al.* (1991) found that that RBC counts had increased 4 days post-altitude. The increased volume of blood not only increases the pressure-overload on the system, but volume-overload-induced hypertrophy also comes into play. This results in repetition of sarcomeres in series, increasing mycoyte length and therefore chamber size, *via* eccentic hypertrophy (Grossman *et al.* 1975), resulting in enlargement of the whole heart (Fig. 3.20). However, it is important to bear in mind that exposure to hypoxia generally also causes dehydration, reducing plasma volume (Bartsch and Saltin, 2008) and causing an increase in the viscocity and thus force required by the heart to pump blood. It is therefore likely that a combination of

both pressure- and volume-overload hypertrophy have caused the observed enlargement of the heart.

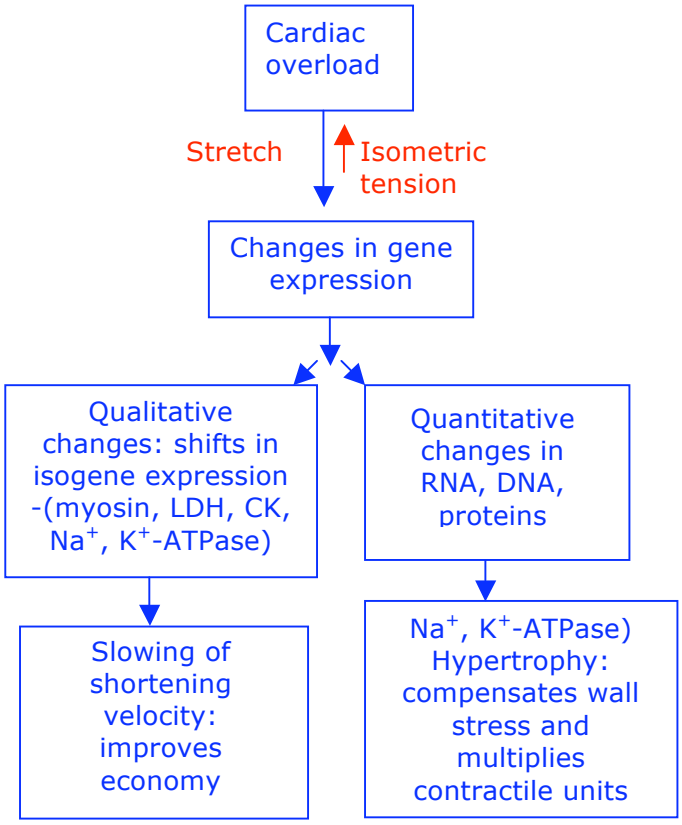

Figure 3.20 Changes in cardiac gene expression occuring in response to chronic mechanical overload (From Swynghedauw, 1989)

3.4.1.2.2 Angiogenesis in the heart and diaphragm

Cardiac angiogenesis has a critical involvement in the adaptive mechanism of cardiac hypertrophy (Sano *et al.* 2007). The wide array of factors acting on the heart are likely to result in angiogenesis: mechanical stretch may be responsible for the angiogenesis seen in the right ventricle and the subepicardium, resulting in sprouting angiogenesis, and hyperaemia (initiated by hypoxia) results in an increase in tissue metabolites

followed by an increase in blood flow and vasodilatation, and this may cause vessel splitting through an increase in shear stress.

According to the LaPlace relationship, wall tension (T) is proportional to the product of intraventricular pressure (P) and ventricular radius (r), expressed by the following equation (Klabund, 2004).

$$T \alpha P.r$$

It can be extrapolated from this that the wall tension experienced by the subepicardium will be greater than that imposed on the subendocardium (as it is further away from the centre of the ventricle), and also as a result of the curvature of the ventricle (Fig. 3.21). Due to the increased wall tension experienced in the outer wall of the heart, a greater amount of stretch-induced angiogenesis could be expected to occur in the subepicardium.

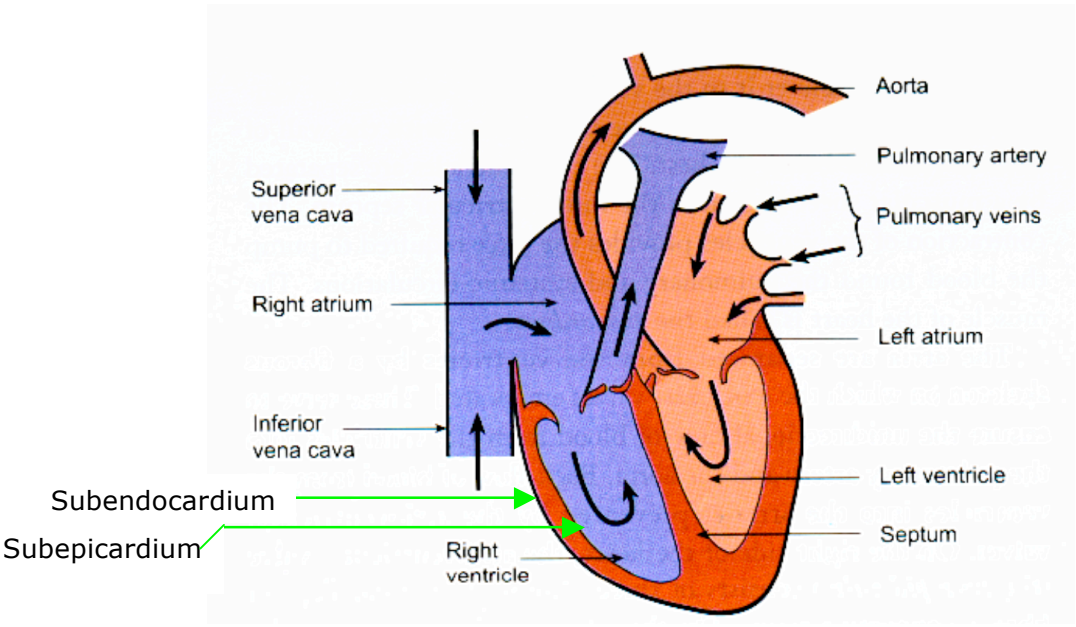

Figure 3.21 Illustration of the increased distance to the subepicardium compared to the subendocardium from the centre of the ventricle, thus an increased wall tension (From Pocock and Richards, 2006)

The C:F of the diaphragm also increased significantly under 10% hypoxia. The carotid body is sensitive to the partial pressure of O_2 in the arterial blood (Gonzalez *et al.* 1992) and, on hypoxic stimulation, releases dopamine. This enhances the action potential frequency in the sensory fibres of the carotid sinus nerve, resulting in an increase in the respiration rate and an increase in blood flow in the diaphragm (Mochizuki-Oda *et al.* 1997). In addition, the increased depth of breathing associated with exposure to hypoxia may be responsible for providing the mechanical stretch required to induce an increase in capillarity.

3.4.1.2.3 Induction of HIF under hypoxic and non-hypoxic conditions

There is growing evidence that the up-regulation of HIF-1 is not limited solely to hypoxic stress but can be induced by growth factors, cytokines, hormones and nitric oxide, along with mechanical factors (Richard *et al*. 2000). Milkiewicz *et al*. (2007) showed that HIF-1α mRNA level can be increased in non-hypoxic endothelial rat cells by mechanical stretch, confirming the *in vivo* data of Williams *et al.* (2006). However, it is well known that HIF-1α is post-translationally regulated under hypoxia (Brahimi-Horn *et al.* 2005; Kaelin and Ratcliffe, 2008). Kim *et al.* (2002) found that HIF-1 protein plays an important role in the induction of VEGF in non-ischaemic and mechanically stressed myocardium of the rat, being regulated by stretch-activated channels ($Gd3^+$-sensitive stretch-activated cation channels). Furthermore, Sano *et al* (2007) showed how pressure-overload, following severe transverse aorta constriction in the heart, promoted vascular growth by HIF-1-dependent induction of angiogenic factors. HIF-1α was increased from day 3 and when using HIF-1α conditional knockout mice, caused a significant decrease in the angiogenic response and maladaptive hypertrophy during chronic pressure overload. These data suggest that angiogenesis seen here may be due to stretch-induced HIF-regulated angiogenesis.

Whether hypoxia plays a role in the induction of angiogenesis seen in the heart is still to be determined. As a result of cardiac hypertrophy, an increase in the diffusion

distance from capillaries to muscle fibres occurs, resulting in a reduced O_2 supply within the myocardium (Sano *et al.* 2007) and thus a stimulus for the hypoxic induction of HIF. The effect of exercise on capillary growth in skeletal muscle has been well studied (Bigard *et al.* 1991; Abdelmalki *et al.* 1996). The resulting tissue PO_2 determined under conditions of physical activity in skeletal muscle (3-4mmHg, Wagner, 2001) provides strong evidence for the induction of HIF under hypoxia. Whether the PO_2 in active cardiac tissue reaches these low levels remains unknown. Thus, a combination of both mechanical stretch and hypoxia may be responsible for initiating the upregulation of HIF under chronic systemic hypoxia, leading to the observed cardiac angiogenesis.

3.4.1.3 Effects of hypoxia in the hindlimb

3.4.1.3.1 Hypoxia failed to elicit significant angiogenesis

Hypoxia at 10% or 12% failed to elicit any significant angiogenesis in the EDL with or without DMOG. However, 10% hypoxia + DMOG was sufficient to increase C:F values in the soleus. These findings are consistent with a number of studies that have failed to show an increase in capillarity with systemic hypoxaemia alone in phasic muscles such as the EDL, though have shown significant increases in the C:F in muscle with predominantly oxidative fibres such as the soleus. However, there is much controversy associated with the latter finding. A similar degree of hypoxaemia to that used here (12%) induced angiogenesis in the soleus muscle of the rat after 3 wks (Deveci *et al*. 2001), although a longer exposure period of 6 wks induced regional capillarity in all skeletal muscles studied (Deveci *et al.* 2002). Snyder *et al. (*1985) found no change in the C:F in the gastrocnemius and diaphragm muscles of rats exposed to hypoxia for 5 wks, and similarly, Hoppeler *et al.* (1990) found no change in the C:F of human M. vastus lateralis in subjects exposed to >5000m (~11%) for 8 wks. However, Olfert *et al* (2001) found that a stimulus of 12% O_2 for 8 wks was sufficient to increase the C:F of the gastrocnemius muscle of the rat, the above studies illustrating the varying responses seen.

One of the main issues noted in a hypoxic environment is that the animals become fairly immobile with lethargy. The EDL is composed of mixed fibre types and is a phasic muscle, thus only used when needed. Thus, conditions rendering the animal hypoxic and lethargic may not be sufficient to induce a sufficient degree of oxidative stress, nor the level of physical activity required for the stimulation of angiogenesis. Being a mixed fibre type with a lower density of capillaries and mitochondria when compared to an oxidative fibre type, the EDL may be less sensitive to changes in the PO_2 of the surrounding environment and thus more likely to withstand changes in O_2 delivery. Thus, a combination of a lack of movement and an insufficiently low blood PO_2 suggest that threshold levels required to stimulate the pathways leading to angiogenesis in the EDL were not reached.

The soleus is composed mainly of slow twitch oxidative fibres, with a large number of mitochondria and a high amount of myoglobin, along with a dense network of capillaries. It functions in postural support and therefore is constantly active. This investment in systems to maximise O_2 diffusion suggests that the PO_2 gradient is more critical here, with an increased sensitivity to changes in O_2 levels, resulting in greater changes in the capillary supply as shown.

3.4.1.3.2 Exercise and hypoxia

The results of this study suggest that an additional stimulus to hypoxia is needed to reach the angiogenic threshold in a mixed muscle such as the EDL. However, studies under conditions of both cold and hypoxia have still only shown changes in the capillarity of oxidative fibres such as the soleus (Banchero *et al.* 1985; Suzuki *et al.* 1997). The additional stress of exercise on top of hypoxia culminates in remodelling of the skeletal muscle in some studies (Bigard *et al.* 1991; Abdelmalki *et al.* 1996; Wagner, 2001, Prior *et al.* 2003). This, however, is another area of controversy, as other studies have shown no change in the capillarity after episodes of intense training at altitude (Truijens *et al.* 2003; Ventura *et al.* 2003). Care must be taken when interpreting studies that have not

accounted for changing fibre size with exercise and hypoxia. Atrophy or hypertrophy of the muscle fibres, experienced under hypoxia or exercise respectively, will both lead to changes in capillary density, thus reflecting the change in functional capillarity but not necessarily a change in capillary growth.

3.4.1.3.3 Lactic acid and haemodynamics

It has been shown that catecholamines, released from the adrenal medulla in response to sympathetic nerve activation by hypoxia, stimulate lactate production in skeletal muscle (Qvisth *et al.* 2008). The influence of catecholamines on the local blood flow in skeletal muscle is a controversial issue, however. Studies have suggested vasoconstriction, vasodilatation, or no vascular reaction (Kurpad *et al.* 1995; Clark *et al.* 1995). Haemodynamic changes caused by lactic acid could therefore be another factor responsible for either the capillary changes shown in the soleus muscle or for the lack of capillary growth seen in the EDL muscle. In respect to our model, if vasodilatation was induced by lactic acid accumulation, the resultant vasodilatation-induced shear stress may be responsible for switching on angiogenesis in the soleus. This is because it will be working harder under hypoxia compared to a phasic muscle (such as the EDL) due to its tonic activity.

3.4.2 Confounding factors

3.4.2.1 The threshold for HIF induction

Elucidating the actual threshold at which HIF is induced *in vivo* has proven difficult. In tissue cultures, HIF-1 activity has been shown to be extremely variable from one cell line to another, though studies have shown that maximal HIF-activation occurs at 0.5% O_2 (Rosenburger *et al.* 2005), and half-maximal activation is found at 1.5-2% O_2, corresponding to PO_2 values of about 10 to 15 mm Hg (Jiang *et al.* 1996). Ji *et al.* (2007) have shown threshold levels for inducing VEGF in myocytes (Fig. 3.21), and from this it may be possible to estimate levels at which HIF may be induced as it, along with

other stimuli such an inflammatory factors, is responsible for switching on VEGF under hypoxia.

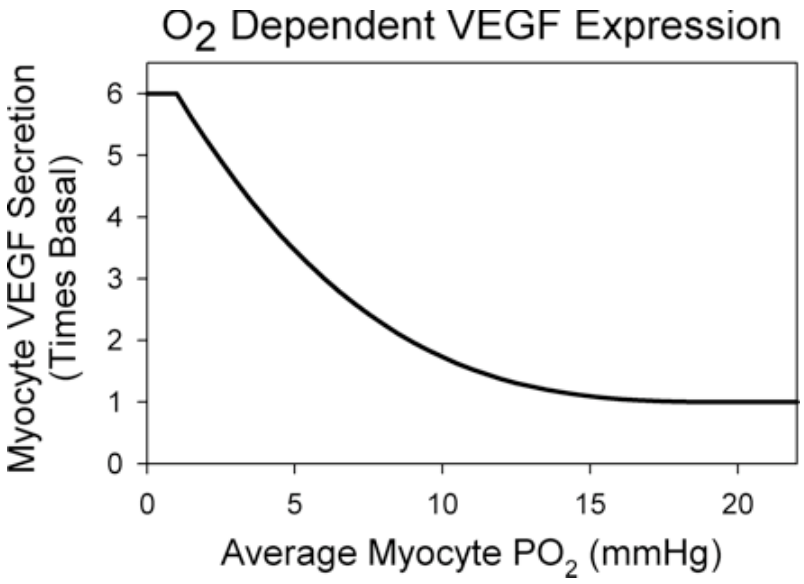

Figure 3.22 A graph illustrating how myocyte hypoxia increases VEGF secretion. Secretion in hypoxic muscle fibers (<1 mmHg) is 6-fold greater compared to that in well-oxygenated muscle fibers (>20 mmHg). (Taken from Ji *et al.* 2007)

There are many limitations associated with the methods currently available for measuring O_2 in mammalian tissue and bodily fluids (Vanderkooi *et al.* 1991). Despite the well-established method of using polarographic microelectrodes to determine tissue PO_2, the spatial resolution is low and it has been found that the electrode itself consumes O_2 and ultimately disturbs and damages the tissue (Maxwell, 2003). Using a blood gas analyser (GEM 4000, Instrumentation), the PO_2 of venous blood in our control animals at 12% hypoxia was 42mmHg, and at 10% hypoxia was 21mmHg. It has been shown that the arterial PO_2 of rats at 8% is 30mmHg and at 12% is 45mmHg (Ray, unpublished), therefore it is reasonable to postulate that the tissue PO_2 for the mice at 10% O_2 lies somewhere between 35mmHg and 42mmHg. However, being able to predict the actual threshold for HIF activation from *in vitro* experiments is complicated, and the current challenge is still to try and determine what the actual circumstances for HIF activation

are. These observations suggest that a hypoxic stimulus of 10% O_2 was not sufficient for HIF activation, as seen from the lack of angiogenesis in the hindlimb skeletal muscles.

3.4.2.2 Mouse strain

A range of studies have examined the strain-specific characteristics of mice. Scholz *et al.* (2002) observed that the C57Bl6/J strain exhibited an early normalisation of blood flow following a femoral artery occlusion, suggesting that there was a denser pre-existing network of collateral vessels compared to the Balb/C strain that was also studied. This observation may account for the lack of angiogenesis occurring in the EDL in chronic hypoxia: a pre-existing network of collaterals may increase the threshold for HIF-mediated angiogenesis to be activated under hypoxic conditions, allowing maintenance of a sufficient blood flow through the tissue despite the hypoxic conditions.

The ventilatory response to hypoxia depends on the pattern and intensity of hypoxic exposure and varies with the strain of animal (Powell *et al*. 1998). Newborn and juvenile animals of a wide range of species show a characteristic biphasic response to hypoxia of an initial augmentation for 1-2 min, followed by a subsequent depression in minute ventilation (Bissonnette *et al*. 2001). This study found that the depressive phase is lacking in the acute response of C57Bl6/J mice to hypoxia, from postnatal days 1-3. Intermittent hypoxia and reoxygenation occur under many pathological conditions, and the respiratory response to this varies with time. The different time courses of these two components, causing a return to pre-hypoxic ventilatory baseline values, are defined as short term potentiation (STP), and studies carried out by Han *et al.* (2000) show the absence of STP in the BL6 strain of mouse. This further supports the presence of the unusual respiratory phenotype as proposed by Bissonnette *et al.* (2001). Comparative morphology of lung structure suggests that C57 mice have a relatively large mass-specific lung volume compared with other inbred strains (Zwemer *et al*. 2007). Zhangm *et al.* (2004) showed that hypoxic conditioning of this strain caused a reduction in

pulmonary vascular permeability, proposing a protective role to maintain pulmonary diffusive capacitance.

On exposure to hypoxia, some mammals will try to maximise the efficiency of their O_2 usage, whereas others will lower their metabolic demand for O_2. Zwemer *et al.* (2007) found that the C57BL6/J strain was naturally more tolerant to hypoxia compared to another strain, CD-1, on the basis of differential metabolic changes when subjected to hypoxic conditioning. The C57BL6/J switched to metabolising ketones, a more efficient fuel. D-β-hydroxybutyrate was found to increase 5 minutes post hypoxic simulus, though by 30 min had declined again, as opposed to the CD-1 strain which showed no change. Taken together, the combination of these factors may account for the improved hypoxic response in this strain of mouse, and thus the lack of change in capillary growth in the hindlimb, as the animal works to counteract physiological changes occuring due to the low $P0_2$.

3.4.2.3 DMOG and the HIF-system

DMOG is a small peptide that inhibits the actions of prolyl hydroxylases on the HIF transcription factor, mimicking hypoxia. Consequently, DMOG may only be effective in inducing HIF-mediated angiogenesis if the hypoxia threshold is not reached by the $P0_2$ of the environment itself. The effect of DMOG *in vivo* under hypoxic conditions is still uncertain though it targets PHDs 1-3 and FIH, all of which are involved in degradation of the HIF-1α subunit under normoxic conditions, but it also targets all members of the prolyl hydroxylase family, possibly having abrogating effects. One of the members of the PHD family is involved in collagen synthesis (C-P4H), and as collagen is a component of the BM, repression of this PHD may interfere with new BM formation during angiogenesis, thus leading to neovascular instability and possible regression.

The DMOG used in these experiments was from Frontier Science and its purity shown to be slightly different from a batch used in previous experiments from a different

source (CHPT 2). However, time did not permit using a newly synthesised batch of DMOG from Oxford on repeated experiments in the hypoxic chamber.

Targeting the 'HIF-system' involves HIF-1α, HIF-2α and HIF-3α. HIF-1α was the original isoform identified, though it was subsequently shown that there were several interaction partners with HIF-1β**.** One was a novel bHLH-PAS protein originally named EPAS-1, now known as HIF-2α, which shares 48% sequence homology with HIF-1α (Tian *et al.* 1997). It has been shown to form a functional heterodimer with HIF-1β and this complex is capable, as HIF-1, of activating transcription factors from the HRE of target genes (Krieg *et al.* 2000). Despite high conservation in amino acid sequence and hypoxia-dependent activation, HIF-1α and HIF-2α have been shown to exhibit quite distinct, non-redundant physiological roles, with some different transcriptional targets and differing levels in tissues: HIF-2α shows a more restricted pattern of expression that includes the developing lung, vasculature, and catecholamine-producing cells (Semenza, 2004). Its differential expression pattern was depicted *via* immunohistochemical staining, molecular analysis, and a number of phenotypic studies (Stroka *et al.* 2001; Wiesener *et al.* 2002). HIF-2α has been shown to be prevalent in endothelial cells (ECs) and is thought to be an important regulator of vascularisation, as shown by its ability to specifically activate the angiopoietin receptor, Tie-2 (Tian *et al.* 1997). It was also found that the hypoxia-induced proliferative response of pulmonary artery fibroblasts was solely HIF-2α dependent (Eul *et al.* 2006). This adds further support to its potential role in development of the vascular system, and the theory that both HIF-1α and HIF-2α act in a cell-specific manner on both common and specific targets (Fig. 3.22).

Uchida *et al.* (2004) demonstrated that both HIF-1α and HIF-2α sub-units were similarly upregulated by acute hypoxia but differentially regulated by chronic hypoxia, with HIF-1α disappearing fairly rapidly, but HIF-2α remaining at a higher and more stable level. This may have been due to a reduction in the stability of HIF-1α mRNA. This finding supports the additional study that was carried out at 6% hypoxia for 1 and 6 h

(CHPT 3.3.1.4), with an inability to detect HIF-1α though HIF-2α being present albeit at decreased levels following the 6 h exposure. As has been demonstrated by the above studies and by Ginouves *et al.* (2008), both HIF-1α and HIF-2α show a comparable response to hypoxia. Thus, that HIF-2α is also upregulated suggests a similar response would likely have been seen with HIF-1α if visualisation of the protein had been achieved.

Another interaction partner that was identified for HIF-1β was HIF-3α. It has been shown to exhibit a completely different expression pattern and levels under hypoxia with mRNA levels increasing significantly with the duration of the hypoxia in a variety of tissues: lung, heart, kidney and liver (Heidbreder *et al.* 2003). This suggests that regulation occurs in a very different manner. However, Li *et al.* (2006) found that HIF-3α functions in a complementary rather than a redundant way with HIF-1α, in protection against hypoxic damage in alveolar ECs. This suggests that it may also be involved in the angiogenic response seen here.

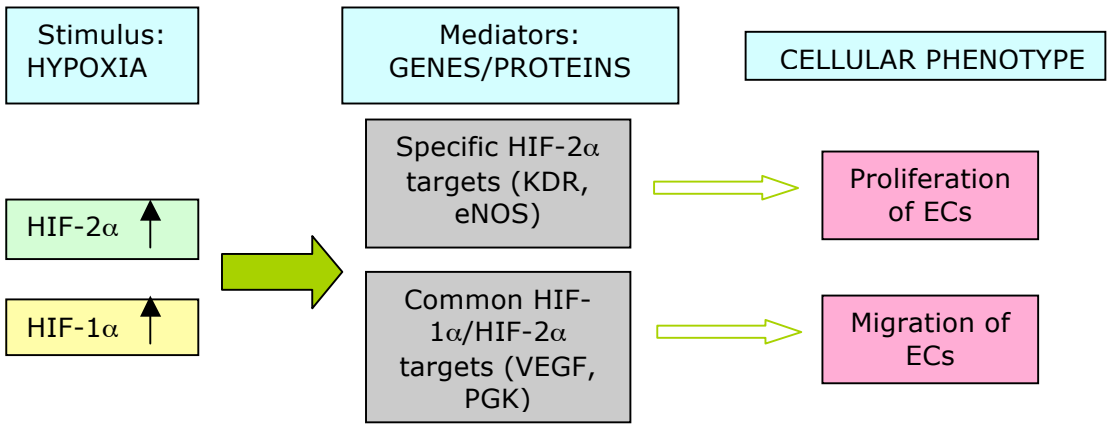

Figure 3.23 HIF-1α and HIF-2α operate *via* both common and specific targets to mediate cellular effects (Modified from Eul *et al.* 2006)

3.4.2.4 PHD2 is the key O_2 sensor and PHD overactivation during chronic hypoxia reduces HIF-α levels

3.4.2.4.1 PHD regulation of HIF

The contribution of each of the three PHDs to the regulation of HIF remains unclear. Using RNA silencing, Appelhoff *et al.* (2004) showed that each of the three isoforms (PHD1-3) contributed in a non-redundant manner to the regulation of both HIF-1α and HIF-2α, and that the abundance of the enzyme present under each condition in differing cell types determined its influence. The PHDs have observable specificities for different prolyl hydroxylation sites on each HIFα subunit and exhibit differential selectivity between both HIF-1α and HIF-2α, modifying the degree and extent of HIF protein activation. They have different expression profiles and subcellular localisation patterns, and this supports findings that they are not equally required *in vivo* (Hirsila *et al.* 2003). All exhibit abundance in specific tissues, along with being widely expressed: PHD2 mRNA is most abundant in adipose tissue, PHD3 is most abundant in the heart, and PHD1 is expressed to a higher degree in the testes (Oehme *et al.* 2002). However, data on skeletal muscle upregulation of the PHDs are limited.

It has recently been demonstrated that PHD2 is the key O_2 sensor under hypoxic conditions (Berchner-Pfannschmidt *et al.* 2008), thus despite not being successful in being able to evaluate the protein expression of PHD1 and PHD3 *via* Western blots under hypoxia, obtaining data for PHD2 under these circumstances has proven most useful. Individual silencing of both PHD1 and PHD3 in a variety of cell types has shown that neither have an effect on the stability of HIF under either normoxia or hypoxia (Berra *et al*. 2003). However, silencing of PHD2 stabilised and activated HIF-1α under both of these conditions. Furthermore, Takeda *et al.* (2007) illustrated how both PHD1$^{-/-}$ and PHD3$^{-/-}$ mice did not show any apparent angiogenic defects, though a conditional knockout of PHD2 produced a phenotype with evidence of hyperactive angiogenesis and

vasodilatation in a multitude of organs (heart, liver, lung, kidney, brain and testes), further suggesting that angiogenesis under hypoxia may occur *via* capillary splitting.

3.4.2.4.2 Increased levels of PHDs under chronic hypoxia

It has been demonstrated that chronic hypoxia causes an increase in the pool of available PHDs, overactivating all 3 isoforms and causing a subsequent decrease in HIF-α levels, a property deemed necessary for cell survival (Ginouves *et al.* 2008). These findings are in contrast to acute hypoxia, where PHD inactivation ensures HIF-1α stabilisation. It is after this inactivation that a new O_2 homeostasis is established, with increasing levels of PHDs and decreasing levels of HIFα.

Stiehl *et al. (*2006) showed that PHD2 remained upregulated over 10 days under chronically hypoxic conditions *in vitro.* Along with this, Huang *et al.* (2002) observed that PHD2 has the highest specific activity toward the primary hydroxylation site of HIF-1α, and residual binding of recombinant PHD2 to HIF-1α ODD peptides *in vitro* occurs, further suggesting a repressive function of PHD2 on HIF-1α following exposure to chronic hypoxia (Stiehl *et al.* 2006). These data support findings shown here in the EDL that the upregulation of PHD2, as determined by densitometry, was 2.3-fold higher after 10% hypoxia for 2 wks when compared to control values (and only had a 0.57x change when DMOG was present). A similar trend was seen in the heart and soleus, though with lower fold increases, supporting the notion that PHDs may exhibit different levels in different tissues at different time points. The finding of decreasing levels of HIF-2α after 6 h at 6% hypoxia, and undetectable levels at 2 wks, along with an inability to detect HIF-1α, support the findings that PHD2 is active in the suppression of HIF following a hypoxic exposure. Along with this, PHD2 has been shown to be a direct target gene of HIF-1α as it contains a HRE (Metzen *et al.* 2005).

3.4.3 Gene expression under hypoxia

A multitude of genes are targeted by HIF, some showing distinct, others inter-relating functions (Fig. 3.2). VEGF is known to form many interactions under normoxia and hypoxia: it is negatively modulated by one of its receptors, Flt-1, positively regulated by another of its receptors, Flk-1, acts on iNOS to increase its expression, and is known to be regulated by both HMOX-1 and TGF-β, among many others. The extent to which these interactions are modified under systemic hypoxia remains unknown, though their upregulation by HIF-1 illustrates a primary response to the hypoxic stimulus. Clearly evident from the data are the different expression levels seen among tissues, both between and within genes, as has been shown for HIF-1α and a range of HIF-regulated genes (Stroka *et al.* 2001; Stiehl *et al.* 2006). Of all genes studied, only EPO and iNOS were actively up and down-regulated in all tissues, largely without an apparent pattern, with the exception of EPO expression in the heart, liver and leukocytes which all showed a characteristic initial increase, followed by decreased expression. Basal gene expression levels of EPO and magnitude of change varied within each tissue, ranging from a 9.5-fold increase in the liver to a 4000-fold increase in the soleus. mRNA expression of EPO in the liver, heart and leukocytes correlated well with the 3 h time point peak in plasma protein (21-fold increase from control values), along with the significantly increased mRNA expression at 3 h in the kidney.

Out of the 7 tissues, the soleus was the only one in which expression levels of all genes were changed, either in a positive or negative direction. The soleus composition (above) suggests that it is fairly sensitive to changes in O_2 supply and this may be why it experiences variations in levels of these hypoxia-regulated genes. Furthermore, the EDL was the only tissue where mostly unchanged levels of gene expression were seen, though in 4 genes (iNOS, HIF, EPO and Flt-1) there was an increase in gene expression by 1 wk. Again, its phenotype suggests that it may be less sensitive to changes in the

PO_2 of the surrounding environment, and hence hypoxia-regulated genes are unresponsive.

3.4.3.1 EPO mRNA and protein expression

Before birth, the liver is the main site of EPO production, though in adults the kidney produces around 90% of systemic EPO. This is supported by the differential basal levels and fold-change on exposure to hypoxia seen in this study, with the kidney expressing average CT levels around 10,000 and the liver being around 1 by 3 h of hypoxia. Clearly evident from this study, a range of tissues have been shown to express EPO, though no structural or functional differences of EPO coming from these different sources have been described (Wiedemann and Johnson, 2009).

Until fairly recently, the role of EPO was thought restricted purely to erythropoiesis. However, it has since been shown to possess other functions, namely protection of neurons against ischaemic brain injury in stroke patients (Ehrenreich *et al.* 2002), significantly improving cardiac function following myocardial infarction by reducing myocyte apoptosis (Parsa *et al.* 2003) and having a protective effect on oxidative renal injury in rats (Kasap *et al.* 2008). Thus, mRNA expression levels detected in the heart and liver in this study may be representative of its protective role in these organs. EPO mRNA has also been shown present in the lung and spleen (Tan *et al.* 1991, Semenza *et al.* 1990), albeit at very low levels. The role of these organs for local and systemic EPO homeostasis is still largely unkown, and the same may be said about expression patterns in the soleus and EDL. However, as with above, EPO may be offering a protective effect against hypoxemia in these tissues.

The spectrum of different levels of EPO regulation became broader with the unexpected finding that there is a link between VEGF and hepatic EPO expression (Tam *et al*. 2006). Hepatic and systemic inhibition of VEGF, as well as conditional deletion of VEGF gene in the liver, induced hepatic EPO expression, which increased the haematocrit and led to polycythaemia in rodents. This was thought to be achieved by interfering with

Flk-1 stimulation. However, there appear to be no similarities in the VEGF, Flk-1 and EPO mRNA expression levels in the present study.

That EPO expression in leukocytes follows a similar pattern to that seen in the plasma response bodes well for the use of leukocytes as a circulating indicator of EPO in response to systemic hypoxia in humans (CHPT 7). As EPO is a downstream gene of HIF, it is a reasonable expectation that it would act as a suitable surrogate measure for HIF-upregulation under hypoxic conditions.

3.4.3.2 Control of EPO by the HIF-system: An emerging role for HIF-2α

It is well known that HIF-1α is post-translationally regulated under hypoxia, although mRNA upregulation has been shown under both hypoxic and normoxic conditions (Richard *et al*. 2000; Kim *et al.* 2002; Roy *et al.* 2004). It has long been thought that HIF-1α is the key factor activating EPO transcription and was the original isoform identified as binding to the 3' regulatory element on the HRE of the EPO promoter (Semenza *et al.* 1991). Using gene silencing *in vitro*, this being later supported by an *in vivo* model (Gruber *et al.* 2007), it was subsequently shown that HIF-2α was largely in control of the same regulatory sequence on the EPO gene (Warnecke *et al.* 2004), and that HIF-1α knockdown only has a small effect on EPO transcription compared with the major reduction observed following HIF-2α inhibition (Gruber *et al.* 2007). Whether the lack of significant change in HIF-1α mRNA seen here is due to an insufficient hypoxic stimulus remains a possibility, though the lack of relationship between HIF-1α and EPO mRNA may be due to the above observation: it is HIF-2α that is largely in control of EPO, hence examining HIF-2α mRNA expression may provide a better representation of its relationship and regulation of EPO.

3.4.3.3 iNOS mRNA

HIF-1α protein and mRNA (Thompson *et al.* 2008) have been shown to upregulate iNOS expression both *in vitro* (Han *et al.* 2007) and *in vivo* (Fagan *et al.* 2001). An HRE in

murine macrophages has been identified and shown to be hypoxia-inducible (Melillo *et al.* 1995). iNOS is known to play a role in the human defence against invading pathogens, and along with being upregulated by HIF-1α is under the control by a variety of inflammatory factors (Kröncke *et al.* 1998). Its role is to synthesise NO as part of the cytotoxic defense, which may also initiate vasodilation of blood vessels on spillover, an important adaptation under systemic hypoxia to increase blood flow and reconstitute the O_2 supply to parts of the body.

Figure 3.24 NO-dependent mechanisms in and the protective effects of adaptation to hypoxia. SOD = superoxide dismutase; GS = glutathione; HSP = heat shock protein; PG = prostaglandins (From M*anukhina et al.* 2006)

iNOS has been associated with ischaemic preconditioning and cardioprotection, whereby an episode of ischaemia triggers an early phase of protection against further episodes of ischaemia. Ischaemia is thought to induce transcription factors (HIF and NF-κb) which subsequently induce iNOS expression, followed by NO release, offering cardioprotection as soon as 24 h following the initial attack (Lowenstein, 1999; Xi *et al.* 2004). Figure 3.23 illustrates the relationships between HIF-1, iNOS and and NO, along with the downstream effects, including those of vasoprotection and anti-stress defense.

A late response is seen in most tissues illustrated here, suggesting that iNOS is

involved in the chronic adaptation to hypoxia. Interestingly, an early response is seen in the leukocytes, suggesting that these peripheral cells may represent an efficient circulating marker of hypoxia, adding further support to their use in CHPT 7. The response in the leukocytes is consistent with that seen in the bone marrow, though occurring slightly earlier, the bone marrow being one site for leukocyte degradation (King *et al.* 1990). This suggests that leukocytes may act as sentinel cells, playing a role in educating the bone marrow on levels of hypoxia.

3.5 Conclusions

Despite both 10% and 12% hypoxia being sufficient to cause hypertrophy of the heart (as a response to the increased workload required to pump blood around the body and against constricting vessels), only 10% O_2 was low enough to induce an angiogenic response in the heart and diaphragm of this strain of mouse. The response seen here is thought to be an indirect effect of hypoxia, being mechanically-mediated by stretch due to a combination of increased ventilation, a higher total volumetric flow of blood and pressure overload. This observation is supported by the fact that hypoxaemia at this level was not low enough to induce blood vessel growth in the hindlimb. The proposed effect of DMOG to enhance any angiogenic growth occurring was not seen in the hindlimb, heart or diaphragm, though there is evidence for its effects in the soleus at 10% hypoxia. Studies have shown that this strain of mouse is very resistant to both systemic hypoxia and local ischaemia, so it is likely that in order to induce a sufficient response in the EDL muscle of the hindlimb, the hypoxic stress on the system needs to be magnified with the use of an additional stimulus such as exercise. Angiogenesis has been induced under locally hypoxic (ischaemic) conditions in a range of studies. However, systemic and local hypoxia may act differently, or have different thresholds for inducing capillary growth, and that may be why similar changes are not seen here. Systemic hypoxia at 10% was sufficient to induce changes in a variety of HIF-regulated genes, namely iNOS and EPO, which were up and down-regulated in all tissues studied. The most reactive tissue was the soleus, consistent with it being an oxidative tissue with an increased sensitive to changing O_2 levels. Leukocytes appear to be sensitive to gene expression alteration under hypoxia, and this gives support to using them as a circulating indicator of HIF-regulated hypoxic stress in humans.

3.6 Future experiments

If the hypoxic stimulus threshold for stimulating angiogenesis was not reached due to an insufficiently low PO_2 of the blood, an obvious experiment to stress the physiological system of the animal to a greater degree would be to incorporate an exercise component into the hypoxic chamber exposure, for example a running wheel. Despite the described hypoxia-resistance characteristics of the C57Bl6/J mice mentioned above, it may be that increasing the hypoxic stress imposed on this strain of mouse to critical levels would be sufficient to induce a reponse. It would also be interesting to record O_2 levels in the muscle tissue using a hypoxyprobe (O_2 sensitive dye) or optodes, an optical sensor device that measures oxygenation of a dye with the aid of a chemical transducer, to determine differential O_2 concentrations within tissue. To overcome the non-specific action of the DMOG, it would be useful to either develop a compound that is specific to target PHD 1, 2 and 3, and FIH alone, or explore using knockout mice. RNA silencing has already been used and shown to have success in mouse embryos. It is still very much in its infancy, though with a promising future. The benefits of using knockout mice over chemical ablation include the lack of effects of toxicity which may be present and unknown, the fact that knockouts are specific and chemicals may still involve a lack of specificity, and finally, that the problem of dosage is not an issue in this instance. Investigating HIF-2α mRNA expression (under 10% hypoxia) in tissues studied here, would possibly provide a useful indicator of its role in the regulation of EPO.

Chapter 4

FEMORAL ARTERY LIGATION

4.1 Introduction

Ligation of the femoral artery in the hindlimb of the mouse will cause an area of local ischaemia and is an efficient surrogate model used to study the effects of peripheral vascular disease in man, on a molecular and physiological level. Chronic ischaemia in humans occurs as a consequence of peripheral arterial occlusive disease (PAD) which leads to obstruction of large arteries, e.g. in the leg. The reduction in blood flow causes a chronic deficiency of O_2 supply to the surrounding tissues and this ultimately results in the development of ulcers and, at worst, gangrene and necrosis of the lower limb (Scholz *et al.* 2003). Rodent models are used to study limb ischaemia on a relatively acute scale as opposed to the usual chronic timescale upon which PAD occurs in humans. Nevertheless, these models are invaluable for understanding the molecular mechanisms governing these conditions, of which the pathways are possible targets for chemical manipulation and clinical investigation.

Both angiogenesis and arteriogenesis are important mechanisms of restoring blood flow following limb ischaemia. Arteriogenesis is the remodelling of the existing arteriolar connections into larger calibre vessels following occlusion of the vessel (Prior *et al.* 2004). These vessels are microvascular, thin-walled conduits that are composed of an endothelial lining, an internal elastic lamina, and one or two layers of smooth muscle cells (Longland, 1953). Arteriogenesis is responsible for the expanded collateral network that improves blood flow in distal areas of the affected limb, whereas angiogenesis is responsible for the extension of small vessel growth within the immediate ischaemic regions, it being an extremely responsive and productive system (Silvestre *et al.* 2000). Angiogenesis is a complex phenomenon which involves capillary sprouting, in contrast to the arterial remodelling seen in arteriogenesis. It consists of several distinct processes, which include endothelial migration and proliferation, extracellular proteolysis, endothelial differentiation (capillary tube formation) and vascular wall remodelling (Buschmann & Schaper, 1999).

4.1.1 Hypoxia Inducible Factor (HIF)

The molecular mechanisms of angiogenesis in limb ischaemia have been thoroughly investigated (Tuomisto *et al.* 2004, Ho *et al.* 2006) and HIF shown to be extremely important in the initiation of new vessel growth *via* transcriptional activation of a number of downstream genes. As previously described (CHPT 1), HIF is a master regulator of O_2 homeostasis and its activation depends on stabilisation of the O_2-dependent degradation domain (ODD) of the α-subunit. The constitutively expressed β-subunit binds with the O_2-regulated α-subunit and is translocated to the nucleus of the cell where it binds to consensus domains of target genes. After binding to the HRE on target genes, transcriptional activation of genes responsible for cellular, whole tissue and whole animal adaptation to hypoxia, are activated. Critical to limb ischaemia, angiogenic responsive genes such as VEGF, angiopoietins and MMPs are subsequently activated, initiating new blood vessel growth in order to partially restore blood flow in the affected area.

4.1.2 Therapeutic angiogenesis

An important challenge for therapeutic angiogenesis is the need to target the angiogenic response to ischaemic areas. Studies report that up to 1000 people per million per year develop critical limb ischaemia (Bobek *et al.* 2006), and a further 150, 000 patients require lower limb amputation for the condition. The endogenous angiogenic response to hypoxia seems to be impaired in patients with PAD, and therapeutic angiogenesis seeks to augment collateral vessel formation using a variety of possible interventions (Collinson and Donnelly, 2004). By-pass grafting surgery, percutaneous transluminal angioplasty and surgical revascularisation are reserved for patients with severe critical limb ischaemia (Collinson and Donnelly, 2004; Bobek *et al.* 2006), though many of these patients are poor candidates for these procedures.

The concept of therapeutic angiogenesis was first introduced in 1989 by a German gynaecologist named Michael Hockel (Bobek *et al.* 2006), who described it as a process of improving blood flow to ischaemic tissue by inducing neovascularisation using

angiogenic agents, administered by gene transfer, recombinant protein or chemicals (Khan *et al* 2003). Despite some initial setbacks and negative clinical trial results, a substantial amount of progress has been made over recent years in the area of targeting angiogenesis therapeutically (Emanueli and Madeddu, 2001; Selke *et al.* 1998). Therapeutic angiogenesis was initially validated in mice, dogs, and pigs and was subsequently approved for use in human clinical testing. A wide range of therapies have been utilised, some yielding limited success, others showing a significant improvement in vascularisation and alleviation of the ischaemia (Table 4.1). The studies have used a variety of treatments, patient selection criteria and endpoints. Many advantages and disadvantages are associated with all types of therapy. Gene transfer is useful for ensuring persistent expression of the factor. However, non-specific gene transfer to other cell types and lack of regulation of gene expression prove problematic in many cases. One of the main drawbacks of growth factor administration such as VEGF is that it renders vessels leaky and unstable (Dvorak et al, 1999). VEGF and bFGF are also potent vasodilators and this may cause unwanted hypotension. Studies suggest that sole administration of VEGF is insufficient to form stable, mature vessels as numerous growth factors, such as Ang-1 and TGF-β are required for the formation of stable vessels (Bobek *et al.* 2006). Treatment with VEGF in the first clinical studies has been well tolerated, though there has been variable success of trials and this suggests that multi-agent gene therapy may be necessary to achieve sufficiently stable blood vessel growth, and to ensure effective clinical outcome in patients. The possibility of using stem cells is also a source of growing excitement (Real *et al.* 2008). HIF-1α-transduced endothelial progenitor cells (EPCs) were administered to nude mice with hindlimb ischaemia and IHC showed enhanced neovascularisation *in vivo*, along with both limb and toe necrosis being significantly reduced, 14 days post transplantation (Jiang *et al.* 2008).

A number of chemicals have been used to indirectly target HIF by inhibiting the PHDs which regulate HIF-1α. DMOG is a PHD and FIH inhibitor, subsequently upregulating HIF activity. Initial studies *in vitro* demonstrated its efficiency at inducing

HIF-1α (Jaakola *et al.* 2001). Subsequent studies have shown its use in enhancing the angiogenic response to limb ischaemia (Milkiewicz *et al.* 2005). TM6089 and TM6008 are two novel compounds that have been shown to induce angiogenesis by binding to the active site of PHD2 (Nangaku *et al.* 2007). Ethyl 3,4-dihydroxybenzoate (EDHB), 6-chlor-3-hydroxychinolin-2-carbonic acid-N-carboxymethylamid (S956711) and L-mimosine (L-mim) all demonstrated similar effects to hypoxia by inducing HIF-1α in both human and rodent cells (Warnecke *et al.* 2003). Animals treated with EDHB displayed significantly increased viability and enhanced exercise performance in hypoxia (Kasiganesan *et al.* 2007). PR39 is a macrophage-derived peptide that acts in a similar way to the above chemicals, inhibiting the degradation of HIF-1α and producing accelerated formation of the vasculature in mice (Li et al. 2000). Directly targeting HIF-1α has long been an attractive method of upregulation, using the iron chelator desferrioxamine or cobalt chloride, leading to an increased muscle capillary supply (Tanaka et al. 2005).

Treatment	**Outcomes**
Intra-arterial $VEGF_{165}$ gene transfer	Increased collaterals
Intra-muscular $VEGF_{165}$ transfer	Increased collaterals in all limbs
Intra-arterial bFGF protein transfer	Improved calf blood flow though lack of positive results at cessation
IV bFGF protein transfer	Peak walking time increased
Intra-arterial VEGF gene transfer	Improved vascularity
Intra-muscular $VEGF_{121}$ gene transfer	No change

Table 4.1 Summary of published clinical studies of therapeutic angiogenesis in patients with PAD (Adapted from Collinson and Donnelly, 2004)

The aim of this study was to evaluate the levels of local hypoxia required to initiate angiogenesis, and to elucidate whether chemical manipulation of HIF-1α stability would enhance these responses.

4.2 Methods

4.2.1 Study design: Femoral artery ligation

We chose to exploit the use of DMOG in altering the response to unilateral ligation, both in the C57BL6/J and C57BL10/J strains of mouse, to determine efficiency of the drug in restoring blood flow in the hindlimb following occlusion of the femoral artery after 1 and 2 wks, and to determine if there were any differences in strain response. Experiments were performed on groups of C57BL6/J and C57BL10/J mice (n=6 in each experimental group). Each group received DMOG (8mg.0.5mL^{-1} saline) (CHPT 2.1) *via* i.p. injection every other day, with the initial injection 2 days before surgery.

4.2.1.2 Surgery

Under aseptic conditions, mice were anaesthetised starting initially with 5% isofluorane and decreasing to 2.5% with O_2 as a carrier. 0.2mL.100g^{-1} Temgesic® was given prior to surgery for postoperative analgesia. The vein was visualised through the skin and an incision was made through the skin alongside the vein at the top of the underside of the leg (Fig. 4.1). Fine forceps were used to clear away the fascia and remove connective tissue that was attached to the artery and vein. The forceps were then used to dissect down between the artery and vein (also on all sides of the artery) to obtain good separation, with care taken to avoid trauma to the adjacent nerve. The artery was lifted up at a minimal distance away from the animal and a piece of suture thread (10,0 polyamide monofilament) was passed underneath. A double knot was tied and the remaining suture thread trimmed to a minimum. Two drops of the antibiotic Depocillin® (300mg.mL^{-1}) was applied to the exposed area and excess was removed after leaving it to be absorbed for a short time. The wound was closed with 4/5 sutures (6,0 vicryl monofilament) and any dried blood removed to minimise the risk of infection. The mice were allowed normal access to food and water to aid recovery. They were then sacrificed after the experimental period of 1 or 2 wks *via* cervical dislocation.

Ligation of the femoral artery was attempted in two different locations along the artery to determine whether the placement of the suture affected the degree of ischaemia experienced. Subsequent analysis of the tissue confirmed that ligating the artery either above and below the saphenous branch of the artery produced no signifcant difference in the degree of capillary growth.

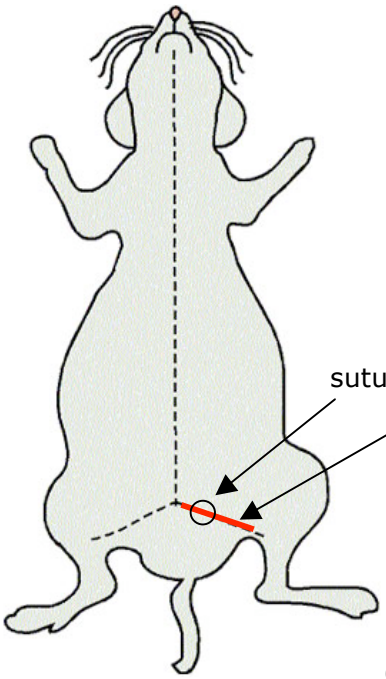

(National Institute of allergy and infectious disease www3.niaid.nih.gov)

Figure 4.1 Location of the area for incision before ligation of the femoral artery

On a number of mice, a Transonic® flow probe (probe and meter) was used to confirm the absence of blood flow following ligation (Fig. 4.3). Figure 4.2 illustrates normal blood flow. The ultrasound bounces off red blood cells flowing through the vessel and this gives a measurement of flow.

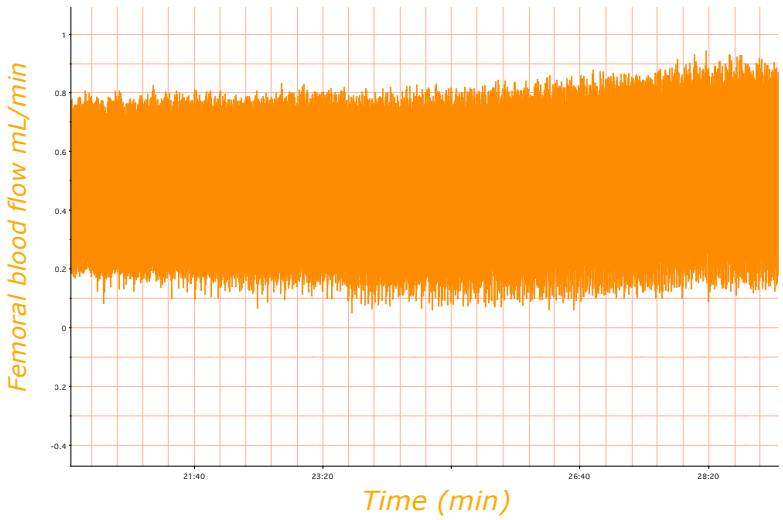

Figure 4.2 Flow probe data obtained by ultrasound from an unligated femoral artery of a C57Bl6/J mouse showing presence of blood flow through the artery

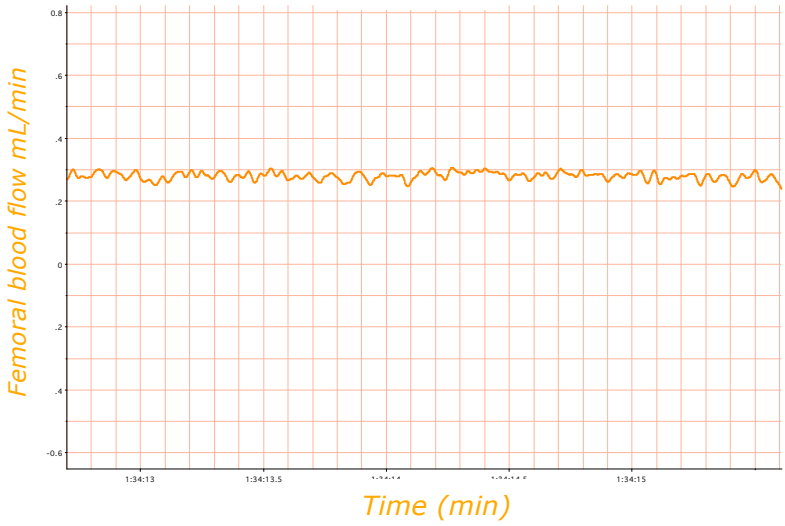

Figure 4.3 Flow probe data obtained by ultrasound from the ligated femoral artery of a C57Bl6/J mouse showing a clear lack of flow

4.2.1.3 Tissue processing

EDL muscles from ipsilateral limbs were taken (CHPT 2.2) and stored on corks at -80°C after being snap-frozen in isopentane cooled in liquid nitrogen (CHPT 2.3). Tissue was sectioned and stained (CHPT 2.3), and capillary and fibre numbers (C:F) counted (CHPT

2.4) using lectin staining. On a selection of slides, lectin and DAPI staining were used to look for the presence of macrophage nuclei, suggesting infiltration and inflammation.

4.3 Results

There was no significant change in the capillary to fibre ratio (C:F) of the EDL muscle in C57BL6/J mice that underwent unilateral ligation of the femoral artery at either 1 or 2 wks (Table 4.2). There was a significant decrease in the capillary density (CD) for mice administered with DMOG during the 1 wk ligation and a significant increase in the mean fibre area (MFA) for mice at 1 wk without DMOG. There was also a significant difference between the MFA for mice during the 1 wk ligation ± DMOG when compared to control values. Mean body mass was 25.6g ± 1.06 (±SEM).

Experiment	**C:F**	**CD** (cap.mm^{-2})	**MFA** (μm^2)
Control (n=6)	1.26 ± 0.02	885 ± 67	1521 ± 102
Control D (n=6)	1.26 ± 0.05	856 ± 141	1674 ± 58
1 wk no D (n=6)	1.31 ± 0.07	736 ± 69	1418 ± 62
1 wk D (n=6)	1.26 ± 0.05	766 ± 30	1554 ± 90
2 wk no D (n=7)	1.33 ± 0.05	839 ± 62	1630 ± 69
2 wk D (n=7)	1.32 ± 0.04	925 ± 44	1501 ± 40

C:F = capillary to fibre ratio, CD = capillary density, MFA = mean fibre area, mean ± SEM. Statistics performed using ANOVA with Dunnetts post hoc test. 'n' is defined in the table. D = DMOG

Table 4.2 C:F, CD and MFA for the EDL muscle following femoral artery ligation in C57BL6/J mice. No significant differences were determined.

The 2 wk ligation was repeated in the C57BL10/J strain of mouse to determine if there were any strain-specific differences as shown in Table 4.3. There was no change in capillary growth in the hindlimb with or without DMOG, though, as is shown in both strains, there is a tendency for a higher though not significant C:F ratio in the ligated limb in both treated and untreated animals.

Lectin and DAPI staining were used to test for the presence of leukocytes, which would otherwise suggest that inflammation may have been a driving force behind any angiogenesis seen. No evidence of an inflammatory presence was seen.

Experiment	**C:F**	**CD** (cap.mm^{-2})	**MFA** (μm^2)
Control (n=6)	1.25 ± 0.02	1015 ± 59	1367 ± 112
2 wk no D (n=6)	1.31 ± 0.05	961 ± 78	1452 ± 89
2 wk D (n=6)	1.36 ± 0.07	1032 ± 101	1372 ± 69

C:F = capillary to fibre ratio, . CD = capillary density, MFA = mean fibre area, mean ± SEM. §=P<0.05 vs. control. Statistics performed using ANOVA with Dunnett's post test. 'n' is defined in the table. D = DMOG

Table 4.3. C:F, CD and MFA for the EDL muscle following femoral artery ligation in C57BL10/J mice. No significant difference was seen between any of the groups.

The average body mass for the C57BL6/J strain of mouse was 26.8 ± 0.24g, with the average EDL mass being the same as control (9.0 ± 0.2mg). Average body mass of the C57BL10/J mouse was 25.1 ± 0.17g, with an average EDL mass of 9.2 ± 0.01mg.

As described, previous studies using DMOG have shown a significant increase in capillary growth. This finding was not reproduced here and therefore investigations into the purity of the DMOG were carried out (CHPT 2.1). Due to a slight discrepancy between 2 batches of DMOG obtained from different sources, a new batch of the original DMOG was synthesised and used in subsequent experiments. However, as shown in Table 4.4, significant capillary supply changes in both DMOG and non-DMOG treated C57BL6/J animals were unable to be shown.

Experiment	**C:F**	**CD** (cap.mm^{-2})	**MFA** (μm^2)
Control (n=6)	1.26 ± 0.02	885 ± 67	1521 ± 102
Control D (n=6)	1.26 ± 0.05	856 ± 141	1674 ± 58
2 wk no D (n=4)	1.25 ± 0.05	639 ± 21§*	1597 ± 62
2 wk D (n=4)	1.34 ± 0.04	577 ± 22§*	1788 ± 69

C:F = capillary to fibre ratio, . CD = capillary density, MFA = mean fibre area, mean ± SEM, §=P<0.05 vs. control,, *= P<0.05 vs.control D Statistics performed using ANOVA with Dunnetts as a posthoc test. 'n' is defined in the table. D = DMOG

Table 4.4 C:F, CD and MFA for the EDL muscle in the femoral artery ligation in C57BL6/J mice using newly synthesised DMOG.

4.4 Discussion

The aim of this study was to determine whether use of a chemical upregulator of HIF would enhance the angiogenic response occurring following ligation of the femoral artery. Previous studies have shown beneficial local effects of HIF enhancement on blood vessel growth *in vivo* under artificial circumstances using polyethylene sponge assays (Willam *et al.* 2002; Warnecke *et al.* 2003), and the pro-angiogenic effects of DMOG have previously been shown by a member of our group (Milkiewicz *et al*. 2004). However, a number of difficulties arose, based upon the initial inefficiency of the DMOG, due to the possible upregulation of anti-angiogenic factors alongside pro-angiogenic factors, and finally upon realisation of the limits the use of this strain of mouse may have.

4.4.1 Effects of ligation in the hindlimb

Despite neither the C57BL6/J or the C57BL10/J strain of mouse exhibiting a significant increase in the capillary to fibre ratio (C:F) in either DMOG or non-DMOG treated limbs at 2 weeks, there was a tendency for the C:F to be obviously increased compared to the control animals. When the newly synthesised batch of DMOG was trialled these same trends were seen, though the difference between the DMOG and non-DMOG treated animals was more convincing, with the DMOG-treated animals exhibiting a higher C:F compared to those without, though both showing a significantly decreased capillary density. Animals studied at 1 wk showed no obvious change at all. These data suggest that the stimulus switching on blood vessel growth under these conditions was not substantial enough.

4.4.1.1 The threshold to induce angiogenesis

The findings in this study are in accordance with a large number of studies that have been unable to show an increase in the capillarity of skeletal muscles in the rat hindlimb (Dawson and Hudlicka, 1990; Hudlicka *et al.* 1994; Cherweck *et al.* 2000), suggesting

that the threshold for inducing angiogenic growth factors under conditions of femoral artery ligation is at a higher level than obtained by ligation alone, or/and there is a parallel increase in anti-angiogenic factors which inhibit the pro-angiogenic circumstances required for new vessel growth. As discussed in CHPT 3.4.2, the *in vivo* PO_2 threshold to induce HIF-activation is unknown, due to difficulty in obtaining reliable methods by which to measure tissue PO_2. However, estimates can be made based on extrapolations from cell work (Jiang *et al.* 1996), leading to the suggestion that the tissue hypoxia was insufficient in this model (see CHPT 3).

4.4.1.2 Fibre type-specific induction of angiogenesis

It has been shown that fibre type influences the response to ligation in the rabbit (Cherwek *et al.* 2000). Despite lack of change in the C:F ratio in either the soleus or TA muscle of the hindlimb in this study, Cherwek *et al.* (2000) observed a much greater upregulation of VEGF in the soleus compared to the TA. These data suggest that properties specific to this muscle fibre type such as a higher capillary and mitochondrial density make it more sensitive to changes in O_2 delivery, and therefore changes in growth factors are more likely here when compared to a mixed fibre type such as the TA or EDL which may be less sensitive to changes in O_2 delivery. This is supported by the finding that long term limitation of blood flow supplying both glycolytic and oxidative skeletal muscle fibres affects oxidative fibres more (Dawson and Hudlicka, 1990), further suggesting that the degree of resulting O_2 delivery was lower due to tissue metabolism and thus closer to the threshold level for inducing angiogenic growth.

4.4.1.3 Additional stimuli inducing angiogenesis

As was postulated for exposure to systemic hypoxia (CHPT 3), an additional stimulus may be required to reach the threshold required for switching on capillary growth in the EDL and other skeletal muscle, despite an apparent upregulation of angiogenic growth factors (Lloyd *et al.* 2003). Capillary growth following ligation has been induced with an

additional stimulus such as exercise (Deschenes and Ogilvie, 1999; Lloyd *et al.* 2003), although angiogenesis was induced in muscles with a high proportion of oxidative fibres such as the medial gastrocnemius as opposed to the EDL with a mixed fibre composition, electrical stimulation (Hudlicka *et al.* 1994), and muscle overload (Deveci and Egginton, 2002). However, additional stresses such as these have been shown to induce an inflammatory response (Hudlicka *et al.* 1993). A method of increasing capillarity using electrical stimulation without muscle damage was shown by Hudlicka *et al.* (1994) whereby mild intermittent stimulation allowed the muscle to replete glycogen stores, resulting in an improved perfusion pressure and lower muscle fatigue, and an increased C:F ratio. It remains unclear whether angiogenesis under such conditions is due to a lowering of the hypoxic threshold or the imposition of muscle work, i.e. the relative importance of metabolic or mechanical stimuli for capillary growth.

4.4.2 The inefficiency of DMOG

Although investigations were made into the purity of the DMOG, the recorded discrepancies between the two batches (CHPT 2.1) may be insignificant based on the fact that the C:F ratio appeared to show similar changes after using either. However, studies looking at the effect of femoral artery ligation and an additional stimulus such as exercise found changes in oxidative muscles such as the soleus, suggesting that it may be beneficial to incorporate this in the future to maximise the potential for observing the proposed effect of DMOG. It is possible that DMOG also has a threshold below which it is not activating the HIF system to its full potential, and this may have been the case here if the bioavailability was underestimated. It may also work differently in different skeletal muscles, depending on fibre type and depending on the amount or type of PHD enzyme present, as different levels have been reported in different tissues (Appelhoff et al. 2004). Differential expression in skeletal muscle has not been explored as yet.

These experiments involved repetition of a protocol using DMOG that had previously been utilised both in vivo (Mikiewicz et al. 2005) and in vitro, many of the

latter experiments taking place in the Ratcliffe Laboratory, Oxford, both with its desired effect of demonstrating HIF-1α upregulation. Mole (unpublished) demonstrated an in vitro dose-response curve for dimethyloxalylglycine, confirming that between 200μM and 500 μM DMOG is required to achieve maximal induction of HIF-1α when lysates from stimulated HeLa cells were analysed by HIF-1α Western blot. It was from these in vitro data that in vivo values published in the literature, were extrapolated. The next logical step would have been to do a dose response in vivo but time was not permitting. (This is discussed in CHPT 8, Future directions).

4.4.3 The confounding factor of mouse strain

The C57BL6/J strain is becoming an increasingly popular model for target gene disruption, though literature based on characterisation of the strain-specific phenotypes suggest significant differences exist in this strain compared to others such as the Balb/c and CD-1 strains. These differences are thought to influence their response to surrounding environmental and imposed experimental conditions. As described in CHPT 3.4.2.2, studies have shown that the respiratory response of the C57BL16/J mouse to hypoxia is abnormal as this strain rapidly switches to metabolising ketones, a more efficient fuel, under hypoxic stress (Zwemer et al. 2007). Studies into this strain have also revealed that the C57BL6/J mouse has a denser network of pre-exisiting collaterals, offering a higher degree of protection against ischaemic insult. This resulted in blood flow through the femoral artery returning to normal rapidly, following ligation of the femoral artery (Zbindeen et al. 2006). A pre-existing collateral vasculature has been identified in various parts of the circulation of a number of species, though the number and size of these anastomoses differs between species and tissues (Helisch et al. 2006). The result is that differing degrees of protection against ischaemic insult are offered and thus the driving force to reach the threshold which would then initiate angiogenesis, also differs.

Helisch et al. (2006) studied 3 different strains of mouse (C57BL6/J, Balb/c and 129S2/Sv) following a femoral artery occlusion, using laser doppler imaging, visible light

oximetry, and treadmill testing. C57BL6/J mice exhibited the most complete recovery as this strain appeared to have a high number of visible collaterals immediately following ligation, and no tissue hypoxia or damage was seen in these areas when compared to the Balb/c strain of mouse. This confirmed findings of Shireman et al. (2005). However, it is important to remember that along with inter-species differences, there is considerable inter-animal variability in the functionality of pre-existing collaterals, despite the animals being genetically similar (Zbindeen *et al.* 2006).

Results from a further study support the implication that genetic heterogeneity plays a major role in determining the response to hypoxic conditions. Ward *et al.* (2007) found that of 4 different strains of mouse used, C57BL6/J, 129S2/Sv, Balb/c and CD-1, a strain-dependent expression of angiogenic growth factors was shown, with the C57BL6/J showing only an intermediate increase of angiogenic growth factors, namely VEGF and Ang-2, compared with the other strains. C57BL10/J mice are also known to differ from C57BL6/J mice with regard to various hematological and coagulation parameters, as well as in their inflammatory response to an infectious challenge (Peters *et al.* 2002), though differences in capillary growth under the ischaemic conditions imposed here were not obvious.

The C57BL6/J strain of mouse therefore appears to be fairly resistant to these experimental interventions and, due to the differing intrinsic mechanisms specific to each strain, it is difficult to know which is the most suitable surrogate model for human disease. Although these data may prove helpful in providing insights into the magnitude of the variety of responses present in humans, a review of gene expression in this model would provide extremely useful information to aid understanding of the different pathways upregulated, posing further stimulation for research into the most effective and beneficial methods of manipulating the molecular pathway underlying ischaemia, and to a greater understanding of the disease itself.

4.4.4 Trauma following surgery and inflammation-induced angiogenesis

A variety of responses are seen following ligation of the femoral artery in the mouse and it is thought that the role inflammation plays is grossly underestimated. The variation in outcomes among studies is due, among other factors previously discussed, to the location of the suture and whether or not both the artery and vein are ligated as a dual procedure (Richardson *et al.* 2001), altering the degree of ischaemia and the amount of trauma induced. Ziv *et al.* (2004) carried out a longitudinal MRI tracking study subsequent to ligation of the femoral artery in the hindlimb of the mouse. They noted that in the early stages of ischaemia, most of the angiogenesis occurring was in the subcutaneous fat as opposed to the injured muscle, the former of which showed no evidence of damage from the ischaemia. In the muscle, vascular permeability was elevated in the first few days, propagating tissue damage, though it subsequently resolved a few days later. Scholz *et al.* (2003) showed that ischaemia-induced damage following ligation developed gradually, shown by the decay of high-energy phosphates and tissue glycogen, and that only 21 days post-surgery was evidence of cell death diminished. There are data to show a lack of muscle necrosis or evidence of inflammation in rats, based on macrophage staining (Brown *et al.* 2003), and our data further support this.

One of the main factors differing in models of femoral artery ligation is the location of the suture and thus degree of ischaemia and damage inflicted. Ziv *et al* (2004) used a location of the ligation further upstream than the present study, and this resulted in a much higher degree of ischaemia as evidenced by loss-of-function of the hindlimb for the first few days. However, difficulty in reaching this location due to proximity to the abdominal wall, and the presence of copious white adipose tissue, may have been responsible for inflicting trauma that led to this inflammation. Another illustration of the effects of extreme ischaemia were shown after the entire left superficial femoral artery and vein, from just below of deep femoral arteries to popliteal artery and vein, were ligated, cut, and excised (Masaki *et al.* 2002), resulting in auto-amputation.

These effects of ischaemia were not present in our model, as mice regained full use of the limb the day after surgery when ligating the artery above and below the saphaenous.

These data suggest that the degree of ischaemia induced was not extreme enough to elicit the significant angiogenic response expected under these conditions, and that depending on the size of the incision and the damage caused upon isolation of the artery, inflammation and muscle damage can be avoided. However, a study following gene expression after acute hindlimb ischaemia found that inflammation-associated genes were also induced after sham surgery, suggesting that the trauma of the operation itself has the potential to induce a number of changes in gene expression (Lee *et al.* 2004).

Evidence of inflammation at either 1 or 2 wks in these studies was not seen on analysis of WBC infiltration. However, this does not confirm an initial absence of inflammation, or absence of an inflammatory mediated HIF-stimulated pathway operating (Fig. 4.4) as opposed to the postulated hypoxia-mediated HIF pathway being stimulated, because, as is indicated by the above studies, inflammatory consequences were immediately counteracted on a molecular level, and transformation back to a more homeostatic environment was evident after a short period of time. It is therefore possible that the angiogenic response seen here was due to a combination of an initial inflammation-induced HIF-upregulation, this being superceded and driven by a hypoxia-induced HIF-response once inflammation had been suppressed. However, the extent and position of the ligation will most likely determine the amount of inflammation induced. Due to the less invasive method used here, it is likely that inflammation contributed only a minor amount.

4.4.4.1 Differential upregulation of HIF

There has been substantial interest in the cross-talk between two hypoxia-responsive factors: HIF and nuclear factor κB (NFκB). Although HIF is widely known as being a key player in the cellular response to hypoxia, it is one amongst a host of factors sensitive to

changes in surrounding O_2 concentrations. NFκB is a family of transcription factors that become activated following stimulation by pro-inflammatory factors such as cytokines. Despite showing evidence of the independent stimulation of pathways leading to the upregulation of hypoxic gene expression, a significant level of cross-talk has been demonstrated (Taylor, 2008) (Fig. 4.4), and along with NFκB being implicated in maintaining basal levels of HIF-1α gene expression *in vivo* (Rius *et al.* 2008), HIF-1α has been shown to regulate some of NFκB signalling (Taylor, 2008).

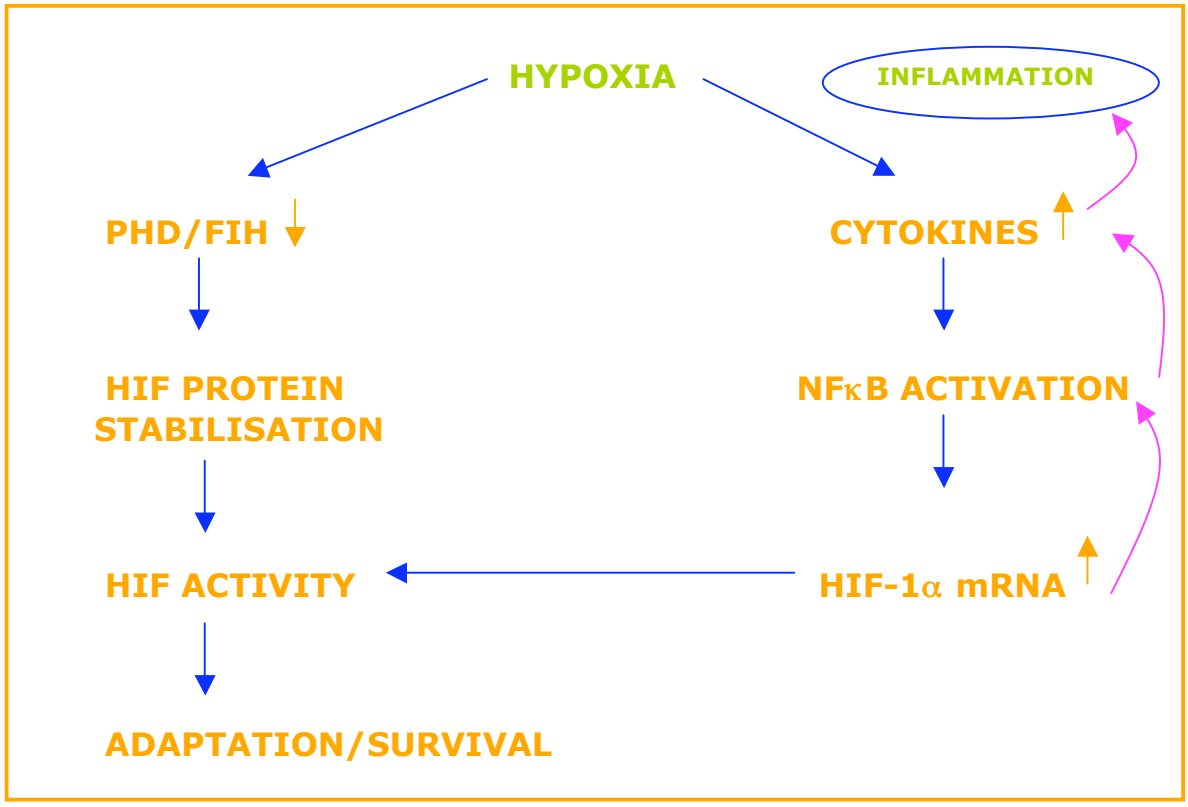

Figure 4.4 Illustration of the cross talk between HIF-1α and NFκB under hypoxia (Adapted from Taylor, 2008)

4.4.5 Upregulation of anti-angiogenic factors

A very fine balance exists between pro- and anti-angiogenic factors and the driving stimulus for new blood vessel growth that occurs when this balance is disrupted (Figg and Folkman, 2008). The upregulation of anti-angiogenic factors is largely ignored in

studies of ischaemia, which usually focus on the changes in pro-angiogenic factors that are occuring. An example is VEGF-A which has 5 isoforms, each of which differ in their degree of heparin affinity (Springer *et al.* 2007). VEGF splicing in the terminal exon results in a family of isoforms that have a 94-98% homology with the mentioned VEGF isoforms, but are antiangiogenic and known as $VEGF_{xxx}b$ (Bates *et al.* 2002). $VEGF_{165}b$ isoforms constitute large percentages of the total VEGF protein in non-angiogenic tissues (up to 82% in the colon; Ladomery *et al.* 2006), though a smaller percentage in angiogenic tissues such as the placenta (Carmeliet *et al.* 1999). Their amounts in skeletal muscle remains unknown. The balance of pro- to anti-angiogenic VEGF isoforms determines the disease state of tissue. There appears to be a splicing switch in the proximal C-terminal which increases the ratio of pro- to anti-angiogenic isoforms of VEGF, and is clearly shown to be associated with a number of diseases (Ladomery *et al.* 2006). Thus the regulation of splicing and the switch to a pro-angiogenic state, is a key event in the development of many diseases, suggesting possible reasons as to why many studies show an upregulation of angiogenic growth factor genes (Tuomisto *et al.* 2004) and proteins (Lloyd *et al.* 2003) but no capillary growth. A recent study also showed that chronic hypoxia attenuates VEGF-stimulated signalling in primary human coronary artery endothelial (HCAE) cells by down-regulating Flk-1 expression, suggesting a possible further explanation for the impaired angiogenic responses seen here (Olsezewska-Pazdrak *et al.* 2009).

4.5 Conclusions

Ligation of the femoral artery in the hindlimb of the C57BL6/J mouse for either 1 or 2 wks was insufficient to induce a significant angiogenic response in the skeletal muscle with or without the PHD inhibitor, DMOG. There were a number of setbacks which impacted on this study: the use of a potentially impure chemical to mimic the effects of hypoxia, did not show expected blood vessel growth, and it was later discovered that the strain of mouse being used may have been more resistant to ischaemic challenge when compared with other strains. Different studies utilise different ligation points on the artery, with those who placed their suture higher than used here obtaining a visual physiological retardation of hindlimb and movement. This suggests that in order to reach the potential threshold for HIF activation and a subsequent significant increase in capillary growth, the intervention needs to induce a higher degree of ischaemia. However, this is confounded by the high degree of inflammation and muscle fibre damage that may be incurred. The role that inflammation played *vs* hypoxia in this model is unknown here.

4.6 Future experiments

An important component of studying the pro-angiogenic response is looking at the anti-angiogenic factors that are also subsequently upregulated, and which may be preventing angiogenesis from occurring. An example of an anti-angiogenic factor is endothelin 1. If the intervention of ligation of the femoral artery was insufficient, an additional stress on system with DMOG may provide a sufficient stimulus in order to induce angiogenesis. Using an additional stress such as exercise may also be necessary to enable threshold levels required to stimulate blood vessel growth *via* HIF. An iliac ligation is an alternate method of limiting blood flow to the hindlimb, though may induce an increased level of ischaemia due to its higher location. Finally, it would be interesting to study these effects in the more responsive soleus muscle of the hindlimb.

Chapter 5

EXTIRPATION

5.1 Introduction

Removal of a synergist muscle will induce functional overload in the remaining muscle as a compensation for the change in load bearing. Along with a resulting increase in muscle mass, the muscle stretch created by this situation stimulates the sprouting form of angiogenesis, whereby abluminal sprouting of endothelial cells (ECs) through the basement membrane occurs (Zhou *et al.* 1998). This initiates the formation of an extended network of capillaries, maintaining blood flow to the elongating muscle fibres and providing sufficient O_2 supplies required for driving new protein synthesis to support an increase in the number of serial sarcomeres (Goldspink *et al.* 1991). There are a number of models representing how functional overload can be used to induce an increase in capillary supply and these models are extremely useful in studying the effects of, and recovery shown, following a variety of clinical situations (e.g. muscle ablation). Alongside removal of a synergistic muscle, electrical stimulation of the muscle or nerve supplying it (Egginton *et al.* 2001; Hudlicka *et al* 2003), or increased load bearing with the use of an additional weight (Gupta and Zak, 1998; Awede *et al.*1999), are all recognised models used to induce an increased fibre size and capillary growth.

5.1.2 Sensing stretch

Blood vessels are constantly subjected to haemodynamic forces such as shear stress, transmural pressure and cyclical strain that change during a cardiac cycle. Muscle stretch in capillaries is sensed primarily by stretch-activated ion channels (Lansman *et al.* 1987) on ECs which are located at the interface between the blood and the vessel wall. Arteries also sense stretch using receptors within smooth muscle cells such as TRPC6, a cation channel which is sensitive to deformation (Spassova *et al.* 2006). Any alterations in stretch or shear induce transformational changes in the vessel wall as a homeostatic mechanism to accommodate the new conditions (Lehoux *et al.* 1998), and this remodelling is characterised by altered morphology of the blood vessels. At the cellular

level, mechanical forces exert changes on the cytoskeleton, gene expression and the proliferation and survival of cells: when subjected to cyclic stretching, almost every type of cell has been found to align nearly perpendicular to the primary stretching axis (Wang *et al.* 2001) and stess fibres are known to assemble in the same direction (Shirinsky *et al.* 1989). Under elevated shear stress conditions, bovine aortic endothelial cells undergo a change in cell morphology, resulting in an increase in central stress fibres and fibronectin fibrils (Thoumine *et al.* 1995a) and a change in the structure and composition of the extracellular matrix (ECM) (Thoumine *et al.* 1995b). It is assumed that similar mechanisms facilitate mechanotransduction of stretch.

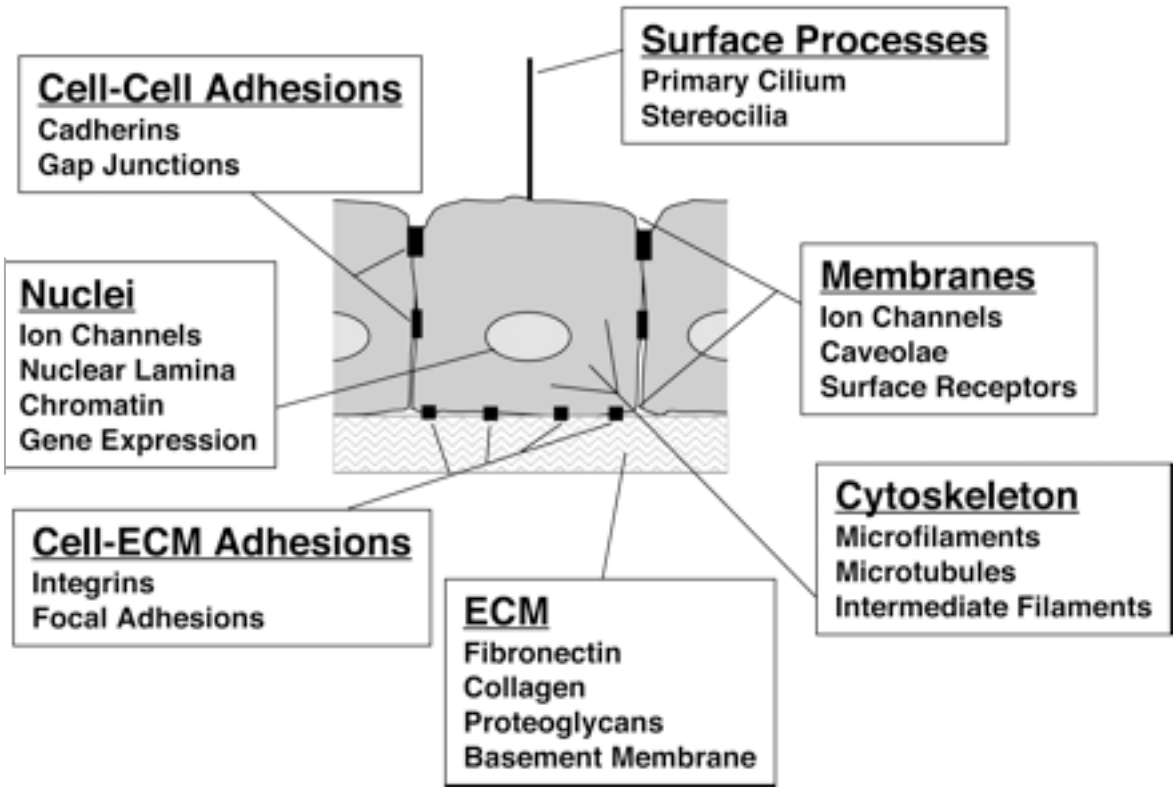

Figure 5.1 Mechanisms of mechanotransduction within and between endothelial cells (From Ingber, 2006)

The cytoskeleton is thought to be the main sensor of mechanical stretch, being responsible for transmitting signals throughout the cells (Ingber, 2006). Stretch-activated ion channels, integrins, growth factor receptors and the ECM, among numerous other structures, have all been shown to contribute to the mechanotransduction response (Ingber 2006; Lehoux *et al.* 1998) (Fig. 5.1). One proposed model for signal transmission is that stretch-sensitive ion channels undergo conformational change when the membrane bilayer distorts. These channels are relatively non-selective, and it was shown that stretch induced an increase in intracellular calcium and other divalent cations (Lansman *et al.* 1987, Davis *et al.* 1992). Tension-dependent changes in the orientation of collagen causes distortion of interconnected basement membrane scaffolds (Fig. 5.2), and this in turn induces changes in the cytoskeleton within associated endothelial cells.

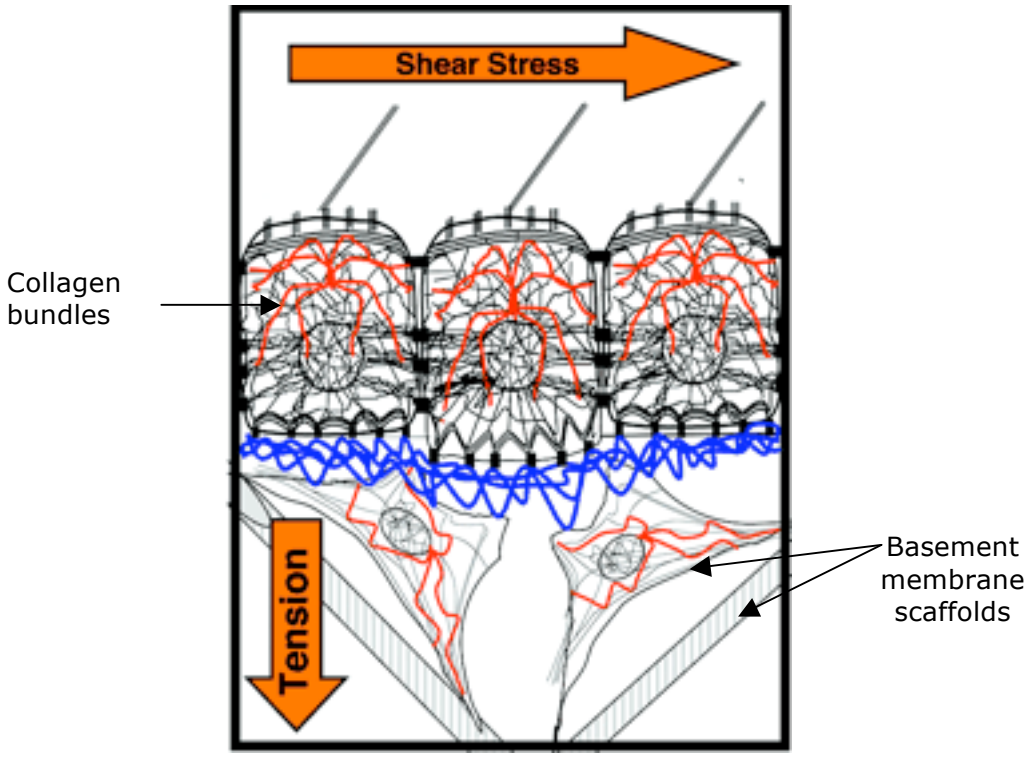

Figure 5.2 Illustration of cellular mechano-responsiveness and connections between the ECM, cells, cytoskeletal networks, and nuclei: changes are channelled through the cytoskeleton to basal cell-ECM adhesions. Red and blue lines represent tension-dependent changes in cytoskeletal structure. (From Inger, 2006)

5.1.3 Endothelial cell gene responses and capillary network remodelling

5.1.31 Endothelial cells

The mechanical stretch imposed on ECs following muscle activity, or in this case overload, results in upregulation of a number of genes. The MAP kinase cascade is a major pathway through which signals derived from growth factors and mechanical strain are transduced into regulation of gene expression and protein synthesis. This pathway involves sequential phosphorylation and activation of cytoplasmic protein kinases (Lehoux *et al.* 1998). Diverse pathways link mechanical strain to MAP kinase activation in vascular cells, and it is thought that integrins are likely involved in these transmission pathways. Castilla *et al.* (1999) found an increase in VEGF mRNA in bovine aortic endothelial cells, following disruption of intercellular junctions caused by mechanical stretch. Matrix metalloproteinase 2 (MMP-2), a protein involved in the breakdown of extracellular matrix, has been shown to be upreguated *via* the ERK1/2 and JNK pathways (Milkiewicz *et al.* 2007), both of which are critical regulators of cell differentiation, cell physiology and neuronal function.

5.1.3.2 Capillary network remodelling

Capillary network remodelling is essential to enable physiological adaptation following functional overload. Two morphologically distinct forms of angiogenesis: sprouting and splitting, induced by contrasting mechanical stimuli, both lead to the formation of fully functional mature capillaries (Hudlicka, 1998). Muscle stretch and overload stimulates abluminal sprouting of endothelial cells through the basement membrane. These sprouts then grow and fuse with other capillaries to form functional anastomoses (Zhou *et al.* 1999). Egginton *et al. (*2000) have shown that the basement membrane (BM) degradation seen here is unique to this form of angiogenesis, occurring only at sprout tips. Following this disruption, the ECs migrate through the gap that is formed into the interstitium where they develop central lumens and eventually form anastomoses with

other vessels. This type of migration is seen in response to an external (abluminal) stimulus; an internal (luminal) stimulus, such an increased shear stress induced by hyperaemia (as a result of exercise or hypoxia, for example) mediates the intraluminal splitting form of angiogenesis which occurs without BM breakdown or sprouting.

5.1.3.3 The role of non-hypoxically inducible HIF in stretch-induced angiogenesis

These different forms of angiogenesis are accompanied by a differential expression pattern of angiogenic mediators (Williams *et al.* 2006b). For example, both stretch and shear stress increase VEGF, while only stretch increases MMPs (Rivilis *et al.* 2002) and only shear stress increases nitric oxide synthase (NOS) activity (Williams *et al.* 2006a). It was recently shown that the expression of HIF-1α and HIF-2α can also be modulated by mechanical forces, along with the known stimulus of low O_2 tension (Richard *et al*. 2000; Kim *et al.* 2002). Milkiewicz *et al.* (2007) interestingly showed that both HIF-1α and HIF-2α, on a protein and mRNA level, played a core role in stretch-induced angiogenesis, though not shear-induced splitting angiogenesis, confirming a role noticed earlier for HIF-1α (Williams *et al.* 2006b). Furthermore, using real-time PCR, Chang *et al.* (2003) showed that levels of HIF-1α mRNA increased 2.1 fold in cultured vascular smooth muscle cells after cyclical stretch for 4 hours.

5.1.4 Skeletal muscle hypertrophy and capillarity

The structural integrity of the capillary wall is such that capillary distensibility is largely determined by support provided by the tissue in which it is located (Kindig *et al.* 1998). In skeletal muscle, capillaries appear not to change a great deal in reponse to changes in perfusion pressure (Bosman *et al.* 1995) and it has been postulated that this is due to the structural interactions of the surrounding muscle, coupled with capillary-myocyte struts (Kindig *et al.* 1998). As sarcomere length increases, the tortuosity of capillaries is lowered as they become more highly aligned wih the longtudinal muscle fibre axis. James (1981) showed that capillaries in hypertrophied muscle become more highly

orientated and further stretching most likely results in a decrease in the luminal diameter (Kindig *et al.* 1998). A multitude of studies have addressed the issue of whether the contortions of these blood vessels are sufficient to induce changes in the blood flow to the muscle, thus affecting O_2 delivery (Poole *et al.* 1997; Kindig *et al.* 1999). It has been shown that resting and maximal levels of blood flow following 2 weeks of extirpation are similar, suggesting that increased blood flow is not responsible for initiating expansion of the capillary bed following overload, and that the subsequent increase in capillary supply normalises any changes in blood flow arising (Egginton *et al.* 1998). This adds further support to the finding that HIF can be upregulated under normoxic conditions.

It has been demonstrated that using a mouse model for extirpation mirrors changes seen in the well-studied rat model (Williams *et al.* 2006a), sufficiently for conclusions to be drawn based on comparisons with other studies. It has previously been demonstrated that extirpation of the TA results in an increase in the C:F ratio of the remaining EDL muscle (Egginton *et al.* 1998). Inter-strain variation in mice has not been studied under conditions of extirpation, although this was examined in the femoral artery ligation model in CHPT 4 with no obvious differences observed. However, it was thought to be beneficial to explore differences between the C57Bl6/J and C57Bl10/J strains of mouse, these being most commonly used in studies of this kind, with results often used interchangeably on the assumption that there are no strain-specific response to stretch. Gene array analysis (Wlliams *et al.* 2006) showed upregulation of HIF-1α, suggesting that it may be responsible for driving capillary growth under normoxic conditions. However, mechansims governing its regulation under conditions of stretch may be different to those under hypoxia. Whether DMOG, the oxoglutarate analogue which works by inhibiting prolyl-hydroxylases (PHDs) 1–3 and factor inhibiting HIF (FIH), has the same effect on HIF levels and downstream effects under conditions of stretch, in correspondence with the already known conditions of hypoxia (Milkiewicz *et al.* 2005), was investigated. This model was used to determine the efficiency of this drug in

enhancing muscle capillarity following removal of a synergist muscle in two different strains of mouse.

5.2 Methods

5.2.1 Study design: extirpation

The procedure involved unilateral surgical removal of the tibialis anterior (TA) muscle in the mouse hindlimb, then re-suturing the skin to allow recovery for 1 or 2 wks, resulting in overload of the synergistic extensor digitorum longus (EDL) muscle. Experiments were performed on groups of C57Bl6/J and C57Bl10/J mice (n=6 in each experimental group). Each group received DMOG (8mg.0.5ml^{-1} saline) (CHPT 2.1) *via* i.p. injection every other day, with the initial injection 2 days before surgery.

5.2.1.1 Surgery

Mice were anaesthetised under aseptic conditions starting with 5% isofluorane and decreasing to 2.5% with O_2 as a carrier. 0.2ml.100g^{-1} Temgesic® was given prior to surgery for postoperative analgesia. An incision was made through the skin at the base of the TA tendon and the scalpel used to cut through the skin and fascia, all the way to the top of the muscle. Forceps were used to free the tendon from surrounding fascia and lift it, allowing room to cut it free with a scalpel blade. The muscle was lifted as high as possible without inflicting any damage and excised close to the top with one clean slice. The end of the cut muscle was put onto the muscle stub to stem the bleeding and induce coagulation. Two drops of antibiotic (300mg.ml^{-1} Depocilin®) were applied and any excess removed after allowing absorption for a short time. The wound was sealed with 4 sutures (6,0 vicryl monofilament) and any dried blood removed to minimise the risk of infection or irritation for the animal. Mice were allowed normal access to food and water to aid recovery and were sacrificed after the experimental period *via* cervical dislocation.

5.2.1.2 Tissue processing

EDL muscles from surgically affected limbs were taken (CHPT 2.2) and stored on corks at -80°C after being snap-frozen in isopentane cooled in liquid nitrogen (CHPT 2.3). Tissue

was sectioned and stained (CHPT 2.3) and capillary and fibre numbers (C:F) counted as described in CHPT 2.4, using lectin staining.

5.3 Results

5.3.1 Capillary changes in skeletal muscle following extirpation surgery

5.3.1.1 Lectin staining

Extirpation surgery was initially conducted on C57Bl6/J mice over a period of 2 weeks, with and without DMOG. There was a significant increase between the control and control DMOG *vs.* extirpated leg without DMOG (Table 5.1), with an insignificant yet noticeably raised capillary to fibre ratio (C:F) in the extirpated leg with DMOG. There was a significant change in the mass of EDL muscle in the extirpated leg compared to control (Table 5.3). With the exception of the capillary density (CD) in the 2 wk no DMOG group which showed a significant increase when compared to control and control DMOG, the mean fibre are (MFA) or CD did not change significantly from control values (see Chapter 3 for a photo of capillary lectin staining).

Experiment	**C:F**	**CD** (cap.mm^{-2})	**MFA** (μm^2)	**RM$_{EDL}$ (%)**
Control	1.26 ± 0.02	885 ± 67	1521 ± 102	0.031± 0.002
Control D	1.26 ± 0.05	937 ± 118	1363 ± 86	0.030± 0.003
2 wk no D	1.36 ± 0.05 §*	1118 ± 76 §*	1262 ± 81	0.062± 0.002§*
2 wk D	1.30 ± 0.03	923 ± 94	1345 ± 234	0.041± 0.002

Table 5.1 Mean C:F, CD and MFA ±SEM for the EDL muscle in the extirpated leg in C57Bl6/J mice (n=6). §=*P*<0.05 vs. control, *= *P*<0.05 vs. control DMOG as determined by ANOVA with Dunnetts post-hoc test, D=DMOG.

Surgery was repeated on C57Bl10/J mice over a period of 2 weeks with and without DMOG. There was a significant increase between control and extirpated C:F values for mice with and without DMOG (Table 5.2). There was a significant increase in muscle

mass between the extirpated *vs.* control muscle (Table 5.3), though no significant changes in MFA or CD in this study.

Experiment	**C:F**	**CD** (cap.mm^{-2})	**MFA** (μm^2)	**RM$_{EDL}$ (%)**
Control	1.23 ± 0.06	990 ± 43	1427 ± 51	0.030±0.001
2 wk no D	1.43 ± 0.04 §	1095 ± 22	1308 ± 40	0.042±0.002§
2 wk D	1.36 ± 0.02§	907 ± 44	1514 ± 81	0.041±0.001§

Table 5.2 C:F, CD and MFA for the EDL muscle in the extirpated leg in C57Bl10 mice (n=6) §=*P*<0.05 vs. control, as determined by ANOVA with Dunnetts post-hoc test (mean±SEM shown, D=DMOG)

	C57Bl6/J Mass of EDL (g)	**C57Bl10/J Mass of EDL (g)**
Control mean±SE	0.009g±0.0004	0.009±0.0007
DMOG-treated mean±SE	0.009±0.0002	0.011±0.0007
Non-DMOG treated mean±SE	0.010±0.0003	0.01±0.0006

Table 5.3 EDL mass (g) in C57Bl6/J and C57Bl10/J mice (n=6) treated with and without DMOG (mean±SE, determined using descriptive statistics with excel. No significant difference as determined by ANOVA with Dunnetts post-hoc test)

5.4 Discussion

The aim of this study was to determine whether a differential angiogenic response would be seen in either of 2 strains of mice (C57Bl6/J and C57Bl10/J) under conditions created by synergist extirpation-induced muscle overload. The second aim was to determine if chemical manipulation of the PHDs (affecting the HIF pathway) under these conditions would have a similar effect to that seen under hypoxia, of enhancing HIF availability and downstream capillary growth.

A limiting factor when using extirpation as a method to induce angiogenesis is that a level of inflammation will be present following the invasive nature of the surgery, along with factors involved in wound healing. It has been shown that gene responses 3 days post-surgery is the earliest point at which no clinical signs of inflammation are seen (Williams *et al.* 2006b). Zhou *et al.* (1999) found no histological evidence of inflammation 1 wk following extirpation surgery, suggesting that any angiogenesis at this point is likely to be as a result of muscle stretch as opposed to other conflicting factors involved in inflammation.

5.4.1 Effects of extirpation in the hindlimb

Most studies on extirpation are based on rat models, with the first mouse model being demonstrated by Williams *et al.* (2006a). Their study confirmed that the mouse model can be used comparatively with previous data reported for the rat, allowing cross-species comparisons.

5.4.1.1 Removal of a synergist muscle stimulates capillary growth

Extirpation in the hindlimb of the C57Bl6/J mouse resulted in a significant increase in capillary growth in both non- and DMOG-treated groups of animals. The increase in C:F ratio seen following extirpation surgery is in accordance with other studies (Egginton *et al.* 1998; Zhou *et al*. 1999; Williams *et al.* 2006a). Repetition of the surgery on the C57Bl10/J exhibited a similar pattern: the increase in C:F ratio was significantly higher

compared to control in both treated and untreated animals, though still lower compared to previous values of 1.54 seen in this strain (Williams *et al.* 2006a). The change in the C67Bl10/J mouse was greater than that seen in the C57Bl6/J mouse (16.3% *vs.* 7.9% increase in non-DMOG treated animals and 10.6% *vs.* 3.2% respectively, in the DMOG-treated animals). Williams *et al.* (2006a) found that the peak rate of angiogenesis occurred between 3 and 7 days in the C57Bl10/J mouse, with only a modest increase between 14 and 28 days. Thus, capillary growth seen here most likely reflects near maximum extent of growth that may occur under these conditions.

The greater change seen in the C57Bl10/J compared to the C57Bl6/J mice illustrates that inter-strain differences do exist, although subtle and statistically insignificant. A differential response may be as a result of differences in fibre type composition: it has been suggested that glycolytic fibres have a greater capability for angiogenesis, possibly due to their greater girth which is usually supplied by fewer capillaries, thus making them more susceptible to hypoxia (Deveci *et al.* 2001). This is supported by data from Ahmed *et al.* (1997) who showed that the capillary supply to human skeletal muscle was scaled with respect to fibre size, though noted that this was independent of fibre type. Differences in fibre type could easily be explored, though no data on differences in composition is presently available.

5.4.1.2 Changes in muscle mass associated with extirpation surgery

In both cases an increase in EDL muscle mass, although not significant, was observed. Overload of the EDL enhances protein synthesis and this is correlated with an increase in muscle fibre diameters, a minor change in fibre type, and only a modest change in the number of fibres present (Hudlicka *et al.* 1982; Egginton *et al.* 1998; Badr *et al.* 2003). There is also an increase in collagen deposition in muscles subjected to stretch during limb lengthening (Laurent *et al.* 1985), as also seen with electrical stimulation (Hansen-smith *et al.* 1996), suggesting this may be a common response to increased muscle

activity.

5.4.2 Oxygen supply and demand

5.4.2.1 Upregulation of protein synthesis and maintenance of blood flow

Protein metabolism is a metabolically expensive process and is upregulated under conditions following extirpation where the number of serial sarcomeres is increased to compensate for the increase in load bearing (Goldspink *et al.* 1995). However, the O_2 demand enabling this to occur is not thought to be excessive, suggesting that O_2 is not the limiting factor. As mentioned above, it has been shown that changes in fibre type and size are only subtle (Hudlicka *et al.* 1982; Egginton *et al.* 1998; Badr *et al.* 2003), adding support to the notion that changes in metabolism and global O_2 consumption are minimal following removal of a synergist muscle, and thus hypoxia is not a stimulating factor for capillary growth here. Furthermore, Egginton *et al.* (1998) showed that resting and maximal levels of blood flow following 2 wks of extirpation are similar to controls, suggesting that O_2 delivery is maintained following surgery and thus is not the major factor initiating new blood vessel growth. The recent observations that HIF can be upregulated under non-hypoxic conditions along with the already known hypoxic stimulus, lends support to the notion that HIF-stimulated blood vessel growth under stretch can occur under normoxic conditions.

5.4.2.2 Chemical manipulation of the HIF pathway with DMOG: Evidence for the upregulation of HIF-1α and HIF-2α under non-hypoxic stretch

Richard *et al.* (2000) was one of the first to show an upregulation of HIF-1α protein *in vitro* in vascular smooth muscle cells (VSMCs), under non-hypoxic conditions of the introduction of fetal calf serum and serotonin, independently, followed soon after by Kim *et al.* (2002) who illustrated the protein presence under mechanical strain in non-hypoxic rat myocardium *in vivo*. Furthermore, Chang *et al.* (2003) showed that HIF-1α mRNA also increased under conditions of non-hypoxic stretch *in vitro* in rat VSMCs. These

studies provide clear evidence for the presence of HIF-1α under conditions of stretch, and under conditions whereby O_2 supply is maintained (see above), allowing the assumption that chemical manipulation of the PHDs and thus HIF levels (DMOG) should have a similar effect to what is seen in ischaemia, in facilitating the growth of new vessels under conditions of overload. As is evident here, the desired effect is not seen, in fact, the opposite trend was observed.

5.4.3 DMOG

5.4.3.1 Multiple targets of DMOG

DMOG not only targets PHD1-3, but the whole of the prolyl 4-hydroxylase (PHD) family. Of these, 2 animal PHD families are known today: collagen PHDs (also known as C-P4Hs), endoplasmic reticulum luminal enzymes that have a central role in the synthesis of all collagens, and HIF-P4Hs, nuclear and cytoplasmic enzymes that play a key role in the response of cells to hypoxia (Koivunen *et al.* 2007). The C-P4Hs act on Xaa-Pro-Gly sequences in collagens and more than 20 collagen-like proteins, leading to their degradation. Collagen deposition is an important part of new skeletal muscle remodelling (Winter and Page, 2000) and interference in this process may influence fibre lengthening and capillary formation: collagen type IV also forms an important part of the basement membrane surrounding the capillary. It is therefore possible that DMOG interfered with the collagen synthesis pathway and thus hindered the subsequent development of muscle fibres and capillaries.

5.4.3.2 The confounding factor of DMOG efficiency

Investigations made into the efficiency of the DMOG used in these experiments revealed that the initial batch used in CHPT 4 was chemically modulated when compared to an initial batch. The newly synthesised batch, from the same source as the original, was used in these extirpation experiments. Results obtained from CHPT 4 suggest that the recorded discrepancies between the two batches may be insignificant based on the fact

that the C:F ratio in the hindlimb following ligation of the femoral artery in CHPT 4 appeared to show similar changes following the use of either batch. It is possible that the threshold required to stimulate HIF was not reached, and thus augmentation of the HIF system to its full potential was not achieved. As suggested previously, DMOG may also work differently in different skeletal muscles, depending on fibre type composition and on the amount or type of PHD enzymes present, which is known to be variable in different tissues. However, differential expression among skeletal muscle has not been explored as yet.

5.5 Conclusions

Extirpation in the hindlimb of both the C57Bl6/J and C57Bl10/J strain of mouse was successful in inducing an increased capillary growth in the EDL muscle, causing subtle changes in muscle mass. This effect was seen to a greater magnitude in the C57Bl10/J strain, suggesting that inter-strain differences may be an important variable to consider when comparisons between models and findings are used. A similar finding was observed in the ligation model (CHPT 4), although the general trend was the same. DMOG was predicted to enhance the capillary supply to a greater extent than extirpation alone. However, treated animals seemed to express lower C:F ratios than those without DMOG, suggesting that DMOG is having an effect on collagen synthesis in the overloaded muscle, or that the mechanism by which HIF is acting under conditions of stretch is different to those under hypoxia.

5.6 Further experiments

It would be interesting to further examine cross strain variability in the response to extirpation using a variety of strains, including those that have already been studied such as Balb/C, using muscle fibre type staining as one method of investigating what differences may exist. Enhancing the degree of overload achieved could be explored by removing a different muscle such as the plantaris. This was done by Degens *et al.* (1992) who observed a much greater 32% increase in muscle mass. It would be useful to develop a chemical inhibitor that specifically targeted each of PHD1-3 to overcome any confounding factors, such as interference with non-HIF pathways. Using knockout mice to illustrate which of the PHDs are most important in this model would, along with a gene array analysis, be a useful track to investigate in order to determine underlying differences in phenotypes. Accordingly, this has been further explored in CHPT 6.

Chapter 6

GENE ARRAYS

6.1 introduction

Gene microarray technology has made it possible to characterise the RNA expression of thousands of genes across numerous tissue samples and under varying conditions, and is a powerful technology that offers comprehensive profiling of gene expression. The benefits of being able to group together collections of genes that may previously have been unknown to operate under postulated conditions are only just being realised.

6.1.1 Differential involvement of PHDs in capillary growth following muscle overload

HIF was originally known to become active under conditions of hypoxia but it has recently been shown that non-hypoxic conditions such as stretch, e.g. induced by removal of the synergist muscle in the hindlimb, can also upregulate HIF on both an mRNA and protein level (Milkiewicz *et al.*, 2005; Richard *et al.*, ; Williams *et al. 2006*). Under normoxia, modification of the ODD within the HIF protein by members of the 2-oxo-glutarate-dependent dioxygenase superfamily (PHD 1-3) inhibits HIF activity. Appelhoff *et al.* (2004) showed that each of the three isoforms of PHD contributes in a non-redundant manner to the regulation of both HIF-1α and HIF-2α, with each expressing a different specificity for hydroxylation sites on the HIF-α subunit, thus modifying the degree and extent of HIF activation. PHD 1-3 have differential localisation patterns, exhibiting abundance in specific tissues, further supporting findings that they are not equally required *in vivo* (Hirsila *et al.* 2003).

6.1.2 Genetic manipulation of mouse models

6.1.2.1 Knockouts

A fundamental goal of biological science is to determine the physiological function of identified proteins. This has been done in a multitude of ways. *In vitro* studies provide an appropriate way of manipulating and studying a protein in a more simple setting,

though it is difficult to draw conclusions when such a large, unknown proportion of the system is missing. A range of inhibitors specific to the PHD pathway are available, and have been trialled in a number of animal and cell models. Ethyl 3,4-dihydroxybenzoate (EDHB), 6-chlor-3-hydroxychinolin-2-carbonic acid-N-carboxymethylamid (S956711) and L-mimosine (L-mim) all demonstrated similar effects to hypoxia by inducing HIF-1α in both human and rodent cells (Warnecke *et al.* 2003). However, the unwanted and unknown side effects of these chemicals, and manipulation of pathways without being fully aware of possible redundancies in the system, are a disadvantage.

Developed over two decades ago, genetically modified animals provide a different approach to gene manipulation compared to methods already employed, allowing one to study the effects of redundancy whilst having the assurance that only the specified gene has been interfered with (but still with the possibility of compensation), and that no unwanted chemically-induced side effects are present. The murine model is distinctly beneficial over classical genetic subjects (drosophila, yeast etc.) as mice are more closely related to humans from a physiological perspective, and mouse embryos can be manipulated with ease when compared to other rodent models (Picciotto and Wickman, 1998). Genetically manipulated models such as the knockout (K/O), whereby a gene or genes are made inoperative by the use of a plasmid or DNA construct, are advantageous as they provide greater definition and clarity of the *in vivo* function of molecules that have been studied *in vitro*, and the resulting phenotypes can be studied at many levels.

6.1.2.2 PHD knockout mice

Recent studies of knockout mice have unveiled some interesting phenomena occurring when a single PHD is ablated. PHD1 knockout mice have been shown to lower O_2 consumption in skeletal muscle by reprogramming glucose metabolism from oxidative to more anaerobic ATP production (Aragones *et al.* 2008), resulting in impaired oxidative muscle performance through enhanced protection of the myofibres against ischaemia. The neuronal phenotype of PHD3 knockout mice was studied and shown to exhibit

abnormal sympathoadrenal development and systemic hypotension (Bishop *et al.* 2008). PHD2 K/O mice are embryonically lethal (Schneider *et al.* 2007), although heterozygous mice have been studied and shown to improve tumour perfusion and oxygenation, alongside inhibiting tumour cell invasion and metastasis (Mazzone *et al.* 2009).

PHD2 is thought to be the main PHD O_2 sensor under hypoxic conditions (Berchner-Pfannschmidt *et al.* 2008), though due to its embryonic lethality as a knockdown, PHD1 and PHD3 K/O mice were used alongside wildtype animals in a model of extirpation, which has been shown to induce the HIF pathway *via* stretch as opposed to hypoxia (Williams *et al* 2006; Mikliewicz *et al.* 2007), to establish relationships between genomic and functional responses in skeletal muscle following genetic manipulation of molecular pathways leading to HIF-1α stability. The aim was to elucidate whether groups of genes were differentially regulated and to identify common pathways within each model, to help elucidate whether complementary or redundant routes exist.

6.2 Methods

6.2.1 Deriving knockouts

Rederivation was perfomed by staff at the animal unit in Birmingham (BMSU). Females were used for rederivation at about 5 wk old: they were given an i.p. injection of Pregnant Mare's Serum Gonadotrophin (PMGS) which mimics FSH. Two days after they were given a second injection of Chorulon (mimics LH) and then mated with male PHD1 mice (gift of Prof. C. Pugh, University of Oxford). The following day, mice were checked for vaginal plugs, culled and the embryos removed from the oviduct of the mice. Clusters of embryos were put into M2 media and hyaluronidase added to remove cells that hold the embryos together. They were then collected and washed 3-5 times before being cultured overnight at 37°C in 5% CO_2. The following day, embryos were transferred into the oviduct of a pseudo pregnant female which had been mated with a sterile male. The resultant litter was weaned and the surrogate female screened for viruses. Following this, the litters were removed from the isolator and sent for breeding to produce a colony.

6.2.2 Genotyping (carried out at the university of Birmingham, Department of Physiology)

This was used to determine the genotype of the knockout mice by extracting the DNA, using PCR to amplify samples, which were run on an agarose gel to identify the products and was performed in Birmingham.

6.2.2.1 Protocol

Ear clippings were placed in a 1.5ml Eppendorf with 0.5ml lysis buffer (10 mM Tris-HCl (Sigma-Aldrich, T5941) pH 8.0, 50mM KCl, 0.3% Tween-20 (Sigma-Aldrich, P5927), 0.3% NP40 (Sigma-Aldrich, NP40), 1 mM Ethylenediaminetetraacetic acid (EDTA, Sigma-Aldrich, 43178) and 16µl of 15mg.ml^{-1} Proteinase K (Roche, 03 115 887 0010) (final

concentration of 500µg.ml^{-1}) added. Samples were incubated at 55°C overnight then vortexed to break up remaining tissue. Tubes were spun at 17,900g for 10 min to pellet undigested tissue, the supernatant removed and placed into a newly labelled Eppendorf. All reagents were kept at 4°C from this point. 500µl phenol:choloroform (Sigma-Aldrich, 77617) was added (in a fume hood) and the solution vortexed. Tubes were centrifuged at 17,900g for 10 min, the upper layer removed and 500µl of cold chloroform (Sigma-Aldrich, C2432) was added. After vortexing, layers were allowed to separate (5-10min), then the upper layer removed and kept. 500µl cold isopropanol (Sigma-Aldrich, l9516) was added, the tube inverted then centrifuged at 17,900g for 10 min and the supernatant discarded. 800µl of 70% ethanol (Sigma-Aldrich, 459836) was added and the tubes inverted and flicked to unstick the pellet from the wall. Samples were centrifuged for 10 min at 17,900g, supernatant removed and discarded, then re-spun at 17,900g for 1 min to allow easier removal of excess liquid. The pellet was air dried at RT for 5-10min and 100µl molecular biology grade water (Fisher Scientific, BP-2484-100) added though not mixed, but left at 37°C in the water bath for half an hour. Samples were mixed by aspirating with a micropipette before use. DNA was stored for short periods at 4°C.

6.2.2.2 Primers for PCR

To amplify the gene of interest *via* PCR, primer sequences were provided by the Wellcome Laboratory in Oxford and made by Alta Bioscience (University of Birmingham).

PHD1 knockout and wild type mouse primers:

WT allele reaction:

With oligos PHDTFOR2 and PHD1NREV;
Wt mouse = band at 900 bp, heterozygous mouse = no band

PHDTFOR2: 5'- AGT CCC TCT GGT TCT AGA GTG GGG –3'
PHD1NREV: 5'- TCT CAG CAT CTC ATC ACT CCC CTG –3'

Recombinant allele reaction:
With oligos NEOPHD1N and PHD1NREV;
Wt mouse = no band; heterozygous = 590 bp

NEOPHD1N: 5'- TTG CAT CGC ATT GTC TGA GTA GGT GT –3'
PHD1NREV: 5'- TCT CAG CAT CTC ATC ACT CCC CTG –3'

PHD3 knockout and wild type mouse primers
WT allele reaction:
With oligos mPHD3-1 and mPHD3-2;
Wt mouse = band at 357 bp, heterozygous = no band

mPHD3-1: 5'- CGA GAT GCC TCT GGG ACA CAT CAT –3'
mPHD3-1: 5'- GGA CCG CTC CTT GAC ATA GTA TTT –3'

Recombinant allele reaction:
With oligos NEO0770 and NEO1360;
Wt mouse = no band; heterozygous = band 590 bp

NEO0770: 5'- CGA CGG GCG TTC CTT GCG CAG –3'
NEO1360: 5'- CGG ATC GAT CCC CTC AGA AGA AC –3'

6.2.2.3 PCR protocol

A total of 20µl mix per tube was made up of 0.2µl of each primer (4pmol.µl^{-1}), 1µl RedTaq (1unit/µl: 1 unit incorporates 10 nmol of total dNTPs into acid-precipitable DNA), 2µl 10x PCR buffer (100 mM Tris-HCl, pH 8.3, 500 mM KCl, 11mM $MgCl_2$ and 0.1% gelatin: both RedTaq and buffer provided by Sigma-Aldrich D4309), 0.5µl deoxynucleotide (dNTP) (10 mM each of UltraPure dATP, dCTP, dGTP and TTP, Sigma-Aldrich, D7295) and 1µl of cDNA, brought to a final volume of 20µl with nuclease-free water (Fisher Scientific, BP2484-100). Samples were denatured by heating to 95°C for 1 min, followed by 30 cycles of: 95°C for 30 s, 63°C for 30 s, and 72°C for 2 min. Samples remained at 72°C for 10 min and were then held at 4°C until use.

6.2.2.4 Gel electrophoresis

The products of the PCR were run on a 2% agarose gel (made with 1X TAE buffer, see below) alongside a 1 Kb Plus DNA Ladder (Invitrogen SKU# 10787-018) to determine whether the gene of interest was present.

6.2.2.4.1 Solutions

50x TAE buffer (1L): 1M glacial acetic acid (Sigma-Aldrich, A9967), 0.5M EDTA pH 8.0 (Sigma-Aldrich, 43178), 2M TRIZMA base (Sigma-Aldrich, T1503).

6.2.2.4.2 Protocol

6g of agarose (Sigma-Aldrich, A9539) and 300ml of 1xTAE buffer were mixed then microwaved for 1 min to dissolve the agarose, then left to cool. 3µl ethidium bromide, (at a concentration of 10mg.ml^{-1}, Sigma-Aldrich, E1510) was added and swirled to mix, making a concentration of 1µl.100ml^{-1}. The gel was poured into a tank of appropriate size, a comb inserted, and left to set for 20-30 min. The gel holder was put into a tank filled with 1x TAE buffer, covering the gel by at least 2mm. The first well was loaded with 5µl marker and the remaining wells with 12µl of PCR samples. The gel was run at 100V for 20 min, then visualised using UV light and a computer with a gel-imaging device (Gene Genius Bio Imaging System with the Gene Snap programme).

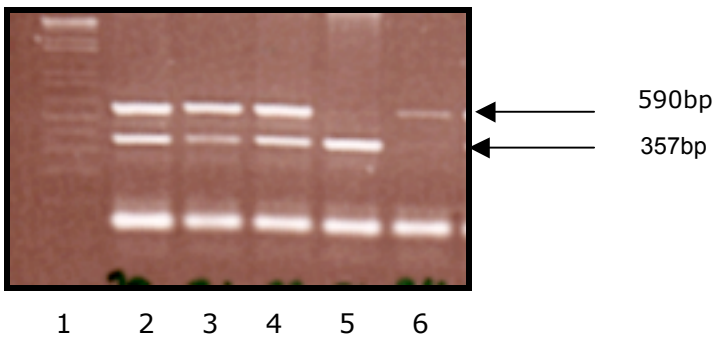

Figure 6.1 Illustration of genotyping results run on a gel following PCR: lane 1 = ladder, lane 2-4 = heterozygotes, lane 5 = wildtype (WT) (357bp), lane 6 = PHD3 K/O (590bp)

6.2.3 Study design: PHD knockouts

PHD1 K/O, PHD3 K/O and wild type (WT) mice (n=3 in each group) underwent unilateral extirpation surgery as described (CHPT 5.2.1.1) and were then sacrificed by cervical dislocation after 1 wk. EDL muscle from the surgically affected leg was removed for analysis (see below).

6.2.3.1 Tissue processing

EDL muscles from ipsilateral limbs were taken (CHPT 2.2) and stored on corks at -80°C after being frozen in isopentane cooled in liquid nitrogen (CHPT 2.3), or directly snap-frozen in Eppendorf tubes in liquid nitrogen. Tissue was sectioned and stained (CHPT 2.3) and capillary and fibre numbers (C:F) counted as described in CHPT 2.4, using lectin staining.

6.2.4 Gene arrays

6.2.4.1 RNA extraction

See Methods 2.5 for Qiagen RNA extraction and test for purity.

6.2.4.2 Gene arrays (carried out at the Wellcome Laboratories in the University of Oxford)

RNA quantity was measured using a NanoDrop ND-1000 spectrophotometer (NanoDrop Technologies, Wilmington, DE) and RNA quality checked using RNA6000 Nano Assay on Agilent bioanalyzer 2100 (Agilent Technologies, Santa Clara, CA). An RNA Integrity Number (RIN) above 7 indicates that the sample is acceptable, along with demonstrating that clear 28S and18S bands are present.

Commercially available high-density oligonucleotide arrays, from Illumina Genome-Wide Expression BeadChips (Mouse Ref-8 v2, Illumina, San Diego, California, USA) were used with 25697 probes representing 18118 Mouse transcripts. In brief, 500ng of total RNAs were reverse transcribed to synthesise first- and second- strand

complementary DNA (cDNA), purified on spin columns, and *in vitro* transcription to synthesise biotin-labelled complementary RNA (cRNA). A total of 750ng of biotin-labelled cRNA was hybridised to Mouse Ref-8 Expression BeadChip (Illumina Inc., San Diego, CA) at 58°C for 18 h. The hybridised BeadChip was washed and labelled with streptavidin-Cy3 according to the manufacturers protocols. Chips were scanned with Illumina BeadScan, and scanned images imported into BeadStudio 3.2.6 (Illumina Inc) for analysis.

A list of differentially expressed transcripts was generated and standard criteria applied (see results 6.3.1.2). The following comparisons were made: (a) WT EXT *vs.* WT, PHD1 K/O *vs.* WT, PHD1 K/O EXT *vs.* PHD1 K/O, PHD1 K/O EXT *vs*. WT EXT, and PHD1 K/O EXT *vs.* PHD3 K/O EXT (WT=wildtype, EXT=extirpation, K/O=knockout). Microarray data was interrogated with reference to gene ontology (GO) databases which describe gene products in terms of their associated biological processes, cellular components and molecular functions, and KEGG pathways, a collection of manually drawn pathway maps looking at molecular interaction and reaction networks for metabolism, genetic information, cellular processes and human diseases (among others) using the Database for Annotation, Visualization and Integrated Discovery (DAVID).

6.3 Results

6.3.1.1 Changes in capillarity

There was no significant difference between the capillary to fibre ratio (C:F) of WT EXT and PHD1 K/O mice *vs* WT mice (Table 6.1). Capillary density (CD) was significantly raised in both PHD K/O EXT groups, along with PHD3 K/O mice alone. The mean fibre area (MFA) was significantly lowered in all K/O and K/O + EXT animals. Mean body mass for WT animals was 29.1 ± 1.4g, for PHD1 K/O was 32.9 ± 3.2g, and for PHD3 K/O was 32.3 ± 7.2g. Mean EDL mass of extirpated leg was 16.0 ± 2mg in PHD1 K/O mice and 14.0 ± 1.0mg in PHD3 K/O mice (compared to 9.0mg ± 0.4, CHPT 5).

Experiment	**C:F**	**CD** (cap.mm^{-2})	**MFA** (μm^2)
WT	1.29 ± 0.08	555.0 ± 27.5	2068 ± 118.9
WT EXT	1.37 ± 0.15	703.3 ± 94.5	1854.5 ± 55.3
P1 K/O	1.46 ± 0.01	655.3 ± 11.4	1576.6 ± 104.9§
P1 K/O EXT	1.34 ± 0.03	753.8 ± 29.5§	1344.2±46.9§
P3 K/O	1.36 ± 0.11	788.2 ± 80.2§	1312.1± 84.5§
P3 K/O EXT	1.30 ± 0.05	730.1 ± 25.7§	1388.0 ± 59.6§

Table 6.1 C:F and CD for PHD1 knockout (P1 K/O), PHD3 K/O (P3 K/O) and wild type animals with and without 1 week of extirpation (EXT), n=3 (mean ± SEM). §=*P*<0.01 *vs.* WT. Statistics were performed by ANOVA using Dunnetts as a post-hoc test.

6.3.1.2 Gene arrays

Gene lists were determined using adjusted *P*<0.05 (Fisher Exact *P*-values) and fold change (FC) of ± 0 to determine which genes were up and down-regulated, with the exception of WT *vs.* WT EXT and PHD1 K/O EXT *vs.* WT EXT: little change was found in gene expression in the former (*P*-values were all >0.05) so *P*<0.1 and FC ±1.5 was used,

and using $P<0.05$ for the latter resulted in an unmanageable number of genes for analysis with DAVID, so $P<0.001$ was used, along with an FC of 2 (Appendix VI). Functional annotation charts were produced from DAVID using GO terms, and a false discovery rate (FDR) of 10% or less as the standard criteria for determining which terms were significantly up- or down-regulated (Appendix V).

Heat maps were created from the gene lists generated (above). Using functional clustering (DAVID) gave an enrichment score (ES) representative of the overall closeness of an annotation cluster, after considering each of its members. The enrichment of each cluster is determined by the *P*-value (above) of each of the groups members, i.e. a greater ES is indicative of a group consisting of lower *P*-values, suggesting that members within the group have shown noticeable change, following treatment, in either in a positive or negative direction. Genes from groups with an ES >1.5 were chosen to create heat maps, this being used as standard criteria.

Colours in the heat map represent the intensity in each sample relative to the average intensity across all samples for that particular gene. The heat map was made using z-values, calculated as:

(Sample Intensity - mean intensity for gene)/standard deviation for gene

For example, if a sample had a mean intensity Z=0, it is shown as black on the heat map; if it is higher than the average (Z>0) it is shown as red on the heat map, and if less than the average (Z<0) it is coloured green. Converting to Z scores is done to make all the genes in the heat map visually comparable, regardless of their overall intensity.

6.3.1.2.1 Validity of samples

6.3.1.2.1.1 RNA quality control (QC) (Carried out at the Wellcome Laboratories at the University of Oxford)

Before carrying out the gene array, QC was carried out for all sample using an RNA integrity programme called the Agilent 2100 Bioanalyser which automatically generates the ratio of the 18S to 28S ribosomal subunits using its software (Fig 6.2). It also provides an RNA integrity number (RIN) (which should lie between 8 and 10 for a good quality sample) as further indication of the quality of the RNA, providing the assessor with an accurate determination of the quality of the samples to be used in the gene array.

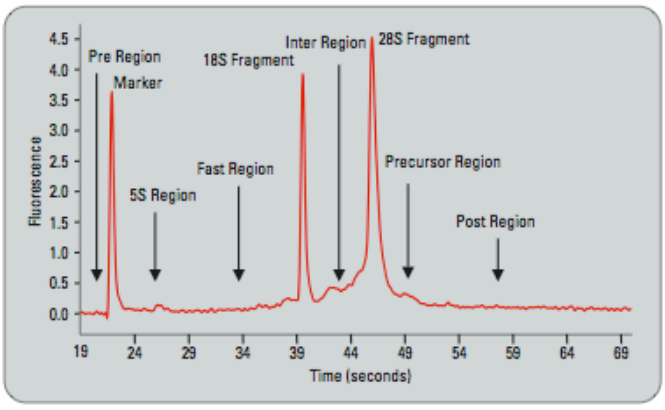

Figure 6.2 Electropherogram indicating regions indicative of RNA quality (see Agilent's 2100 Bioanalyser website)

6.3.1.2.1.2 Log intensity plots following gene array

Scatterplots were made to illustrate which samples were appropriate for use in subsequent analyses. Intensity values were plotted for all probes on the array in one sample compared to another. Fig 6.3 illustrates samples unsuitable for analysis, whereas Fig 6.4 illustrates samples which are. A number of samples were unsuitable for use (PHD3 K/O mouse tissue) due to inadequate storage and consequent degradation, hence

analyses are not equally balanced with respect to 'n'. A tight cluster of points (Fig. 6.4) on the diagonal indicates a pair of samples which are very similar: ideally all pairwise comparisons should show this. A much greater spread is seen with the poor quality samples indicated in Fig. 6.3.

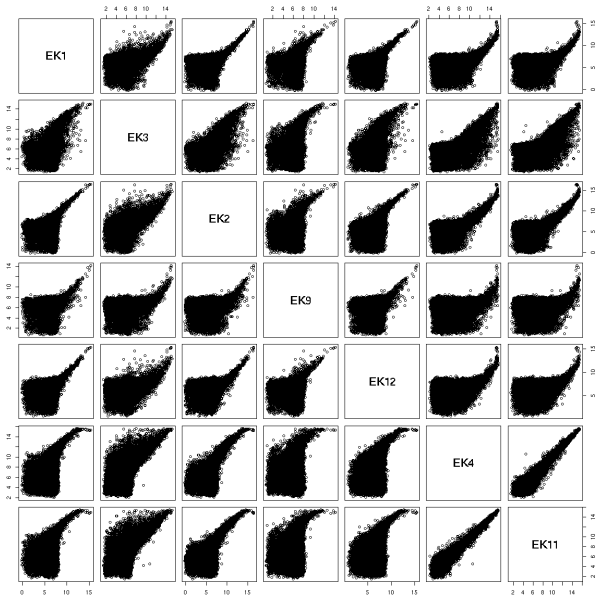

Figure 6.3 Illustration of samples with poor quality

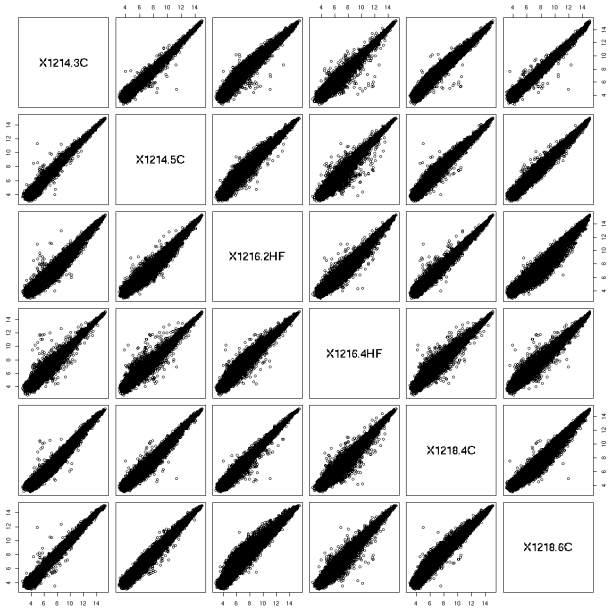

Figure 6.4 Illustration of good quality samples

Fig 6.5 illustrates the group of outliers (a) and normalised box plots following removal of the degraded samples (b).

(a) (b)

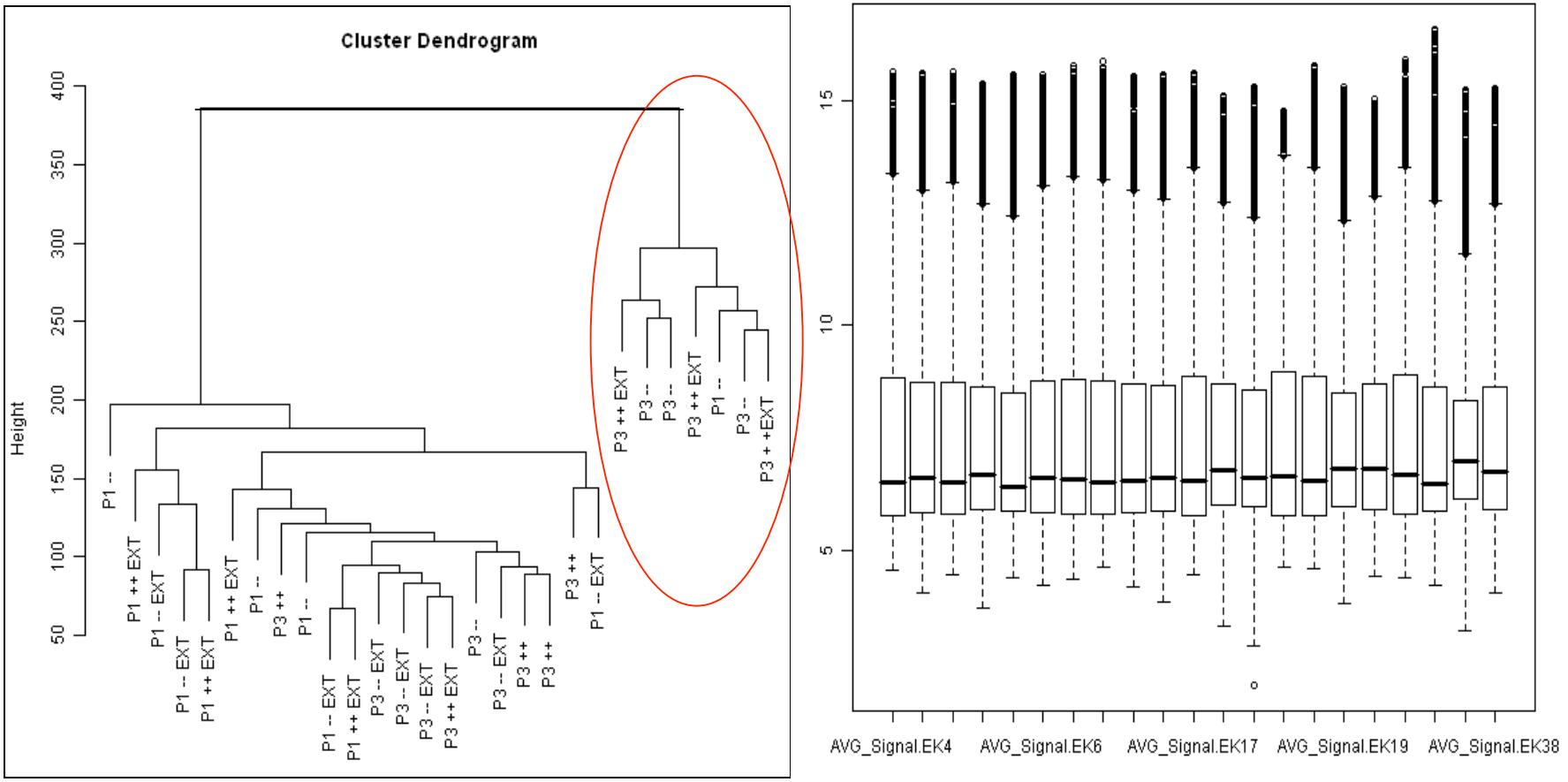

Figure 6.5(a) Dendrogram illustrating a group of outliers from the rest of the group which were excluded, and (b) Boxplot illustrating normalised data following removal of outliers

6.3.1.2.1.3 Principal component analysis (PCA)

PCA represents a method of summarising the variance present in the gene expression data, translating this into 2 dimensions, resulting in a plot with points that represent each sample: the more similar the samples are, the closer they are together. Figure 6.6 clearly illustrates that PHD3 K/O EXT samples are closely related, along with WT, though WT EXT, PHD1 K/O EXT and PHD1 K/O all have samples (within the total of 3) distinctly different from each other. This is most likely due to naturally occurring differences between mice (biological variability), or individual differences in response to surgical intervention.

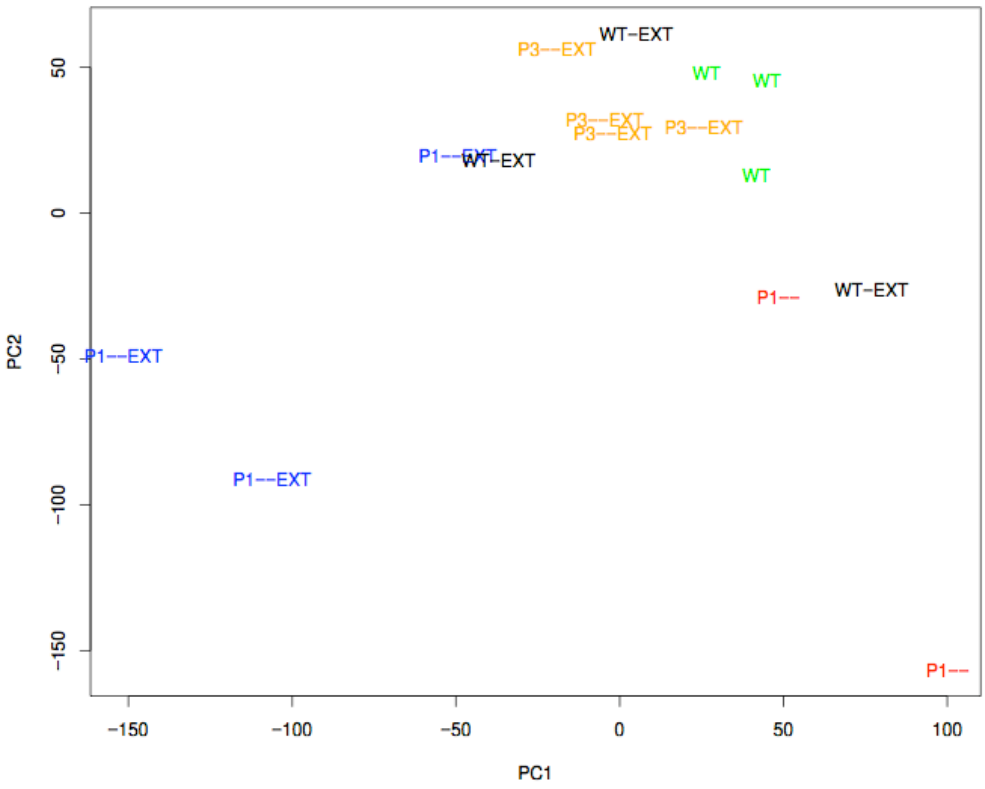

Figure 6.6 PCA of all samples in this study to illustrate how related samples are to each other

6.3.1.2.2 Validation of knockdown

Validation of the PHD3 knockdown is shown (Fig 6.7), with a 20 fold lower expression when compared to WT. Each boxplot shows the range of intensities measured for each particular probe targeting either PHD1 or PHD3, for all samples with a particular genotype (i.e. PHD1 K/O, PHD3 K/O and WT). The genotypes are represented on the 'x' axis. These boxplots represent the spread of expression intensity across these samples, and thus give an idea of the success level of the knockdown which was achieved (an intensity on the 'y' axis of 6 or below is regarded as background noise).

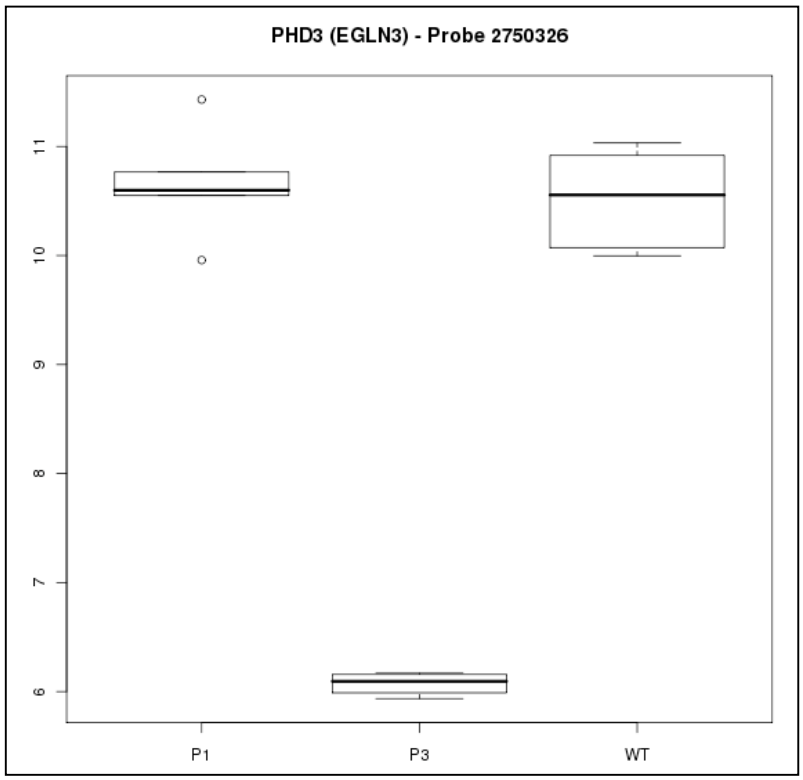

Figure 6.7 Log scale intensity plotted against PHD3 gene expression (P3), PHD1 gene expression (P1) and wildtype

High quality RNA was shipped to Oxford for RNA analysis and due to inadequate storage was degraded in nearly all PHD3 groups: only viable data from PHD3 K/O + EXT was obtained from PHD3 K/O mice group.

Unfortunately, less knockdown was seen in the PHD1 K/O mice (Fig. 6.8) as illustrated by the spread of values with a log intensity ranging from around 7 to just below 8.5. Values under 6 are recognised as background.

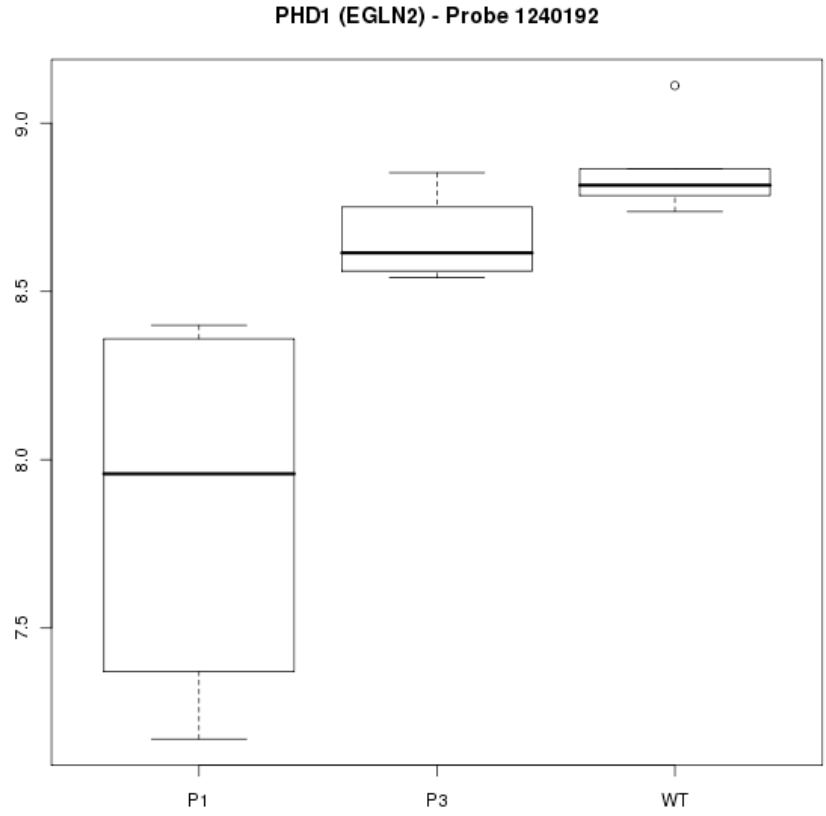

Figure 6.8 Log scale intensity plotted against PHD1 gene expression (P1), PHD3 gene expression (P3) and wildtype (WT)

6.3.1.2.3 Comparisons between groups

Heat maps were produced using gene lists adapted with standard criteria (above) and are in Appendix IV. Heat maps were also produced using functional clustering (DAVID)

and these identified specific groups of genes significantly upregulated in functional groups with an ES >1.5.

6.3.1.2.3.1 WT EXT vs. *WT*

Figure 6.9 demonstrates comparisons in genes between WT animals with and without extirpation (as determined by functional clustering with DAVID with an ES >1.5). Due to lack of significant change in genes between groups, the heat map produced from the gene list alone was very similar, so only one is shown). Both groups show a very similar response. This is illustrated further by the grouping of WT EXT next to WT by dendrogram bars. Coloured bars beneath dendrograms illustrate different groups.

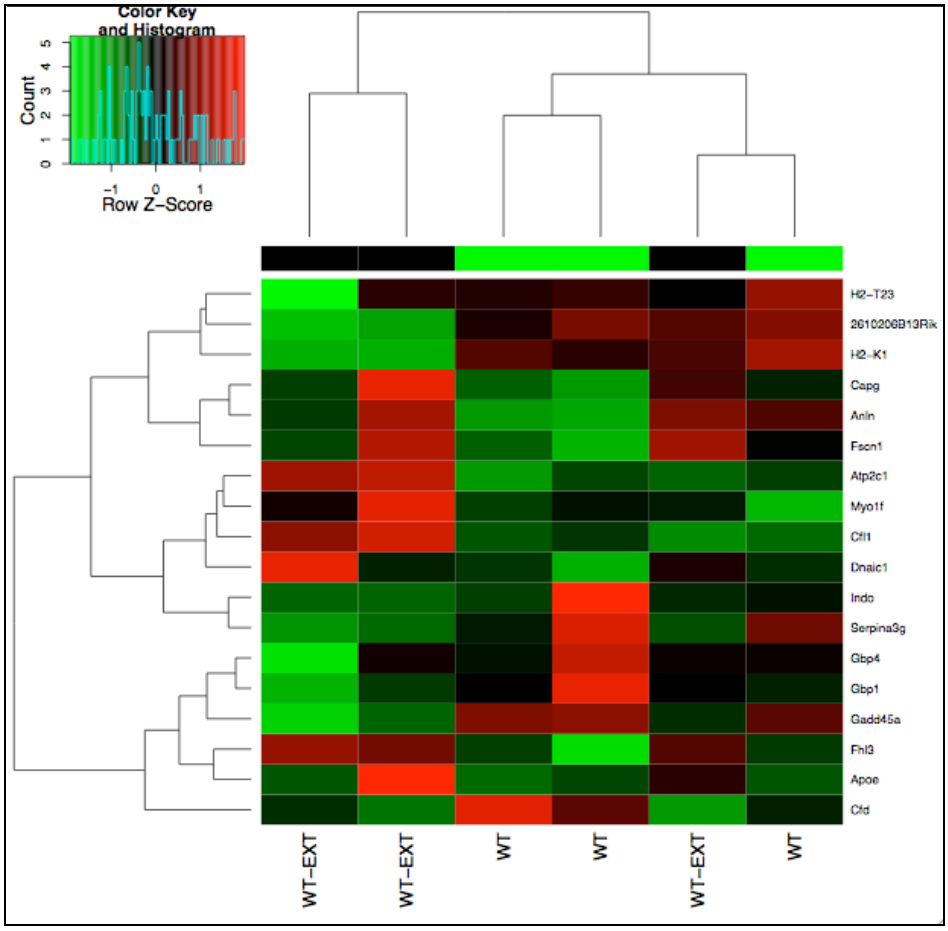

Figure 6.9 A heat map illustrating genes up- (red) and down-regulated (green) in wildtype (WT) mice with extirpation (EXT) *vs.* WT alone (n=3 in each group)

6.3.1.2.3.2 PHD1 K/O vs. *WT*

Figure 6.10 demonstrates reciprocal changes between PHD1 K/O (P1--) mice and WT mice very clearly (from functional clusters with an ES >1.5). However, as noted (6.3.1.2.2), it was shown that knockdown of PHD1 was not achieved very successfully. This is illustrated here, with the second column (denoted P1--) showing less similarity to column 1, also P1 K/O, the opposite of what would be expected for mice with the same genotype. This is further evidenced by dendrogram bars (placed on top of the heat map). These bars are not representative of absolute values, only of relationships between experimental groups.

Obvious reciprocal change between groups is shown as 'A': genes related to DNA damage response, stress response and antigen processing and presentation are upregulated in WT animals and down-regulated in PHD1 K/O mice. In the sub category 'B' were a collection of genes related to sensory perception and stimulus detection, cell communication, and signal transduction: these were all upregulated in PHD1 K/O mice.

6.3.1.2.3.3 PHD1 K/O EXT vs. PHD1 K/O

Figure 6.11 (from functional clustering) illustrates clear reciprocal changes in gene expression levels between PHD1 K/O mice with extirpation as an intervention, and PHD1 K/O mice alone. Dendrogram bars at the top of the heat map show clear segmentation between the two groups.

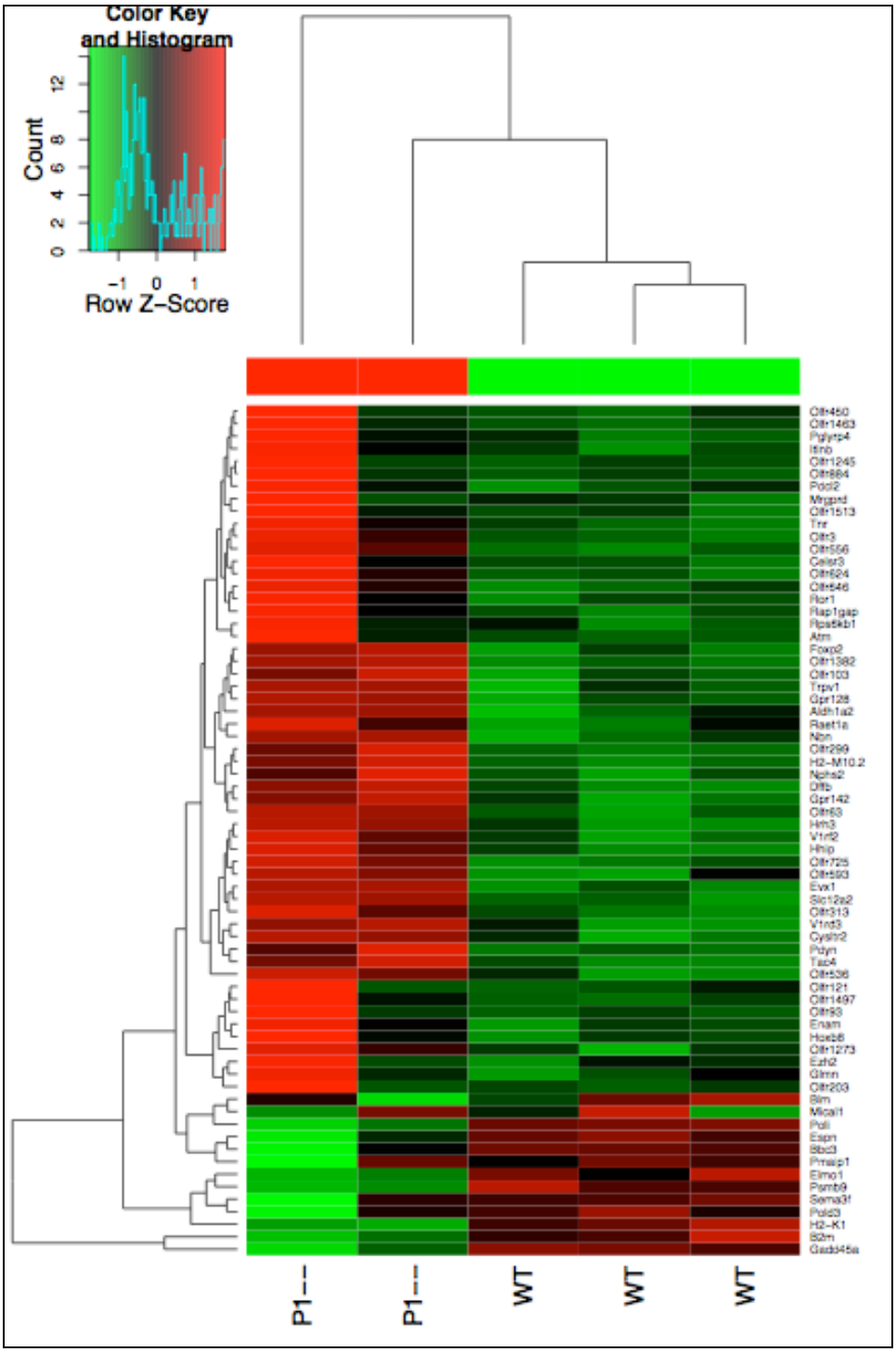

Figure 6.10 A heat map illustrating genes up- (red) and down-regulated (green) in PHD1 K/O mice *vs.* wildtype (WT), derived from functional clusters with an ES>1.5. (n=3 in each group)

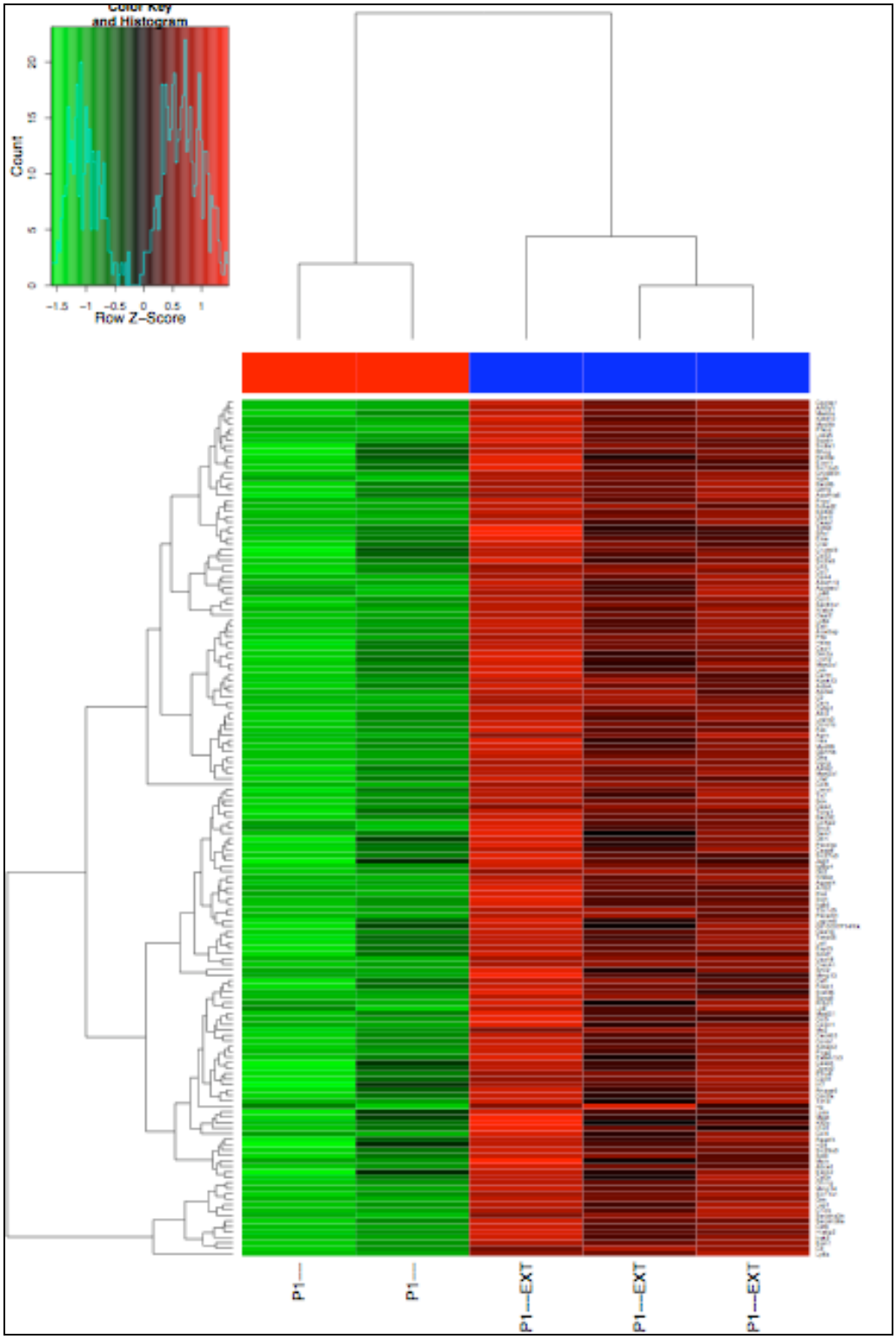

Figure 6.11 A heat map illustrating genes up- (red) and down-regulated (green) PHD1 K/O extirpation (EXT) (columns 3-5) vs. PHD1 K/O mice (columns 1-2), derived from functional clusters with an ES>1.5. (n=3 in each group)

6.3.1.2.3.3 PHD1 K/O EXT vs. WT EXT

Figure 6.12 (from functional clustering) again clearly illustrates differential and reciprocal upregulation of gene expression in PHD1 K/O *vs.* WT mice, both having had unilateral extirpation. Column 3 further illustrates issues noted (above) that the WT EXT mouse genotype overlaps with the WT genotype with inconsistencies, and column 5 relates to the partial knockdown of the P1 K/O mouse, as mentioned (6.3.1.2.3.2).

A subset of genes have been identified where patterns of reciprocal change are shown (A, B, C). Genes in A, involved mainly in glycolysis, are shown to be upregulated in WT EXT compared to PHD1 K/O EXT mice. Similar functions are upregulated in C, along with genes related to oxidative stress. B identifies genes, again upregulated in the WT EXT phenotype, that are associated with apoptosis and mitochondrial function.

6.3.1.2.3.4 PHD3 K/O EXT vs. WT EXT

Input of gene lists into DAVID revealed low ES, <1.5, indicating that although 34 genes were classified as upregulated and 23 genes down-regulated, none of these represent functional terms that were significantly changed in this intervention. Thus, a heat map was produced using $P<0.01$ and ± 0 FC (Fig. 6.13).

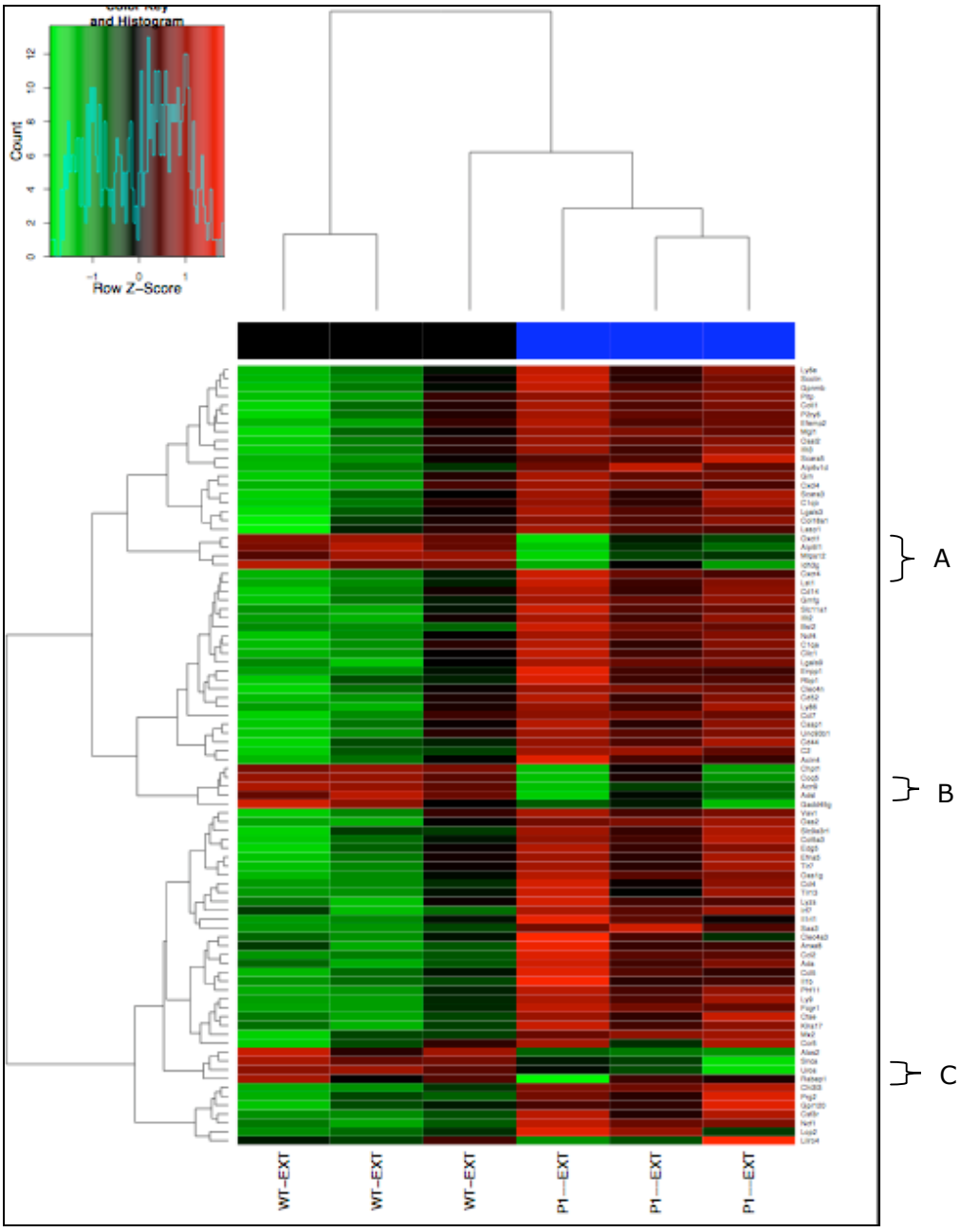

Figure 6.12 A heat map illustrating genes up- (red) and down-regulated (green) in PHD1 K/O EXT (columns 4-6) vs. wild type mice with extirpation (WT EXT) mice (columns 1-3), derived from functional clusters with an ES>1.5. n=3 in each group

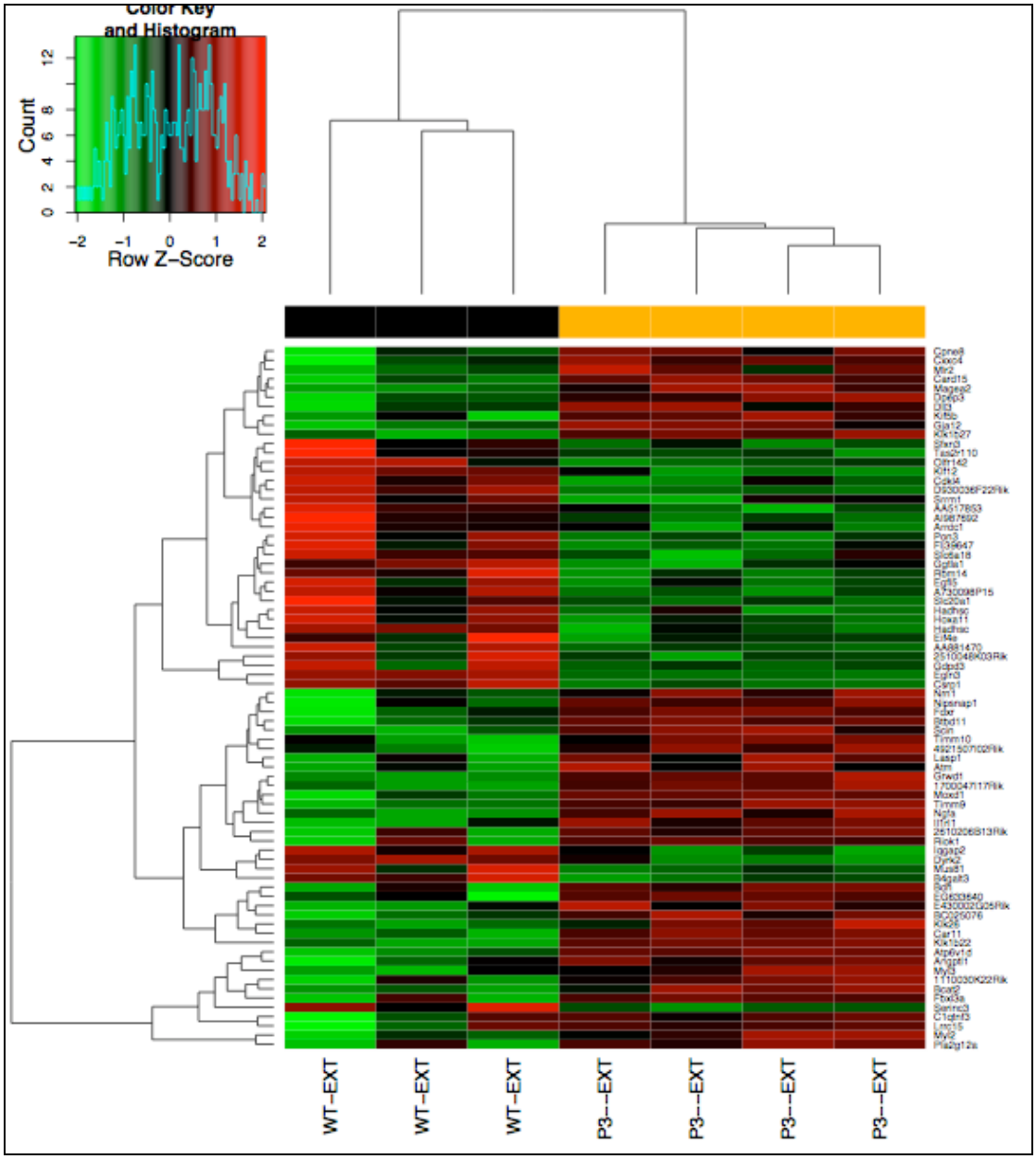

Figure 6.13 A heat map illustrating genes up- (red) and down-regulated (green) in PHD3 K/O mice with extirpation (EXT) (columns 4-7) vs. wildtype (WT) EXT mice (columns 1-3), derived from gene lists with $P<0.01$ and ±0 FC. n=3 in each group

6.3.1.2.3.5 PHD1 K/O EXT vs. *PHD3 K/O EXT*

Figure 6.14 (from functional clustering) gives a fine illustration of reciprocity in gene changes when one or other of the PHD isoforms, 1-3, is ablated.

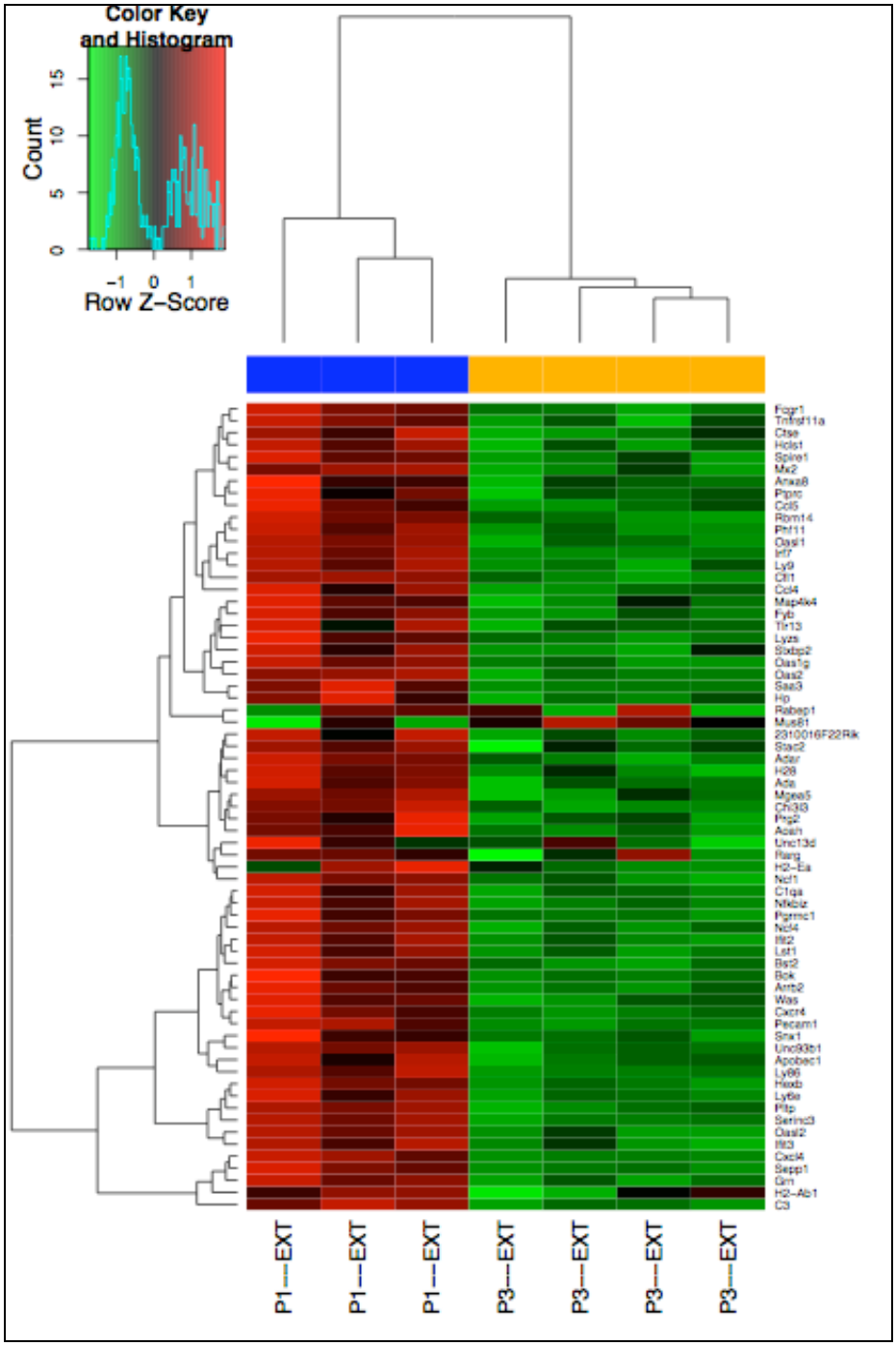

Figure 6.14 A heat map illustrating genes up- (red) and down-regulated (green) PHD1 K/O mice with extirpation (EXT) (columns 4-6) vs. PHD3 K/O EXT (columns 1-3), derived from functional clusters with an ES>1.5. n=3 in each group

6.3.1.2.4 Analysis of upregulated gene expression across groups

Potentially interesting up- and down-regulated genes identified using criteria (above) and GO terms are shown in Table 6.2 and 6.3, respectively. Evidence for an inflammatory response and an increase in metabolism to fuel the observed increase in protein turnover and angiogenesis are all seen. Interestingly, PHD3 is upregulated in the PHD1 K/O EXT model.

	WT EXT *vs.* WT	**PHD1 K/O *vs.* WT**	**PHD1 K/O EXT *vs.* WT EXT**	**PHD1 K/O EXT *vs.* PHD1 K/O**	**PHD3 K/O EXT *vs.* WT EXT**	**PHD1 K/O EXT *vs.* PHD3 K/O EXT**
Angiogenesis	MMP 3, 12		MMP 2, 3, 12, 13	MMP 13, 14	Angiopoietin-like 1	MMP 13
	IGF		TGF-β	TGF-β	Schinderin	PHD3
			Syndecan 3	Syndecan 3	Lim and SH3 protein	Syndecan 3
			Rho-GTPase activating protein 9			Rho-GTPase activating protein 9
			Cd248			
			TIMP-1			
			Tenascin			
			Adam 12			
Cell cycle		cDNA sequence BC002059	Endothelial differentiation, sphingolipid G-protein coupled receptor 5	Cell division cycle 2 homolog	cDNA sequence BC025076	cDNA sequence BC006779
			Cell division cycle associated 2	Cell division cycle associated 2		
			EGF containing fibulin-like ECM protein	MAD2 (mitotic arrest deficient, homolog)-like 1		
Apoptosis		DNA fragmentation factor (β)		Caspase 1, 4, 8	Kinesin family member 5B	

Protein metabolism	Procollagen type XIV α1		Procollagen type V α3	Procollagen type V α2	Dipeptidase 3	
	Ubiquitin specific peptidase	Ubiquitin C	Procollagen type XVIII α1		Kallikrein 1-related peptidase	
			Cathepsin E, C, S, Z	Cathepsin Z		Cathepsin E, S, Z
Fatty acid metabolism		Esterase		Phospholipase C, λ2	Phospholipase A2	Phospholipase C, λ2
	Phospholipid transfer protein	Acyl-coA synthetase long-chain member 3	Phospholipid transfer protein	Phospholipid transfer protein		
	Apolipoprotein B	Fatty acid binding protein 7	Apolipoprotein C-I	Apolipoprotein B		
				Elongation of very long chain fatty acids		
Immune response	Tenascin N	Tenascin R				
			Toll-like receptor 7, 13	Toll-like receptor 7, 13		Toll-like receptor 13
	Chemokine (C-C motif) ligand 7, 8		Chemokine (C-X-C motif) ligand 4	Chemokine (C-X-C motif) ligand 1		Chemokine (C-X-C motif) ligand 4
			Chemokine (C-C motif) receptor 5	Chemokine (C-C motif) ligand 4, 8		Chemokine (C-C motif) ligand 4, 5
	Interleukin 13 receptor α1		Interleukin 1 β, Interleukin 1 receptor-like 1	Interleukin 1 receptor-like 1	Interleukin 1 receptor-like 1	
			Lymphocyte antigen 9	Lymphocyte antigen 6, 9, 86		Lymphocyte antigen 9, 86
			Colony stimulating factor 1 and 3 receptor	Colony stimulating factor 1 and 3 receptor		Colony stimulating factor 1 receptor
		Platelet activating factor	Platelet activating factor	Platelet activating factor		NFκB

		acetylhydrolase 2	acetylhydrolase isoform 1β	acetylhydrolase isoform 1β		
Cell adhesion molecules		Cadherin EGF lag 7-pass receptor 3	CD44 antigen	PECAM-1		
		Protocadherin λ subfamily A	CD53			
			VCAM-1			
			Adam 12			
			Integrin β 7	Integrin α5		
Mitochondrial function		Cytochrome P450, family 2, 21	Thromboxane a synthase 1		Branched chain aminotransferase 2, mitochondrial	Electron transferring flavoprotein α
					Translocase of inner mitochondrial membrane 9, 10	ATP-synthase, mitochondrial F0 complex
Glycolysis		Aldehyde dehydrogenase 1	Aldehyde dehydrogenase 3			
		Aldolase 3, c isoform				

Table 6.2 A subset of upregulated genes identified as potentially interesting following GO analysis. (Matrix metalloprotease: MMP, transforming growth factor β: TGF-β, insulin-like growth factor: IGF, epidermal growth factor: EGF, extracellular matrix: ECM)

Common across most comparisons, apoptotic and cell division factors are also shown to decrease, along with mitochondrial function and glycolysis-related genes. PHD1 is down-regulated in the PHD1 K/O, which provides confirmation of its knockdown in this model.

6.3.1.2.5 Analysis of down-regulated gene expression across groups

	WT EXT *vs.* WT	PHD1 K/O *vs.* WT	PHD1 K/O EXT *vs.* WT EXT	PHD1 K/O EXT *vs.* PHD1 K/O	PHD3 K/O EXT *vs.* WT EXT	PHD1 K/O EXT *vs.* PHD3 K/O EXT
Apoptosis	Dynactin 1		Dynactin 4			
	Growth arrest and DNA-damage inducible 45 γ	Growth arrest and DNA-damage inducible 45 α	Growth arrest and DNA-damage inducible 45 γ			
	Calpain 2	Bcl-2 binding component		DNA fragmentation factor β		Apoptotic chromatin condensation inducer
Cell division		Histone 1				Histone 2
		Adenosine deaminase, β1	Cell division cycle 34 homolog			CDNA sequence BC004044
		Polymerase (DNA-directed) iota				DNA segment, Chr 4
		Polymerase (DNA-directed) Δ3				Cell division cycle 34 homolog
Mitochondrial function	Cytochrome p450, family 2, subfamily E	Mitochondrial intermediate peptidase	Mitochondrial ribosomal protein S12			Translocase of inner mitochondrial membrane 8
			Isocitrate dehydrogenase 3			Isocitrate dehydrogenase 3
			Mitochondrial carrier homolog 2			Mitochondrial carrier homolog 2
			Coenzyme Q5 homolog, methyltransferase			Coenzyme Q5 homolog, methyltransferase
						Mitochondrial ribosomal protein L3

Glycolysis	Aldehyde dehydrogenase		Phosphorylase kinase α1			Succinate-coA ligase α
			Pyruvate dehydrogenase			NADH dehydrogenase 1 α, 6
						Acetyl-coenzyme A dehydrogenase
Angiogenesis					PHD3	
Inflammation	Guanylate nucleotide binding protein 1					
	macrophage activation 2					

Table 6.3 A subset of down-regulated genes identified as potentially interesting following GO analysis

6.4 Discussion

This study was designed to investigate whether relationships between genomic and functional responses exist in skeletal muscle, following genetic manipulation of molecular pathways leading to HIF-1α stability. The PHDs have been shown to contribute in a non-redundant manner to the regulation of HIF-1α (Appelhoff *et al.* 2004), suggesting that a differential gene response should be seen following specific PHD ablation.

6.4.1 Changes in hindlimb capillarity

A clear trend exists (as already shown, CHPT 5) between WT and WT EXT mice, with extirpation inducing an increase, although not significant, in the capillary to fibre ratio (C:F). Interestingly, in both PHD1 and PHD3 K/O mice, the C:F is noticeably higher, (not-significant) in non-intervention animals. This suggests a trend towards impaired angiogenesis in K/O animals with EXT as an intervention, although the reduced (mean fibre area) MFA seen in all K/O and K/O EXT mice suggests that a reduction in fibre size is responsible for the observed reduction in C:F and increased capillary density (CD). Thus, angiogenesis seems to be impaired in both PHD1 K/O and PHD3 K/O mice. There are insufficient existing experimental data on skeletal muscle phenotype in PHD knockout mice to support this observation from other studies. Interestingly, mean muscle mass within each knockout group was higher than that observed following extirpation in CHPT 5, suggestive of enhanced protein synthesis following PHD ablation (see 6.4.2.2.4).

6.4.2 Gene expression

6.4.2.1 Validity of samples

Before and after gene arrays were carried out, the purity and concentration of the samples was determined as described (6.3.1.2.1). On doing so, a number of samples were unfortunately eliminated due to degradation that may have occurred because of

inadequate storage conditions (freezer breakdown in Oxford). Between some of the remaining samples, namely PHD1 K/O, PHD1 K/O EXT and WT EXT, significant variation in the gene expression of samples was seen and may exist due to naturally occurring inter-animal variability. An adequate PHD3 knockdown was achieved, though the knockdown in PHD1 animals was not achieved to the level desired, and this may have affected the results seen here.

6.4.2.2 Cross-intervention analysis

WT mice appeared to exhibit little difference in gene expression when compared to WT EXT, evidenced by differential gene expression levels being insignificant ($P>0.1$), and may be due to reasons mentioned above. Increasing the sample number would greatly help to increase confidence. However, with the exception of WT and WT EXT mice, all groups exhibited clear reciprocal changes in gene expression patterns, i.e. where genes were up-regulated in one genotype and intervention, the same genes were seen to be down-regulated in the contrasting situation, for example WT extirpation *vs.* PHD1 K/O extirpation.

6.4.2.2.3 Inflammatory pathways

A number of key pathways were stimulated which appeared to be upregulated as a common response to extirpation in both WT and PHD1 K/O animals. Genes involved in the inflammatory response were increased following extirpation surgery. Previous studies have shown that the earliest point at which no clinical signs of inflammation are seen is at 3 days (Williams *et al.* 2006b), and this is supported by a lack of visual inflammation 1 wk following extirpation surgery (Zhou *et al.* 1999). Here, inflammatory response genes are still significantly upregulated, suggesting that a subclinical inflammatory response may still play a role in these early phases (1 wk) post-surgery, further suggesting that angiogenesis may be stimulated through inflammatory pathways, as well as or instead of the stretch-induced mechanism which is well-known (Egginton *et*

al. 1998; Zhou *et al*. 1999; Williams *et al.* 2006a). In common with another study (Williams *et al.* 2006b), tenascin was upregulated in WT EXT mice, and Toll-like receptors 7 and 13 were commonly upregulated in PHD1 K/O EXT mice, both of which are known to play a role in inflammation. Tenascin is an ECM glycoprotein that has a number of isoforms. Tenascin N was upregulated in WT EXT mice: despite characterisation of the sequence and structure of the molecule, little is known about its physiological role. Another isoform, tenascin R, was upregulated in PHD1 K/O mice. This plays a role in the developing and adult nervous system. Although not upregulated here, tenascin C is a mechano-regulated, morphogenic ECM protein associated with tissue remodelling (Fluck *et al.* 2008).

That NFκB was upregulated in PHD1 K/O EXT *vs*. PHD3 K/O EXT supports the above suggestion that the angiogenesis seen here may be as a result of inflammatory-induced conditions. NFκB is a family of transcription factors that become activated following stimulation by pro-inflammatory factors such as cytokines, such as those listed here (chemokines and interleukins), and it has been implicated in maintaining basal levels of HIF-1α gene expression *in vivo* (Rius *et al.* 2008) (CHPT 4, Fig. 4.4).

6.4.2.2.4 Upregulation of energy producing pathways provides fuel for an increase in protein synthesis

Following removal of a synergist muscle, an increase in muscle mass occurs in the remaining muscle to compensate for the change in load bearing. Protein synthesis is an energetically expensive process, though required for supporting an increase in the number of serial sarcomeres (Goldspink *et al.* 1991), along with increasing collagen deposition in muscles subjected to stretch during limb lengthening (Laurent *et al.* 1985). Common amongst both WT and PHD1 K/O animals was an increase in collagen synthesis, evidenced by the upregulation of procollagen (although differing isoforms) in both WT EXT and PHD1 K/O EXT. Cathepsin E, C, S and Z were also upregulated, consistent with a model of extirpation (Goldspink *et al* 1995), in PHD1 K/O EXT mice. These are

prominent proteases involved in protein metabolism, and this suggests a role for these enzymes in tissue remodelling during muscle hypertrophy.

Fuelling this necessary adaptation following the intervention are an increase in fatty acid metabolism, mitochondrial function and glycolysis (Table 6.3), although these genes were significantly upregulated in knockout mice only. The latter finding is supportive of a study showing that PHD1 deficiency results in an adaptation from oxidative to more anaerobic ATP production (Aragones *et al.* 2007).

6.4.2.2.5 Upregulation of angiogenic factors and cell adhesion molecules

The muscle stretch created by extirpation stimulates the sprouting form of angiogenesis, whereby abluminal sprouting of ECs through the basement membrane occurs (Zhou *et al.* 1998). This is in contrast to the splitting form of angiogenesis where ECs send filopodial processes into the capillary lumen which then join and form a separate branch, and this subsequently propogates down the capillary (Zhou *et al.* 1998), this not involving any degradation of the BM. As expected, none of the significantly regulated genes related to angiogenesis were seen in PHD1 K/O mice alone.

PHDs act in the regulation of the HIF-α subunit, and have been shown to exhibit non-redundant roles in the regulation of this transcription factor (Appelhoff *et al.* 2004). Interestingly, in the PHD1 K/O EXT model, PHD3 is shown to be significantly upregulated, alongside PHD1 which is shown to be significantly down-regulated. The latter finding gives support to the absence of gene expression in this model. Though this significant upregulation provides evidence to suggest that there is redundancy acting within this system.

MMPs play a critical role in breaking down the BM of the vessel and the ECM *via* release of ECM-bound growth factors. The increased vascular permeability due to a combination of VEGF and the MMPs enables extravasation of plasma proteins that lay down a provisional scaffold for migrating cells (Carmeliet, 2003). A number of studies have shown the necessity of MMPs in sprouting angiogenesis (Rivilis *et al.* 2002): MMP-2

is a well-studied member of the group, and shown to be upregulated here. It is also known to be upregulated by the membrane associated MMP-14. It has a specificity to degrade collagen type IV, the most prevalent protein in skeletal muscle basal lamina (Rullman *et al.* 2009). MMP-2 has also been shown important for successful regeneration of experimentally damaged muscle fibres in the mouse (Kherif *et al.* 1999).

Accordingly, MMP-3, 12, 13 and 14 all showed significant upregulation in PHD1 K/O mice with extirpation, with MMP-3 and 12 also upregulated in WT EXT mice. The MMP-3 gene encodes an enzyme which degrades fibronectin, laminin, collagens III, IV, IX, and X, and cartilage proteoglycans and is thought to be involved in wound repair (Entrez-gene). The MMP-12 enzyme degrades soluble and insoluble elastin, whereas MMP-13 protein cleaves type II collagen more efficiently than types I and III. This may be involved in articular cartilage turnover and cartilage pathophysiology. TIMP-1, a tissue inhibitor of metalloproteases, has also been shown upregulated under conditions of extirpation in the PHD1 K/O animal, in agreement with a recent study showing an upregulation of both MMP-2, 14 and TIMP-1 following exercise training in humans (Rullman *et al.* 2009). Likewise, Heinemeier *et al.* (2007) and Rivilis et al (2002) found a parallel upregulation of TIMP-1 alongside MMP-2 in rat skeletal muscle, suggesting that a complex feedback system is operating under conditions of ECM degradation.

Schinderin and Lim and SH3 protein are upregulated in PHD3 K/O EXT mice. The former is involved in ECM remodelling, and Lim and SH3 is involved in cell migration, indicative that an angiogenic stimulus is prevalent.

TGF-β regulates cell proliferation, migration, ECM production, and the differentiation of a wide variety of cell types (Piek *et al*. 1999). It is involved in the development of the vascular system and affects the function of ECs (Goumans *et al.* 2003), playing a role in the development of new blood vessels. A positive correlation between mechanical loading of cells and TGF-β expression has also been shown in both *in vitro* and *in vivo* studies, on a large variety of human and animal cell and tissue types (Villarreal and Dillmann, 1992; Lindahl *et al.* 2002; Ruwhof *et al.* 2000). Furthermore,

Lindahl *et al.* (2002) demonstrated that promoter activation in procollagen-α1 (upregulated here in PHD1 K/O EXT mice) cardiac fibroblasts is TGF-β -dependent, so their parallel upregulation supports known findings.

Syndecan 3 is also upregulated in PHD1 K/O EXT mice, when compared to both WT EXT and PHD3 K/O EXT. It is known to play an important role in skeletal muscle differentiation (Aird, 2007), though is not thought to play as much of a role in vascular development as syndecan-1, which regulates integrin activation during angiogenesis (Beauvais *et al.* 2009).

Angiopoietin-like receptor 1 is upregulated in PHD3 K/O EXT mice. Unlike ANG-2, these molecules do not bind to the angiopoietin-specific receptor, TIE2, and are known as orphan ligands. They have a potent activity for regulating angiogenesis as proangiogenic or antiangiogenic factors, suggesting that their receptors may be expressed on endothelial cells (Oike *et al.* 2004).

Cell adhesion molecules have been shown to contribute to the mechanotransduction response (Ingber 2006; Lehoux *et al.* 1998) involved in transmitting changes in the cytoskeleton within associated ECs into a genomic and functional response. Integrins are heterodimeric transmembrane proteins whose main function is as receptors for most of the structural components of the ECM and several matrix-associated growth factors and proteases (Hynes, 1992). Integrin α5 and β7 were upregulated in PHD1 K/O EXT mice, along with CD44 antigen, CD53, PECAM-1 and VCAM-1. Both the integrins, PECAM-1 and VCAM-1 have been shown to be important in angiogenesis: VCAM-1, expressed on ECs and thought to be upregulated by VEGF (Ding *et al* 2003), and PECAM-1, a 130KDa glycoprotein located mainly along the lateral plasma membrane (DeLisser *et al.* 1997), have both been shown necessary for new vessel formation by inhibition of their action *in vitro* and *in vivo*. Adam 12 is another cell adhesion molecule which was upregulated here. It is a transmembrane protein containing both a disintegrin and metalloprotease domain, thus it potentially has both cell adhesion and protease activities (Primakoff and Myles, 2000).

6.4.2.2.6 Down-regulated functions

A multitude of factors were down-regulated, many of which also exist in the same functional categories as those that were also upregulated, including those involved in mitochondrial function, glycolysis and cell division. This suggests that feedback mechanisms exist which depress enhanced functions in these specific categories, on attainment of a certain level of expression, to maintain homeostasis. The possibility exists that realignment of the pathways involved in any of the above categories (such as glycolysis), by both up- and downregulation of genes, may not change the flux through the pathway, particularly if these genes code for elements that do not have an effect on the rate limiting step in the pathway (e.g. equilibrium enzymes).

6.5 Conclusions

Specific ablation of PHD1, with the added intervention of extirpation surgery, results in the upregulation of a number of genes involved in the inflammatory response, glycolysis and mitochondrial metabolism, the latter two possibly providing the fuel for an enhanced protein synthesis in response to the induced overload. Angiogenic and cell adhesion genes are also seen to be increased, suggestive of a permissive environment for new blood vessel growth. However, histological evidence suggests that this is not translated into a physiological angiogenic response, as evidenced by the lack of significant increase in the C:F of the EDL in the hindlimb. Skeletal muscle hypertrophy is clearly evident from the change in EDL muscle mass, thus this is suggestive of a dissociation between an increase in muscle mass and new blood vessel growth, i.e. a time lag between gene expression, translation and activity. The possibility exists that a number of anti-angiogenic factors have also been upregulated, which have yet to be defined, and this means that the angiogenic balance is not permissive in the direction of new blood vessel growth, though this remains to be determined. PHD3 was significantly upreglated in the PHD1 knockout mouse, suggesting that in agreement with published literature, these two may act in a non-redundant manner.

6.6 Future directions

One of the main drawbacks of this study was the low number of animals that were used. Increasing animal number in future studies may increase statistical significance, and improve confidence in the findings of inter-variability, naturally occurring *in vivo.*

Had time permitted, it would have been useful to undertake more extensive data mining of the genomic response by combining microarray data and subjecting it to parsimonious clustering analysis. This would provide empirical evidence for consistent gene up-regulation that could be validated by more quantitative genomic (qRT-PCR) and proteomic (multiplex ELISA) methodologies.

Chapter 7

SYSTEMIC HYPOXIA

7.1 Introduction

The ability to translate the effect of animal models, and in particular the murine response, into a functional human response is a controversial and still largely undetermined area in many cases. I therefore undertook a translational study to investigate the similarities in systemic response to hypoxia in both mouse and man. Following determination of the time course of HIF-1α and HIF-1α activated gene expression in several tissues in the mouse, including leukocytes (see CHPT 3), the objective of this part of my thesis was to observe if this HIF-driven gene expression in leukocytes (already observed in the murine model on a carefully selected number of genes) could be used as a viable indicator of the systemic response to hypoxia in man, thus possessing potential for use as hypoxia-responsive indicators. This parallel response to systemic hypoxia in both mouse and man (an upregulation of HIF-regulated gene expression under hypoxia in leukocytes) could serve as a useful indication of the potential this murine model has to mirror the human response. In addition, I wanted to determine if the parameters studied in humans could be used as a potential set of markers for fitness at altitude, when related to altitude sickness and O_2 saturation of the blood, the latter an area of contention that has been studied for many years and remains an active area of research.

Due to my long-term fascination with high altitude physiology and response in man, along with my affiliation with a high altitude research group based in Birmingham, I decided that this would be an ideal opportunity to conduct a study in a murine model that allowed partial translation into the human response to hypoxia. The Birmingham Medical Expeditionary Society (BMRES) comprises a group of physicians who formed a charitable research group 25 years ago, interested in investigating mechanisms of altitude illness and how the body adapts to high altitude; I have been a member for 4 years. I was presented with an opportunity to design a follow-up to a chronic high-altitude exposure study in Bolivia performed by the group. The plan was to incorporate

an acute high altitude exposure phase, providing a contrast between the acute setting in the hypoxic chamber and the chronic setting of a slower ascent to the high altitude plateau in Chile. From these data, one may be able to predict the response of an individual on ascent to altitude in the field, by studying their response in the laboratory. The original design for the study involved collaborating with part of the Chilean army, a group of whom would have also been subjects in the chronic exposure part of this study. This wasn't eventually feasible which is unfortunate as it would have added greater power to the study.

"Severe O_2 deprivation at extreme altitudes is only tolerated due to an enormous increase in ventilation which protects the alveolar PO_2 against decreasing inspired values" (West, 1990). This is known as the hypoxic ventilatory response (HVR). After acute exposure to hypobaric conditions, the increase in ventilation occurs within seconds, reaching full intensity within minutes, and a ventilatory acclimatisation occurs after continuous exposure over days (Lahiri *et al.* 2000). It is known that some people with a rapid HVR at altitude are less likely to suffer with the effects of hypoxia (Matsuzawa *et al.* 1989). Hyperventilation causes an increase in the affinity of Hb for O_2, increasing O_2 uploading by the pulmonary capillaries (West, 1990). Pulmonary vasculature O_2 sensors initiate regulation of the hypoxic pulmonary vasoconstrictor response which results in improved ventilation–perfusion matching, and cardiac output (CO) increases in response to the increase demand for O_2.

7.1.1 Physiological impairment caused by ascent to altitude

O_2 deprivation resulting from high altitude exposure in lowlanders impairs mental and physical performance, quality of sleep and general well being. West (2005) noted that symptoms were relieved on administration of O_2. Rapid ascent to high altitude may result in a condition known as acute mountain sickness (AMS). The main features of AMS are headache, accompanied by one or more other symptoms such as light-

headedness, dizziness, loss of appetite, nausea, vomiting, fatigue, lassitude, breathlessness and difficulty sleeping (Hackett and Roach, 2001). The lowest altitude at which individuals appear to be affected is around 2500m (Ward, Milledge and West, 1995). Clinical conditions observed after rapid ascent include an accumulation of fluid: high altitude pulmonary edema (HAPE) or high altitude cerebral edema (HACE). Ascent to high altitude results in an increase in production of reactive O_2 (ROS) and nitrogen species such as superoxide, hydrogen peroxide, hydroxyl radicals, nitric oxide, and peroxynitrite which directly stimulate central CO_2 chemoreceptors in the brain stem (Mulkey *et al.* 2003). These free radicals are known to cause oxidative damage to lipids, proteins and DNA that is thought to be associated with high altitude illness: Bailey (2003) found a greater increase in free radical-mediated biomarkers of lipid peroxidation and sarcolemmal membrane permeability in subjects diagnosed with clinical AMS.

There have been several scoring systems used to diagnose and quantify mountain sickness. These include the Lake Louise Score (LL) (Appendix IV) which is sensitive enough to detect AMS, along with the Environmental Symptom Questionnaire (ESQ) (Appendix IV), both consisting of a multitude of questions which attempt to illustrate the degree of suffering by the subject.

7.1.2 Stimulation and control of erythropoiesis in response to hypoxia

Occurring slower in onset than its cardiopulmonary counterparts, an increase in the number of RBC in the blood (polycythaemia) is a well-known feature of acclimatisation that was first reported by Viault in 1890 (Smith *et al.* 2008). The main determinant of erythropoiesis is the release of the glycoprotein hormone erythropoietin (EPO), mainly from interstitial fibroblasts in the kidneys of the adult (Chavez *et al.* 2006), in response to local O_2 tensions. Very low O_2 tensions *in vitro* have been shown to be required for EPO stimulation, e.g. incubation of hepatic cells with 7mmHg PO_2 for 24 hours (Goldberg *et al.* 1988). Following its release into the circulation, it binds to EPO receptors on erythrocyte progenitor cells and stimulates increased production of RBCs (Zhu *et al.*

2002). The control of EPO synthesis is achieved at a transcriptional level by hypoxia-inducible factor (HIF) (Pugh *et al.* 1991; Maxwell *et al*. 1993), a transcription factor that rapidly accumulates in the nucleus under hypoxia (Fig, 7.1). HIF induces the transcription of a large number of hypoxia-related genes, although it is itself regulated at a post-translational level (Stolze *et al.* 2006) (CHPT 1). An increasingly recognised role for HIF-2α is its dominant role in the regulation of EPO over HIF-1α (Gruber *et al.* 2007).

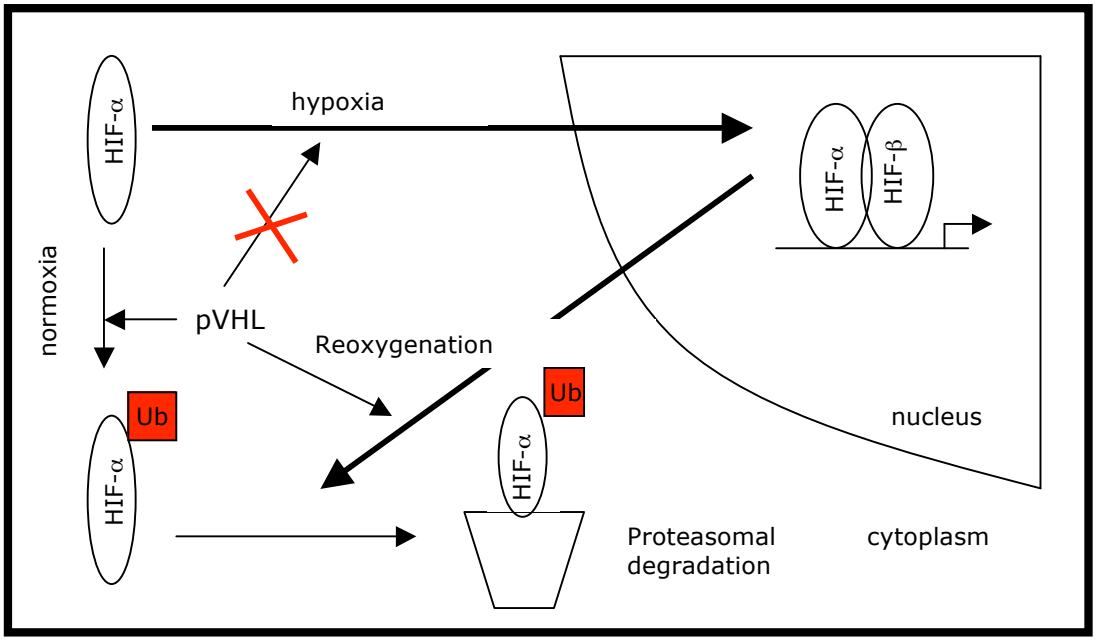

(Adapted from Jewell *et al.* 2001)

Figure 7.1 Schematic diagram of the rapid HIF regulation during normoxia, hypoxia, and reoxygenation. In normoxia, the pVHL (von Hippel-Lindau protein) binds to HIF-α and recruits it to the ubiquitination machinery (Ub) where it is degraded. After exposure to hypoxia, HIF-α production increases causing its accumulation in the nucleus where it dimerises with the HIF-β sub-unit. This functional HIF complex induces transcription of a variety of O_2-regulated genes. Upon reoxygenation, HIF proteins undergo efficient proteasomal degradation.

The increase in red blood cell count (RBCC) following EPO up-regulation augments the O_2-carrying capacity of arterial blood (Soliz *et al.* 2005). It has been shown that the increase in EPO is altitude dependent: altitudes greater than 2100m appear to be a threshold for stimulating a sustained EPO release in man (Ge *et al.* 2002). The EPO concentration in the blood has been shown to increase as soon as 90 min after the

inspiratory PO_2 is lowered (Eckhardt *et al.* 1989), to rise progressively during the first 24 to 48 h, and then decline towards baseline levels over 1-2 weeks (Richalet et al, 1994; Abbrecht and Littell, 1972). This decline continues despite sustained hypoxia and occurs before the expansion of the RBCC. However, haemoglobin (Hb) and haematocrit (Hct) have been shown to be elevated within days of ascent (Richalet et al, 1994): the spleen has been reported to serve as a dynamic reservoir for RBC storage, sequestering 200-250ml of densely packed RBCs. Up to 50% of which may be released during acute hypoxia (Bakovic *et al.* 2005). Acute hypoxia has been shown to play a key role in triggering splenic contraction (Richardson *et al.* 2005; de Bruijn *et al.* 2008).

7.1.3 The multifaceted regulatory role of HIF in response to hypoxia

Inadequate inspiratory O_2 triggers a multifaceted cellular response driven by HIF, governing a global transcriptional response to hypoxia amongst different cell and tissue types. This further enables the body to adapt and acclimatise to the surrounding low O_2 environment. Changes induced include shifts in metabolic pathways such as up-regulation of glycolysis, alongside the previously mentioned up-regulation of erythropoiesis. HIF is an extremely labile protein in normoxia, but in hypoxia HIF-1α degradation is reduced, resulting in increased intracellular levels (Fig. 7.2). Within 2 min of hypoxic exposure, HIF protein accumulates in the nucleus (Fig. 7.1). These features make studying HIF-protein levels a challenge.

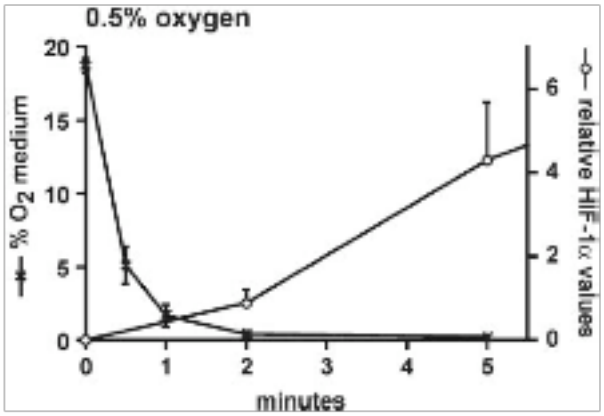

Figure 7.2 Graph showing HIF-1α kinetics compared with the decrease in O_2 concentration in the medium during the first 5 min of hypoxia in nuclear extracts of a human epithelial carcinoma celll line (HeLaS3 cells) exposed to 0.5% O_2 using tonometry (mixing a fluid with the appropriate gas concentration) (From Jewell *et al.* 2001)

7.1.3.1 Control of downstream genes by HIF-1 and HIF-2

Despite high conservation in amino acid sequence and hypoxia-dependent activation, HIF-1α and HIF-2α have been shown to exhibit quite distinct, non-redundant physiological roles, with some different transcriptional targets and differing levels in tissues (Stroka *et al.* 2001). As HIF-2α has been shown to play an important role in the regulation of EPO, it is important to consider downstream consequences arising from its activation, alongside HIF-1α. A multitude of genes are targeted by both HIF isoforms that are of interest in this study (CHPT 1, Table 1.1) and which may provide a surrogate representation of HIF activation, also forming interactions between themselves (CHPT 3, Fig 3.1).

7.1.4 Individual variability in the EPO response to hypoxia and its association with AMS

EPO production under hypoxia is governed by a great deal of inter-individual variability (Ge *et al.* 2001) although the cause of this remains largely unknown. However, Jedlickova *et al.* (2003) found evidence indicating that this variability was not genetically determined. Sutherland *et al.* (unpublished) studied plasma EPO concentration in

subjects taken to 5200m over 4 days and found that EPO 'responders', i.e. those who experienced a rapid increase in their plasma EPO concentration, suffered less with acute mountain sickness (AMS) compared to 'non–responders'. This is logical: individuals who experience a more rapid increase in EPO are able to increase their RBCC and thus O_2-carrying capacity faster than those who are slower with a lower magnitude of response, thus predisposing them to a lower risk of developing sickness at altitude. This remains an area of controversy: a number of studies found no change in EPO levels in AMS+ *vs.* AMS-subjects at altitude (Tissot van Patot *et al.* 2005, Basu *et al.* 2007), while AMS+ subjects had an increased EPO level when compared to well subjects (Huang *et al.* 2008). In addition, a number of studies that have found significantly increased EPO levels in subjects who developed HAPE (Basu *et al.* 2007; Pavliceck *et al.* 2000). EPO has been widely studied for its role in improving athletic performance after altitude exposure: 'living high, training low'. It has been shown that athletes who were non-responders, i.e. who did not show an improvement in performance following a sojourn at altitude, had a smaller and less sustained increase in EPO when compared to 'responders' (Chapman *et al.* 1998). This is consistent with the original hypothesis. Discrepancy among studies may reflect the fact that EPO has been shown to be a key factor modulating not only an increase in RBCC, but also affecting the HVR, carotid body activity, and hypoxic ventilatory acclimatisation (Soliz *et al.* 2005).

7.1.5 Diurnal EPO variation, and associations with sex and age

Erythropoietin production at altitude seems mainly influenced by changes in pH and the affinity of O_2 for haemoglobin. However, a number of studies have demonstrated diurnal variations in EPO expression: Klausen *et al.* (1996) showed that the lowest concentrations were seen between 8am and 4pm, with peaks occurring at 4am. It is logical that EPO peaks coincide with the observation that many people experience a significant drop in their blood O_2 saturation while sleeping, especially if cheyne stoke breathing is occurring (oscillation in the pattern of ventilation between apnea and

tachypnea under hypoxic conditions), and this theory is supported by a study done by Cahan *et al.* (1992), who found that EPO peaked at similar time points in their study. Thus, it is seemingly important to maintain a constant sampling time point following a period of rest to normalise O_2 saturations, and that sampling should most suitably occur in the waking hours, providing a more true representation of EPO levels as a reflection of the resting O_2 saturation, as opposed to under the more hypoxic induction experienced when sleeping.

Women and female animals are well known to cope better than males when exposed to decreased PO_2 at high altitude and this coincides with the observation that women are less susceptible to hypoxia-related illness at sea level (Soliz *et al.* 2000). Soliz *et al.* (2009) were the first to demonstrate that EPO modulates hypoxic ventilation in a sex-dependent manner, both in mouse and man. They found that EPO acts at both the brain stem in the central respiratory centres, and the carotid body cells at the periphery. It is well known that the ovarian steroids, progesterone and oestrogen, are potent ventilatory stimulants (Lefter *et al.* 2007), and data on illness at altitude (AMS, HACE and HAPE) suggest that these steroids play a protective role (Basnyat and Murdoch, 2003). Mukundan *et al.* (2002) found that both hormones can directly influence the expression of EPO.

A study done in 1981 by Peterson *et al.* showed that the HVR strongly decreased with age, by 50% in a group of 65-79 year olds when compared to a younger age group. The production of endogenous thiols are known to modulate the production of EPO, and a further study has shown that plasma thiol decreases with age, and corresponding shifts in the plasma redox state (i.e. the amount of damaging free radicals present) are thought to contribute to age-related impairment of EPO responses (Hildebrandt *et al*. 2002).

7.1.6 Normobaric hypoxia *vs.* hypobaric hypoxia

There are as yet no studies to date that expose subjects to an equal time treatment of both normobaric and hypobaric hypoxia with a crossover experimental design. A number of studies have looked at the intermittent hypoxic response under both normobaric and hypobaric conditions, (i.e. short periods of time at hypoxia followed by a soujourn at normoxia) and some suggest that the physiological response of humans to hypobaric hypoxia is markedly different to that under normobaric hypoxic conditions. Savourey *et al.* (2003) found that hypobaric hypoxia leads to a greater hypoxemia, hypocapnia, blood alkalosis and a lower O_2 arterial saturation when compared to normobaric exposure, and that intermittent hypobaric hypoxic exposure is more likely to aid acclimatisation. However, this is a controversial area with other studies finding intermittent normobaric hypoxia successful at aiding acclimatisation, the latter a useful practise for example in training army personnel (Muza, 2007). This is clearly an area that needs further investigation.

The first set of experiments were conducted to determine if it is possible to determine the susceptibility of an individual to AMS on exposure to high altitude, based on their plasma EPO response. The second part was used to determine if leukocytes could be used as a viable, minimally invasive surrogate marker of activation of the HIF-system under hypoxia. Leukocytes are the first nucleated cells, after pulmonary cells, to be exposed to O_2 tension variations (Mounier *et al.* 2008), and their life-span remains unchanged under hypoxic conditions (Birks *et al.* 1975). They express a variety of HIF-regulated genes, and as measuring HIF protein proved too labile in this study to be a useful marker, gene expression of HIF-1α and a collection of downstream genes regulated by HIF under hypoxia was deemed the most likely to provide an accurate representation of systemic HIF activation. Subsequently, the downstream gene response was evaluated to determine if any relationship exists with AMS at altitude.

7.2 Methods

7.2.1 Experimental design

Twenty subjects participated in a two-part study involving an acute and chronic exposure to hypoxia; all subjects were members of the BMRES who volunteered themselves for the study. Each subject signed a consent form to enable their inclusion in the study and ethical approval was obtained from the South Birmingham Ethics Committee. In the acute exposure (phase I), baseline normoxic measurements were made in a laboratory followed by 6-hour exposure to 12% O_2 in a normobaric hypoxic chamber (the equivalent of about 4600m), maintained at room temperature (RT). This altitude was chosen as it is greater than that deemed necessary for EPO induction, it follows a similar altitude to a number of studies in this area, and subjects were to be based at a similar altitude in Chile, phase II. Measurements were repeated at the end of the hypoxic exposure. Subsequently, the study involved a chronic exposure (phase II). Baseline measurements were taken in Chile at sea level in Arica, and at Parinacota (4392m), 4 days post-altitude exposure. The ascent profile is shown in Fig. 7.3. Subjects comprised 6 female and 14 male with a mean age of 43 ± 17 years, and a mean body mass of 75.7 ± 10.4kg.

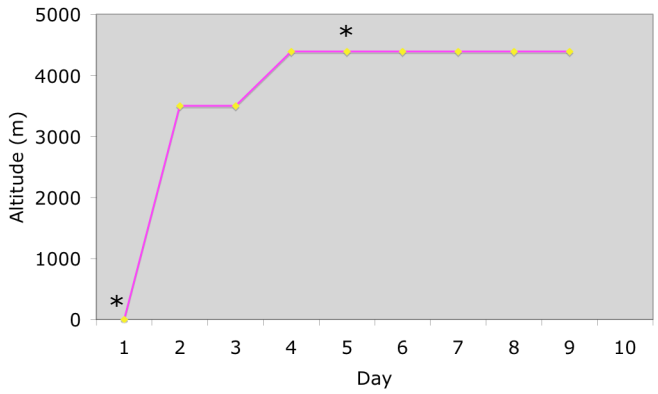

Figure 7.3 Ascent profile in Chile. (* indicates where blood samples were taken)

During the experimental sampling and measurement period, the degree of AMS was determined using the LL and ESQ scoring systems. An arbitrary value of a LL score (self + clinical) of >=3 plus a headache, was used alongside an ESQ score of >=0.7 to diagnose those suffering with AMS, as has been used in a number of studies (Tissot van Patot *et al.* 2005; Roeggla *et al.* 1996; Maggiorini *et al.* 1998; Dellasanta *et al.* 2007). The following calculation was used to determine the ESQ score, with the score per question represented as 'Q':

$$ESQscore=(Q1*0.489+Q2*0.465+Q3*0.446+Q4*0.346+Q5*0.501+Q6*0.519+Q7*0.387+Q8*0.347+Q9*0.413+Q10*0.692+Q11*0.584)/25.95*5$$

Oxygen saturation was measured using a pulse oximeter, a non-invasive method of determining the percentage of haemoglobin (Hb) saturated with O_2. The PO_2 and PCO_2 were determined from venous and arterialised capillary blood samples (ear lobe: these samples were only able to be collected during phase I), along with haematocrit (Hct) and Hb levels (Appendix III), which were obtained in both phases. Venous blood for plasma and leukocytes was drawn and processed as described in 7.2.1.2 and 7.2.1.3.

7.2.2 Plasma separation from blood

Blood was drawn into a 10ml purple top vacutainer tube by a trained physician who was an expert phlebotomist,at a constant time point of in the morning, both in the acute and chronic phase of the study, and centrifuged at RT for 30 min at 400g. Plasma was withdrawn and aliquoted into Eppendorf tubes which were then flash frozen in liquid nitrogen and stored at -80°C. ELISAs were used to analyse EPO, VEGF and sFlt-1 expression at each time point (R&D Systems, DEP00, DVE00 and DVR100), the kit being used as per the manufacturer's instructions (CHPT 2.7). The kit for VEGF measures $VEGF^{165}$, an isoform of VEGF-A and this is the isoform that is referred to for the rest of the chapter.

7.2.3 mRNA extraction from leukocytes

PaxGene tubes (PreAnalytix, 762165) were used to store 2.5ml blood for subsequent mRNA extraction. PaxGene tubes contain a stabilising agent that halts further change in gene expression, allowing quantification of gene expression at the time of the blood sample. The PreAnalytix blood RNA extraction kit (BD Biosciences, 762174) was used according to the manufacturers instructions. cDNA was made and RT-PCR carried out (CHPT 2.6). The following genes were analysed for their expression under normoxic and hypoxic conditions: HIF-1α (Hs00936368_m1), EPO (Hs01071097_m1), VEGF-A (Hs00900055_m1), Flk-1 (Hs009211700_m1), HMOX-1 (Hs01110250_m1), iNOS (Hs00167248_m1), and ALD-A (Hs00605108_g1). A selection of probes for carbonic anhydrase IX (CAIX) and sFlt were trialed under a variety of conditions using different controls, though attempts to study gene expression in leukocytes were not successful for these genes.

See Appendix II for details on HIF nuclear extraction from leukocytes.

7.3 Results

For raw data showing absolute data plots of mRNA gene expression, Hct, Hb, PO_2 and PCO_2 values, and plasma protein values, see Appendix III.

7.3.1 Changes on a physiological level

7.3.1.1 AMS

The criteria used to diagnose AMS was a LL score of >=3 and an ESQ score of >=0.7. Based on this, a small proportion of individuals were categorised (Table 7.1) with 4 out of the total 10 subjects diagnosed with AMS, suffering during both the acute and chronic exposure.

AMS in phase I and II	AMS in phase I only	AMS in phase II only
3, 12, 18, 20	9, 10, 16	11, 21, 22

Table. 7.1 Individuals diagnosed with AMS based on the LL and ESQ scoring systems as described (anonymised ID shown)

7.3.1.2 Oxygen saturation

As expected, O_2 saturation was lowered under hypoxic conditions as demonstrated by changes in O_2 saturation (pulse oximetry) and the PO_2 content of the blood (Fig. 7.4). Unfortunately, the latter sample could not be obtained during phase II due to logistical difficulties in the field. Measurements with the pulse oximeter showed a mean of 97.7 ± 0.17% in normoxia and 82.3 ± 1.5% in hypoxia, phase I and 98.8 ± 0.09% at sea level and 88.5 ± 1.1% at high altitude in phase II, both of these being significantly lowered (P<0.0001). Mean PO_2 was in phase I was 42.1 ± 1.0mmHg.

(a) Phase I

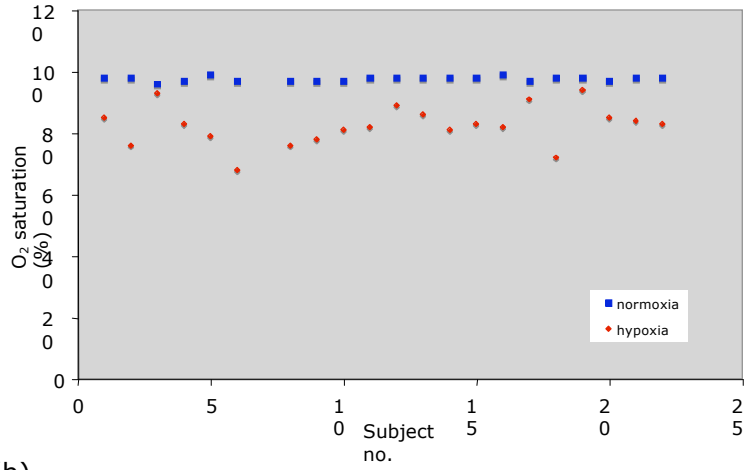

Phase II

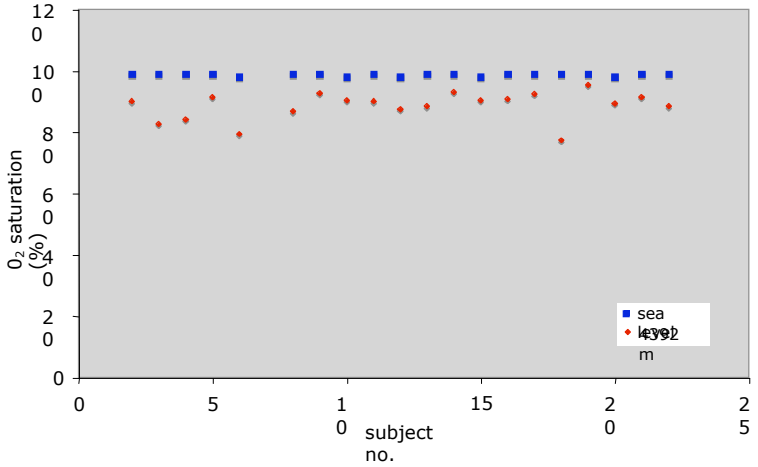

(b)

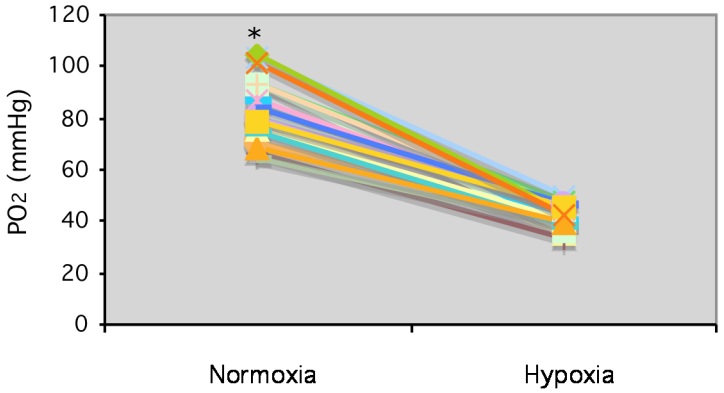

Figure 7.4 Change in % O_2 saturation as seen with (a) finger pulse oximeter and (b) in the PO_2 of an arterialised blood (phase I only), individual values shown, with means for each group calculated. * = $P<0.0001$ as determined with a paired t-test (n=20)

7.3.2 Changes on a molecular level: plasma protein

7.3.2.1 Changes in plasma EPO protein under acute and chronic hypoxia

All individuals showed a rise in plasma EPO (Fig. 7.5) that was significant when analysed with a paired t-test. However, the relative change was different (with the exception of one individual) in phase I compared to phase II (Fig. 7.6). While the magnitude of change was much greater in phase II when compared to phase I (Fig. 7.7), the range was still large.

Table 7.2 Mean plasma EPO (mIU/ml) (±SEM, determined by paired t-test)

	Normoxia	**Hypoxia**	***P*-value**
Phase I	8.50 ± 1.13	18.34 ± 1.44	<0.0001
Phase II	11.21 ± 1.02	59.94 ± 7.50	<0.0001

(a) Phase I

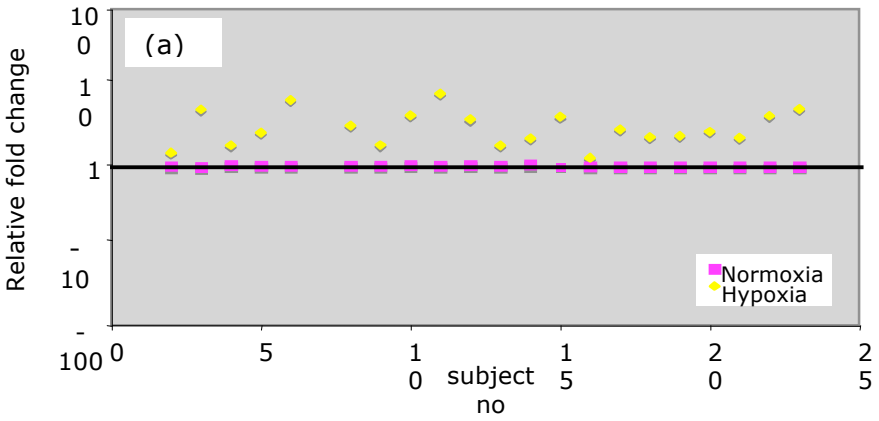

(b) Phase II

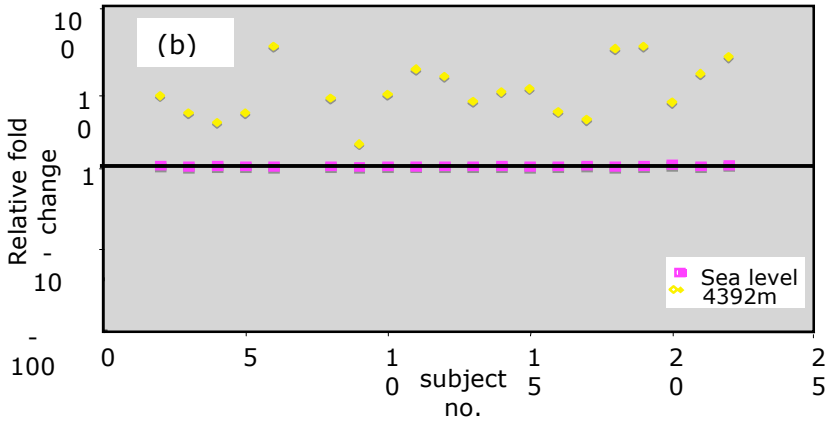

Figure 7.5 Relative fold changes in plasma EPO concentration in (a) phase I and (b) II as determined using an ELISA (n=20)

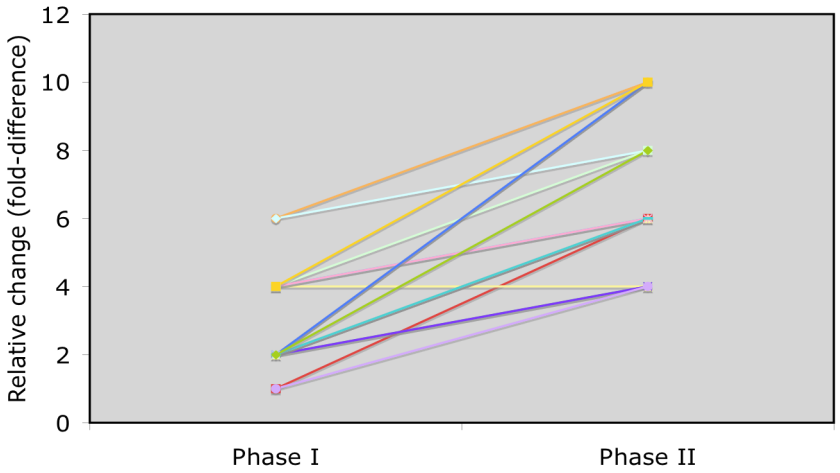

Figure 7.6 Relative fold change in plasma [EPO] in individuals between phase I and phase II on exposure to hypoxia (ELISA)

Figure 7.7 Spread of change in plasma [EPO] between phase I and II. ** = *P*<0.0001, as determined by paired t-test

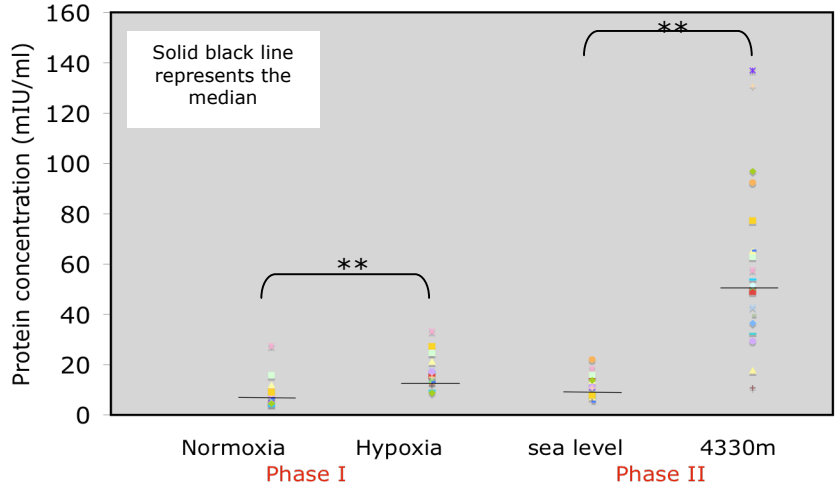

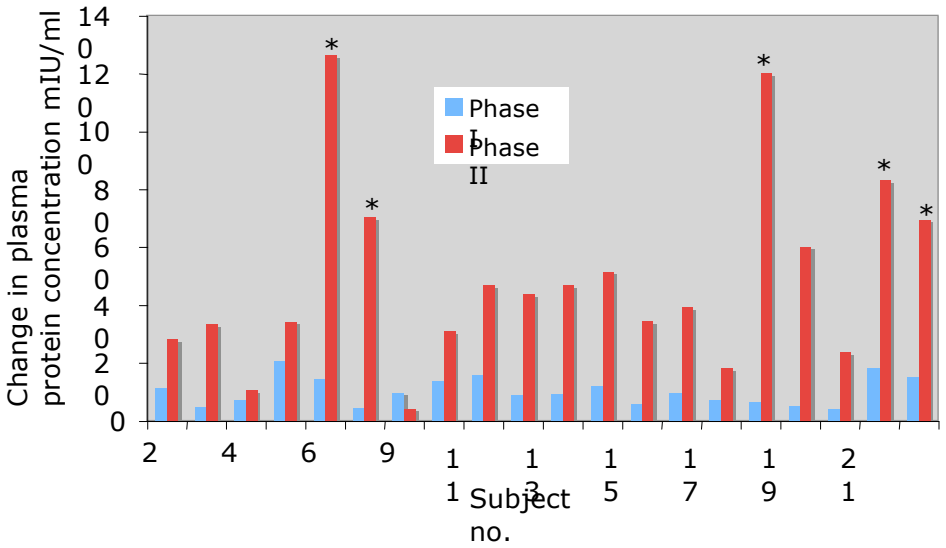

Figure 7.8 Relative changes in plasma [EPO] (mIU/ml) between phase I and II. * indicates those classified as EPO responders based on the arbitrary cut off (explained in the text).

Differentiating responders from non-responders in the acute exposure of phase I was difficult as inter-individual results were similar (Fig. 7.8). A more obvious separation was apparent in phase II, responders being separated from non-responders based on a 40% increase from the mean protein concentration, an arbitrary value based on the lower limit of the response: this 40% cut-off clearly partitioned the EPO responders with a mean of 106.1±11.58mIU/ml from the non-responders with a mean of 44.3 ± 4.3mIU/ml (P=0.05, as determined by paired t-test). Individuals falling within the 'response' category are indicated in Fig. 7.8 (*).

7.3.2.2 Change in plasma VEGF

Plasma VEGF concentration showed a differential response under acute compared with chronic exposure, as evidenced by the relative fold change (Fig. 7.9). After studying the data, a representative value of ±20% was used to indicate whether there had been a notable change in plasma protein expression. (This value was also used for sFlt plasma protein expression). Seven subjects showed a down-regulation, 6 subjects an up-regulation and 7 subjects showed no change in plasma [VEGF] during phase I. Eleven subjects showed a decrease in plasma VEGF in phase II, (6 of these showing a similar response to acute hypoxia), with 9 subjects showing no change at all (5 of these individuals having showed a similar response under acute conditions) (see Table 7.2). A comparison of the change in plasma VEGF under acute and chronic hypoxia is shown in Fig. 7.10.

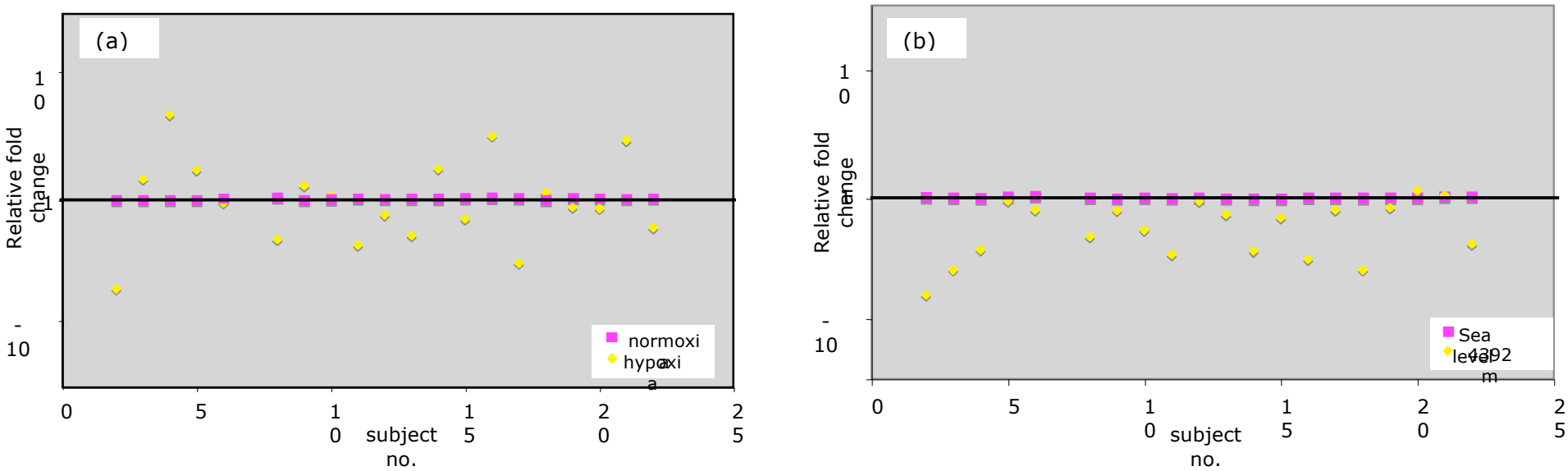

Figure 7.9 Relative fold changes in plasma [VEGF] in (a) Phase I (b) Phase II as determined using an ELISA

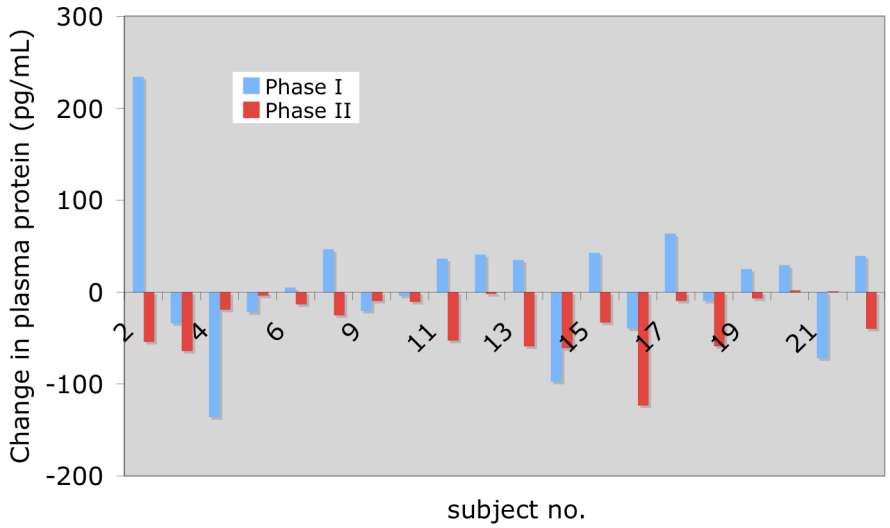

Figure 7.10 Change in VEGF plasma [protein] during phase I and phase II (pg/ml) (determined by ELISA) what is the scale on the ordinate?

7.3.2.3 Change in plasma sFlt

As with VEGF, changes in plasma sFlt under acute and chronic hypoxia appeared to differ, a varied response being shown under the former and a more blunted response under the latter conditions. Using a representative value of ±20% change in expression to distinguish responders from non-responders, 8 subjects showed an increase in protein expression under acute hypoxia compared to 6 subjects under chronic hypoxia, with 6 of these being the same subjects. No subject showed a decrease in expression under chronic conditions compared to 6 who did so under acute hypoxia. Fourteen subjects showed no change under chronic conditions, with 6 of these being the same under acute hypoxia (see Table 7.2). Relative fold change in protein expression is shown (Fig. 7.11) along with the change in protein concentration, a comparison between phase I and II (Fig. 7.12).

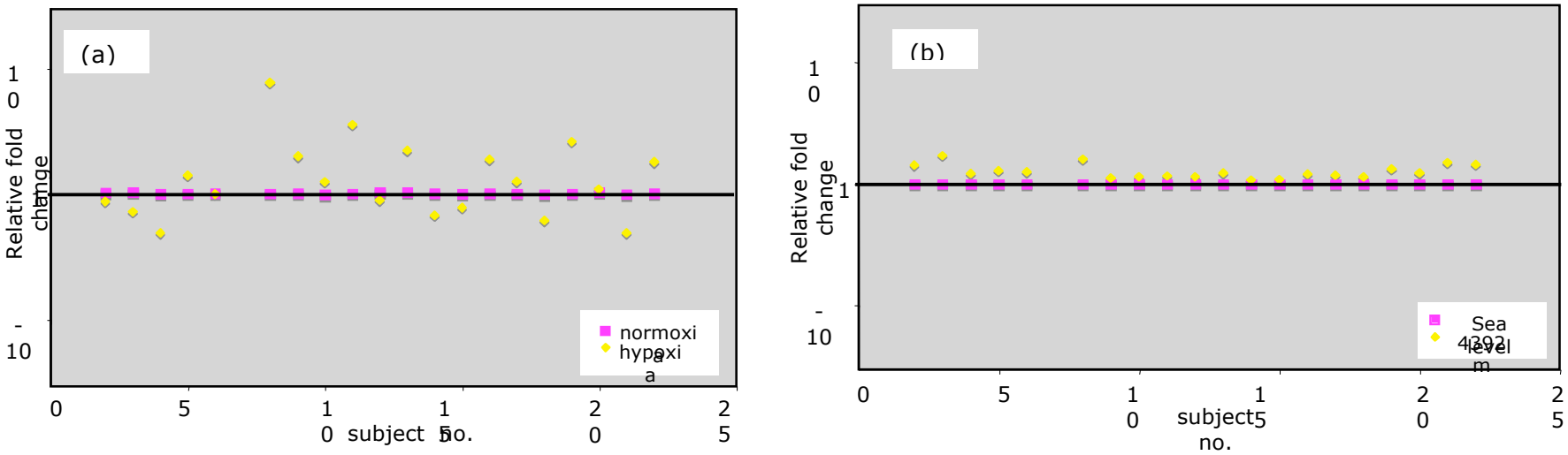

Figure 7.11 Relative fold change in plasma [sFlt-1] in (a) phase I and (b) phase II as determined using an ELISA

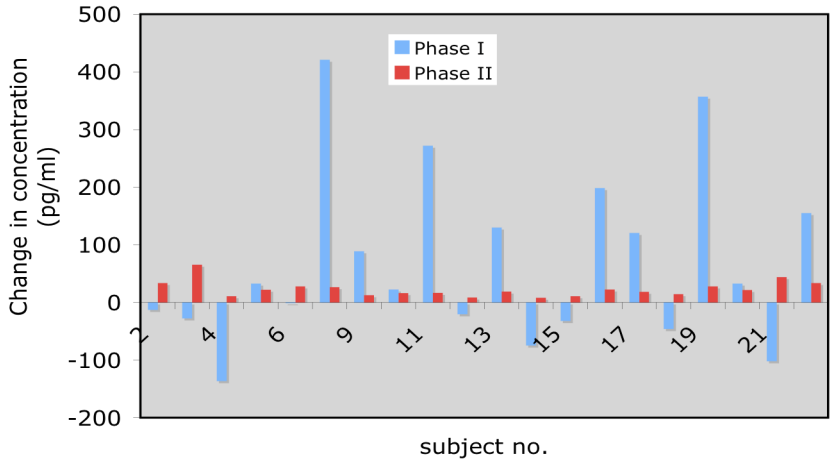

Figure 4.12 Change in sFlt [protein] (pg/ml) (as determined by ELISA)

7.3.2.4 Inconsistent changes in plasma EPO, VEGF and sFlt

Table 7.3 illustrates individual changes seen in plasma protein levels of EPO, VEGF and sFlt during phase I and phase II. It is evident that although all individuals experienced an increase in EPO levels, a varied relationship exists between EPO and corresponding VEGF and sFlt levels. Three individuals showed no change in levels of both VEGF and sFlt, 9 individuals show the same change of either an increase or decrease in both phase I and II, and the remainder exhibit prolific variation in response. All subjects either decreased or maintained VEGF levels in phase II.

Subject no.	Plasma EPO: chamber	Plasma EPO: 4330m	Plasma VEGF: chamber	Plasma VEGF: 4330m	Plasma sFLT: chamber	Plasma sFLT: 4330m
2	↑	↑	↓	↓	↓	↑
3	↑	↑	↑	↓	↓	↑
4	↑	↑	↑	∅	↓	∅
5	↑	↑	↑	∅	↑	∅
6	↑	↑	∅	∅	∅	∅
8	↑	↑	↓	↓	↑	↑
9	↑	↑	∅	↓	↑	∅
10	↑	↑	∅	↓	∅	∅
11	↑	↑	↓	↓	↑	∅
12	↑	↑	∅	∅	∅	∅
13	↑	↑	↓	↓	↑	∅
14	↑	↑	↑	↓	↓	∅
15	↑	↑	↓	↓	∅	∅
16	↑	↑	↑	↓	↑	∅
17	↑	↑	↓	∅	∅	∅
18	↑	↑	∅	∅	↓	∅
19	↑	↑	∅	∅	↑	↑
20	↑	↑	∅	∅	∅	∅
21	↑	↑	↑	∅	↓	↑
22	↑	↑	↓	↓	↑	↑

Table 7.3 Individual response in plasma protein levels. ↑ indicates an increase, ↓ a decrease and ∅ no change (with ±20% change levels as defined in 7.3.2.2)

7.3.2.4.1 Relationship between EPO and sFlt

Although regression analyses indicate a weak relationship (R^2=0.109, phase I; R^2=0.040, phase II), on plotting the relative change in plasma EPO and sFlt protein a positive relationship was seen both phase I and phase II, although this does not reach statistical significance (Fig. 7.13). sFLT is shown as relative change in pg/ml, EPO as mIU/ml

(a)

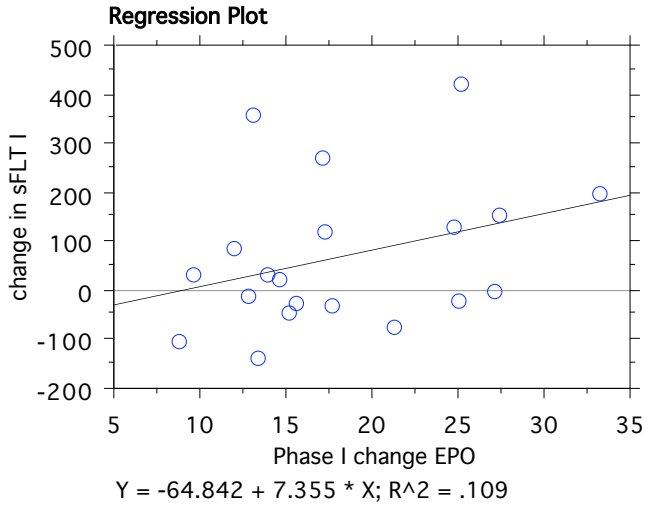

P-value: 0.154

(b)

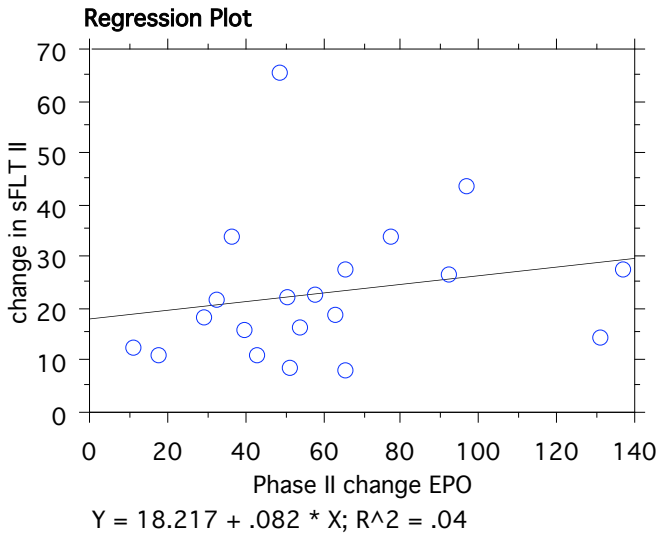

P-value: 0.396

Figure 7.13 Regression analyses of change in plasma EPO [protein] against sFlt plasma [protein] (a) phase I and (b) phase II

7.3.2.4.3 Relationship between plasma VEGF and EPO protein

There was no significant relationship between changes in plasma EPO and VEGF in phase I (P=0.912, R^2=0.001) or phase II (P=0.636, R^2=0.013, Fig. 7.14). VEGF is shown as relative change in pg/ml, EPO as mIU/ml

(a)

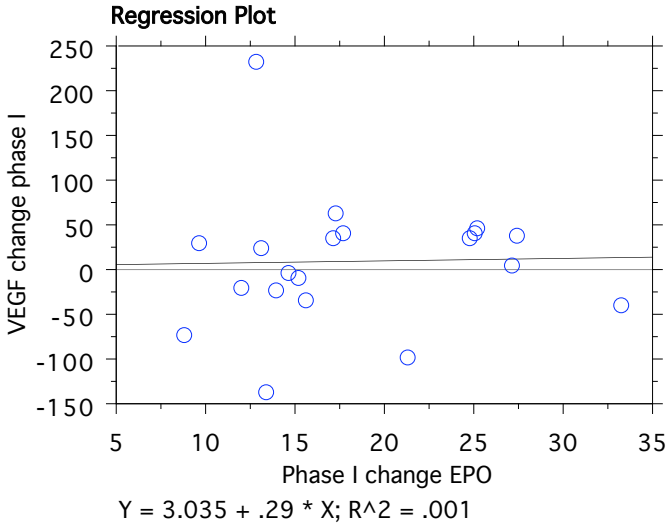

(b)

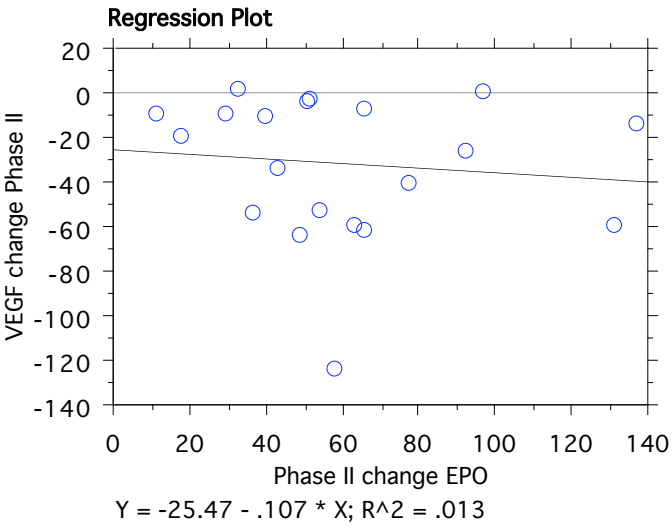

Figure 7.14 Regression analyses of change in plasma [EPO] *vs.* change in plasma [VEGF] protein in (a) phase I and (b) phase II

7.3.2.4.3 Relationship between VEGF and sFlt

A significant relationship was seen between changes in plasma VEGF *vs.* sFlt protein in phase I (R^2=0.327, *P*=0.011). No significant relationship was found between VEGF and sFlt in phase II (R^2=0.027, *P*=0.512, Fig. 7.15). These relationships are further illustrated in Fig. 7.16. sFLT is shown as relative change in pg/ml, VEGF as pg/ml.

(a)

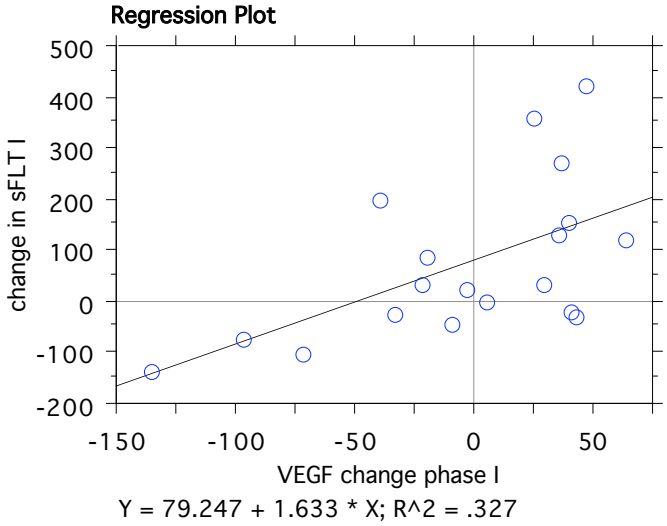

(b)

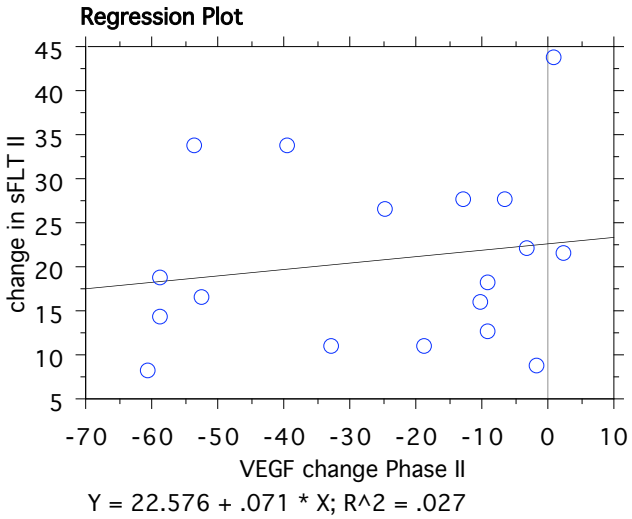

Figure 7.15 Regression analyses showing change in plasma [sFLT] protein *vs.* VEGF plasma [protein] in (a) phase I and (b) phase II.

(a)

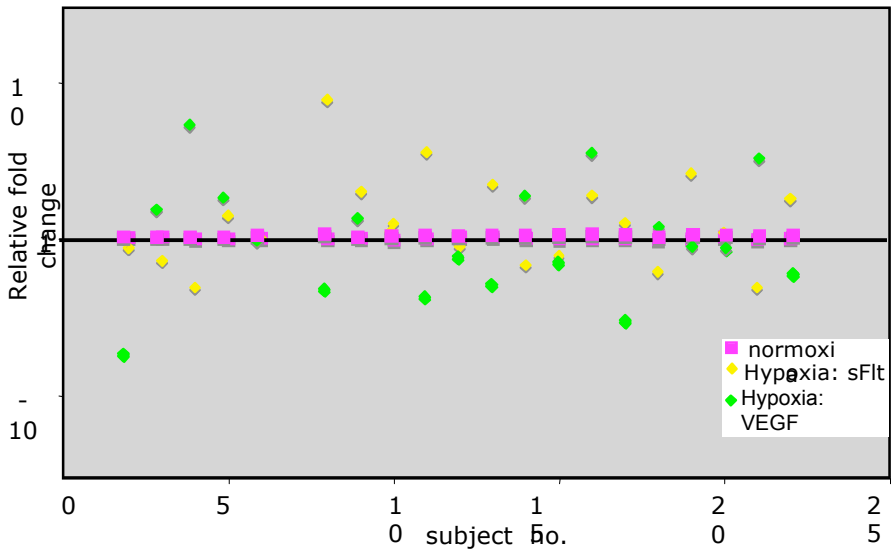

(b)

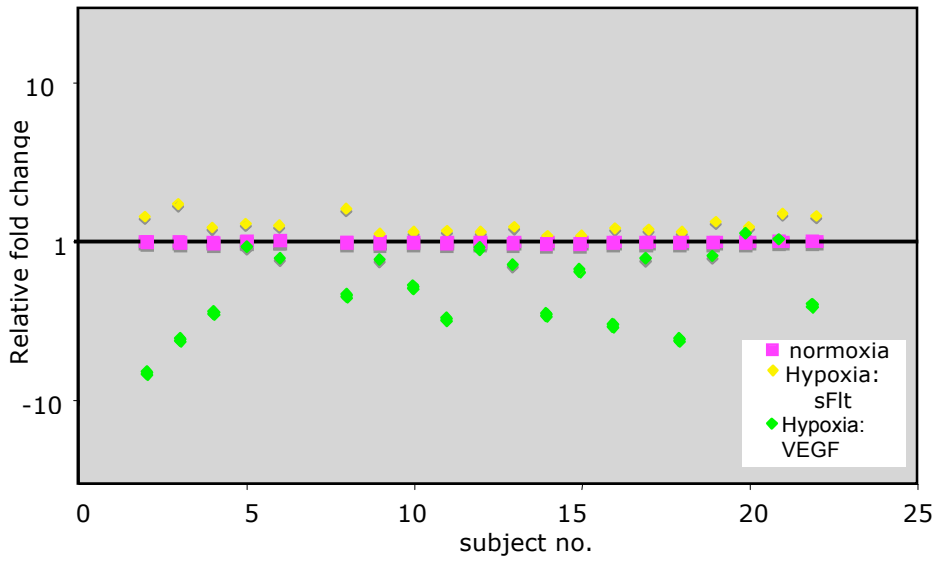

Figure 7.16 Illustration of the changing relationship between plasma VEGF and sFlt protein during (a) phase I and (b) phase II, protein levels as determined by ELISA

7.3.2.5 Plasma protein changes in AMS+ and AMS- individuals

Mean protein concentration generally varied between well subjects and those diagnosed with AMS (Table 7.4). The mean of plasma EPO in phase I showed little change, although subjects with AMS in phase II showed a trend for higher levels of EPO plasma protein. Plasma VEGF levels showed greater a change in phase II with sick individuals tending to show lower levels. A consistent fall in VEGF levels under hypoxia compared with normoxia was observed in Phase II in most subjects, though a number remained unchanged. sFlt showed a different relationship in phase II compared with phase I, with slightly higher levels in sick subjects in phase II, along with the majority of subjects showing increased levels. However, none of these differences were statistically significant using an unpaired t-test.

Protein	**AMS**	**Phase I**	**Phase II**
EPO (mIU/ml)	+	17.8 ± 3.14	70.2 ± 12.8
	-	19.6 ± 1.77	56.1 ± 8.6
VEGF (pg/ml)	+	81.3 ± 20.4	26.6 ± 3.5
	-	91.4 ± 19.3	44.9 ± 11.4
sFlt (pg/ml)	+	227.2 ± 74.4	111.8 ±10.1
	-	271.5 ± 54.2	105.8 ± 6.4

Table 7.4 Mean plasma protein concentration values for EPO, VEGF and sFlt during phase I and II (± SEM), as determined by ELISA. AMS+ n=7, AMS- n=13.

7.3.3 Changes on a molecular level: hypoxia-regulated gene expression

Criteria of ±40% were used to determine whether subjects had shown a change in leukocyte gene expression.

7.3.3.1 Changes in leukocyte Aldolase-A (ALD-A) gene expression

As is clearly shown, the magnitude of change occurring was greater under chronic hypoxia (Fig. 7.17). However, the individual changes were not correlated between phases of the study (Table 7.3). Two out of the 6 individuals who showed no change in expression did so in both phases, while 5 of the 9 subjects who increased ALD-A levels in phase I and 3 of the 5 subjects who showed a decrease in phase I showed no change in phase II.

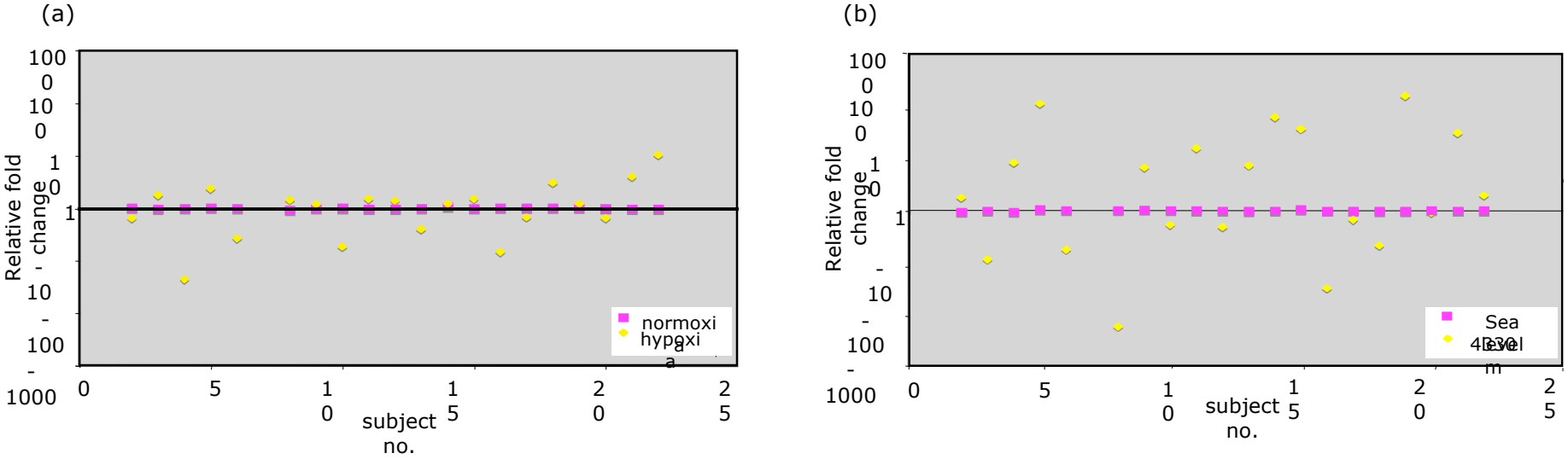

Figure 7.17 Relative fold change in leukocyte ALD-A gene expression during (a) phase I and (b) phase II as determined by qRT-PCR

7.3.3.2 Changes in leukocyte inducible nitric oxide synthase (iNOS) gene expression

A great deal of variability was seen in the leukocyte iNOS mRNA response to hypoxia (Fig. 7.18). In phase I, 8 subjects showed no change compared to one individual in phase II. Of the 5 subjects that showed increased iNOS levels in phase I, 2 of these also did so in phase II, and 3 of the 7 who showed a decrease in phase I showed a similar response in phase II.

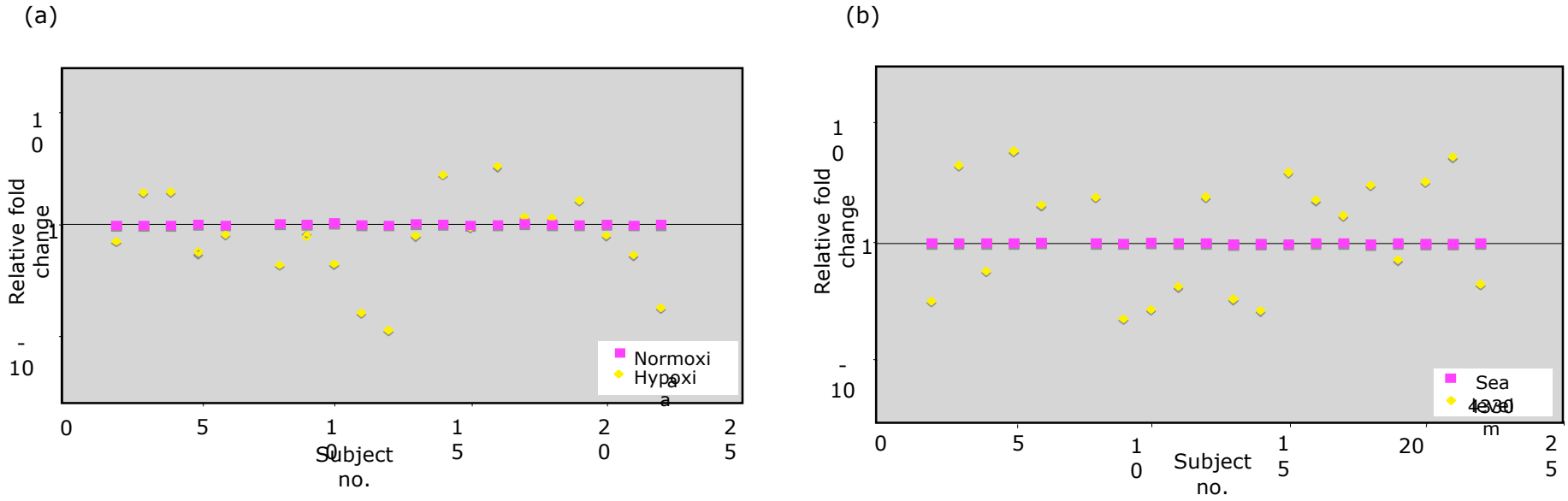

Figure 7.18 Relative fold change in leukocyte gene iNOS expression during (a) phase I and (b) phase II as determined by qRT-PCR

7.3.3.3 Changes in leukocyte haemoxygenase (HMOX-1) gene expression

Chronic hypoxia had a greater effect on the magnitude of HMOX-1 gene expression in the leukocytes (Appendix III). Eleven subjects increased their expression by >=40%: 2 of these showed the same response in phase I, and 8 subjects showed a decrease in expression. Three of these individuals exhibited the same response in phase I (Fig. 7.19). Only 1 person showed no change, compared with 8 who remained unchanged under acute hypoxia conditions.

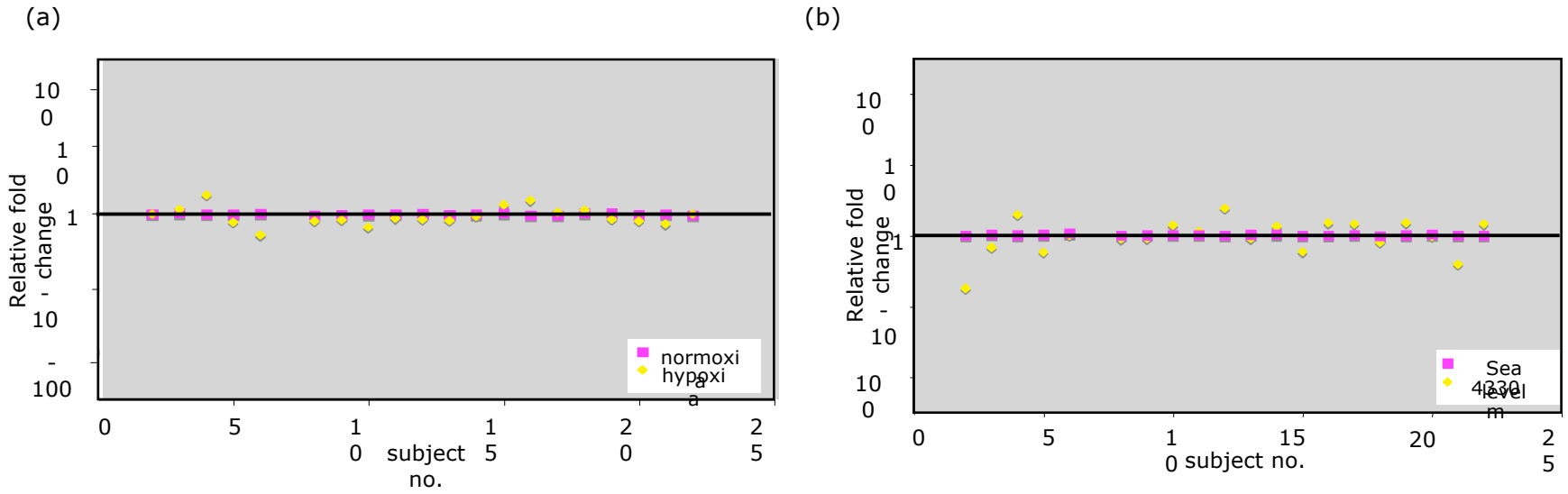

Figure 7.19 Relative fold change in leukocyte HMOX-1 gene expression during (a) phase I and (b) phase II as determined by qRT-PCR

7.3.3.4 Changes in leukocyte fms-like tyrosine kinase-1 (Flk-1) gene expression

Individuals exhibited similar changes in Flk-1 leukocyte gene expression under both chronic and acute hypoxia (Appendix III). Seven subjects showed no change in phase I: four of these had the same response in phase II, ten showed an increase in phase I, 5 showing the same response in phase II; and 3 decreased their expression in both phases (Fig. 7.20).

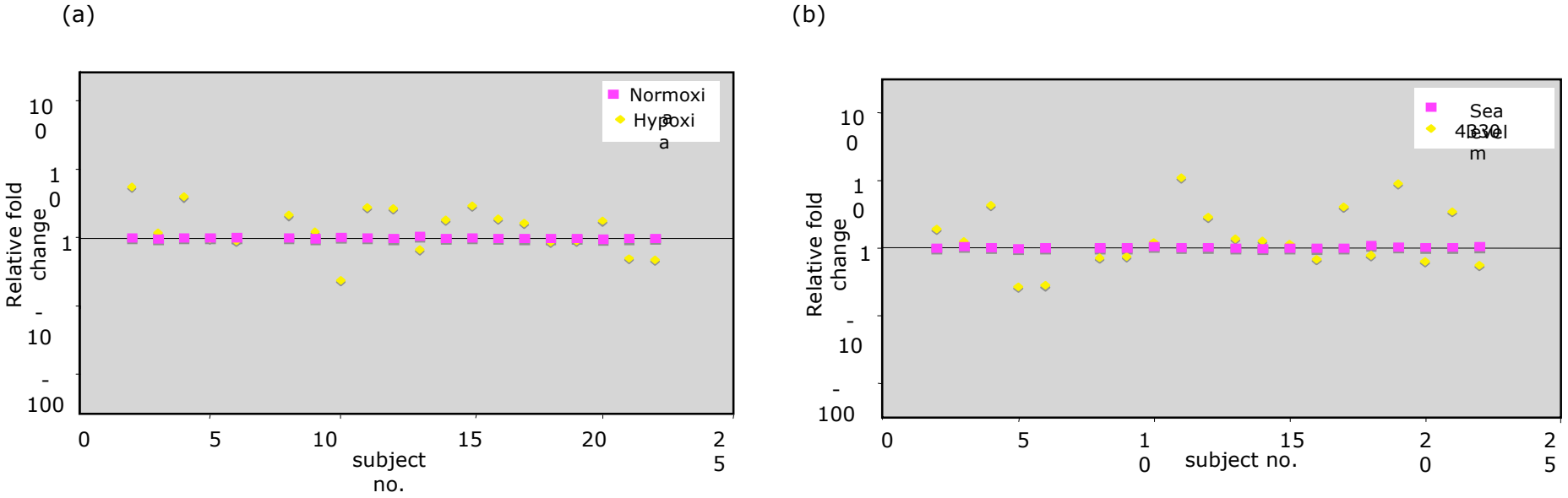

Figure 7.20 Relative fold change in leukocyte Flk-1 gene expression during (a) phase I and (b) phase II as determined by qRT-PCR

7.3.3.5 Changes in leukocyte vascular endothelial growth factor (VEGF) gene expression

Hypoxia generally failed to induce a prominent change in leukocyte VEGF gene expression under either acute or chronic hypoxia (Fig. 7.21, Appendix III). Fourteen of the 20 subjects showed unchanged values in phase I, with 7 of these showing the same response in phase II. Only 3 subjects showed an increase in phase I, compared to 6 in phase II, with the remaining 2 and 3 showing a decrease in phase I and II, respectively.

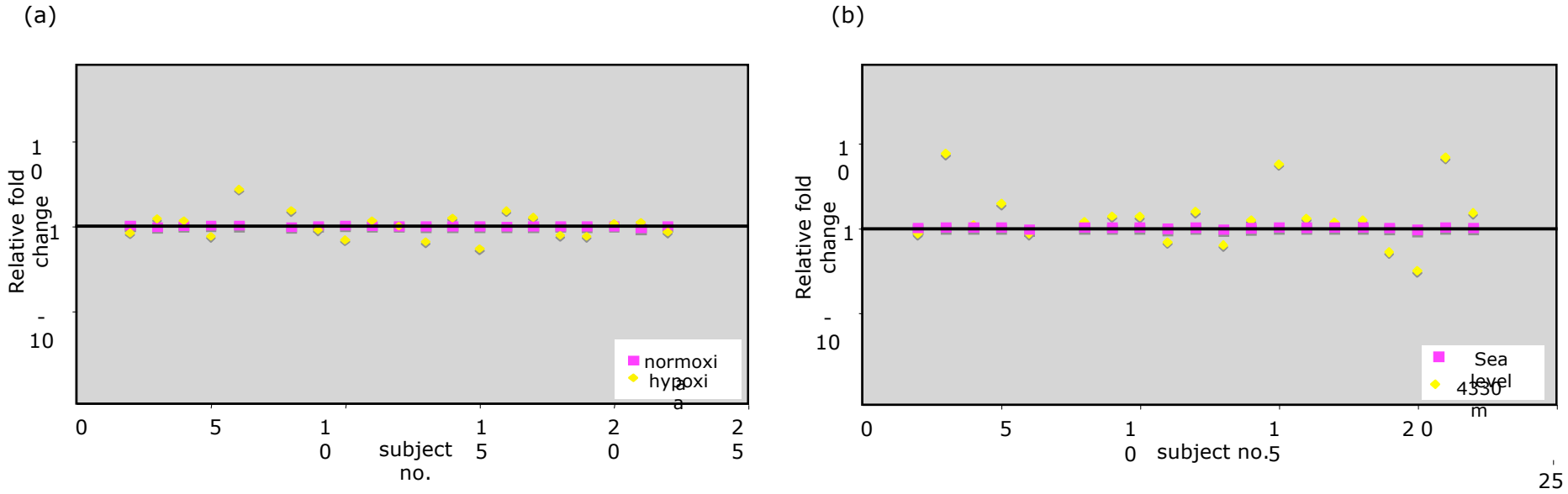

Figure 7.21 Relative fold change in leukocyte VEGF gene expression during (a) phase I and (b) phase II as determined by qRT-PCR

7.3.3.6 Changes in leukocyte erythropoietin (EPO) gene expression

Little correlation was shown in the individual response between phase I and II (Fig. 7.22, Table 7.3). Nine subjects showed unchanged levels during phase I compared with 5 during phase II. Only 7 subjects showed an increase of >=40% in phase I compared to 13 in phase II, with 4 and 2 subjects in phase I and II, respectively, showing a decline in expression.

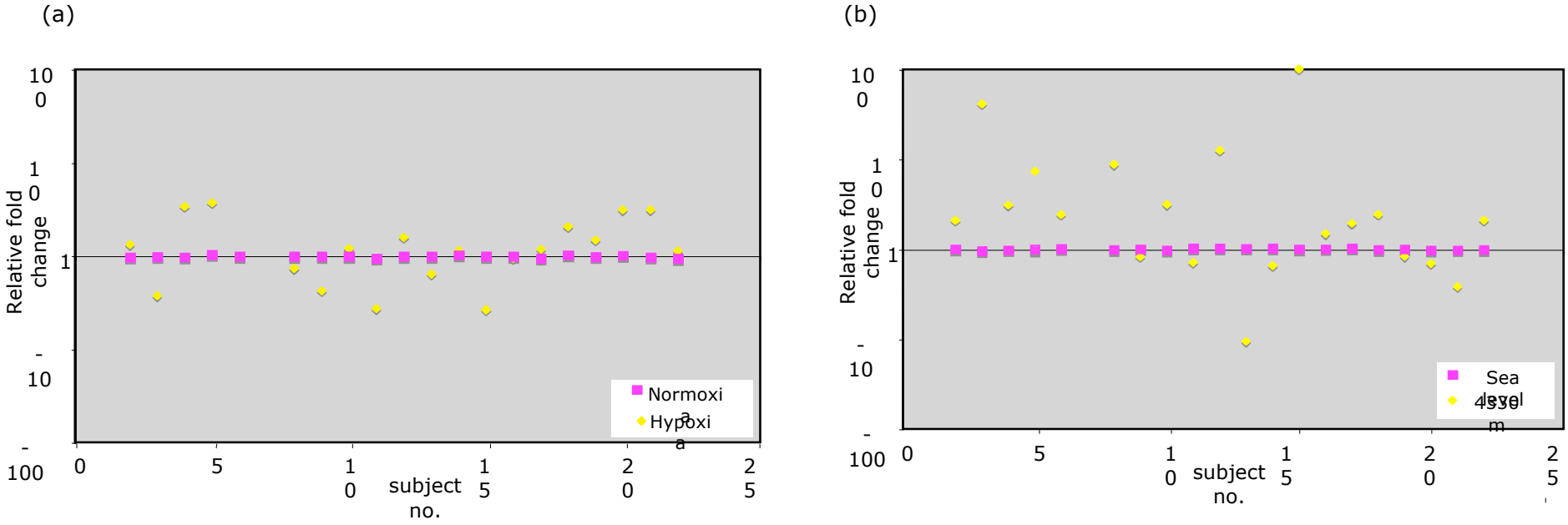

Figure 7.22 Relative fold change in leukocyte EPO gene expression during (a) phase I and (b) phase II as determined by qRT-PCR

7.3.3.7 Changes in leukocyte hypoxia inducible factor-1α (HIF-α) gene expression

Leukocyte HIF-1α mRNA expression remained unchanged in 9 individuals during phase I, with 3 of these also lacking a response in phase II (Fig. 7.23, Table 7.3). Similar numbers, 6 and 7 subjects in phase I and II respectively, showed an increase (4 of these being the same individuals); 5 individuals showed a decrease in expression, with 2 showing the same response out of 8 individuals who decreased expression in phase II.

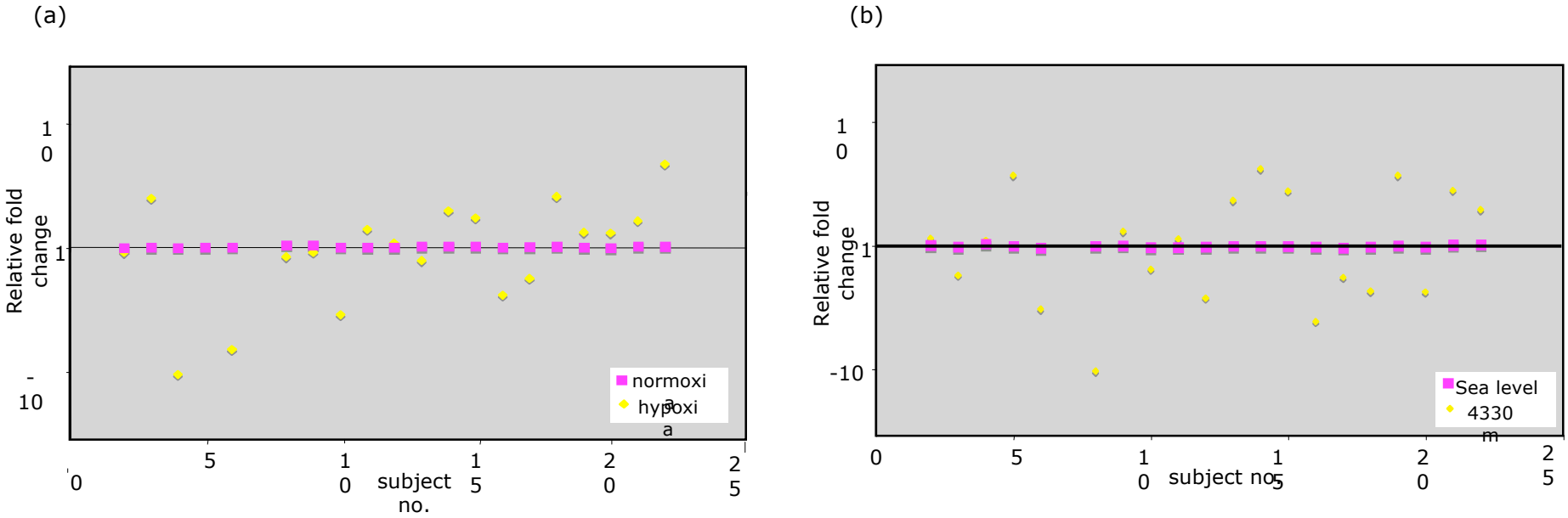

Figure 7.23 Relative fold change in leukocyte HIF-1α gene expression during (a) phase I and (b) phase II, determined by qRT-PCR

7.3.3.8 Summary of changes in mRNA levels of genes regulated by HIF-1α

Table 7.5 clearly demonstrates the undefined relationship that exists between HIF-1α and a selection of its target genes expressed in leukocytes, with arrows indicating the directionality of change based on ± 40%.

	HIF: I	HIF: II	EPO: I	EPO: II	VEGF: I	VEGF: II	ALD-A: I	ALD-A: II	iNOS: I	iNOS: II	FLK-1: I	FLK-1: II	HMOX: I	HMOX: II
2	∅	∅	∅	↑	∅	∅	∅	↑	∅	↓	↑	↑	∅	↓
3	↑	↓	↓	↑	∅	↑	↑	↓	↑	↑	∅	∅	∅	∅
4	↓	∅	↑	↑	∅	∅	↓	↑	↑	↓	↑	↑	↑	↑
5	∅	↑	↑	↑	∅	↑	↑	↑	↓	↑	∅	↓	∅	↓
6	↓	↓	∅	↑	↑	∅	↓	↓	∅	↑	∅	↓	↓	∅
8	∅	↓	∅	↑	↑	∅	↑	↓	↓	↑	↑	∅	∅	∅
9	∅	∅	↓	∅	∅	∅	∅	↑	∅	↓	∅	∅	∅	∅
10	↓	∅	∅	↑	↓	∅	↓	↓	↓	↓	↓	∅	∅	↑
11	∅	∅	↓	∅	∅	∅	↑	↑	↓	↓	↑	↑	∅	∅
12	∅	↓	↑	↑	∅	↑	↑	↓	↓	↑	↑	↑	∅	↑
13	∅	↑	∅	↓	↓	∅	↓	↑	∅	↓	∅	∅	∅	∅
14	↑	↑	∅	∅	∅	∅	∅	↑	↑	↓	↑	∅	∅	∅
15	↑	↑	↓	↑	↓	↑	↑	↑	∅	↑	↑	∅	∅	∅
16	↓	↓	∅	↑	↑	∅	↓	↓	↑	↑	↑	∅	↑	↑
17	↓	↓	∅	↑	∅	∅	∅	∅	∅	↑	↑	↑	∅	↑
18	↑	↓	↑	↑	∅	∅	↑	↓	∅	↑	∅	∅	∅	∅
19	∅	↑	↑	∅	∅	↓	∅	↑	↑	∅	∅	↑	∅	↑
20	∅	↓	↑	∅	∅	↓	∅	∅	∅	↑	↑	∅	∅	∅
21	↑	↑	↑	↓	∅	↑	↑	↑	↓	↑	↓	↑	∅	↓
22	↑	↑	∅	↑	∅	↑	↑	↑	↓	↓	↓	↓	∅	↑

Table 7.5 Change in gene expression (mRNA) during Phase I and phase II with ↑ indicating an increase, ↓ a decrease (based on a 40%± change) and ∅ no change

7.3.4 Association between physiological and molecular changes

7.3.4.1 Relationship between plasma EPO expression and individuals diagnosed with AMS

There appears to be no relationship between individuals diagnosed as suffering with AMS on the basis of questionnaires and the magnitude of their physiological plasma (EPO) response. All subjects exhibited either a 1 or 2-fold change in Phase I, though this was similar to the majority of other non-AMS individuals. The change ranged from 2 to 10-fold in phase II, again showing no difference when compared to non-AMS individuals.

7.3.4.2 Relationship between changes in plasma EPO with changes in PO_2, Hct, Hb and O_2 saturation (%)

7.3.4.2.1 Phase I

There was no evidence for a relationship between changes in plasma EPO and blood O_2 tension (P=0.6823, R^2=0.01) (Fig. 7.25). Interestingly, there was a significant trend for individuals with lower Hct and Hb values to have a higher induction of EPO (Fig 7.26). It seems plausible that this increased EPO response resulted from a poorer capacity to transport O_2 and hence a greater hypoxic signal to the EPO-producing tissues. This is in line with a weak negative relationship with O_2 saturation (Fig 7.24).

7.3.4.2.2 Phase II

Unfortunately, the PO_2 of arterial blood was not obtained. There was again a strong negative relationship between change in EPO with Hct and Hb (both P<0.0001) (Fig. 7.27). This reinforces the observation made in phase I. There were two outliers as shown in Fig 7.26 (red circle). Both of these subjects had AMS in this phase, and were

also outliers when characterised by the leukocyte mRNA response. There was a further outlier (denoted by red arrow, Fig 7.26) though this subject was not characterised by any of the mentioned features. As in phase I, there was a negative relationship with O_2 saturation (R^2=0.237, P<0.05) (Fig. 7.24). The same two outliers had the lowest O_2 saturation in phase II (Fig 7.24, red circle). Unfortunately, the PO_2 of arterial blood was not obtained in phase II.

(a) (b)

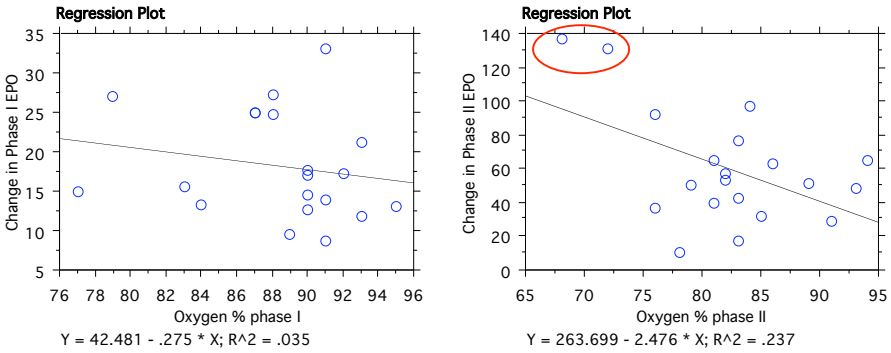

Figure 7.24 Relationship between O_2 saturation and plasma EPO protein response in (a) phase I and (b) phase II

(a) (b) (c)

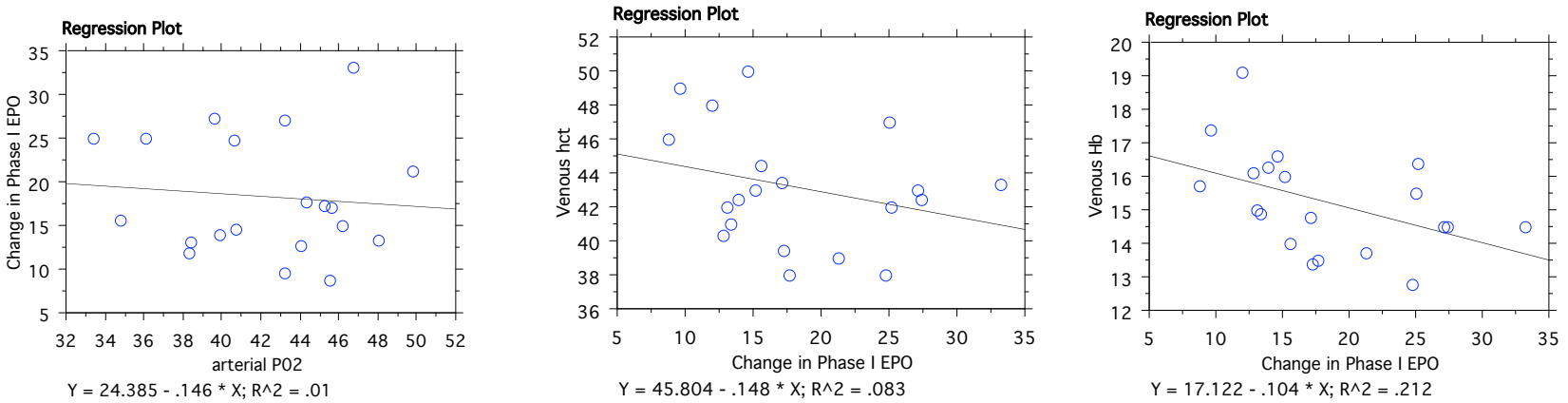

Figure 7.25 Relationship between change in plasma EPO [protein] in phase I with (a) PO_2 (b) Hct (P<0.0001) and (c) Hb (P<0.0001), as determined using regression analyses

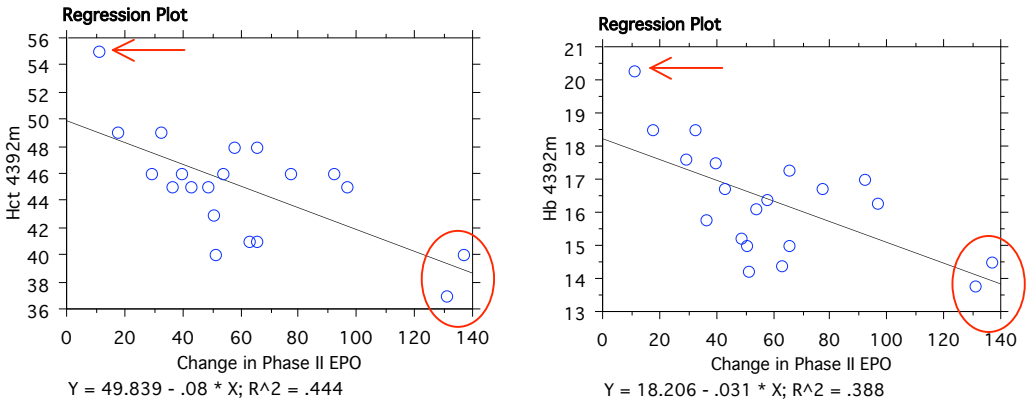

Figure 7.26 Relationship between change in plasma EPO [protein] in phase II with (a) Hct (P< 0.0001) and (b) Hb (P< 0.0001), determined using regression analyses. (Red circles and arrows denote outliers, as explained above).

7.3.4.3 Regression analyses of changes in plasma EPO with downstream hypoxia-activated gene expression

By observing the relationship between plasma EPO protein and the mRNA expression of HIF-1α-regulated genes it was hoped to determine if EPO protein, acting as a surrogate marker of HIF-1α activation, had an influence on downstream gene expression. Analysis of regression coefficients (Table 7.6) indicates little evident relationship, with the exception of VEGF mRNA expression where there was a trend towards a positive relationship (Fig. 7.27, *P*=0.0562).

Gene	Regression Equation		R^2 value		*P*-value	
	Phase I	Phase II	Phase I	Phase II	Phase I	Phase II
ALD-A	Y=-40.828 + 3.181 * X	Y=2.704 – 0.041 * X	0.066	0.136	0.2752	0.1102
iNOS	Y=--0.053 + 0.027 * X	Y=0.366 – 0.005 * X	0.006	0.037	0.7567	0.4158
HMOX-1	Y=433.571 – 85.436 * X	Y=-663.031 - -2.938 * X	0.095	2.953E-4	0.1859	0.9427
VEGF	Y=-268.01 + 29.283 * X	Y=598.73 – 1.16 * X	0.188	0.001	0.0562	0.9082
Flk-1	Y=0.997 – 0.077 * X	Y=0.242 – 0.008 *X	0.122	0.007	0.1319	0.7332
EPO	Y=0.323 – 0.03 * X	Y=3.987 – 0.045 * X	0.152	0.041	0.0890	0.3935
HIF	Y=-0.004 - 0.012 * X	Y=0.043 – 0.001 * X	0.004	0.088	0.7807	0.2041

Table 7.6 Regression values for changes in plasma EPO protein plotted against changes in mRNA expression of HIF-target genes where Y is the gene of interest and X is [EPO]

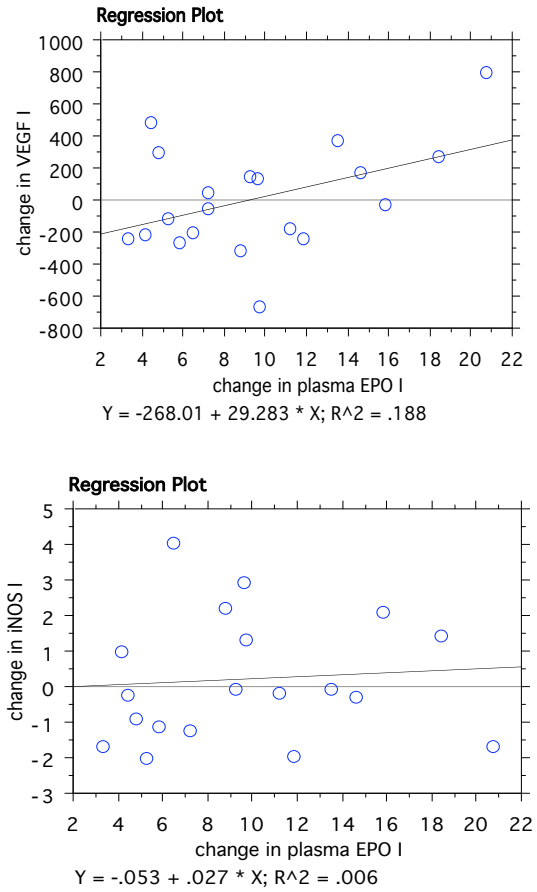

Figure 7.27 (a) A positive relationship between changes in VEGF mRNA and plasma EPO protein in phase I (*P*=0.0562), and (b) illustration of the lack of relationship between changes in iNOS mRNA and EPO plasma protein in phase I (*P*=0.7567)

Outliers were present in the majority of regression analyses graphs, and subsequent identification of these individuals reveals that they were outliers in many gene responses also (Table 7.7). However, correlation of these outliers to AMS scores or % O_2 saturation revealed that none of the outliers from phase I had suffered with AMS, though 3 out of the 6 outliers from phase II had been diagnosed with AMS (subject no. 3, 18 and 21). As seen, subjects 5 and 6 were common to both phases. Furthermore, regression analyses of plasma VEGF with leukocyte VEGF mRNA expression also revealed 2 of the 6 previous outliers who had AMS in phase II (subject no. 3 and 21). Classification of subjects who were EPO responders revealed that 3 of these were also shown to be outliers here (no. 6, 18 and 21).

Outliers common to Phase I		Outliers common to phase II	
Subject no.	Genes involved	Subject no.	Genes involved
		3	iNOS, VEGF, EPO
5	iNOS, HMOX-1	5	ALD-A, Flk-1, HIF-1
6	Flk-1, VEGF, HIF-1	6	ALD-A, iNOS, VEGF, EPO
22	Flk-1, HIF-1	15	ALD-A, VEGF, EPO
		18	ALD-A, iNOS, VEGF, HIF-1, EPO
		21	VEGF, EPO

Table 7.7 Illustration of 'outliers' (denoted by subject no.) revealed in regression analyses of EPO plasma protein with leukocyte mRNA changes. ☐ Indicates subjects who were outliers in both phases.

7.4 Discussion

The first part of this study was designed to determine if EPO 'responders' could be differentiated from 'non-responders' by studying changes in plasma protein levels on exposure to hypoxia, and subsequently correlating these changes with AMS scores and O_2 saturation levels. It has previously been shown that subjects who experienced a rapid rise in EPO production on exposure to low O_2 levels suffered less with AMS (Sutherland, unpublished), possibly due to their enhanced O_2-carrying capacity as a result of an increased Hct, and thus [Hb]. The second part of the study was used to determine if leukocytes can be used as a circulating indicator of HIF-1α activation under hypoxia by studying the mRNA expression of HIF-1α along with a variety of HIF-activated genes, and correlating these findings with AMS scores. Due to difficulties in measuring HIF-protein, EPO protein was used as a surrogate indicator of HIF-activation. The objective was to test whether the findings from these responses would provide information about whether someone is likely to cope better under systemic hypoxia conditions, and thus at high altitude, following on from the observation in CHPT 3 that leukocytes could be used as a viable indicator of HIF-driven gene expression under hypoxic conditions.

7.4.1 Physiological changes under systemic hypoxia

7.4.1.1 Sickness at altitude

On ascent, there is an maximum altitude where an individual can cope sufficiently with the lowered O_2 levels. Extending above this exists a zone whereby the body can tolerate the lower O_2 levels, though is not acclimatised. There is not enough O_2 in this upper zone for the body to function properly and symptoms of hypoxic distress occur: this presents as acute mountain sickness. The scoring system used to distinguish subjects suffering with AMS in this study identified 10 out of

the 20 total subjects, 4 of these appearing in both phase I and II. A degree of controversy exists on determining which scoring system(s) should be used to diagnose those with clinical AMS. Some studies use a LL score of >=5, though using this in our study category eliminated 3 subjects detected using the ESQ who also exhibited notable changes in gene expression. A number of studies have criticised the ESQ scoring system of containing superfluous questions and being validated against only a single item (Maggiorini *et al.* 1998; Dellasanta *et al.* 2007). However, as it identified the same individuals as the LL criteria did in this study, it was decided to utilise both systems.

7.4.1.2 Gender difference and sickness at altitude

Alveolar ventilation and the HVR have been shown to be greater in females than males. This may be due to ovarian hormones, for administration of progesterone and oestrogen has been shown to enhance both alveolar ventilation and the HVR (Aitken *et al.* 1986; Tatsumi *et al.* 1991; Lefter *et al.* 2007). Thus, one may expect there to be a gender differential response at altitude, particularly depending on the part of the menstruation cycle the female is in (higher levels of progesterone during the luteal phase of the cycle) or whether or not the individual was taking the contraceptive pill, the former shown as a more efficient adaptation to the surrounding hypoxia and thus lower levels of AMS. Three out of the 10 AMS+ individuals were females, suggesting that cycle time-points may be important and that increasing population size in this study could yield some interesting information concerning the relationship between hormones and response to hypoxia. As an addition to a future study, finding out the cycle phase each individual female was in could aid in understanding this differential response.

7.4.1.3 Age effect at altitude

As described (introduction), links have been postulated between the effect aging has on the body and its ability to cope at altitude when compared to the younger generation. There was no evidence in this study to suggest that the older members of the group (72 years old) coped in a different manner to the rest of the population, based on the fact that their O_2 saturations and AMS scores were not outstanding.

7.4.2 Response and adaptation to hypoxia: the HIF system

Studies of human physiological adaptation to altitude have long sought to determine whether genetic factors play a part in determining how well a person responds on exposure to lowered O_2 availability. The phenotype possessed by Western people is distinct from that shown by native populations such as Tibetan high altitude residents, who may have been subject to natural selection based on their capacity to have adapted to life at high altitude.

HIF is a highly conserved heterodimer, playing a central role in O_2 homeostasis. More than 40 of the HIF-regulated genes have been identified to play a key role in the response to hypoxia (Moore *et al.* 2006) and variation has been shown to occur in these genes by studying single nucleotide polymorphisms (SNPs) (Howell *et al.* 2002; Hanaoka *et al.* 2003), which alters circulating plasma levels and thus the individuals response to hypoxia. However, further studies are required to confirm whether the genetic variants seen in HIF-targeted pathways do protect some individuals more than others.

Observation of HIF-1α protein changes on exposure to hypoxia was not possible because of a difficulty in preventing its degradation due to its very short half-life on exposure to normoxia. It is recognised that HIF-1α activates EPO by binding to the 3' regulatory element on the HRE of the EPO promoter (Semenza

et al. 1991), and more recently that HIF-2α affects control *via* the same regulatory sequence on the EPO gene (Warnecke *et al.* 2007). Consequently, HIF-1α knockdown only has a small effect on EPO transcription. Available evidence is consistent with a working hypothesis that HIF is the key O_2 sensor in hypoxia and that it is in direct control of EPO under these conditions. This provides the rationale for using EPO as a surrogate measure of HIF activation, and studying the transcriptional activation of downstream genes known to contain the HRE bound by HIF.

7.4.3 Molecular effects of systemic hypoxia

7.4.3.1 EPO plasma protein: using EPO as a surrogate marker for HIF activation and hypoxic up-regulation

In agreement with a well-established phenomenon, subjects in this study experienced a rise in plasma EPO levels on exposure to hypoxia. The literature suggests that plasma EPO levels result from *de novo* synthesis of EPO in the kidney as opposed to release from preformed-stores (Schooley and Mahlmann, 1972; Scholz *et al.* 1990) though its synthesis is dependent on available iron stores.

The time course of the EPO response is consistent with the greater mean significant increase in concentration seen in the chronic hypoxia exposure of phase II, a 434% increase, when compared to the 116% increase in the acute exposure of phase I. This time course is in accordance with a number of studies in rodents (Clemons *et al.* 1987; Schooley *et al.* 1972), although in contrast, data shown in CHPT 3.3.2.2 shows plasma EPO in a mouse model rose to its highest value by 3 h, but fell significantly thereafter.

The differing environments created by the chamber in phase I compared to the change in ambient temperature and other surrounding conditions

experienced high in the mountains, including the conditions on ascent (i.e. physical activity) and duration of exposure, may be in part responsible for the noticeable differences between the acute and chronic setting in this study. The differential response between the normobaric hypoxic environment and the hypobaric hypoxic environment was observed by Savourey *et al.* (2003, see introduction).

7.4.3.1.2 Classifying EPO responders and looking at correlations with altitude sickness

Individuals experienced different fold changes in each phase of the study, with all but one showing a greater relative increase in phase II. The observation that there is a variable inter-individual EPO response supports previous findings (Ge *et al.* 2001), and this enabled subjects to be grouped accordingly, i.e. individuals could be grouped based on whether they experience a prominent plasma EPO response or not (Chapman *et al.* 1998). It is evident from the data that differentiating responders from non-responders in the acute exposure of phase I was difficult, possibly due to an insufficient hypoxic stimulus or length of exposure, meaning that inter-individual differences were less obvious. Data from the chronic hypoxia of phase II enables separation into arbitrary high-responder and low-responder groups, allowing a more meaningful correlation with previous data sets that were also obtained in the field, as opposed to the chamber: responders were separated from non-responders based on a 40% increase from the mean protein concentration of values lying on the lower limit of response. Fig. 7.8 clearly shows a separation between the two. There was a statistical significance between the mean of the EPO responders *vs.* non-responders ($P<0.05$), grouping 5 subjects out of the total 20: three of these had AMS, and interestingly, 3 out of these were also shown to be outliers on analysis of the mRNA response of a number of HIF-regulated genes in leukocytes.

Looking at changes in mean [EPO] for AMS+ and AMS- individuals revealed little change in phase I, though a higher [EPO] for AMS+ compared to AMS- subjects in phase II. Though not significant, this suggests that EPO 'responders', i.e. those with higher levels of EPO, include a larger number of AMS+ individuals.

It is thus reasonable to suggest that EPO responders are more likely to suffer with AMS when compared to non-responders, though a more highly powered study is required to validate this proposal. This conclusion contradicts the hypothesis that increased EPO levels lead to increased RBC production and an enhanced O_2 carrying capacity, thus decreasing susceptibility to hypoxia-induced AMS. Rather, EPO levels seem to reflect those individuals with the greatest level of tissue hypoxia. This is compatible with the finding, as discussed below, that subjects with the lowest Hb values had the highest EPO response.

7.4.3.1.2 Relationship between EPO and AMS with O_2 saturation and haematological changes

7.4.3.1.2.1 Oxygen saturation

It is widely thought that the level of erythropoietic activity in mammals is ultimately determined by the ratio of O_2 supply to demand in tissues producing erythropoietin. It has been suggested that O_2 saturation is a more important determinant of the EPO response than O_2 tension (Weil *et al.* 1968; Pavlicek *et al.* 2000). This finding has been replicated in the present study with a negative relationship shown: the lower the O_2 blood saturation, the higher the change in plasma EPO. This relationship was stronger and significant in the chronic hypoxia of phase II, with 2 outliers that were consistent in having both the lowest Hct and Hb scores: they had the lowest O_2 saturations along with the greatest change in plasma EPO. One of the individuals was categorised as suffering with AMS in this phase, with both being labelled outliers in the leukocyte mRNA response. This suggests that changes in circulating O_2 levels was not a proximate cause of

altitude illness as low O_2 saturations can only be attributed to one of the seven AMS+ individuals, though low O_2 levels are a cause of higher circulating EPO levels. However, there was no significant difference or noticeable variation from mean O_2 saturation values for AMS+ subjects and EPO responders, suggesting that O_2 level is an unreliable determinant of sickness at altitude. A possible explanation for this counterintuitive result is that the O_2 saturation values were determined by external application of a saturation-measuring device to a finger. The values were visible to the subject who was readily able to increase O_2 saturation values by taking a few deep breaths. In this way, subjects who had been suffering with hypoxia were able to temporarily reverse this. In the same way, subjects who demonstrate cheyne stoking while asleep may have apparently normal respiration patterns when awake. Clearly, the EPO response is not confined to the level of hypoxia when fully awake and consciously or subconsciously hyperventilating.

7.4.3.1.2.2 Changes in Hct and Hb

A negative relationship is seen between absolute Hct, Hb and plasma EPO in the hypoxic exposure of both phases, showing that subjects with a higher Hct and thus Hb have an increased carrying capacity for O_2. This suggests that the stimulus for EPO up-regulation is less than in individuals who have a low Hct and Hb: it is in the latter that the greatest change in EPO is seen from normoxia. The two outliers described in 7.4.3.1.2.1 are also seen here, their low Hct and Hb levels correlating with low O_2 saturations.

There is evidence that contraction of the spleen on exposure to hypoxia can increase the RBCC (Kam *et al.* 1999). The spleen is known to contract under hypoxia causing release of stored RBCs (Richardson *et al.* 2005; Bakovic *et al.* 2005). This increase is not evident in phase I of these studies (see Appendix III) and may be due to the circumstances surrounding the acute hypoxic exposure:

individuals were sedentary or supine for most of the 6 hour exposure, having no physiological imperative to move, and thus would have been under different autonomic control when compared to the more active situation in the field.

The association between EPO levels and Hct from the literature is variable. A lot of the data come from early studies where some groups demonstrated marked polycythaemia on exposure to hypoxia (Barcroft *et al.* 1923; Hurtado *et al.* 1945; Merino, 1950), and others found no change in RBCC until a significant amount of time at altitude had passed: during the 1st two months at altitude, Reynafarje *et al.* (1959) were unable to detect an increase in RBCC, though following this and up until 6 months post-altitude exposure, Hct began to increase. This observation is supported by a shorter study by Faura *et al.* (1969) who found that the Hct changed very little following seven days at altitude. In a meta-analysis conducted by Sawka *et al.* (2000), greater evidence pointed to an unaltered volume of RBC. These discrepancies were thought to be due to the different methods used to assess volume, but this has since been since been disregarded (Sawka *et al.* 2000).

Possibilities for discrepancies between data sets involve haemoconcentration leading to a decrease in plasma volume (McLean *et al.* 2006), due to dehydration which is known to increase under hypoxia, and possibly due to changes in oncotic balance, as proteins have been shown to leave the vascular space due to an increased capillary permeability (Sawka *et al.* 2000). However, these findings are controversial. The degree of haemoconcentration relates to the magnitude of hypoxic stress imposed, thus differing degrees will be seen in these studies as different altitudes have been studied (Sawka *et al.* 2000)

Along with these observations under chronic hypoxia, there has been a wealth of studies looking at the effect of 'living high, training low' as a mechanism for increasing RBCC and thus athletic ability and performance: some have shown that 4 weeks of intermittent hypoxic training have no effect on RBCC, despite

increasing EPO levels (Gore *et al.* 2006), where others have shown that a maximal period of 4 weeks is required to reap any benefits (Wilber *et al.* 2007). The former observation lends support to the argument that a longer period is required for blood volume expansion, including an increase in Hct: Pugh (1964) observed that the largest volume expansion in an altitude acclimatisation study over 5000m for 4 months, and that changes opposing this may be due to haemoconcentration due to reasons mentioned above.

It is possible to propose a time line over which EPO and Hct are induced (Fig. 7.28), which suggests that the time points looked at in this study, along with data from above studies, fall short of maximal responses seen in both of these haematological variables. This study merely provides a dynamic snapshot of changes occurring, not an end-point assay.

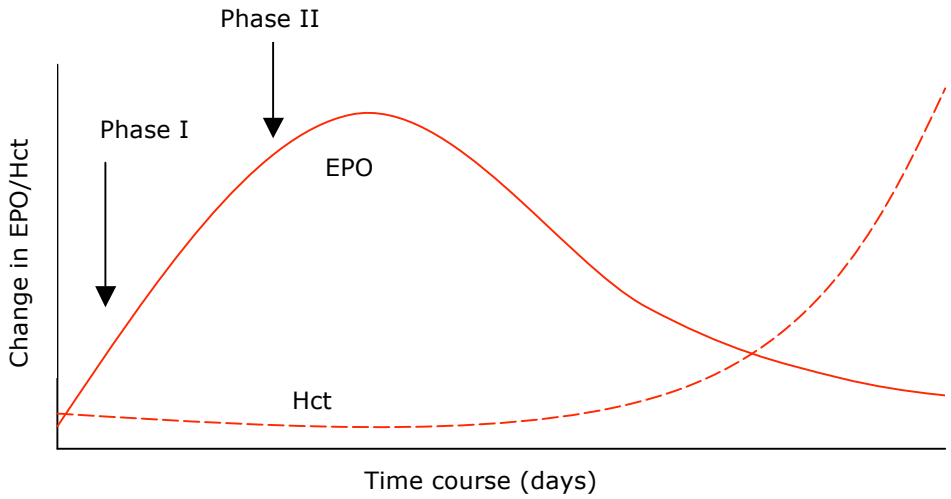

Figure 7.28 Time course of hypothesised EPO (solid line) and Hct (dotted line) changes under hypoxia, with approximate timing of phase I and II

7.4.3.2 Inability to predict the hypoxic response of an individual using leukocytes as a circulating marker of gene expression

The expression of HIF-1α has been well documented in circulating leukocytes (Khahil *et al*. 2008; Mounier *et al.* 2008; Pialoux *et al.* 2009), along with the expression of its downstream target genes. Circulating leukocytes have the ability to mirror the body's tissues and organs in health and disease (Dhahbi *et al.* 2007), and were deemed a useful indicator of gene up-regulation under hypoxic conditions, as hypoxia has been shown to cause their up-regulation (Sanidas *et al.* 2000). However, one main factor must be taken into account: a shift will be continually occurring of the type and number of circulating leukocytes. Leukocytes are composed of polynuclear neutrophils (60–70%), lymphocytes (30%), monocytes (5%), polynuclear eosinophils (2%), and polynuclear basophils (<1%) (Testart-Paillet *et al.* 2007). It is impossible to ascertain which members of the population were involved in the hypoxic response without a differential count, which is not reported in studies showing up-regulation of these genes, nor was such a count conducted here. Individual differential counts are extremely variable. However, studies showing differential leukocyte counts following exposure to hypoxia have revealed unremarkable changes (Bolling *et al.* 1997; Bailey *et al.* 2000). The life span of leukocytes ranges from 6 hours to around many years for some T lymphocytes, depending on the type of leukocyte studied (Van Dyke *et al.* 1951). Hypoxia is known to decrease neutrophil apoptosis (Hannah *et al.* 1995), an otherwise major mechanism in the resolution of acute inflammation (Mecklenburgh *et al.* 2002). In concert with their relative abundance under normal conditions, this suggests that the leukocyte population under hypoxia may be largely made up of neutrophils, and that our results are largely reflecting neutrophil gene expression.

It is important to consider the fact that circulating leukocytes and the genes they express can be altered not only by hypoxic but inflammatory conditions (Baudry *et al.* 1998). There is evidence that hypoxia can induce an inflammatory response in immune cells and endothelial cells, validated by the finding that levels of circulating interleukins and C-reactive protein are upregulated in response to hypoxic conditions at high altitude (Hartmann *et al.* 2002). Distinguishing between stimulation of these genes by either of the two conditions was not possible in this study. An acute stimulus of 12% hypoxia has also been shown to alter the morphology of the circulating leukocyte, inducing crater-like formations and a disruption of the cellular membrane (Sanidas *et al.* 2000). How this impacts on gene expression remains unknown.

7.4.3.2.1 Significant inter- and intra-individual variability in gene expression under hypoxia

There was a large amount of inter-individual variation that occurred in the HIF-1α leukocyte response to hypoxia, in agreement with previous studies (Mounier *et al.* 2006, 2008), and this may reflect the above observations of a changing leukocyte population due to varying life spans. This variability may also be explained by DNA sequence variations resulting from HIF-1α gene polymorphisms in the promoter region of the HIF-1α gene (Prior *et al.* 2006). Other studies have shown an up-regulation during the first 2 h of hypoxia, followed by a down–regulation of expression, with suggestions that the naturally occurring antisense HIF-1α is responsible for these changes (Pialoux *et al.* 2009). This is consistent with antisense levels increasing in proportion to HIF-1α mRNA expression (Mounier *et al.* 2006). As our study only followed HIF-1α gene expression after 6 hours in phase I, and 4 days in phase II, it is possible that down-regulation of HIF-1α had already occurred.

As with HIF-1α, a large variation was shown in HIF-regulated gene mRNA expression, with an inability to reveal consistent changes across any of the gene

responses for an individual, or to enable a correlation with HIF-1α mRNA expression. This again may be linked with the varying life span of the leukocyte and/or down-regulation of HIF expression at the time points chosen for this study.

7.4.3.2.2 Using HIF-1α mRNA to predict the plasma EPO response

HIF-1α is a post-translationally regulated protein (Brahimi-Horn *et al.* 2005, Kaelin and Ratcliffe, 2008), although its regulation on a transcriptional level has also been described (Milkiwiecz *et al.* 2005; Mounier *et al.* 2008; Pialoux *et al.* 2009). Indeed, when studied along a time course of 12 h, it has been shown that plasma EPO levels, and VEGF, follow similar kinetics to that of HIF-1α mRNA levels, suggesting that regulation may occur on a transcriptional level (Pialoux *et al.* 2009). In agreement with a previous study (Mounier *et al.* 2006), prediction of whether an individual will be an EPO responder or a non-responder at altitude from HIF-1α mRNA levels was not possible. The variable positive and negative response of HIF-1α mRNA levels did not correlate with the consistent rise in plasma EPO levels in this study.

7.4.3.2.3 Using plasma EPO protein to predict the HIF-regulated gene response

Little is known of the effect HIF-1α mRNA expression has on HIF-1α protein levels under these circumstances, and it is unfortunate that HIF protein levels could not be assayed in this study. Mounier *et al.* (2006) found variable, though generally unchanged levels of HIF-1α protein along with mRNA levels. Based on this uncertainty, it is difficult to determine whether using EPO as a surrogate measure for HIF-protein activation is appropriate.

Regression analyses of EPO protein with downstream gene responses showed little association between the two, with only VEGF mRNA expression

showing a weak correlation. However, there were a number of individuals consistently appearing as outliers in a number of genes. Out of these 6 outliers, 3 were diagnosed with AMS and 3 were part of a group of 5 EPO responders identified. Two of these outliers were common to both phases of the study. This suggests that although none of the individual genes *per se* are able to be used as a valid discriminator defining the EPO response to hypoxia or susceptibility to AMS, the possibility exists of being able to predict either of these rises with an enhanced number of factors studied, and/or increasing the sample number to increase the power of the study.

7.4.3.3 VEGF and sFlt plasma protein

The VEGF and associated sFlt plasma protein response to hypoxia is one that has long been studied, with widespread failure for a conclusive end-point to be reached. Possible reasons for this include the fact that some investigations have looked at total circulating VEGF protein and others only at free VEGF, i.e. VEGF that is not bound to its cognate receptors, and studies have used samples inconsistently from either plasma or serum, another factor which may alter the outcome. Studying VEGF in blood plasma rather than serum is recommended, as one storage site for VEGF is platelets and VEGF release has been shown to increase on clotting, thus levels may reflect blood platelet counts in addition to any hypoxia-induced response (Jelkmann, 2001). A further confounding factor is that the time period after exposure to high altitude differs in many of these studies. Because of this, data from different studies has been shown to vary by up to three orders of magnitude (Jelkmann, 2001). In this study, an ELISA kit that measures only free VEGF-A in the plasma was used.

7.4.3.3.1 Changes in VEGF

VEGF is a vascular permeability factor and its gene expression has been shown to increase under hypoxia both *in vitro* (Gleadle *et al.* 1995) and in an *in vivo* mouse

model (Marti and Risau, 1998). A link has therefore been postulated between a hypoxia-induced increase in vascular leakage in the brain and lungs, subsequently leading to HACE or HAPE, respectively, due to its known characteristic of increasing membrane permeability (Behzadian *et al.* 2003). A greater amount of free VEGF is seen in some AMS+ subjects, suggesting it may contribute to the pathology of high altitude illness. Studies generally find that VEGF levels increase in plasma under hypoxia, though evidence for the association between either AMS and/or clinical oedema is weak and remains so following this study: In phase I, a variable individual response in plasma VEGF was seen, subjects exhibiting both positive and negative changes. In phase II, however, effects were more consistent and there were only negative or unchanged values, suggesting that the response is different under chronic compared to the acute exposure to hypoxia, becoming blunted following a longer time exposure. Alternatively, the response may be due to the differing environment provided by the hypobaric *vs.* the normobaric exposure to hypoxia, as discussed earlier (see Introduction).

These results are consistent with a number of previous studies, demonstrating continued uncertainty surrounding the VEGF response of an individual to hypoxia. The failure to be able to correlate altitude sickness or other parameters studied (such as PO_2) has been seen previously (Nilles *et al.*2009, Pavlicek *et al.* 2000), although one study has found that individuals suffering with AMS have a higher amount of free plasma VEGF (Tissot van Patot *et al.* 2005).

Inconsistent changes were also shown in AMS+ subjects and EPO responders in relation to VEGF, with no apparent correlation being seen. One explanation for the variation seen in the above-mentioned studies is the differing time scales upon which they occurred: all were based at a similar height of between 4000-4200m, though from 1 day of exposure (Pavlicek *et al.* 2000) to 2 days (Maloney *et al.* 2000*,* Nilles *et al.*2009). Plasma samples for VEGF on the chronic study time point here were taken on day 4 and at the slightly more

elevated altitude of 4392m. Taken together, the timescale of the adaptive physiological response may therefore play a role in determining the different outcomes seen in these studies.

It is important to be aware of the role that the immune system can play in VEGF activation, with the possibility that any plasma VEGF seen may have been induced by inflammatory factors, as well as or instead of hypoxia. Schobersberger *et al.* (2000) found a significant long-lasting increase in serum VEGF that was accompanied by activation of the immune system (increased levels of interleukin-6 and neopterin), although Pavlicek *et al*. (2000) provided evidence against any clinically relevant inflammation in the development of HAPE which can occur as a subsequent development of AMS.

7.4.3.3.2 Changes in sFlt

Tissot van Patot *et al.* (2005) showed a decrease in the amount of circulating sFlt in subjects diagnosed with AMS, along with the above-mentioned increase in free plasma VEGF, supporting the proposed hypothesis that more VEGF is therefore available to participate in the pathology surrounding HACE and HAPE (as less sFLT is available to titrate the effect of the free VEGF).

Our study showed largely unchanged levels of sFlt in both AMS+ and AMS- subjects during both phases. This finding does not provide support to the above theory. The response of both sFlt and VEGF was more blunted in phase II with only unidirectional changes occurring, though in a negative direction for VEGF and in a positive direction for sFLT when compared to baseline values for each phase. This indicates that there is less bioavailable VEGF to participate in the proposed pathogenesis associated with HACE or HAPE under chronic hypoxia, suggesting that either (i) a feedback mechanism is operating which acts to maintain fairly constant levels of VEGF activity, similar to those under normoxia, after a prolonged period of exposure to hypoxia (i.e. 4 days here), (ii) that the hypoxic stimulus to induce changes in levels of VEGF and sFlt was inadequate, or (iii) that

the time frame associated with exposure to hypoxia, either normobaric or particularly hypobaric, was too long to see the acute changes previously reported: Tissot van Patot *et al.* (2005) found changes occurring following a 20 h exposure.

Regression analyses between EPO and sFlt indicated a positive relationship, although not significant, allowing us to postulate a possible influence of EPO, and indirectly HIF, upon sFlt. However, no relationship was shown between EPO and the HIF-responsive VEGF, suggesting that *in vivo* regulation is likely to be multi-factorial.

7.4.3.4 Confounding factors from the study

7.4.3.4.1 Control of EPO by the HIF-system: An emerging role for HIF-2α

There is firm evidence that HIF-1α is the key factor activating EPO transcription. However, HIF-2α, which shares 48% sequence homology with HIF-1α (Tian *et al.* 1997),

is now also known to play an important role in controlling EPO production, and controversy exists around which of the two isoforms plays the greater role. HIF-1α was the original isoform identified as binding to the 3' regulatory element on the HRE of the EPO promoter (Semenza *et al.* 1991). Using gene silencing *in vitro*, and later supported by an *in vivo* model (Gruber *et al.* 2007), it was subsequently shown that HIF-2α was largely in control of the same regulatory sequence on the EPO gene (Warnecke *et al.* 2004). The role of HIF-1α protein in the control of EPO remains controversial, but an ELISA to measure HIF-2α protein levels was not available. In addition, Mounier *et al.* (2006) were not able to determine HIF-2α mRNA levels in leukocytes, suggesting that it is not expressed, therefore its presence here was not able to be determined. HIF-2α is in control of the same genes as HIF-1α, in this study, though without further insight to its

presence in this study, establishing whether the EPO expression was under the control of HIF-1 or HIF-2, remains unclear.

7.4.3.4.2 Controversy surrounding the determination of clinical AMS

Scoring systems used to determine whether an individual is suffering from AMS or not are deemed insufficient by many for assessing whether physical symptoms evident are a result of the altitude or other surrounding factors that may be present. The LL system has long been used and is useful on many clinical levels, along with the ESQ. However, studying changes on a molecular level requires a more intimate approach to accurately identify who is ill and who is not, so that confidence in correlating changes on a protein and haematological level with sickness can be increased.

7.5 Conclusion

Acute responses to hypoxia are those occurring practically instantaneously with the environmental change. Acclimatory responses are defined as adjustments requiring some fraction of the organism's lifetime, from minutes to days, to reach a new steady state (Hochachka *et al.* 1998). It is evident that many of the changes occurring during the acute exposure of phase I are different in magnitude and directionality when compared to the chronic exposure of phase II, and these changes may be attributed to the different environment provided by normobaric *vs.* hypobaric hypoxia. The change in EPO seen here is a good indicator of the physiological response to hypoxia, though no significant correlation could be made with sex or age of the subject and the degree of their response. EPO responders were shown to increase EPO levels faster, though this was not translated into increased Hct and Hb levels as the literature would suggest, or to individuals suffering less with AMS. This suggests that the system is influenced by a range of factors which influence feedback mechanisms, making pathways less straightforward than previously thought. Biological feedback mechanisms and possible genetic variations also mean that translation of this change into a downstream cascade system modulated by HIF produces a very variable response, clearly shown as inter-individual variation in and between proteins and genes and this suggests that multiple metrics are required to measure response to hypoxia resulting in AMS. The plasma VEGF and sFlt response shown has added to the confusion surrounding theories of links with illness at altitude, either in the form of AMS or the more serious HACE or HAPE, with no definitive associations being seen in the acute exposure, and although a decrease in plasma VEGF was seen with a corresponding increase in sFLT under chronic hypoxia, no correlations could be made with individuals suffering with AMS. The idea of using circulating leukocytes as an indicator of the hypoxic activation of genes was deemed logical following observation of their upregulation

in murine leukocytes, and leukocytes have been known to efficiently represent the body's tissues and organs in health and disease, so could be assumed to be an efficient measure of the systemic hypoxic response. However, their heterogeneity in relation to type and lifespan causes difficulties in their collective use for assessing response to hypoxia.

7.6 Future directions

An important future step would be to carry out counts of leukocytes and a platelet count, to determine whether an inflammatory-based immune response was present in response to hypoxia, which may otherwise influence the gene response seen. A differential count of leukocytes would also be useful to determine whether one species of leukocyte made up the majority of the population present, and whether this influenced the results seen, based on their relative half-lifes, for example, a species of leukocyte with a short half life may show a different level of gene expression when compared to a leukocyte with a longer half life. Furthermore, study of the variety of factors implicated in an immune response to confirm whether inflammation may also be playing a role in activation of these HIF-regulated proteins and genes may be insightful. It would be beneficial (on a study that encompasses as many factors as this) to incorporate larger subject numbers to increase the power in this study and provide more definite evidence for each of the changes observed, alongside increasing the selection of genes studied and evaluating changes in these genes on a protein level as well. Developing a more efficient AMS scoring system would represent a more pragmatic approach to defining sickness at altitude. Finally, as new technologies are revolutionising the study of adaptation of the human body to stress, comprehensive gene screening and comparisons between situations of hypoxia and normoxia could resolve these issues.

Chapter 8
DISCUSSION

8 Discussion

When challenged with the situation of low O_2 in the surrounding environment, be it local or systemic, the body undergoes a series of adaptations which subsequently aid acclimatisation. On a physiological level, an increase in ventilation rate and cardiac output ensue in response to acute hypoxia, followed closely by an upregulation of factors on a molecular level when hypoxic conditions are maintained. These mediate erythropoietic, metabolic and angiogenic changes, among many others. Central to controlling changes on both these levels is a transcription factor which acts as a global effector of change under both hypoxic and normoxic conditions, HIF. A common theme among experiments in CHPT 3 and 5 was to elucidate what level of local hypoxia or systemic hypoxaemia was necessary to initiate angiogenesis, and whether use of a chemical stabiliser of HIF would enhance this response. Studying these models is not only useful for deducing the necessary conditions for initiating blood vessel growth, but act as valuable surrogate measure for clinical conditions such as peripheral vascular disease and chronic obstructive pulmonary disease, respectively.

Systemic changes to hypoxia are evidenced in CHPT 3 by an increase in capillarity in the diaphragm and heart of mice under conditions of 10% hypoxia. This illustrates how angiogenesis, presumably mediated by HIF although not confirmed here, can be upregulated not only under conditions of hypoxia, but also stretch as a consequence of a increased ventilation and greater overload, respectively. HIF-mediated upregulation under non-hypoxic conditions has been demonstrated previously (Kim et al. 2002; Williams et al. 2006b; Milkiewicz et al. 2007). That similar angiogenic effects weren't seen in the EDL of the hindlimb suggests the need for a greater hypoxic stimulus, such as may be achieved with exercise. Elucidating the PO_2 required for HIF activation in vivo and the

subsequent induction of angiogenesis is an area of controversy due to difficulties in securing accurate measurements of tissue PO_2, but it may well be that the threshold for activating HIF was not reached here. However, a muscle with a more oxidative fibre type, the soleus, was more responsive to hypoxaemia than the mixed fibre type of EDL. This has been shown in other studies (Deveci et al. 2001, 2002) suggesting that fibre type plays a crucial role in determining tissue responsiveness. Consistent with this finding, the mRNA response following exposure to 10% hypoxia was most significantly altered in the soleus.

HIF availability is under tight control under both normoxia and hypoxia by members of the PHD family, PHD 1-3. Following from previous observations that chemical manipulation of the PHDs can alter HIF-1α stability (Jaakola et al. 2001; Warnecke et al. 2003; Milkiewicz et al. 2005), experiments were conducted to elucidate whether the finding of an increased capillarity in the hindlimb of the mouse following ligation of the femoral artery and treatment with the PHD inhibitor, DMOG, would be seen in both a model of systemic hypoxia and overload, along with a replicated finding in the femoral ischaemia model. In both models of the hypoxic induction of HIF (systemic and local), no evidence for an enhanced capillarity was seen in the hindlimb following treatment with DMOG. This primarily suggests that the threshold for inducing HIF-1 may not have been reached as tissue hypoxia was insufficient: the position of the ligation may have an influence upon the degree of ischaemia. Ziv et al (2004) ligated the artery further upstream than our study, inducing a higher degree of ischaemia (as evidenced by loss of limb function). The confounding factor here though is the possibility of inflammation due to the more invasive nature of the surgery, which can also play a role in inducing angiogenesis (NFκB-mediated HIF-1 activation). Alternatively, a less well studied area when observing angiogenesis following ischaemia is the upregulation of a number of anti-angiogenic factors (e.g. thrombospondin-1, endostatin, and angiostatin) alongside pro-angiogenic factors. In this case, it emphasises the delicate balance determining whether

angiogenesis is activated or not remained, the 'angiogenic switch', which is still unresolved.

HIF-1α has been shown to be upregulated under conditions of stretch, such as those experienced following removal of a synergist muscle in the hindlimb (extirpation), resulting in angiogenesis. So examining whether a similar response would be seen following manipulation of HIF-1α stability as with femoral artery ligation (Milkiewicz *et al*. 2005), may help to shed light on the presence of alternate pathways leading to the upregulation of HIF in response to different physiological challenges. The hypothesised response of an enhanced capillarity, greater than that achieved by extirpation alone, was not evident. This suggests that under conditions of stretch, HIF is either acting *via* a different pathway, or DMOG is impacting on the regulatory system in an unfavourable way: DMOG has been shown to have an affect on other members of the PHD family involved in collagen synthesis, namely C-P4Hs (Koivunen *et al*. 2007), a necessary component of recovery following extirpation (in angiogenesis and increased sarcomere length) (Laurent *et al*. 1985; Winter and Page, 2000). It proved, it may be the case that the potential of such chemical manipulation as therapeutic angiotherapy is limited.

Confounding factors impacted upon each of the other studies: subsequent to both the systemic and acute hypoxia studies (CHPT 3 and 5), it was realised that the strain of mouse being used was particularly resistant to both challenge by systemic hypoxia and ischaemia, modulating its metabolic fuel and ventilation under systemic hypoxia, and possessing an innately greater CD in skeletal hindlimb muscles, translating into a greater capacity to maintain sufficient O_2 delivery under systemic hypoxia, and the ability to rapidly restore blood flow following occlusion of the artery. Thus, this strain of mouse has been shown less useful in these studies as reaching a level of local hypoxia suitable for HIF activation without imposing dangerous levels of systemic hypoxaemia is a challenge.

A variation of the strain was used (C57Bl10/J) in both the femoral artery ligation and extirpation models, and an enhanced response was seen in this strain when compared to C57Bl6/J. This clearly illustrates that inter-strain differences do exist, albeit subtle and statistically insignificant, though it would be interesting to investigate factors such as variability in fibre type composition which may be responsible for this response.

The viability of DMOG was also questioned and found to be slightly different in molecular structure (using NMR and MS) to that used in previous experiments (Milkiewicz et al. 2005). However, repetition of experiments with a newly synthesised batch again failed to produce an enhanced C:F in affected limbs, suggesting that DMOG also has a threshold below which it is not activating the HIF system to its full potential, and this may have been the case here if the bioavailability was underestimated.

The unwanted and unknown side effects of the use of chemicals to manipulate biological pathways, without being fully aware of possible redundancies in the system, are a disadvantage. The use of genetically modified animals, allowing one to study the effects of redundancy whilst having the assurance that only the specified gene has been directly interfered with, has been revolutional for many studies, and was used here to identify the differential response of animals with either PHD1 or PHD3 gene ablation. In vitro data has shown that PHDs contribute in a non-redundant manner to the regulation of HIF-1α (Appelhoff et al. 2004), so the effect of manipulating either of these pathways should help to elucidate whether a similar scenario exists in the more complex, interactive situation in vivo. The reciprocal gene changes seen in PHD1 and PHD3 K/O mice shows that redundancy is present. Significant upregulation of genes involved in protein remodelling was evident by muscle hypertrophy (suggesting that protein remodelling is occurring downstream of gene expression), though translation of the observed angiogenic gene response into downstream physiological effects was lacking, giving support to the complexity of the

angiogenic response, and suggesting, as mentioned above, that anti-angiogenic factors may play a role in inhibiting pro-angiogenic signal from being physiologically active.

The well-studied erythropoietic adaptations following systemic hypoxia were clearly evidenced by the increased plasma EPO in the mouse by 3 h post-hypoxia (CHPT 3) and by raised levels of a greater magnitude in humans following both an acute and chronic exposure to hypoxia (CHPT 4). EPO 'responders' were shown to increase EPO levels faster, though this wasn't translated into increased Hct and Hb levels, adding to the literature controversy associated with the multitude of variables in each study affecting the outcome. No significant relationship was seen between EPO levels and AMS+ subjects, although there was a trend for sickness to be associated with a greater increase in plasma [EPO]. This is in accordance with lower Hct and Hb levels, allowing one to hypothesise that individuals who suffer at altitude do so due to impaired polycythaemia and thus insufficient blood O_2-carrying capacity, despite having higher levels of EPO.

As EPO is known to be regulated by HIF (Semenza et al. 1991), it was deemed a suitable surrogate indicator demonstrating HIF upregulation, as studying HIF directly proved too difficult. As HIF is known to be regulated on a post-translational level under hypoxia (Brahimi-Horn et al. 2005; Kaelin and Ratcliffe, 2008), the lack of change in mRNA transcripts was expected, as seen. Data from CHPT 3 encouraged the use of leucocytes as a circulating marker of the systemic hypoxic response in humans, as the expression of HIF-1 α and its downstream target genes have been identified here (Khahil et al. 2008; Mounier et al. 2008; Pialoux et al. 2009). A number of HIF-regulated genes were seen to change, e.g. the leucocyte EPO mRNA response mirrored the plasma [EPO], giving support to the proposed utility of this approach in humans. A greater variability was seen in human leucocyte mRNA response in the selected genes, though the study confirmed that leucocytes do appear to be sensitive to gene

expression alteration under hypoxia. This variability may be naturally occurring or because of the differing half-life of the leucocyte population, meaning that gene expression differed with each new population. Biological feedback mechanisms and possible genetic variations (DNA sequence variations resulting from HIF-1α gene polymorphisms in the promoter region of the HIF-1α gene) have been observed (Prior et al. 2006) mean that translation of this change into a downstream cascade modulated by HIF produces a very variable response. Whether the mRNA response seen here is translated into a protein response remains to be determined, though it may be that regulation of a number of these genes occurs post-translationally, suggesting that the mRNA response may not be a true indicator of an individuals hypoxic response. Thus, the idea of using circulating leucocytes as an indicator of the hypoxic activation of genes seems logical as they have been known to efficiently represent the body's tissues and organs in health and disease. However, their feasibility in relation to varying life spans remains controversial, and accurate determination of AMS susceptibility is likely to require a panel of responsive indices.

Future work

A range of difficulties encountered in these studies provides the basis for future experiments, which may help explain discrepancies observed. One major factor highlighted is the effect mouse strain can have upon the response and outcome to differing experimental and thus environmental stimuli. Animal models have long been used to model disease, and one of the primary aims of research is to find an animal model that can be used as a surrogate model to mirror the human response to disease, as experimenting on human subjects is not always feasible. Carrying out a broad study to incorporate a variety of mouse strains in order to determine differential responses to imposed conditions, may help to identify the most suitable strains available for proposed models.

The HIF system is complicated and variable, and one of the big problems in trying to understand its biology is its lability, meaning that isolation of this normoxically-degraded and hypoxically-upregulated protein is a major challenge, as was found here. This could be overcome by conducting experiments in a hypoxic chamber that would prevent the otherwise inevitable exposure to normoxia. Another issue in understanding its downstream effects are encountered due to the wide range of factors that also impact upon HIF-regulated genes, presumably in an interactive manner. Within the systems studied here it is possible that inflammation played a role in initiating angiogenesis, as evidenced by upregulation of inflammatory factors (CHPT 6) 1 wk following extirpation, when histological evidence of angiogenesis has been shown. To proteins under HIF control under these circumstances, and to elucidate which pathways are activated e.g. hypoxia and/or inflammation, it may prove necessary to perform nuclear pull down assays, allowing the detection of proteins that bind *in vitro* to an immobilised HIF recombinant protein. The disadvantages of this approach are that although *in vitro* experiments provide large amounts of useful data, they are

not able to replicate the complexity of the *in vivo* environment, but may highlight some of the important pathways and/or cellular mechanisms in operation here.

Laser capture microdissection (LCM) is a method for isolating specific cells of interest from microscopic regions of tissue that has been sectioned, allowing the selection of cells with a minimum resolution of several microns and also allowing the analysis of cells of interest that are free of neighbouring contaminants which may otherwise confound experimental results (Edwards, 2007). These cells can then be used in a wide range of downstream assays such as LOH (loss of heterozygosity) studies, gene expression analysis at the mRNA level or in a wide range of proteomic assays such as 2D gel analysis, Western blotting, reverse phase protein array and protein profiling. Many of these have already been used on tissue and leucocyte samples here, though the advantages of studying isolated cells include the speed of isolation, the fact that no lesions are incurred on isolation, and the ability to study a small subset of cells provides an accurate assessment of gene expression levels that may be critical to understanding their mechanisms of action. This technique would be very useful when combined with a study of the anti-angiogenic factors present under conditions of femoral artery ligation, which may represent the confounding factor inhibiting angiogenesis under conditions that otherwise should provide a pro-angiogenic environment. For example, $VEGF^{165b}$ is an inhibitory form of VEGF that has been shown to constitute large percentages of the total VEGF protein in non-angiogenic tissues (Ladomery *et al.* 2006), the balance of pro- to anti-angiogenic VEGF isoforms apparently determining the disease state of tissue, and thus whether or not the angiogenic switch is activated in a positive direction.

PHD2 is the key O_2 sensor exhibiting regulation over HIF-1α (Berchner-Pfannschmidt *et al.* 2008), though its ablation leads to embryonic lethality. More is known about the function of this PHD *in vitro* than the other two enzymes, so investigating its presence in a new *in vivo* model would be extremely beneficial. In adult mice deficient for PHD2 by conditional knockout, HIF-1α accumulated in

both the kidney and liver, inducing EPO expression (Takeda *et al.* 2008). Generating PHD2 knockouts with somatic mutations is possible by Cre-mediated recombination and this would be interesting to provide comparisons with the PHD1 and PHD3 knockout mice already used with muscle extirpation, where hypoxia is thought to play no role, and also to observe responses in the femoral artery ligation or an iliac ligation model, where hypoxia is thought to be the key factor initiating the angiogenic response.

My studies with DMOG did not yield useful data. Whether this was due to lack of potency in the preparations given to me or to model used remains to be determined. As outlined previously, the *in vitro* model described by Jaakola *et al.* (2001) would answer the first question. Regarding the mouse model, the pharmacological and toxicological properties of DMOG have not been fully investigated. The effect of varying doses of DMOG on vitals (including measuring temperature *via* an anal probe, heart rate using an ECG, and blood pressure using a saline-filled catheter inserted into the left ventricle *via* the carotid artery connected to a blood pressure monitor) in the murine model are necessary. Once established, Western Blotting and mRNA quantification of HIF and PHD expression in the heart and skeletal leg muscles could be performed. Time course studies would be necessary to fully understand its effects.

Factors determining how well an individual fares on exposure to altitude are still largely undetermined, possibly as a multitude of factors are responsible for an individuals response, and looking at many components of the complex system *in vivo* at one time is too complicated. Thus, research groups have only tried to identify one aspect at a time. Gene array technology has made it possible to characterise the RNA expression of thousands of genes across numerous tissue samples and under varying conditions, and would prove very useful in assessing changes at a gene expression level, that occur in sick *vs.* well individuals under the systemic hypoxia at altitude to help uncover the multi-faceted response that seems to be occurring.

APPENDICES

Appendix I

A.1.1 Mean mouse mass (g) 12% hypoxia ± SEM (n=6 per group)

Day	1 wk DMOG	1 wk no DMOG	2 wk DMOG	2 wk no DMOG	4 wk DMOG	4 wk no DMOG
0	25.6 ± 1.03	26.8 ± 0.52	26.0 ± 1.2	25.0 ± 1.13	26.2 ± 0.19	24.8 ± 0.46
3	25.1 ± 0.68	26.2 ±1.12	24.6 ± 0.4	23.7 ± 0.49	25.1 ± 0.69	24.1 ± 1.06
5	26.0 ± 0.89	26.2 ± 0.34	25.7 ± 0.12	24.4 ± 0.99	25.6 ± 0.72	24.5 ±0.88
7			26.7 ± 0.79	25.2 ± 0.25	26.0 ± 0.45	25.0 ± 0.75
10			26.7 ± 0.61	25.2 ± 0.85	26.5 ± 1.11	25.1 ± 1.03
12			27.3 ± 1.05	25.9 ± 0.1	26.8 ± 0.85	25.4 ± 0.97
14					27.6 ± 0.96	25.8 ± 0.26
17					27.7 ± 0.71	25.8 ± 0.49
19					28.3 ± 0.64	26.5 ± 0.47
21					28.4 ± 0.62	26.6 ± 0.77
24					28.1 ± 0.2	26.4 ± 1.14
26					27.8 ± 0.33	26.0 ± 0.65

A.1.2 Mean mouse mass (g) under 10% hypoxia ± SEM (n=12 per group)

Day	2 wk DMOG	2 wk no DMOG
0	25.3 ± 0.65	25.5 ± 0.94
3	24.1 ± 1.02 §	24.6 ± 0.68 §
5	24.5 ± 0.48 §	24.1 ± 0.71 §
7	25.3 ± 0.22	25.1 ± 0.78
10	25.0 ± 0.88	25.3 ± 1.14
12	25.6 ± 0.57	25.2 ± 0.72

Appendix II

A.2.1 HIF protein extraction from WBCs

A.2.1.1 White blood cell isolation from whole blood

All centrifugation steps were carried out at RT. Blood was drawn into two 10ml purple top vacutainer tubes (EDTA-treated) and tubes inverted several times. Blood was diluted and mixed 1:1 with cold 1xPBS. 20ml of this was layered upon an equal volume of Histopaque 1077 (Sigma, 10771) in 2x50ml falcon tubes. Tubes were spun at RT for 30 min at 400 RCF. Following centrifugation, a generous layer of the opaque interface (buffy layer) from each tube was removed using a pasteur pipette, and combined into one 50ml tube on ice. 20ml 1xPBS was added and mixed. Tubes were spun for 10 mins at 250 RCF. The supernatant was removed, the pellet resuspended with 10ml 1xPBS in a 15ml tube and spun for 10 mins at 250 RCF. The supernatant was removed and resuspended with 10ml 1XPBS, then spun for 10 min at 250 RCF. The supernatant was removed and the pellet resuspended in 250µl 1xPBS and protease inhibitors (PI was made up during last 10 min spin). The sample was transferred to an eppendorf and frozen in liquid nitrogen, then stored at -80°C.

A.2.1.2 HIF nuclear protein extraction

HIF-1 resides in the nucleus under hypoxic conditions and thus a nuclear extraction buffer was used to isolate the protein.

A.2.1.2.1 Solutions

Lysis Buffer A- 1ml

HEPES	100µl
$MgCl_2$, NaF	100µl
KCl	100ul
DTT	5µl
NP-40	10µl
Na_3VO_4	10µl
Protease Inhibitors	140µl
PMSF	1µl
H_20	535µl

Lysis Buffer B- 1ml

HEPES	200µl
$MgCl_2$, NaF	100µl
NaCl	100ul
DTT	5µl
Glycerol	250µl
Na_3VO_4	10µl
Protease Inhibitors	140µl
PMSF	1µl
H_20	195µl

To make 50 ml of the following:

1.19g 100mM HEPES pH 7.9
15mM $MgCl_2$, 50mM NaF
0.15g $MgCl_2$
0.1g NaF
0.37g 100mM KCl
1.84g 200mM Na_3VO_4 (100x)
(Adjust to pH 10, then boil till colourless. Repeat until it remains colourless)
12.27g 4.2M NaCl
10% NP-40 (100x)

0.5ml:

17.4mg (in EtOH) 200mM PMSF (0.5ml) (freeze)

200µl:

3mg 100mM DTT (keep frozen)

Protease inhibitor cocktail (make fresh daily or freeze, according to manufacturers guidelines)

A.2.1.2.2 Protocol

Eppendorfs were brought to RT on ice from -80°C and spun for 5 mins at 1000 RCF at 4°C. The supernatant was removed and 1ml of buffer A added to the cell pellet which was then vortexed to break up the pellet. The sample was spun at 16,000 RCF for 5 min at 4°C. The cystolic supernatant was removed, 100µl of buffer B added and the sample vortexed. Samples were left on ice for 20 mins before a final vortex and subsequent centrifugation at 16,000 RCF for 5 min at 4 °C. The supernatant was aliquoted to eppendorfs and frozen at -80°C.

A.2.1.3 HIF ELISA

HIF protein was analysed using a HIF transcription ELISA kit (Panomics, EK1020) as per the manufacturers instructions.

A.3.1 Data from exposure to 12% in the normobaric hypoxic chamber, Phase I

A.3.1.1 Venous blood

Subject	Hb [g/dl]		Hct [%]		PCO_2 (mmHg)		PO_2 (mmHg)	
Number	NORM	HYP	NORM	HYP	NORM	HYP	NORM	HYP
2	15.9	14.0	45.0	44.5	49.0	43.2	31.0	22.7
3	13.3	14.9	40.0	41.0	43.8	31.8	28.4	36.2
4	13.0	16.3	41.5	42.5	44.5	40.9	30.3	24.3
5	13.3	14.5	42.0	43.0	54.3	36.0	31.1	30.1
6	13.9	16.4	42.0	42.0	49.8	36.6	23.9	25.5
8	17.5	19.1	44.0	48.0	52.1	38.2	21.3	27.3
9	15.8	16.6	46.0	50.0	46.6	46.1	36.5	25.0
10	14.3	14.8	43.0	43.5	44.7	41.1	36.7	20.8
11	14.3	15.5	44.0	47.0	40.1	34.0	68.3	49.7
12	11.8	12.8	37.5	38.0	43.6	38.8	30.3	36.0
13	11.3	13.7	36.0	39.0	43.7	33.3	27.9	32.8
14	13.1	13.5	39.0	38.0	49.8	40.0	30.1	34.4
15	13.6	14.5	42.0	43.3	45.9	44.7	42.1	27.4
16	12.4	13.4	39.5	39.5	41.5	39.7	47.6	30.7
17	13.6	16.0	40.0	43.0	48.0	42.1	25.3	20.2
18	13.4	15.0	39.0	42.0	50.3	42.6	29.6	16.8
19	16.2	17.4	48.0	49.0	39.1	42.4	56.3	23.3
20	14.7	15.7	45.0	46.0	46.6	39.7	39.4	27.4
21	14.8	14.5	43.0	42.5	47.4	43.3	21.9	19.2
22	14.5	15.8	44.0	46.0	45.6	45.6	51.3	30.0

Hb: haemoglobin, Hct: haematocrit, PCO_2: partial pressure carbon dioxide, PO_2, partial pressure oxygen, (blue= subjects with AMS)

A.3.1.2 Arterialised capillary

Subject Number	Hb [g/dl]		Hct [%]		PCO_2 (mmHg)		PO_2 (mmHg)	
	NORM	HYP	NORM	HYP	NORM	HYP	NORM	HYP
2	14.5	14.7	43.0	45.0	35.5	26.4	78.8	34.8
3	13.6	13.8	41.5	42.0	33.5	28.2	92.7	48.0
4	14.8	15.0	43.0	45.0	34.4	22.5	86.8	39.9
5	14.3	13.3	43.0	42.0	37.6	29.8	70.8	43.2
6	15.0	14.2	45.0	43.0	37.8	30.5	66.2	33.4
8	15.7	14.7	43.0	45.3	35.9	29.3	64.3	38.3
9	17.0	17.3	50.0	52.5	38.3	33.0	86.4	40.7
10	15.0	14.2	46.0	45.0	35.7	26.6	81.1	45.6
11	14.5	15.5	45.0	47.0	37.1	28.5	92.8	36.1
12	11.5	12.6	40.0	38.0	35.5	24.8	76.0	40.6
13	12.3	12.4	41.0	41.0	32.8	26.9	103.3	49.8
14	13.5	13.4	39.5	40.0	37.2	34.0	87.2	44.3
15	13.0	13.3	49.5	44.0	41.5	32.5	79.9	46.7
16	13.4	13.9	38.8	41.0	33.5	31.2	92.7	45.2
17	13.4	16.0	41.0	44.0	38.2	30.8	84.0	46.2
18	11.4	13.6	39.0	42.0	32.7	28.3	74.7	38.4
19	15.5	15.7	49.0	48.5	31.1	30.7	105.0	43.2
20	15.4	15.6	47.5	46.0	37.0	30.8	78.7	45.5
21	13.8	14.3	43.0	44.0	37.0	31.1	68.6	39.6
22	14.6	15.6	44.5	47.5	42.1	35.5	101.6	41.9

Hb: haemoglobin, Hct: haematocrit, PCO_2: partial pressure carbon dioxide, PO_2, partial pressure oxygen, (blue= subjects with AMS)

A.3.2 Data from exposure to 4392m, Phase II

A.3.2.1 Venous blood

Subject Number	Hb [g/dl]		Hct [%]	
	NORM	HYP	NORM	HYP
2	14	15.8	43	45
3	13.6	15.2	41	45
4	15.5	18.5	43	49
5	15.2	15	43	43
6	14.2	14.5	45	40
8	16.5	17	45	46
9	17.3	20.3	49	55
10	15.9	17.5	44	46
11	17.2	16.1	46	46
12	14.6	14.2	43	40
13	12.6	14.4	42	41
14	15.7	15	40	41
15	16.2	16.7	45	45
16	13.3	16.4	40	48
17	14.4	17.6	40	46
18	13.1	13.8	39	37
19	18.9	17.3	50	48
20	14.6	18.5	45	49
21	16.2	16.3	42	45
22	17.4	16.7	48	46

Hb: haemoglobin, Hct: haematocrit, PCO_2: partial pressure carbon dioxide, PO_2, partial pressure oxygen, (blue= subjects with AMS)

A.3.3 AMS scores and O_2 saturation

A.3.3.1 Phase I

Normoxia

No.	LL-self	LL clinical	LL total	ESQ	Head-ache	SaO_2 (%)
2	0	0	0	0.000	N	98
3	1	0	1	0.090	Y	96
4	0	0	0	0.000	N	97
5	0	0	0	0.000	N	99
6	0	0	0	0.000	N	97
8	0	0	0	0.000	N	97
9	0	0	0	0.000	N	97
10	0	0	0	0.000	N	97
11	0	0	0	0.000	N	98
12	4	0	0	0.000	N	98
13	1	0	1	0.067	N	98
14	0	0	0	0.000	N	98
15	0	0	0	0.000	N	98
16	0	0	0	0.000	N	99
17	0	0	0	0.000	N	97
18	1	0	1	0.000	N	98
19	0	0	0	0.000	N	98
20	0	0	0	0.000	N	97
21	0	0	0	0.000	N	98
22	0	0	0	0.000	N	98

Hypoxia

No.	LL-self	LL clinical	LL total	ESQ	Head-ache	SaO_2 (%)
2	0	0	0	0.000	N	76
3	9	1	10	2.360	Y	93
4	0	0	0	0.000	N	83
5	1	0	1	0.090	Y	79
6	1	0	1	0.090	Y	68
8	2	0	2	0.270	Y	76
9	3	1	4	0.457	Y	78
10	4	1	5	0.462	Y	81
11	3	1	4	0.487	N	82
12	2	1	3	0.090	Y	89
13	2	0	2	0.239	Y	86
14	1	0	1	0.179	Y	81
15	1	0	1	0.000	N	83
16	7	1	8	1.597	Y	82
17	1	0	1	0.090	Y	91
18	5	1	6	0.658	Y	72
19	1	0	1	0.094	Y	94
20	8	1	9	2.386	Y	85
21	2	0	2	0.184	Y	84
22	1	0	1	0.094	Y	83

LL: lake louise criteria, ESQ: environmental symptoms questionnaire, Y: yes, N: no, SaO_2: oxygen saturation (pulse oximetry)
Blue fill indicates those diagnosed with AMS

A.3.3.2 Phase II

Normoxia

No.	LL-self	LL clinical	LL total	ESQ	Head-ache	SaO_2 (%)
2	0	1	1	n/r	N	99
3	0	0	0	n/r	N	99
4	0	0	0	n/r	Y	99
5	0	1	1	n/r	N	99
6	0	0	0	n/r	N	98
8	1	0	1	n/r	N	99
9	0	0	0	n/r	N	99
10	0	0	0	n/r	N	98
11	0	0	0	n/r	N	99
12	2	0	2	n/r	Y	98
13	0	0	0	n/r	Y	99
14	0	0	0	n/r	N	99
15	0	0	0	n/r	Y	98
16	0	0	0	n/r	N	99
17	0	0	0	n/r	N	99
18	1	0	1	n/r	N	99
19	0	0	0	n/r	N	99
20	4	1	5	n/r	Y	98
21	0	0	0	n/r	N	99
22	0	0	0	n/r	N	99

Hypoxia

No.	LL-self	LL clinical	LL total	ESQ	Head-ache	SaO_2 (%)
2	0	2	2	0.000	N	90
3	2	2	4	0.472	Y	83
4	1	1	2	0.000	N	84
5	1	0	1	0.100	N	91
6	1	1	2	0.075	N	79
8	2	1	3	0.000	N	87
9	0	0	0	0.000	N	93
10	1	0	1	0.000	Y	90
11	4	1	5	0.277	Y	90
12	3	0	3	0.258	Y	87
13	0	0	0	0.000	N	88
14	1	0	1	0.090	Y	93
15	3	1	4	n/r	N	90
16	0	0	0	0.000	N	91
17	0	0	0	0.000	N	92
18	7	1	8	0.895	Y	77
19	0	0	0	0.000	N	95
20	6	1	7	1.125	Y	89
21	5	0	5	0.461	Y	91
22	6	1	7	0.858	Y	88

LL: lake louise criteria, ESQ: environmental symptoms questionnaire, Y: yes, N: no, SaO_2: oxygen saturation (pulse oximetry)
Blue fill indicates those diagnosed with AMS

A.3.4 Plasma protein concentrations as determined by ELISA

A.3.4.1 EPO (mIU/ml)

	Phase I		Phase II	
Subject no.	Normoxia	Hypoxia	Normoxia	Hypoxia
2	9.4	12.8	8.3	36.5
3	4.4	15.6	15.7	48.9
4	8.6	13.4	7.1	17.8
5	6.7	13.9	16.4	50.6
6	6.4	27.1	10.8	136.9
8	10.5	25.1	22	92.3
9	7.6	11.9	6.7	10.8
10	4.9	14.6	8.7	39.6
11	3.6	17.1	6.9	53.8
12	9.2	25.0	7.7	51.5
13	15.8	24.7	16	62.9
14	12.0	21.2	13.7	65.2
15	5.9	17.7	8.3	42.7
16	27.4	33.2	18.3	57.5
17	7.6	17.2	11.2	29.4
18	7.9	15.1	10.8	130.8
19	6.6	13.1	5.2	65.3
20	4.4	9.6	8.6	32.2
21	4.6	8.7	13.8	96.8
22	8.9	27.3	7.8	77.2

A.3.4.2 sFLT (pg/ml)

	Phase I		Phase II	
Subject no.	Normoxia	Hypoxia	Normoxia	Hypoxia
2	94	82	75	109
3	100	73	89	154
4	274	139	46	57
5	92	124	72	94
6	101	100	105	133
8	73	494	40	66
9	102	191	109	122
10	94	117	106	123
11	116	388	94	110
12	136	116	56	65
13	122	252	76	95
14	233	159	95	103
15	150	119	116	128
16	239	437	104	127
17	494	614	94	112
18	130	84	95	109
19	234	591	80	108
20	539	572	88	110
21	209	107	84	128
22	206	361	72	106

A.3.4.3 VEGF (pg/ml)

	Phase I		Phase II	
Subject no.	Normoxia	Hypoxia	Normoxia	Hypoxia
2	49	283	64	11
3	100	66	86	23
4	165	29	31	12
5	44	22	41	37
6	51	56	57	44
8	32	79	48	23
9	82	62	46	36
10	64	60	23	13
11	20	56	81	28
12	110	150	24	23
13	29	64	225	166
14	224	127	98	37
15	85	127	112	79
16	51	12	181	58
17	20	84	46	36
18	67	58	80	21
19	120	145	38	32
20	131	160	16	18
21	101	30	45	46
22	47	87	68	28

Appendix IV

Lake Louise AMS Scoring System

Time	**am**	**pm**	**am**	**pm**	**am**	**pm**	**am**	**pm**	**am**	**pm**
Headache										
None at all	0	0	0	0	0	0	0	0	0	0
Mild headache	1	1	1	1	1	1	1	1	1	1
Moderate headache	2	2	2	2	2	2	2	2	2	2
Severe headache, incapacitating	3	3	3	3	3	3	3	3	3	3
Gastrointestinal symptoms										
Good appetite	0	0	0	0	0	0	0	0	0	0
Poor appetite ot nausea	1	1	1	1	1	1	1	1	1	1
Moderate nausea or vomiting	2	2	2	2	2	2	2	2	2	2
Severe, incapacitating nausea and vomiting	3	3	3	3	3	3	3	3	3	3
Fatigue and/or weakness										
Not tired or weak	0	0	0	0	0	0	0	0	0	0
Mild fatigue/weakness	1	1	1	1	1	1	1	1	1	1
Moderate fatigue/weakness	2	2	2	2	2	2	2	2	2	2
Severe fatigue/weakness	3	3	3	3	3	3	3	3	3	3
Dizziness/lightheadedness										
None	0	0	0	0	0	0	0	0	0	0
Mild	1	1	1	1	1	1	1	1	1	1
Moderate	2	2	2	2	2	2	2	2	2	2
Severe, capacitating	3	3	3	3	3	3	3	3	3	3
Difficulty Sleeping										
Slept as well as usual	0	0	0	0	0	0	0	0	0	0
Did not sleep as well as usual	1	1	1	1	1	1	1	1	1	1
Woke many times, poor night's sleep	2	2	2	2	2	2	2	2	2	2
Could not sleep at all	3	3	3	3	3	3	3	3	3	3

Environmental symptoms questionnaire

Please mark each: 0 Not at all 1 Slight 2 Somewhat 3 Moderate 4 Quite a bit 5 Extreme

	am	pm	am	pm	am	pm	am	pm	am	pm
I feel lightheaded										
I have a headache										
I feel dizzy										
I feel faint										
My vision is dim										
My coordination is off										
I feel weak										
I feel sick to my stomach										
I've lost my appetite										
I feel sick										
I feel hungover										
Total										

Appendix V

A.5.1 Gene lists

A.5.1.1 WT *vs.* WT EXT

A.5.1.1.2 Upregulated

Gene symbol	Gene name
Anln	ANILLIN, ACTIN BINDING PROTEIN (SCRAPS HOMOLOG, DROSOPHILA)
Pltp	PHOSPHOLIPID TRANSFER PROTEIN
Serinc3	SERINE INCORPORATOR 3
C1qtnf3	C1Q AND TUMOR NECROSIS FACTOR RELATED PROTEIN 3
Lyzs	LYSOZYME
Ms4a7	MEMBRANE-SPANNING 4-DOMAINS, SUBFAMILY A, MEMBER 7
Tnn	TENASCIN N
Cldn10	DNA SEGMENT, CHR 14, ERATO DOI 728, EXPRESSED
Dlk1	DELTA-LIKE 1 HOMOLOG (DROSOPHILA)
Ggcx	GAMMA-GLUTAMYL CARBOXYLASE
Eif2s3y	EUKARYOTIC TRANSLATION INITIATION FACTOR 2, SUBUNIT 3, STRUCTURAL GENE Y-LINKED
Ugt1a10	UDP GLYCOSYLTRANSFERASE 1 FAMILY, POLYPEPTIDE A10
Apobec1	APOLIPOPROTEIN B EDITING COMPLEX 1
Ccl12	CHEMOKINE (C-C MOTIF) LIGAND 12
Atp2c1	RIKEN CDNA 1700121J11 GENE
Epm2aip1	EPM2A (LAFORIN) INTERACTING PROTEIN 1
AA881470	EST AA881470
Cbr2	CARBONYL REDUCTASE 2
Fscn1	FASCIN HOMOLOG 1, ACTIN BUNDLING PROTEIN (STRONGYLOCENTROTUS) PURPURATUS)
Adamts4	A DISINTEGRIN-LIKE AND METALLOPEPTIDASE (REPROLYSIN TYPE) WITH THROMBOSPONDIN TYPE 1 MOTIF, 4
Lcn2	LIPOCALIN 2
Emb	EMBIGIN
Sfrp2	SECRETED FRIZZLED-RELATED SEQUENCE PROTEIN 2
Unc93b1	UNC-93 HOMOLOG B1 (C. ELEGANS)
Gdpd3	GLYCEROPHOSPHODIESTER PHOSPHODIESTERASE DOMAIN CONTAINING 3
Dnaic1	DYNEIN, AXONEMAL, INTERMEDIATE CHAIN 1
Ccl7	CHEMOKINE (C-C MOTIF) LIGAND 7
Vamp8	VESICLE-ASSOCIATED MEMBRANE PROTEIN 8
Mmp12	MATRIX METALLOPEPTIDASE 12
Fhl3	FOUR AND A HALF LIM DOMAINS 3
Capg	CAPPING PROTEIN (ACTIN FILAMENT), GELSOLIN-LIKE
4930583H14Rik	RIKEN CDNA 4930583H14 GENE
Prc1	PROTEIN REGULATOR OF CYTOKINESIS 1
Chrng	CHOLINERGIC RECEPTOR, NICOTINIC, GAMMA POLYPEPTIDE
Usp39	UBIQUITIN SPECIFIC PEPTIDASE 39
Mt3	METALLOTHIONEIN 3
Igfbp4	INSULIN-LIKE GROWTH FACTOR BINDING PROTEIN 4
C4b	COMPLEMENT COMPONENT 4B (CHILDO BLOOD GROUP)
Tomm22	RING FINGER PROTEIN 13

Cfl1	COFILIN 1, NON-MUSCLE
Myo1f	MYOSIN IF
Mest	MESODERM SPECIFIC TRANSCRIPT
Col14a1	PROCOLLAGEN, TYPE XIV, ALPHA 1
Mmp3	MATRIX METALLOPEPTIDASE 3
Ankrd2	ANKYRIN REPEAT DOMAIN 2 (STRETCH RESPONSIVE MUSCLE)
Apoe	APOLIPOPROTEIN E
Col3a1	PROCOLLAGEN, TYPE III, ALPHA 1
H2-Ab1	HISTOCOMPATIBILITY 2, CLASS II ANTIGEN A, BETA 1
Clec4n	C-TYPE LECTIN DOMAIN FAMILY 4, MEMBER N
Lrrc15	LEUCINE RICH REPEAT CONTAINING 15
Ccl8	CHEMOKINE (C-C MOTIF) LIGAND 8
2810021J22Rik	RIKEN CDNA 2810021J22 GENE
Serpina3n	SERINE (OR CYSTEINE) PEPTIDASE INHIBITOR, CLADE A, MEMBER 3N
Pkig	PROTEIN KINASE INHIBITOR, GAMMA
Junb	JUN-B ONCOGENE
Il13ra1	INTERLEUKIN 13 RECEPTOR, ALPHA 1

A.5.1.1.2 Down-regulated

Gene symbol	**Gene name**
Xist	INACTIVE X SPECIFIC TRANSCRIPTS
Gadd45a	GROWTH ARREST AND DNA-DAMAGE-INDUCIBLE 45 ALPHA
H2-K1	HISTOCOMPATIBILITY 2, K1, K REGION
H2-T23	HISTOCOMPATIBILITY 2, T REGION LOCUS 23
Cdo1	CYSTEINE DIOXYGENASE 1, CYTOSOLIC
Slc15a2	SOLUTE CARRIER FAMILY 15 (H+/PEPTIDE TRANSPORTER), MEMBER 2
Capn2	CALPAIN 2
1110020G09Rik	RIKEN CDNA 1110020G09 GENE
EG633640	SIMILAR TO CG10866-PA
Aldh1a7	ALDEHYDE DEHYDROGENASE FAMILY 1, SUBFAMILY A7
Indo	INDOLEAMINE-PYRROLE 2,3 DIOXYGENASE
Cfd	COMPLEMENT FACTOR D (ADIPSIN)
Myl3	MYOSIN, LIGHT POLYPEPTIDE 3
Zfp68	ZINC FINGER PROTEIN 68
Tmc7	TRANSMEMBRANE CHANNEL-LIKE GENE FAMILY 7
Mup2	MAJOR URINARY PROTEIN 2
Cyp2e1	CYTOCHROME P450, FAMILY 2, SUBFAMILY E, POLYPEPTIDE 1
Gbp4	MACROPHAGE ACTIVATION 2
Riok1	RIO KINASE 1 (YEAST)
Mal	MYELIN AND LYMPHOCYTE PROTEIN, T-CELL DIFFERENTIATION PROTEIN
Gvin1	GTPASE, VERY LARGE INTERFERON INDUCIBLE 1
Serpina3g	SERINE (OR CYSTEINE) PEPTIDASE INHIBITOR, CLADE A, MEMBER 3G
EG546166	HYPOTHETICAL PROTEIN LOC546166
Gbp1	GUANYLATE NUCLEOTIDE BINDING PROTEIN 1
Dctn1	DYNACTIN 1
2610206B13Rik	RIKEN CDNA 2810449K13 GENE

A.5.1.2 PHD1 K/O *vs.* WT

A.5.1.2.1 Upregulated

Gene symbol	Gene name
Olfr299	OLFACTORY RECEPTOR 299
V1rf2	VOMERONASAL 1 RECEPTOR, F2
EG432743	HYPOTHETICAL GENE SUPPORTED BY AK077314
Cyp21a1	CYTOCHROME P450, FAMILY 21, SUBFAMILY A, POLYPEPTIDE 1
Olfr536	OLFACTORY RECEPTOR 536
Olfr121	OLFACTORY RECEPTOR 121
1300012G16Rik	RIKEN CDNA 1300012G16 GENE
Olfr1245	OLFACTORY RECEPTOR 1245
BC002059	CDNA SEQUENCE BC002059
2010309E21Rik	RIKEN CDNA 2010309E21 GENE
4921510J17Rik	RIKEN CDNA 4921510J17 GENE
Kctd8	POTASSIUM CHANNEL TETRAMERISATION DOMAIN CONTAINING 8
Olfr884	OLFACTORY RECEPTOR 884
BC060632	CDNA SEQUENCE BC060632
4930521A18Rik	RIKEN CDNA 4930521A18 GENE
Gpr128	G PROTEIN-COUPLED RECEPTOR 128
Timm22	TRANSLOCASE OF INNER MITOCHONDRIAL MEMBRANE 22 HOMOLOG (YEAST)
Olfr725	OLFACTORY RECEPTOR 725
4933421E11Rik	RIKEN CDNA 4933421E11 GENE
Pafah2	PLATELET-ACTIVATING FACTOR ACETYLHYDROLASE 2
Pdyn	PRODYNORPHIN
Lgi1	LEUCINE-RICH REPEAT LGI FAMILY, MEMBER 1
Gpr142	G PROTEIN-COUPLED RECEPTOR 142
Pknox2	PBX/KNOTTED 1 HOMEOBOX 2
Dffb	DNA FRAGMENTATION FACTOR, BETA SUBUNIT
Cysltr2	CYSTEINYL LEUKOTRIENE RECEPTOR 2
Olfr624	OLFACTORY RECEPTOR 624
Fabp7	FATTY ACID BINDING PROTEIN 7, BRAIN
1700109H08Rik	RIKEN CDNA 1700109H08 GENE
Olfr103	OLFACTORY RECEPTOR 103
Elmo1	RIKEN CDNA C230095H21 GENE
Hhip	HEDGEHOG-INTERACTING PROTEIN
Trpv1	TRANSIENT RECEPTOR POTENTIAL CATION CHANNEL, SUBFAMILY V, MEMBER 1
Evx1	EVEN SKIPPED HOMEOTIC GENE 1 HOMOLOG
Btnl2	BUTYROPHILIN-LIKE 2
H2-M10.2	HISTOCOMPATIBILITY 2, M REGION LOCUS 10.2
Blm	BLOOM SYNDROME HOMOLOG (HUMAN)
Olfr593	OLFACTORY RECEPTOR 593
Rps6kb1	RIBOSOMAL PROTEIN S6 KINASE, POLYPEPTIDE 1
Zp1	ZONA PELLUCIDA GLYCOPROTEIN 1
Speer8-ps1	SPERMATOGENESIS ASSOCIATED GLUTAMATE (E)-RICH PROTEIN 8, PSEUDOGENE 1
Olfr556	OLFACTORY RECEPTOR 556
Atm	ATAXIA TELANGIECTASIA MUTATED HOMOLOG (HUMAN)
Padi3	PEPTIDYL ARGININE DEIMINASE, TYPE III
F12	COAGULATION FACTOR XII (HAGEMAN FACTOR)
Itlnb	INTELECTIN B
Hrasls5	HRAS-LIKE SUPPRESSOR FAMILY, MEMBER 5
Ezh2	ENHANCER OF ZESTE HOMOLOG 2 (DROSOPHILA)

Olfr63	OLFACTORY RECEPTOR 63
Olfr203	OLFACTORY RECEPTOR 203
Ror1	RECEPTOR TYROSINE KINASE-LIKE ORPHAN RECEPTOR 1
Eif4e1b	GENE MODEL 273, (NCBI)
Otc	ORNITHINE TRANSCARBAMYLASE
Olfr3	OLFACTORY RECEPTOR 3
Polr3k	POLYMERASE (RNA) III (DNA DIRECTED) POLYPEPTIDE K
Mrgprd	MAS-RELATED GPR, MEMBER D
Stx19	RIKEN CDNA A030009B12 GENE
Aldh1a2	ALDEHYDE DEHYDROGENASE FAMILY 1, SUBFAMILY A2
Btc	BETACELLULIN, EPIDERMAL GROWTH FACTOR FAMILY MEMBER
Pcsk4	PROPROTEIN CONVERTASE SUBTILISIN/KEXIN TYPE 4
Uts2	UROTENSIN 2
Nphs2	NEPHROSIS 2 HOMOLOG, PODOCIN (HUMAN)
Gm397	GENE MODEL 397, (NCBI)
Mlstd1	MALE STERILITY DOMAIN CONTAINING 1
Lin28	LIN-28 HOMOLOG (C. ELEGANS)
Olfr450	OLFACTORY RECEPTOR 450
V1rd3	VOMERONASAL 1 RECEPTOR, D3
Yars	TYROSYL-TRNA SYNTHETASE
1700025E21Rik	RIKEN CDNA 1700016K02 GENE
Muc10	MUCIN 10, SUBMANDIBULAR GLAND SALIVARY MUCIN
Aldoc	ALDOLASE 3, C ISOFORM
Cacng5	CALCIUM CHANNEL, VOLTAGE-DEPENDENT, GAMMA SUBUNIT 5
Olfr313	OLFACTORY RECEPTOR 313
Foxp2	RIKEN CDNA 2810043D05 GENE
Olig3	OLIGODENDROCYTE TRANSCRIPTION FACTOR 3
Pdcl2	RIKEN CDNA 1700010B22 GENE
Cyp2c29	CYTOCHROME P450, FAMILY 2, SUBFAMILY C, POLYPEPTIDE 29
LOC621852	SIMILAR TO SIMILAR TO TESTIS EXPRESSED HOMEOBOX 2
Zfp54	ZINC FINGER PROTEIN 54
Mdm1	TRANSFORMED MOUSE 3T3 CELL DOUBLE MINUTE 1
Fbxw11	F-BOX AND WD-40 DOMAIN PROTEIN 11
Tnrc4	TRINUCLEOTIDE REPEAT CONTAINING 4
Nbn	NIBRIN
4930433I11Rik	RIKEN CDNA 4930433I11 GENE
Rchy1	RING FINGER AND CHY ZINC FINGER DOMAIN CONTAINING 1
Hrh3	HISTAMINE RECEPTOR H 3
Pnmt	PHENYLETHANOLAMINE-N-METHYLTRANSFERASE
Rap1gap	RAP1, GTPASE-ACTIVATING PROTEIN 1
Acsl3	ACYL-COA SYNTHETASE LONG-CHAIN FAMILY MEMBER 3
Sumf2	SULFATASE MODIFYING FACTOR 2
Gdpd3	GLYCEROPHOSPHODIESTER PHOSPHODIESTERASE DOMAIN CONTAINING 3
Tac4	TACHYKININ 4
Spata16	SPERMATOGENESIS ASSOCIATED 16
Olfr646	OLFACTORY RECEPTOR 646
Gp9	GLYCOPROTEIN 9 (PLATELET)
Olfr1463	OLFACTORY RECEPTOR 1463
Cth	CYSTATHIONASE (CYSTATHIONINE GAMMA-LYASE)
1110005A03Rik	RIKEN CDNA 1110005A03 GENE
Olfr1497	OLFACTORY RECEPTOR 1497
Thnsl1	EXPRESSED SEQUENCE AW413632
Enam	ENAMELIN
Prrt3	PROLINE-RICH TRANSMEMBRANE PROTEIN 3
Glmn	GLOMULIN, FKBP ASSOCIATED PROTEIN
Mical1	MICROTUBULE ASSOCIATED MONOXYGENASE, CALPONIN AND LIM DOMAIN CONTAINING 1
Ceacam14	CEA-RELATED CELL ADHESION MOLECULE 14
D19Ertd386e	DNA SEGMENT, CHR 19, ERATO DOI 386, EXPRESSED
Adh5	ALCOHOL DEHYDROGENASE 5 (CLASS III), CHI POLYPEPTIDE

Tnr	TENASCIN R
Lsm11	U7 SNRNP-SPECIFIC SM-LIKE PROTEIN LSM11
Negr1	NEURONAL GROWTH REGULATOR 1
Syt13	SYNAPTOTAGMIN XIII
Es1	ESTERASE 1

A.5.1.2.2 Down-regulated

Gadd45a	GROWTH ARREST AND DNA-DAMAGE-INDUCIBLE 45 ALPHA
Csf1	COLONY STIMULATING FACTOR 1 (MACROPHAGE)
Slc8a1	SOLUTE CARRIER FAMILY 8 (SODIUM/CALCIUM EXCHANGER), MEMBER 1
Slc25a17	SOLUTE CARRIER FAMILY 25 (MITOCHONDRIAL CARRIER, PEROXISOMAL MEMBRANE PROTEIN), MEMBER 17
Sema3f	SEMA DOMAIN, IMMUNOGLOBULIN DOMAIN (IG), SHORT BASIC DOMAIN, SECRETED, (SEMAPHORIN) 3 F
Ap1g1	ADAPTOR PROTEIN COMPLEX AP-1, GAMMA 1 SUBUNIT
Fbxo7	F-BOX ONLY PROTEIN 7
Foxc1	FORKHEAD BOX C1
Arrdc3	ARRESTIN DOMAIN CONTAINING 3
2700094K13Rik	RIKEN CDNA 2700094K13 GENE
Zfp30	ZINC FINGER PROTEIN 30
Mgat1	MANNOSIDE ACETYLGLUCOSAMINYLTRANSFERASE 1
2310037I24Rik	RIKEN CDNA 2310037I24 GENE
2210009G21Rik	RIKEN CDNA 2410004I22 GENE
Akap10	A KINASE (PRKA) ANCHOR PROTEIN 10
Riok1	RIO KINASE 1 (YEAST)
Gvin1	GTPASE, VERY LARGE INTERFERON INDUCIBLE 1
Espn	ESPIN
Cog2	COMPONENT OF OLIGOMERIC GOLGI COMPLEX 2
Eml3	ECHINODERM MICROTUBULE ASSOCIATED PROTEIN LIKE 3
EG546166	HYPOTHETICAL PROTEIN LOC546166
EG630499	SIMILAR TO HISTOCOMPATIBILITY 2, Q REGION LOCUS 10
Adarb1	ADENOSINE DEAMINASE, RNA-SPECIFIC, B1
Psmb9	PROTEOSOME (PROSOME, MACROPAIN) SUBUNIT, BETA TYPE 9 (LARGE MULTIFUNCTIONAL PEPTIDASE 2)
Poli	POLYMERASE (DNA DIRECTED), IOTA
Zfp275	ZINC FINGER PROTEIN 275
Bbc3	BCL-2 BINDING COMPONENT 3
Taf6	TAF6 RNA POLYMERASE II, TATA BOX BINDING PROTEIN (TBP)-ASSOCIATED FACTOR
B2m	BETA-2 MICROGLOBULIN
Pmaip1	PHORBOL-12-MYRISTATE-13-ACETATE-INDUCED PROTEIN 1
H2-K1	HISTOCOMPATIBILITY 2, K1, K REGION
Ddx21	DEAD (ASP-GLU-ALA-ASP) BOX POLYPEPTIDE 21
1700102P08Rik	RIKEN CDNA 1700102P08 GENE
Trim36	TRIPARTITE MOTIF-CONTAINING 36
Avpr1a	ARGININE VASOPRESSIN RECEPTOR 1A
Lhfp	LIPOMA HMGIC FUSION PARTNER

Trim30	TRIPARTITE MOTIF PROTEIN 30
Musk	MUSCLE, SKELETAL, RECEPTOR TYROSINE KINASE
Slc25a16	SOLUTE CARRIER FAMILY 25 (MITOCHONDRIAL CARRIER, GRAVES DISEASE AUTOANTIGEN), MEMBER 16
Tmem16f	TRANSMEMBRANE PROTEIN 16F
Tef	THYROTROPH EMBRYONIC FACTOR
Commd8	COMM DOMAIN CONTAINING 8
Jag1	JAGGED 1
Ift140	INTRAFLAGELLAR TRANSPORT 140 HOMOLOG (CHLAMYDOMONAS)
Cyfip1	CYTOPLASMIC FMR1 INTERACTING PROTEIN 1
Dusp18	DUAL SPECIFICITY PHOSPHATASE 18
Nkd1	RIKEN CDNA 2810434J10 GENE
Coil	COILIN
Galnt2	EXPRESSED SEQUENCE AI480629
Mipep	MITOCHONDRIAL INTERMEDIATE PEPTIDASE
4930550C14Rik	RIKEN CDNA 4930550C14 GENE
Pold3	POLYMERASE (DNA-DIRECTED), DELTA 3, ACCESSORY SUBUNIT
Gadd45a	GROWTH ARREST AND DNA-DAMAGE-INDUCIBLE 45 ALPHA
Csf1	COLONY STIMULATING FACTOR 1 (MACROPHAGE)
Slc8a1	SOLUTE CARRIER FAMILY 8 (SODIUM/CALCIUM EXCHANGER), MEMBER 1
Slc25a17	SOLUTE CARRIER FAMILY 25 (MITOCHONDRIAL CARRIER, PEROXISOMAL MEMBRANE PROTEIN), MEMBER 17
Sema3f	SEMA DOMAIN, IMMUNOGLOBULIN DOMAIN (IG), SHORT BASIC DOMAIN, SECRETED, (SEMAPHORIN) 3 F
Ap1g1	ADAPTOR PROTEIN COMPLEX AP-1, GAMMA 1 SUBUNIT
Fbxo7	F-BOX ONLY PROTEIN 7
Foxc1	FORKHEAD BOX C1
Arrdc3	ARRESTIN DOMAIN CONTAINING 3
2700094K13Rik	RIKEN CDNA 2700094K13 GENE
Zfp30	ZINC FINGER PROTEIN 30
Mgat1	MANNOSIDE ACETYLGLUCOSAMINYLTRANSFERASE 1
2310037I24Rik	RIKEN CDNA 2310037I24 GENE
2210009G21Rik	RIKEN CDNA 2410004I22 GENE
Akap10	A KINASE (PRKA) ANCHOR PROTEIN 10
Riok1	RIO KINASE 1 (YEAST)
Gvin1	GTPASE, VERY LARGE INTERFERON INDUCIBLE 1
Espn	ESPIN
Cog2	COMPONENT OF OLIGOMERIC GOLGI COMPLEX 2
Eml3	ECHINODERM MICROTUBULE ASSOCIATED PROTEIN LIKE 3
EG546166	HYPOTHETICAL PROTEIN LOC546166
EG630499	SIMILAR TO HISTOCOMPATIBILITY 2, Q REGION LOCUS 10
Adarb1	ADENOSINE DEAMINASE, RNA-SPECIFIC, B1
Psmb9	PROTEOSOME (PROSOME, MACROPAIN) SUBUNIT, BETA TYPE 9 (LARGE MULTIFUNCTIONAL PEPTIDASE 2)
Poli	POLYMERASE (DNA DIRECTED), IOTA
Zfp275	ZINC FINGER PROTEIN 275
Bbc3	BCL-2 BINDING COMPONENT 3
Taf6	TAF6 RNA POLYMERASE II, TATA BOX BINDING PROTEIN (TBP)-ASSOCIATED FACTOR
B2m	BETA-2 MICROGLOBULIN
Pmaip1	PHORBOL-12-MYRISTATE-13-ACETATE-INDUCED PROTEIN 1

H2-K1	HISTOCOMPATIBILITY 2, K1, K REGION
Ddx21	DEAD (ASP-GLU-ALA-ASP) BOX POLYPEPTIDE 21
1700102P08Rik	RIKEN CDNA 1700102P08 GENE
Trim36	TRIPARTITE MOTIF-CONTAINING 36
Avpr1a	ARGININE VASOPRESSIN RECEPTOR 1A
Lhfp	LIPOMA HMGIC FUSION PARTNER
Trim30	TRIPARTITE MOTIF PROTEIN 30
Musk	MUSCLE, SKELETAL, RECEPTOR TYROSINE KINASE
Slc25a16	SOLUTE CARRIER FAMILY 25 (MITOCHONDRIAL CARRIER, GRAVES DISEASE AUTOANTIGEN), MEMBER 16
Tmem16f	TRANSMEMBRANE PROTEIN 16F
Tef	THYROTROPH EMBRYONIC FACTOR
Commd8	COMM DOMAIN CONTAINING 8
Jag1	JAGGED 1
Ift140	INTRAFLAGELLAR TRANSPORT 140 HOMOLOG (CHLAMYDOMONAS)
Cyfip1	CYTOPLASMIC FMR1 INTERACTING PROTEIN 1
Dusp18	DUAL SPECIFICITY PHOSPHATASE 18
Nkd1	RIKEN CDNA 2810434J10 GENE
Coil	COILIN
Galnt2	EXPRESSED SEQUENCE AI480629
Mipep	MITOCHONDRIAL INTERMEDIATE PEPTIDASE
4930550C14Rik	RIKEN CDNA 4930550C14 GENE
Pold3	POLYMERASE (DNA-DIRECTED), DELTA 3, ACCESSORY SUBUNIT

A.5.1.3 PHD1 K/O EXT *vs.* PHD1 K/O

A.5.1.3.1 Upregulated

Def6	DIFFERENTIALLY EXPRESSED IN FDCP 6
Lyzs	LYSOZYME
Fes	FELINE SARCOMA ONCOGENE
Slc8a1	SOLUTE CARRIER FAMILY 8 (SODIUM/CALCIUM EXCHANGER), MEMBER 1
Casp4	CASPASE 4, APOPTOSIS-RELATED CYSTEINE PEPTIDASE
Abca1	ATP-BINDING CASSETTE, SUB-FAMILY A (ABC1), MEMBER 1
Cdc2a	CELL DIVISION CYCLE 2 HOMOLOG A (S. POMBE)
Birc5	BACULOVIRAL IAP REPEAT-CONTAINING 5
Apobec1	APOLIPOPROTEIN B EDITING COMPLEX 1
Pafah1b3	PLATELET-ACTIVATING FACTOR ACETYLHYDROLASE, ISOFORM 1B, ALPHA1 SUBUNIT
Htatip2	HIV-1 TAT INTERACTIVE PROTEIN 2, HOMOLOG (HUMAN)
Pscdbp	PLECKSTRIN HOMOLOGY, SEC7 AND COILED-COIL DOMAINS, BINDING PROTEIN
Msln	MESOTHELIN
Mx2	MYXOVIRUS (INFLUENZA VIRUS) RESISTANCE 2
Pml	PROMYELOCYTIC LEUKEMIA
Git2	G PROTEIN-COUPLED RECEPTOR KINASE-INTERACTOR 2
Cd84	CD84 ANTIGEN
Slc15a3	SOLUTE CARRIER FAMILY 15, MEMBER 3
Nfkbiz	NUCLEAR FACTOR OF KAPPA LIGHT POLYPEPTIDE GENE ENHANCER IN B-CELLS INHIBITOR, ZETA
Vat1	VESICLE AMINE TRANSPORT PROTEIN 1 HOMOLOG (T CALIFORNICA)
Kctd10	POTASSIUM CHANNEL TETRAMERISATION DOMAIN CONTAINING 10
A630077B13Rik	RIKEN CDNA A630077B13 GENE
Csf3r	COLONY STIMULATING FACTOR 3 RECEPTOR (GRANULOCYTE)
Gmfg	GLIA MATURATION FACTOR, GAMMA
Tgfb3	TRANSFORMING GROWTH FACTOR, BETA 3
Lypla3	LYSOPHOSPHOLIPASE 3
Coro1a	CORONIN, ACTIN BINDING PROTEIN 1A
Btk	BRUTON AGAMMAGLOBULINEMIA TYROSINE KINASE
Pecam1	PLATELET/ENDOTHELIAL CELL ADHESION MOLECULE 1
Actn4	ACTININ ALPHA 4
Mobkl2a	MOB1, MPS ONE BINDER KINASE ACTIVATOR-LIKE 2A (YEAST)
Foxp1	FORKHEAD BOX P1
Coro1c	CORONIN, ACTIN BINDING PROTEIN 1C
Klhl6	KELCH-LIKE 6 (DROSOPHILA)
Emilin2	ELASTIN MICROFIBRIL INTERFACER 2
Arl11	ADP-RIBOSYLATION FACTOR-LIKE 11
Rab8b	RAB8B, MEMBER RAS ONCOGENE FAMILY
Tlr13	TOLL-LIKE RECEPTOR 13
Jag1	JAGGED 1
Ap2a2	ADAPTOR PROTEIN COMPLEX AP-2, ALPHA 2 SUBUNIT
Cyfip1	CYTOPLASMIC FMR1 INTERACTING PROTEIN 1
Ccl4	CHEMOKINE (C-C MOTIF) LIGAND 4
Agpat4	1-ACYLGLYCEROL-3-PHOSPHATE O-ACYLTRANSFERASE 1

	(LYSOPHOSPHATIDIC ACID ACYLTRANSFERASE, DELTA)
Lst1	LEUKOCYTE SPECIFIC TRANSCRIPT 1
Il1rl1	INTERLEUKIN 1 RECEPTOR-LIKE 1
Ep400	E1A BINDING PROTEIN P400
Rab8a	RAB8A, MEMBER RAS ONCOGENE FAMILY
Kcnab2	POTASSIUM VOLTAGE-GATED CHANNEL, SHAKER-RELATED SUBFAMILY, BETA MEMBER 2
1200013B08Rik	RIKEN CDNA 1200013B08 GENE
Litaf	LPS-INDUCED TN FACTOR
Cggbp1	CGG TRIPLET REPEAT BINDING PROTEIN 1
Gpr124	G PROTEIN-COUPLED RECEPTOR 124
Slc35e3	RIKEN CDNA 9330166G04 GENE
Gns	GLUCOSAMINE (N-ACETYL)-6-SULFATASE
Serpinb6a	SERINE (OR CYSTEINE) PEPTIDASE INHIBITOR, CLADE B, MEMBER 6A
Anln	ANILLIN, ACTIN BINDING PROTEIN (SCRAPS HOMOLOG, DROSOPHILA)
Hn1	HEMATOLOGICAL AND NEUROLOGICAL EXPRESSED SEQUENCE 1
Ms4a7	MEMBRANE-SPANNING 4-DOMAINS, SUBFAMILY A, MEMBER 7
Csf1	COLONY STIMULATING FACTOR 1 (MACROPHAGE)
Itga5	INTEGRIN ALPHA 5 (FIBRONECTIN RECEPTOR ALPHA)
Ly86	LYMPHOCYTE ANTIGEN 86
Mad2l1	MAD2 (MITOTIC ARREST DEFICIENT, HOMOLOG)-LIKE 1 (YEAST)
Sh3bgrl3	SH3 DOMAIN BINDING GLUTAMIC ACID-RICH PROTEIN-LIKE 3
Grn	GRANULIN
Plcg2	PHOSPHOLIPASE C, GAMMA 2
Pros1	PROTEIN S (ALPHA)
Bnc2	BASONUCLIN 2
Rrbp1	RIKEN CDNA 5730465C04 GENE
Ttyh3	TWEETY HOMOLOG 3 (DROSOPHILA)
Kcnk13	POTASSIUM CHANNEL, SUBFAMILY K, MEMBER 13
Eml3	ECHINODERM MICROTUBULE ASSOCIATED PROTEIN LIKE 3
Snx1	SORTING NEXIN 1
Bcl3	B-CELL LEUKEMIA/LYMPHOMA 3
Slc11a1	SOLUTE CARRIER FAMILY 11 (PROTON-COUPLED DIVALENT METAL ION TRANSPORTERS), MEMBER 1
Dbnl	DREBRIN-LIKE
AY078069	CDNA SEQUENCE AY078069
Lsp1	LYMPHOCYTE SPECIFIC 1
C4b	COMPLEMENT COMPONENT 4B (CHILDO BLOOD GROUP)
4930570C03Rik	RIKEN CDNA 4930570C03 GENE
Cxcl1	CHEMOKINE (C-X-C MOTIF) LIGAND 1
Flna	FILAMIN, ALPHA
Aif1	ALLOGRAFT INFLAMMATORY FACTOR 1
S100a4	S100 CALCIUM BINDING PROTEIN A4
Glipr2	GLI PATHOGENESIS-RELATED 2
Tcirg1	T-CELL, IMMUNE REGULATOR 1, ATPASE, H+ TRANSPORTING, LYSOSOMAL V0 PROTEIN A3
Laptm5	LYSOSOMAL-ASSOCIATED PROTEIN TRANSMEMBRANE 5
Mest	MESODERM SPECIFIC TRANSCRIPT
Trem2	TRIGGERING RECEPTOR EXPRESSED ON MYELOID CELLS 2C
P2ry6	PYRIMIDINERGIC RECEPTOR P2Y, G-PROTEIN COUPLED, 6
Soat1	STEROL O-ACYLTRANSFERASE 1

Casp1	CASPASE 1
Csrp2	CYSTEINE AND GLYCINE-RICH PROTEIN 2
C1qb	COMPLEMENT COMPONENT 1, Q SUBCOMPONENT, BETA POLYPEPTIDE
C3	COMPLEMENT COMPONENT 3
Dpep2	DIPEPTIDASE 2
Irak3	INTERLEUKIN-1 RECEPTOR-ASSOCIATED KINASE 3
Cerk	CERAMIDE KINASE
Ugcg	UDP-GLUCOSE CERAMIDE GLUCOSYLTRANSFERASE
Ncf4	NEUTROPHIL CYTOSOLIC FACTOR 4
Ccl8	CHEMOKINE (C-C MOTIF) LIGAND 8
Ccnb1	CYCLIN B1
Arrb2	ARRESTIN, BETA 2
Sh3bp2	SH3-DOMAIN BINDING PROTEIN 2
Limk1	LIM-DOMAIN CONTAINING, PROTEIN KINASE
1200002N14Rik	RIKEN CDNA 1200002N14 GENE
Plac8	PLACENTA-SPECIFIC 8
Hexa	HEXOSAMINIDASE A
Cdca2	CELL DIVISION CYCLE ASSOCIATED 2
Slc29a3	SOLUTE CARRIER FAMILY 29 (NUCLEOSIDE TRANSPORTERS), MEMBER 3
C1qtnf3	C1Q AND TUMOR NECROSIS FACTOR RELATED PROTEIN 3
0610007P14Rik	RIKEN CDNA 0610007P14 GENE
Cant1	CALCIUM ACTIVATED NUCLEOTIDASE 1
Scotin	SCOTIN GENE
Cacnb3	CALCIUM CHANNEL, VOLTAGE-DEPENDENT, BETA 3 SUBUNIT
Lgals3	LECTIN, GALACTOSE BINDING, SOLUBLE 3
Tlr7	TOLL-LIKE RECEPTOR 7
Drctnnb1a	DOWN-REGULATED BY CTNNB1, A
Ly9	LYMPHOCYTE ANTIGEN 9
Myo9b	MYOSIN IXB
H28	HISTOCOMPATIBILITY 28
Gpr177	G PROTEIN-COUPLED RECEPTOR 177
Prkcd	PROTEIN KINASE C, DELTA
Sla	SRC-LIKE ADAPTOR
Man2a1	MANNOSIDASE 2, ALPHA 1
Unc93b1	UNC-93 HOMOLOG B1 (C. ELEGANS)
Usp18	UBIQUITIN SPECIFIC PEPTIDASE 18
Cotl1	RIKEN CDNA 2010004C08 GENE
Chrng	CHOLINERGIC RECEPTOR, NICOTINIC, GAMMA POLYPEPTIDE
Rhog	RAS HOMOLOG GENE FAMILY, MEMBER G
Esco2	ESTABLISHMENT OF COHESION 1 HOMOLOG 2 (S. CEREVISIAE)
C920005C14Rik	RIKEN CDNA C920005C14 GENE
Uap1l1	UDP-N-ACTEYLGLUCOSAMINE PYROPHOSPHORYLASE 1-LIKE 1
Arpc1b	ACTIN RELATED PROTEIN 2/3 COMPLEX, SUBUNIT 1B
Ctsz	CATHEPSIN Z
Lmnb1	LAMIN B1
Cd44	CD44 ANTIGEN
Adam19	A DISINTEGRIN AND METALLOPEPTIDASE DOMAIN 19 (MELTRIN BETA)
Cap1	CAP, ADENYLATE CYCLASE-ASSOCIATED PROTEIN 1 (YEAST)
Sec61a1	SEC61 ALPHA 1 SUBUNIT (S. CEREVISIAE)
9130404D14Rik	RIKEN CDNA 9130404D14 GENE
Bok	BCL-2-RELATED OVARIAN KILLER PROTEIN
Gldc	DNA SEGMENT, CHR 19, WAYNE STATE UNIVERSITY 57,

	EXPRESSED
Tspyl3	TSPY-LIKE 3
Cd68	CD68 ANTIGEN
Mmp13	MATRIX METALLOPEPTIDASE 13
Lxn	LATEXIN
Fchsd2	FCH AND DOUBLE SH3 DOMAINS 2
Mbc2	MEMBRANE BOUND C2 DOMAIN CONTAINING PROTEIN
Agrn	AGRIN
C2	COMPLEMENT COMPONENT 2 (WITHIN H-2S)
Ly6a	LYMPHOCYTE ANTIGEN 6 COMPLEX, LOCUS A
Manba	RIKEN CDNA 2410030O07 GENE
BC017643	CDNA SEQUENCE BC017643
Mgl1	MACROPHAGE GALACTOSE N-ACETYL-GALACTOSAMINE SPECIFIC LECTIN 1
Nfatc4	NUCLEAR FACTOR OF ACTIVATED T-CELLS, CYTOPLASMIC, CALCINEURIN-DEPENDENT 4
Rab32	RAB32, MEMBER RAS ONCOGENE FAMILY
Ankfy1	ANKYRIN REPEAT AND FYVE DOMAIN CONTAINING 1
Ptbp1	POLYPYRIMIDINE TRACT BINDING PROTEIN 1
Kif2c	EST X83316
Pltp	PHOSPHOLIPID TRANSFER PROTEIN
Galk1	GALACTOKINASE 1
Fxyd5	FXYD DOMAIN-CONTAINING ION TRANSPORT REGULATOR 5
Slc2a6	SOLUTE CARRIER FAMILY 2 (FACILITATED GLUCOSE TRANSPORTER), MEMBER 6
Ugcgl1	RIKEN CDNA 0910001L17 GENE
Txndc5	THIOREDOXIN DOMAIN CONTAINING 5
Ccl5	CHEMOKINE (C-C MOTIF) LIGAND 5
Rnase6	RIBONUCLEASE, RNASE A FAMILY, 6
Oasl2	2'-5' OLIGOADENYLATE SYNTHETASE-LIKE 2
Col5a2	PROCOLLAGEN, TYPE V, ALPHA 2
Sdc3	SYNDECAN 3
Mgat1	MANNOSIDE ACETYLGLUCOSAMINYLTRANSFERASE 1
BC025575	CDNA SEQUENCE BC025575
Cbr2	CARBONYL REDUCTASE 2
Irf7	INTERFERON REGULATORY FACTOR 7
Mmp14	MATRIX METALLOPEPTIDASE 14 (MEMBRANE-INSERTED)
Oas2	2'-5' OLIGOADENYLATE SYNTHETASE 2
Cx3cr1	CHEMOKINE (C-X3-C) RECEPTOR 1
Sfrp2	SECRETED FRIZZLED-RELATED SEQUENCE PROTEIN 2
Adamts5	A DISINTEGRIN-LIKE AND METALLOPEPTIDASE (REPROLYSIN TYPE) WITH THROMBOSPONDIN TYPE 1 MOTIF, 5 (AGGRECANASE-2)
Upp1	URIDINE PHOSPHORYLASE 1
Zyx	ZYXIN
Elovl1	ELONGATION OF VERY LONG CHAIN FATTY ACIDS (FEN1/ELO2, SUR4/ELO3, YEAST)-LIKE 1
Casp8	CASPASE 8
BC026590	CDNA SEQUENCE BC026590
Ccl7	CHEMOKINE (C-C MOTIF) LIGAND 7
Ecm1	EXTRACELLULAR MATRIX PROTEIN 1
Ube1l	UBIQUITIN-ACTIVATING ENZYME E1-LIKE
Hp	HAPTOGLOBIN
Igfbp4	INSULIN-LIKE GROWTH FACTOR BINDING PROTEIN 4
Rps6ka1	RIBOSOMAL PROTEIN S6 KINASE POLYPEPTIDE 1

Stard5	DNA SEGMENT, CHR 7, ERATO DOI 152, EXPRESSED
Lass5	LONGEVITY ASSURANCE HOMOLOG 5 (S. CEREVISIAE)
Gm2a	GM2 GANGLIOSIDE ACTIVATOR PROTEIN
Cx3cl1	CHEMOKINE (C-X3-C MOTIF) LIGAND 1
Lrp12	LOW DENSITY LIPOPROTEIN-RELATED PROTEIN 12
BC038286	CDNA SEQUENCE BC038286
Oas1g	2'-5' OLIGOADENYLATE SYNTHETASE 1G
Abi3	ABI GENE FAMILY, MEMBER 3
Tyrobp	TYRO PROTEIN TYROSINE KINASE BINDING PROTEIN
Spag5	SPERM ASSOCIATED ANTIGEN 5
Btg1	B-CELL TRANSLOCATION GENE 1, ANTI-PROLIFERATIVE
Myd88	MYELOID DIFFERENTIATION PRIMARY RESPONSE GENE 88
BC004728	CDNA SEQUENCE BC004728
Ext1	EXOSTOSES (MULTIPLE) 1
Ift140	INTRAFLAGELLAR TRANSPORT 140 HOMOLOG (CHLAMYDOMONAS)
Rassf4	RIKEN CDNA 3830411C14 GENE
Alox5ap	ARACHIDONATE 5-LIPOXYGENASE ACTIVATING PROTEIN
Aebp1	AE BINDING PROTEIN 1
Tbc1d5	TBC1 DOMAIN FAMILY, MEMBER 5
Clec4n	C-TYPE LECTIN DOMAIN FAMILY 4, MEMBER N
Lgals3bp	LECTIN, GALACTOSIDE-BINDING, SOLUBLE, 3 BINDING PROTEIN
Cstb	CYSTATIN B
Gpnmb	GLYCOPROTEIN (TRANSMEMBRANE) NMB
Ly6e	LYMPHOCYTE ANTIGEN 6 COMPLEX, LOCUS E
Slc27a3	SOLUTE CARRIER FAMILY 27 (FATTY ACID TRANSPORTER), MEMBER 3
Serpina3n	SERINE (OR CYSTEINE) PEPTIDASE INHIBITOR, CLADE A, MEMBER 3N
Man2b1	MANNOSIDASE 2, ALPHA B1
Spc25	SPINDLE POLE BODY COMPONENT 25 HOMOLOG (S. CEREVISIAE)
Cd52	CD52 ANTIGEN

A.5.1.3.2 Down-regulated

Klf12	KRUPPEL-LIKE FACTOR 12
Olfr299	OLFACTORY RECEPTOR 299
Rdh13	RETINOL DEHYDROGENASE 13 (ALL-TRANS AND 9-CIS)
Pdlim5	PDZ AND LIM DOMAIN 5
Dffb	DNA FRAGMENTATION FACTOR, BETA SUBUNIT
Cysltr2	CYSTEINYL LEUKOTRIENE RECEPTOR 2
Stx19	RIKEN CDNA A030009B12 GENE
1700007I06Rik	RIKEN CDNA 1700007I06 GENE
Tpm3	TROPOMYOSIN 5
Dsg1b	DESMOGLEIN 1 BETA
Olig3	OLIGODENDROCYTE TRANSCRIPTION FACTOR 3

A.5.1.4 PHD1 K/O EXT *vs.* WT EXT

A.5.1.4.1 Upregulated genes

Cdca2	CELL DIVISION CYCLE ASSOCIATED 2
Csf1r	COLONY STIMULATING FACTOR 1 RECEPTOR
Lyzs	LYSOZYME
Tpx2	TPX2, MICROTUBULE-ASSOCIATED PROTEIN HOMOLOG (XENOPUS LAEVIS)
Aldh3b1	ALDEHYDE DEHYDROGENASE 3 FAMILY, MEMBER B1
Ncf1	NEUTROPHIL CYTOSOLIC FACTOR 1
Lasp1	LIM AND SH3 PROTEIN 1
Scotin	SCOTIN GENE
Efemp2	EPIDERMAL GROWTH FACTOR-CONTAINING FIBULIN-LIKE EXTRACELLULAR MATRIX PROTEIN 2
Lgals3	LECTIN, GALACTOSE BINDING, SOLUBLE 3
Tlr7	TOLL-LIKE RECEPTOR 7
Scara3	SCAVENGER RECEPTOR CLASS A, MEMBER 3
Incenp	INNER CENTROMERE PROTEIN
Pqlc3	PQ LOOP REPEAT CONTAINING
Ly9	LYMPHOCYTE ANTIGEN 9
Bst2	BONE MARROW STROMAL CELL ANTIGEN 2
Pafah1b3	PLATELET-ACTIVATING FACTOR ACETYLHYDROLASE, ISOFORM 1B, ALPHA1 SUBUNIT
Pscdbp	PLECKSTRIN HOMOLOGY, SEC7 AND COILED-COIL DOMAINS, BINDING PROTEIN
Apoc1	APOLIPOPROTEIN C-I
Mx2	MYXOVIRUS (INFLUENZA VIRUS) RESISTANCE 2
Itgb7	INTEGRIN BETA 7
Rac3	RAS-RELATED C3 BOTULINUM SUBSTRATE 3
Cd84	CD84 ANTIGEN
Slc15a3	SOLUTE CARRIER FAMILY 15, MEMBER 3
Ctse	CATHEPSIN E
Il1b	INTERLEUKIN 1 BETA
Ifit3	INTERFERON-INDUCED PROTEIN WITH TETRATRICOPEPTIDE REPEATS 3
Vat1	VESICLE AMINE TRANSPORT PROTEIN 1 HOMOLOG (T CALIFORNICA)
Rbp1	RETINOL BINDING PROTEIN 1, CELLULAR
Emr1	EGF-LIKE MODULE CONTAINING, MUCIN-LIKE, HORMONE RECEPTOR-LIKE SEQUENCE 1
Csf3r	COLONY STIMULATING FACTOR 3 RECEPTOR (GRANULOCYTE)
Clic1	CHLORIDE INTRACELLULAR CHANNEL 1
Gmfg	GLIA MATURATION FACTOR, GAMMA
Coro1a	CORONIN, ACTIN BINDING PROTEIN 1A
Scara5	SCAVENGER RECEPTOR CLASS A, MEMBER 5 (PUTATIVE)
Nmi	N-MCY (AND STAT) INTERACTOR
Ctsc	CATHEPSIN C
Prg2	PROTEOGLYCAN 2, BONE MARROW
Unc93b1	UNC-93 HOMOLOG B1 (C. ELEGANS)
Samsn1	SAM DOMAIN, SH3 DOMAIN AND NUCLEAR LOCALIZATION SIGNALS, 1
Usp18	UBIQUITIN SPECIFIC PEPTIDASE 18
Lgals9	LECTIN, GALACTOSE BINDING, SOLUBLE 9

Edg5	ENDOTHELIAL DIFFERENTIATION, SPHINGOLIPID G-PROTEIN-COUPLED RECEPTOR, 5
Btk	BRUTON AGAMMAGLOBULINEMIA TYROSINE KINASE
Lyl1	LYMPHOBLASTOMIC LEUKEMIA
Cotl1	RIKEN CDNA 2010004C08 GENE
4930583H14 Rik	RIKEN CDNA 4930583H14 GENE
Ifitm6	INTERFERON INDUCED TRANSMEMBRANE PROTEIN 6
Ccr5	CHEMOKINE (C-C MOTIF) RECEPTOR 5
Actn4	ACTININ ALPHA 4
C920005C14 Rik	RIKEN CDNA C920005C14 GENE
Cxcr4	CHEMOKINE (C-X-C MOTIF) RECEPTOR 4
Epb4.1l3	ERYTHROCYTE PROTEIN BAND 4.1-LIKE 3
Ctss	CATHEPSIN S
Ctsz	CATHEPSIN Z
Cxcl4	CHEMOKINE (C-X-C MOTIF) LIGAND 4
Rod1	ROD1 REGULATOR OF DIFFERENTIATION 1 (S. POMBE)
Adam12	A DISINTEGRIN AND METALLOPEPTIDASE DOMAIN 12 (MELTRIN ALPHA)
Epb4.1l1	ERYTHROCYTE PROTEIN BAND 4.1-LIKE 1
Cd44	CD44 ANTIGEN
Arl11	ADP-RIBOSYLATION FACTOR-LIKE 11
Tlr13	TOLL-LIKE RECEPTOR 13
Ccl4	CHEMOKINE (C-C MOTIF) LIGAND 4
Gldc	DNA SEGMENT, CHR 19, WAYNE STATE UNIVERSITY 57, EXPRESSED
Lst1	LEUKOCYTE SPECIFIC TRANSCRIPT 1
Il1rl1	INTERLEUKIN 1 RECEPTOR-LIKE 1
Cd53	CD53 ANTIGEN
Cd68	CD68 ANTIGEN
Chi3l3	CHITINASE 3-LIKE 3
Tor3a	TORSIN FAMILY 3, MEMBER A
1200013B08 Rik	RIKEN CDNA 1200013B08 GENE
Mlkl	MIXED LINEAGE KINASE DOMAIN-LIKE
Mmp13	MATRIX METALLOPEPTIDASE 13
Lpxn	LEUPAXIN
Slc9a3r1	SOLUTE CARRIER FAMILY 9 (SODIUM/HYDROGEN EXCHANGER), ISOFORM 3 REGULATOR 1
C2	COMPLEMENT COMPONENT 2 (WITHIN H-2S)
Myo1g	MYOSIN IG
Slfn1	SCHLAFEN 1
Mgl1	MACROPHAGE GALACTOSE N-ACETYL-GALACTOSAMINE SPECIFIC LECTIN 1
Fzd1	FRIZZLED HOMOLOG 1 (DROSOPHILA)
Pltp	PHOSPHOLIPID TRANSFER PROTEIN
Enpp1	ECTONUCLEOTIDE PYROPHOSPHATASE/PHOSPHODIESTERASE 1
Tbxas1	THROMBOXANE A SYNTHASE 1, PLATELET
Ms4a7	MEMBRANE-SPANNING 4-DOMAINS, SUBFAMILY A, MEMBER 7
Slc2a6	SOLUTE CARRIER FAMILY 2 (FACILITATED GLUCOSE TRANSPORTER), MEMBER 6
Ada	ADENOSINE DEAMINASE
BC026585	CDNA SEQUENCE BC026585
Klra17	KILLER CELL LECTIN-LIKE RECEPTOR, SUBFAMILY A, MEMBER 17
Napsa	NAPSIN A ASPARTIC PEPTIDASE
Sp100	NUCLEAR ANTIGEN SP100

Ccl5	CHEMOKINE (C-C MOTIF) LIGAND 5
Fcgr1	FC RECEPTOR, IGG, HIGH AFFINITY I
Arhgap9	RHO GTPASE ACTIVATING PROTEIN 9
Rnase6	RIBONUCLEASE, RNASE A FAMILY, 6
Col5a3	PROCOLLAGEN, TYPE V, ALPHA 3
Oasl2	2'-5' OLIGOADENYLATE SYNTHETASE-LIKE 2
Ly86	LYMPHOCYTE ANTIGEN 86
Sdc3	SYNDECAN 3
Sh3bgrl3	SH3 DOMAIN BINDING GLUTAMIC ACID-RICH PROTEIN-LIKE 3
Pvrl2	POLIOVIRUS RECEPTOR-RELATED 2
4732435N03 Rik	RIKEN CDNA 4732435N03 GENE
Grn	GRANULIN
Plcg2	PHOSPHOLIPASE C, GAMMA 2
E430002G05 Rik	RIKEN CDNA E430002G05 GENE
Ptpn18	PROTEIN TYROSINE PHOSPHATASE, NON-RECEPTOR TYPE 18
Renbp	RENIN BINDING PROTEIN
Gpr120	G PROTEIN-COUPLED RECEPTOR 120
Irf7	INTERFERON REGULATORY FACTOR 7
Vav1	VAV 1 ONCOGENE
Oas2	2'-5' OLIGOADENYLATE SYNTHETASE 2
Fpr-rs2	FORMYL PEPTIDE RECEPTOR, RELATED SEQUENCE 2
Slc11a1	SOLUTE CARRIER FAMILY 11 (PROTON-COUPLED DIVALENT METAL ION TRANSPORTERS), MEMBER 1
Ccl7	CHEMOKINE (C-C MOTIF) LIGAND 7
Ugt1a6a	UDP GLUCURONOSYLTRANSFERASE 1 FAMILY, POLYPEPTIDE A6A
Capg	CAPPING PROTEIN (ACTIN FILAMENT), GELSOLIN-LIKE
Ube1l	UBIQUITIN-ACTIVATING ENZYME E1-LIKE
Lhfpl2	LIPOMA HMGIC FUSION PARTNER-LIKE 2
Lcp2	LYMPHOCYTE CYTOSOLIC PROTEIN 2
Tmem8	TRANSMEMBRANE PROTEIN 8 (FIVE MEMBRANE-SPANNING DOMAINS)
Saa3	SERUM AMYLOID A 3
Ccl2	CHEMOKINE (C-C MOTIF) LIGAND 2
Olfml1	OLFACTOMEDIN-LIKE 1
Blvrb	BILIVERDIN REDUCTASE B (FLAVIN REDUCTASE (NADPH))
Clec4a3	C-TYPE LECTIN DOMAIN FAMILY 4, MEMBER A3
Phf11	PHD FINGER PROTEIN 11
Parp14	RIKEN CDNA 1600029O10 GENE
2810417H13 Rik	RIKEN CDNA 2810417H13 GENE
Antxr1	ANTHRAX TOXIN RECEPTOR 1
Lilrb4	LEUKOCYTE IMMUNOGLOBULIN-LIKE RECEPTOR, SUBFAMILY B, MEMBER 4
Oas1g	2'-5' OLIGOADENYLATE SYNTHETASE 1G
Aif1	ALLOGRAFT INFLAMMATORY FACTOR 1
Gpr114	G PROTEIN-COUPLED RECEPTOR 114
Glipr2	GLI PATHOGENESIS-RELATED 2
Ms4a6d	MEMBRANE-SPANNING 4-DOMAINS, SUBFAMILY A, MEMBER 6D
Cd14	CD14 ANTIGEN
Tyrobp	TYRO PROTEIN TYROSINE KINASE BINDING PROTEIN
Rabep1	RABAPTIN, RAB GTPASE BINDING EFFECTOR PROTEIN 1
C1qa	COMPLEMENT COMPONENT 1, Q SUBCOMPONENT, ALPHA POLYPEPTIDE
Mmp3	MATRIX METALLOPEPTIDASE 3
Anxa8	ANNEXIN A8

Rassf4	RIKEN CDNA 3830411C14 GENE
D14Ertd668e	DNA SEGMENT, CHR 14, ERATO DOI 668, EXPRESSED
Hcst	HEMATOPOIETIC CELL SIGNAL TRANSDUCER
Col18a1	PROCOLLAGEN, TYPE XVIII, ALPHA 1
Trem2	TRIGGERING RECEPTOR EXPRESSED ON MYELOID CELLS 2C
P2ry6	PYRIMIDINERGIC RECEPTOR P2Y, G-PROTEIN COUPLED, 6
Soat1	STEROL O-ACYLTRANSFERASE 1
Casp1	CASPASE 1
C1qb	COMPLEMENT COMPONENT 1, Q SUBCOMPONENT, BETA POLYPEPTIDE
Slc44a1	SOLUTE CARRIER FAMILY 44, MEMBER 1
BC029169	CDNA SEQUENCE BC029169
Clec4n	C-TYPE LECTIN DOMAIN FAMILY 4, MEMBER N
Efna5	EPHRIN A5
Lgals3bp	LECTIN, GALACTOSIDE-BINDING, SOLUBLE, 3 BINDING PROTEIN
Ly6e	LYMPHOCYTE ANTIGEN 6 COMPLEX, LOCUS E
Gpnmb	GLYCOPROTEIN (TRANSMEMBRANE) NMB
Ncf4	NEUTROPHIL CYTOSOLIC FACTOR 4
Abcg1	ATP-BINDING CASSETTE, SUB-FAMILY G (WHITE), MEMBER 1
Atp6v1d	ATPASE, H+ TRANSPORTING, LYSOSOMAL V1 SUBUNIT D
Tgfb1i1	TRANSFORMING GROWTH FACTOR BETA 1 INDUCED TRANSCRIPT 1
Plac8	PLACENTA-SPECIFIC 8
1200002N14Rik	RIKEN CDNA 1200002N14 GENE
Cd52	CD52 ANTIGEN
Ifit2	INTERFERON-INDUCED PROTEIN WITH TETRATRICOPEPTIDE REPEATS 2

A.5.1.4.1 Downregulated genes

Mtch2	MITOCHONDRIAL CARRIER HOMOLOG 2 (C. ELEGANS)
Slc25a11	SOLUTE CARRIER FAMILY 25 (MITOCHONDRIAL CARRIER OXOGLUTARATE CARRIER), MEMBER 11
Coro6	CORONIN, ACTIN BINDING PROTEIN 6
Acn9	ACN9 HOMOLOG (S. CEREVISIAE)
Ncoa4	NUCLEAR RECEPTOR COACTIVATOR 4
Zfp289	ZINC FINGER PROTEIN 289
Lpin1	LIPIN 1
Coq5	COENZYME Q5 HOMOLOG, METHYLTRANSFERASE (YEAST)
Fbxo32	F-BOX ONLY PROTEIN 32
8230402K04Rik	RIKEN CDNA 8230402K04 GENE
Tspyl1	TESTIS-SPECIFIC PROTEIN, Y-ENCODED-LIKE 1
Gadd45g	GROWTH ARREST AND DNA-DAMAGE-INDUCIBLE 45 GAMMA
Mrps12	MITOCHONDRIAL RIBOSOMAL PROTEIN S12
Ech1	ENOYL COENZYME A HYDRATASE 1, PEROXISOMAL
Idh3g	ISOCITRATE DEHYDROGENASE 3 (NAD+), GAMMA
Snca	SYNUCLEIN, ALPHA
Tmem66	TRANSMEMBRANE PROTEIN 66
Sgk3	SERUM/GLUCOCORTICOID REGULATED KINASE 3
Apip	APAF1 INTERACTING PROTEIN
Chpt1	CHOLINE PHOSPHOTRANSFERASE 1
1700034H14Rik	RIKEN CDNA 1700034H14 GENE
Slc35e4	SOLUTE CARRIER FAMILY 35, MEMBER E4
Tpd52l1	TUMOR PROTEIN D52-LIKE 1
Vgll2	VESTIGIAL LIKE 2 HOMOLOG (DROSOPHILA)
Rfc4	REPLICATION FACTOR C (ACTIVATOR 1) 4
5230400G24Rik	RIKEN CDNA 5230400G24 GENE
Phospho1	PHOSPHATASE, ORPHAN 1
Alas2	AMINOLEVULINIC ACID SYNTHASE 2, ERYTHROID
Ush2a	USHER SYNDROME 2A (AUTOSOMAL RECESSIVE, MILD) HOMOLOG (HUMAN)
Nit2	NITRILASE FAMILY, MEMBER 2
Arl6ip2	ADP-RIBOSYLATION FACTOR-LIKE 6 INTERACTING PROTEIN 2
Sar1b	SAR1 GENE HOMOLOG B (S. CEREVISIAE)
Kif17	KINESIN FAMILY MEMBER 17
Gpr146	G PROTEIN-COUPLED RECEPTOR 146
1700102P08Rik	RIKEN CDNA 1700102P08 GENE
Gba2	GLUCOSIDASE BETA 2
Lmcd1	LIM AND CYSTEINE-RICH DOMAINS 1
2410166I05Rik	RIKEN CDNA 2410166I05 GENE
Klf12	KRUPPEL-LIKE FACTOR 12
2010311D03Rik	EXPRESSED SEQUENCE AI314967
S3-12	PLASMA MEMBRANE ASSOCIATED PROTEIN, S3-12
Synj2bp	SYNAPTOJANIN 2 BINDING PROTEIN
Adsl	ADENYLOSUCCINATE LYASE
Oxct1	3-OXOACID COA TRANSFERASE 1
Syngr2	SYNAPTOGYRIN 2
Pdlim5	PDZ AND LIM DOMAIN 5
Dctn4	DYNACTIN 4

Psmd8	PROTEASOME (PROSOME, MACROPAIN) 26S SUBUNIT, NON-ATPASE, 8
Ldb3	LIM DOMAIN BINDING 3
Nudt2	NUDIX (NUCLEOSIDE DIPHOSPHATE LINKED MOIETY X)-TYPE MOTIF 2
Uros	UROPORPHYRINOGEN III SYNTHASE
Sgcg	SARCOGLYCAN, GAMMA (DYSTROPHIN-ASSOCIATED GLYCOPROTEIN)
Phka1	PHOSPHORYLASE KINASE ALPHA 1
Pdhb	PYRUVATE DEHYDROGENASE (LIPOAMIDE) BETA
Hist1h2bh	HISTONE 1, H2BH
Atp5f1	ATP SYNTHASE, H+ TRANSPORTING, MITOCHONDRIAL F0 COMPLEX, SUBUNIT B, ISOFORM 1
Mllt3	DNA SEGMENT, CHR 4, ERATO DOI 321, EXPRESSED
Cdc34	CELL DIVISION CYCLE 34 HOMOLOG (S. CEREVISIAE)

A.5.1.5 PHD3 K/O EXT *vs.* WT EXT

A.5.1.5.1 Upregulated genes

Pla2g12a	PHOSPHOLIPASE A2, GROUP XIIA
C1qtnf3	C1Q AND TUMOR NECROSIS FACTOR RELATED PROTEIN 3
Lasp1	LIM AND SH3 PROTEIN 1
Klk1b22	KALLIKREIN 1-RELATED PEPTIDASE B22
Cxxc4	CXXC FINGER 4
EG633640	SIMILAR TO CG10866-PA
Fdxr	FERREDOXIN REDUCTASE
Timm10	TRANSLOCASE OF INNER MITOCHONDRIAL MEMBRANE 10 HOMOLOG (YEAST)
Timm9	TRANSLOCASE OF INNER MITOCHONDRIAL MEMBRANE 9 HOMOLOG (YEAST)
Btbd11	BTB (POZ) DOMAIN CONTAINING 11
Nipsnap1	4-NITROPHENYLPHOSPHATASE DOMAIN AND NON-NEURONAL SNAP25-LIKE PROTEIN HOMOLOG 1 (C. ELEGANS)
Dpep3	DIPEPTIDASE 3
Atm	ATAXIA TELANGIECTASIA MUTATED HOMOLOG (HUMAN)
Myl3	MYOSIN, LIGHT POLYPEPTIDE 3
Car11	CARBONIC ANHYDRASE 11
E430002G05Rik	RIKEN CDNA E430002G05 GENE
Il1rl1	INTERLEUKIN 1 RECEPTOR-LIKE 1
Myl2	MYOSIN, LIGHT POLYPEPTIDE 2, REGULATORY, CARDIAC, SLOW
Bcat2	BRANCHED CHAIN AMINOTRANSFERASE 2, MITOCHONDRIAL
Moxd1	MONOOXYGENASE, DBH-LIKE 1
Klk1b27	KALLIKREIN 1-RELATED PEPTIDASE B27
Riok1	RIO KINASE 1 (YEAST)
Cpne8	COPINE VIII
Lrrc15	LEUCINE RICH REPEAT CONTAINING 15
Nrn1	NEURITIN 1
Angptl1	ANGIOPOIETIN-LIKE 1
Dll3	DELTA-LIKE 3 (DROSOPHILA)
Atp6v1d	ATPASE, H+ TRANSPORTING, LYSOSOMAL V1 SUBUNIT D
Kif5b	KINESIN FAMILY MEMBER 5B
Magea2	MELANOMA ANTIGEN, FAMILY A, 2
Scin	SCINDERIN
Grwd1	GLUTAMATE-RICH WD REPEAT CONTAINING 1
2610206B13Rik	RIKEN CDNA 2810449K13 GENE
BC025076	CDNA SEQUENCE BC025076

A.5.1.5.1 Downregulated genes

Olfr142	OLFACTORY RECEPTOR 142
Egln3	EGL NINE HOMOLOG 3 (C. ELEGANS)
Tas2r110	TASTE RECEPTOR, TYPE 2, MEMBER 110
Serinc3	SERINE INCORPORATOR 3
AA881470	EST AA881470
Pon3	PARAOXONASE 3
Iqgap2	HYPOTHETICAL PROTEIN A630053O10
Slc6a18	SOLUTE CARRIER FAMILY 6 (NEUROTRANSMITTER TRANSPORTER), MEMBER 18
Arrdc1	ARRESTIN DOMAIN CONTAINING 1
Hoxa11	HOMEO BOX A11
Cdkl4	CYCLIN-DEPENDENT KINASE-LIKE 4
Klf12	KRUPPEL-LIKE FACTOR 12
Ggtla1	GAMMA-GLUTAMYLTRANSFERASE-LIKE ACTIVITY 1
Dyrk2	DUAL-SPECIFICITY TYROSINE-(Y)-PHOSPHORYLATION REGULATED KINASE 2
B4galt3	UDP-GAL:BETAGLCNAC BETA 1,4-GALACTOSYLTRANSFERASE, POLYPEPTIDE 3
Gdpd3	GLYCEROPHOSPHODIESTER PHOSPHODIESTERASE DOMAIN CONTAINING 3
Rbm14	RNA BINDING MOTIF PROTEIN 14
Sfxn3	SIDEROFLEXIN 3
Csrp1	CYSTEINE AND GLYCINE-RICH PROTEIN 1
Slc20a1	SOLUTE CARRIER FAMILY 20, MEMBER 1
Srrm1	SERINE/ARGININE REPETITIVE MATRIX 1
Eif4e	EUKARYOTIC TRANSLATION INITIATION FACTOR 4E
Mus81	MUS81 ENDONUCLEASE HOMOLOG (YEAST)

A.5.1.6 PHD1 K/O EXT *vs.* PHD3 K/O EXT

A.5.1.6.1 Upregulated

Slc29a3	SOLUTE CARRIER FAMILY 29 (NUCLEOSIDE TRANSPORTERS), MEMBER 3
Csf1r	COLONY STIMULATING FACTOR 1 RECEPTOR
Serinc3	SERINE INCORPORATOR 3
Lyzs	LYSOZYME
Tpx2	TPX2, MICROTUBULE-ASSOCIATED PROTEIN HOMOLOG (XENOPUS LAEVIS)
Ncf1	NEUTROPHIL CYTOSOLIC FACTOR 1
Ticam2	TOLL-LIKE RECEPTOR ADAPTOR MOLECULE 2
Ly9	LYMPHOCYTE ANTIGEN 9
Apobec1	APOLIPOPROTEIN B EDITING COMPLEX 1
Bst2	BONE MARROW STROMAL CELL ANTIGEN 2
Stat2	SIGNAL TRANSDUCER AND ACTIVATOR OF TRANSCRIPTION 2
H28	HISTOCOMPATIBILITY 28
Mx2	MYXOVIRUS (INFLUENZA VIRUS) RESISTANCE 2
Itgb7	INTEGRIN BETA 7
Kif21b	KINESIN FAMILY MEMBER 21B
H2-Ea	HISTOCOMPATIBILITY 2, CLASS II ANTIGEN E ALPHA
Cd84	CD84 ANTIGEN
Arl4c	ADP-RIBOSYLATION FACTOR-LIKE 4C
Slc15a3	SOLUTE CARRIER FAMILY 15, MEMBER 3
Ctse	CATHEPSIN E
Unc13d	UNC-13 HOMOLOG D (C. ELEGANS)
Lrmp	LYMPHOID-RESTRICTED MEMBRANE PROTEIN
2310016F22Rik	RIKEN CDNA 2310016F22 GENE
Nfkbiz	NUCLEAR FACTOR OF KAPPA LIGHT POLYPEPTIDE GENE ENHANCER IN B-CELLS INHIBITOR, ZETA
Adar	ADENOSINE DEAMINASE, RNA-SPECIFIC
2010110P09Rik	RIKEN CDNA 2010110P09 GENE
Ifit3	INTERFERON-INDUCED PROTEIN WITH TETRATRICOPEPTIDE REPEATS 3
Aoah	ACYLOXYACYL HYDROLASE
Glycam1	GLYCOSYLATION DEPENDENT CELL ADHESION MOLECULE 1
Emr1	EGF-LIKE MODULE CONTAINING, MUCIN-LIKE, HORMONE RECEPTOR-LIKE SEQUENCE 1
Clic1	CHLORIDE INTRACELLULAR CHANNEL 1
Gmfg	GLIA MATURATION FACTOR, GAMMA
Coro1a	CORONIN, ACTIN BINDING PROTEIN 1A
Ednrb	ENDOTHELIN RECEPTOR TYPE B
Prg2	PROTEOGLYCAN 2, BONE MARROW
Unc93b1	UNC-93 HOMOLOG B1 (C. ELEGANS)
Usp18	UBIQUITIN SPECIFIC PEPTIDASE 18
Lgals9	LECTIN, GALACTOSE BINDING, SOLUBLE 9
Cenpi	FSH PRIMARY RESPONSE 1
Btk	BRUTON AGAMMAGLOBULINEMIA TYROSINE KINASE
Ms4a6b	MEMBRANE-SPANNING 4-DOMAINS, SUBFAMILY A, MEMBER 6B
Spire1	SPIRE HOMOLOG 1 (DROSOPHILA)

Pecam1	PLATELET/ENDOTHELIAL CELL ADHESION MOLECULE 1
Egln3	EGL NINE HOMOLOG 3 (C. ELEGANS)
4930583H14Rik	RIKEN CDNA 4930583H14 GENE
Tnfrsf11a	TUMOR NECROSIS FACTOR RECEPTOR SUPERFAMILY, MEMBER 11A
Btnl2	BUTYROPHILIN-LIKE 2
Ifitm6	INTERFERON INDUCED TRANSMEMBRANE PROTEIN 6
Wnt2	WINGLESS-RELATED MMTV INTEGRATION SITE 2
Dcp1b	DCP1 DECAPPING ENZYME HOMOLOG B (S. CEREVISIAE)
Cxcr4	CHEMOKINE (C-X-C MOTIF) RECEPTOR 4
Fyb	FYN BINDING PROTEIN
Ctss	CATHEPSIN S
Ctsz	CATHEPSIN Z
Cxcl4	CHEMOKINE (C-X-C MOTIF) LIGAND 4
Epb4.1l1	ERYTHROCYTE PROTEIN BAND 4.1-LIKE 1
Hexb	HEXOSAMINIDASE B
Tlr13	TOLL-LIKE RECEPTOR 13
Ccl4	CHEMOKINE (C-C MOTIF) LIGAND 4
Bok	BCL-2-RELATED OVARIAN KILLER PROTEIN
Lst1	LEUKOCYTE SPECIFIC TRANSCRIPT 1
Cd53	CD53 ANTIGEN
Chi3l3	CHITINASE 3-LIKE 3
Tor3a	TORSIN FAMILY 3, MEMBER A
1200013B08Rik	RIKEN CDNA 1200013B08 GENE
Mlkl	MIXED LINEAGE KINASE DOMAIN-LIKE
Ptprc	PROTEIN TYROSINE PHOSPHATASE, RECEPTOR TYPE, C
Mmp13	MATRIX METALLOPEPTIDASE 13
Gtf2e2	GENERAL TRANSCRIPTION FACTOR II E, POLYPEPTIDE 2 (BETA SUBUNIT)
Lpxn	LEUPAXIN
Slc9a3r1	SOLUTE CARRIER FAMILY 9 (SODIUM/HYDROGEN EXCHANGER), ISOFORM 3 REGULATOR 1
Sgpl1	SPHINGOSINE PHOSPHATE LYASE 1
5830472M02Rik	RIKEN CDNA 5830472M02 GENE
Myo1g	MYOSIN IG
Slfn1	SCHLAFEN 1
Mgl1	MACROPHAGE GALACTOSE N-ACETYL-GALACTOSAMINE SPECIFIC LECTIN 1
Mus81	MUS81 ENDONUCLEASE HOMOLOG (YEAST)
Map4k4	NCK INTERACTING KINASE
Ptpra	PROTEIN TYROSINE PHOSPHATASE, RECEPTOR TYPE, A
Pltp	PHOSPHOLIPID TRANSFER PROTEIN
BC006779	CDNA SEQUENCE BC006779
Iqgap2	HYPOTHETICAL PROTEIN A630053O10
Ada	ADENOSINE DEAMINASE
BC026585	CDNA SEQUENCE BC026585
Klra17	KILLER CELL LECTIN-LIKE RECEPTOR, SUBFAMILY A, MEMBER 17
Ccl5	CHEMOKINE (C-C MOTIF) LIGAND 5
Fcgr1	FC RECEPTOR, IGG, HIGH AFFINITY I
Gal	GALANIN
Sepp1	SELENOPROTEIN P, PLASMA, 1
Arhgap9	RHO GTPASE ACTIVATING PROTEIN 9
Rnase6	RIBONUCLEASE, RNASE A FAMILY, 6
Csrp1	CYSTEINE AND GLYCINE-RICH PROTEIN 1
Pgrmc1	PROGESTERONE RECEPTOR MEMBRANE COMPONENT 1

Oasl2	2'-5' OLIGOADENYLATE SYNTHETASE-LIKE 2
Ly86	LYMPHOCYTE ANTIGEN 86
Sdc3	SYNDECAN 3
Grn	GRANULIN
AA881470	EST AA881470
Plcg2	PHOSPHOLIPASE C, GAMMA 2
Ptpn18	PROTEIN TYROSINE PHOSPHATASE, NON-RECEPTOR TYPE 18
Was	WISKOTT-ALDRICH SYNDROME HOMOLOG (HUMAN)
Kcnk13	POTASSIUM CHANNEL, SUBFAMILY K, MEMBER 13
Irf7	INTERFERON REGULATORY FACTOR 7
Mgea5	MENINGIOMA EXPRESSED ANTIGEN 5 (HYALURONIDASE)
Cx3cr1	CHEMOKINE (C-X3-C) RECEPTOR 1
Oas2	2'-5' OLIGOADENYLATE SYNTHETASE 2
Fpr-rs2	FORMYL PEPTIDE RECEPTOR, RELATED SEQUENCE 2
Klra18	KILLER CELL LECTIN-LIKE RECEPTOR, SUBFAMILY A, MEMBER 18
Snx1	SORTING NEXIN 1
Upp1	URIDINE PHOSPHORYLASE 1
Rbm14	RNA BINDING MOTIF PROTEIN 14
Gdpd3	GLYCEROPHOSPHODIESTER PHOSPHODIESTERASE DOMAIN CONTAINING 3
Slc11a1	SOLUTE CARRIER FAMILY 11 (PROTON-COUPLED DIVALENT METAL ION TRANSPORTERS), MEMBER 1
Ss18	SYNOVIAL SARCOMA TRANSLOCATION, CHROMOSOME 18
Lhfpl2	LIPOMA HMGIC FUSION PARTNER-LIKE 2
Tmem8	TRANSMEMBRANE PROTEIN 8 (FIVE MEMBRANE-SPANNING DOMAINS)
Saa3	SERUM AMYLOID A 3
Hp	HAPTOGLOBIN
Oasl1	2'-5' OLIGOADENYLATE SYNTHETASE-LIKE 1
Clec4a3	C-TYPE LECTIN DOMAIN FAMILY 4, MEMBER A3
Phf11	PHD FINGER PROTEIN 11
Cfl1	COFILIN 1, NON-MUSCLE
Oas1g	2'-5' OLIGOADENYLATE SYNTHETASE 1G
Ela1	ELASTASE 1, PANCREATIC
Aif1	ALLOGRAFT INFLAMMATORY FACTOR 1
Tyrobp	TYRO PROTEIN TYROSINE KINASE BINDING PROTEIN
Rabep1	RABAPTIN, RAB GTPASE BINDING EFFECTOR PROTEIN 1
Tcirg1	T-CELL, IMMUNE REGULATOR 1, ATPASE, H+ TRANSPORTING, LYSOSOMAL V0 PROTEIN A3
Myo1f	MYOSIN IF
C1qa	COMPLEMENT COMPONENT 1, Q SUBCOMPONENT, ALPHA POLYPEPTIDE
Anxa8	ANNEXIN A8
Hcls1	HEMATOPOIETIC CELL SPECIFIC LYN SUBSTRATE 1
Rassf4	RIKEN CDNA 3830411C14 GENE
D14Ertd668e	DNA SEGMENT, CHR 14, ERATO DOI 668, EXPRESSED
Stac2	SH3 AND CYSTEINE RICH DOMAIN 2
Trem2	TRIGGERING RECEPTOR EXPRESSED ON MYELOID CELLS 2C
Stxbp2	SYNTAXIN BINDING PROTEIN 2
Gpr65	G-PROTEIN COUPLED RECEPTOR 65
C3	COMPLEMENT COMPONENT 3
H2-Ab1	HISTOCOMPATIBILITY 2, CLASS II ANTIGEN A, BETA 1
Tspan32	TETRASPANIN 32
Rarg	RETINOIC ACID RECEPTOR, GAMMA
Lgals3bp	LECTIN, GALACTOSIDE-BINDING, SOLUBLE, 3 BINDING PROTEIN

Ly6e	LYMPHOCYTE ANTIGEN 6 COMPLEX, LOCUS E
Ncf4	NEUTROPHIL CYTOSOLIC FACTOR 4
Abcg1	ATP-BINDING CASSETTE, SUB-FAMILY G (WHITE), MEMBER 1
Arrb2	ARRESTIN, BETA 2
Pkig	PROTEIN KINASE INHIBITOR, GAMMA
Plac8	PLACENTA-SPECIFIC 8
1200002N14Rik	RIKEN CDNA 1200002N14 GENE
Ifit2	INTERFERON-INDUCED PROTEIN WITH TETRATRICOPEPTIDE REPEATS 2

A.5.1.6.2 Down-regulated

Mtch2	MITOCHONDRIAL CARRIER HOMOLOG 2 (C. ELEGANS)
Pla2g12a	PHOSPHOLIPASE A2, GROUP XIIA
Coro6	CORONIN, ACTIN BINDING PROTEIN 6
Slc25a11	SOLUTE CARRIER FAMILY 25 (MITOCHONDRIAL CARRIER OXOGLUTARATE CARRIER), MEMBER 11
Atp5s	ATP SYNTHASE, H+ TRANSPORTING, MITOCHONDRIAL F0 COMPLEX, SUBUNIT S
Ncoa4	NUCLEAR RECEPTOR COACTIVATOR 4
Gphn	GEPHYRIN
Mreg	WHN-DEPENDENT TRANSCRIPT 2
Uchl5	UBIQUITIN CARBOXYL-TERMINAL ESTERASE L5
EG633640	SIMILAR TO CG10866-PA
Ech1	ENOYL COENZYME A HYDRATASE 1, PEROXISOMAL
Ndufa6	NADH DEHYDROGENASE (UBIQUINONE) 1 ALPHA SUBCOMPLEX, 6 (B14)
Idh3g	ISOCITRATE DEHYDROGENASE 3 (NAD+), GAMMA
Adk	ADENOSINE KINASE
Rab5a	RIKEN CDNA 2410015H04 GENE
Timm8b	TRANSLOCASE OF INNER MITOCHONDRIAL MEMBRANE 8 HOMOLOG B (YEAST)
Sgk3	SERUM/GLUCOCORTICOID REGULATED KINASE 3
Scnm1	SODIUM CHANNEL MODIFIER 1
Apip	APAF1 INTERACTING PROTEIN
Acadm	ACETYL-COENZYME A DEHYDROGENASE, MEDIUM CHAIN
1810049H13Rik	RIKEN CDNA 1810049H13 GENE
Chpt1	CHOLINE PHOSPHOTRANSFERASE 1
Als2	AMYOTROPHIC LATERAL SCLEROSIS 2 (JUVENILE) HOMOLOG (HUMAN)
Ndufc1	NADH DEHYDROGENASE (UBIQUINONE) 1, SUBCOMPLEX UNKNOWN, 1
Acin1	APOPTOTIC CHROMATIN CONDENSATION INDUCER 1
Wbp1	WW DOMAIN BINDING PROTEIN 1
A330049M08Rik	RIKEN CDNA A330049M08 GENE
0610006I08Rik	RIKEN CDNA 0610006I08 GENE
Nit2	NITRILASE FAMILY, MEMBER 2
Txlnb	TAXILIN BETA
Arl6ip2	ADP-RIBOSYLATION FACTOR-LIKE 6 INTERACTING PROTEIN 2
Ptp4a2	PROTEIN TYROSINE PHOSPHATASE 4A2

Lypla1	LYSOPHOSPHOLIPASE 1
Slc15a2	SOLUTE CARRIER FAMILY 15 (H+/PEPTIDE TRANSPORTER), MEMBER 2
Hba-a1	HEMOGLOBIN ALPHA, ADULT CHAIN 1
Kif21a	KINESIN FAMILY MEMBER 21A
Nrbf2	NUCLEAR RECEPTOR BINDING FACTOR 2 PSEUDOGENE
Gpr37l1	DNA SEGMENT, KIST 8
1190002H23Rik	RIKEN CDNA 1190002H23 GENE
Mrpl3	MITOCHONDRIAL RIBOSOMAL PROTEIN L3
E2f6	E2F TRANSCRIPTION FACTOR 6
Gatad1	GATA ZINC FINGER DOMAIN CONTAINING 1
Rpo1-3	RNA POLYMERASE 1-3
Mrpl53	MITOCHONDRIAL RIBOSOMAL PROTEIN L53
Hist1h2bm	HISTONE 2, H3C1
Tef	THYROTROPH EMBRYONIC FACTOR
Csda	COLD SHOCK DOMAIN PROTEIN A
Mcm6	MINICHROMOSOME MAINTENANCE DEFICIENT 6 (MIS5 HOMOLOG, S. POMBE) (S. CEREVISIAE)
Hr	HAIRLESS
Car11	CARBONIC ANHYDRASE 11
Pdlim5	PDZ AND LIM DOMAIN 5
Slc25a34	SOLUTE CARRIER FAMILY 25, MEMBER 34
Ube2g1	UBIQUITIN-CONJUGATING ENZYME E2G 1 (UBC7 HOMOLOG, C. ELEGANS)
Nudt2	NUDIX (NUCLEOSIDE DIPHOSPHATE LINKED MOIETY X)-TYPE MOTIF 2
Mbp	MYELIN BASIC PROTEIN
Sgcg	SARCOGLYCAN, GAMMA (DYSTROPHIN-ASSOCIATED GLYCOPROTEIN)
Decr1	2,4-DIENOYL COA REDUCTASE 1, MITOCHONDRIAL
Atp1b1	ATPASE, NA+/K+ TRANSPORTING, BETA 1 POLYPEPTIDE
AI597479	EXPRESSED SEQUENCE AI597479
Hist1h2bh	HISTONE 1, H2BH
Tceb1	TRANSCRIPTION ELONGATION FACTOR B (SIII), POLYPEPTIDE 1
Atp5f1	ATP SYNTHASE, H+ TRANSPORTING, MITOCHONDRIAL F0 COMPLEX, SUBUNIT B, ISOFORM 1
Grwd1	GLUTAMATE-RICH WD REPEAT CONTAINING 1
Pde6d	PHOSPHODIESTERASE 6D, CGMP-SPECIFIC, ROD, DELTA
Mrps31	MITOCHONDRIAL RIBOSOMAL PROTEIN S31
Mtrf1	MITOCHONDRIAL TRANSLATIONAL RELEASE FACTOR 1
2310039H08Rik	RIKEN CDNA 2310039H08 GENE
Hint3	HISTIDINE TRIAD NUCLEOTIDE BINDING PROTEIN 3
Acn9	ACN9 HOMOLOG (S. CEREVISIAE)
Ythdf2	YTH DOMAIN FAMILY 2
Lpin1	LIPIN 1
Coq5	COENZYME Q5 HOMOLOG, METHYLTRANSFERASE (YEAST)
Klk1b22	KALLIKREIN 1-RELATED PEPTIDASE B22
Gsto1	GLUTATHIONE S-TRANSFERASE OMEGA 1
Mat2b	EXPRESSED SEQUENCE AI182287
Fbxo32	F-BOX ONLY PROTEIN 32
8230402K04Rik	RIKEN CDNA 8230402K04 GENE
Ubc	UBIQUITIN C
Mrps12	MITOCHONDRIAL RIBOSOMAL PROTEIN S12
Prdx3	PEROXIREDOXIN 3
BC004044	CDNA SEQUENCE BC004044

Snca	SYNUCLEIN, ALPHA
Rps6ka5	RIBOSOMAL PROTEIN S6 KINASE, POLYPEPTIDE 5
Tmem126a	TRANSMEMBRANE PROTEIN 126A
Zfp30	ZINC FINGER PROTEIN 30
Etfa	ELECTRON TRANSFERRING FLAVOPROTEIN, ALPHA POLYPEPTIDE
A430005L14Rik	RIKEN CDNA A430005L14 GENE
Cldn15	CLAUDIN 15
LOC654426	ATP SYNTHASE, H+ TRANSPORTING, MITOCHONDRIAL F0 COMPLEX, SUBUNIT F PSEUDOGENE
Homer1	HOMER HOMOLOG 1 (DROSOPHILA)
Hist1h2bk	HISTONE 1, H2BK
Ndufa5	NADH DEHYDROGENASE (UBIQUINONE) 1 ALPHA SUBCOMPLEX, 5
Dtna	DYSTROBREVIN ALPHA
Mkks	MCKUSICK-KAUFMAN SYNDROME PROTEIN
Narg1l	NMDA RECEPTOR REGULATED 1-LIKE
Riok1	RIO KINASE 1 (YEAST)
1700034H14Rik	RIKEN CDNA 1700034H14 GENE
Cutc	CUTC COPPER TRANSPORTER HOMOLOG (E.COLI)
Cldn1	CLAUDIN 1
Greb1	RIKEN CDNA 5730583K22 GENE
Tpd52l1	TUMOR PROTEIN D52-LIKE 1
Cops8	EXPRESSED SEQUENCE AA408242
D10Jhu81e	DNA SEGMENT, CHR 10, JOHNS HOPKINS UNIVERSITY 81 EXPRESSED
Rfc4	REPLICATION FACTOR C (ACTIVATOR 1) 4
5230400G24Rik	RIKEN CDNA 5230400G24 GENE
Dars	ASPARTYL-TRNA SYNTHETASE
Sh3kbp1	SH3-DOMAIN KINASE BINDING PROTEIN 1
Ush2a	USHER SYNDROME 2A (AUTOSOMAL RECESSIVE, MILD) HOMOLOG (HUMAN)
Taf6	TAF6 RNA POLYMERASE II, TATA BOX BINDING PROTEIN (TBP)-ASSOCIATED FACTOR
Sar1b	SAR1 GENE HOMOLOG B (S. CEREVISIAE)
Atp5j	ATP SYNTHASE, H+ TRANSPORTING, MITOCHONDRIAL F0 COMPLEX, SUBUNIT F
Kif17	KINESIN FAMILY MEMBER 17
Suclg1	SUCCINATE-COA LIGASE, GDP-FORMING, ALPHA SUBUNIT
Lmcd1	LIM AND CYSTEINE-RICH DOMAINS 1
2410166I05Rik	RIKEN CDNA 2410166I05 GENE
Slc25a16	SOLUTE CARRIER FAMILY 25 (MITOCHONDRIAL CARRIER, GRAVES DISEASE AUTOANTIGEN), MEMBER 16
2010311D03Rik	EXPRESSED SEQUENCE AI314967
S3-12	PLASMA MEMBRANE ASSOCIATED PROTEIN, S3-12
Egln1	EGL NINE HOMOLOG 1 (C. ELEGANS)
Synj2bp	SYNAPTOJANIN 2 BINDING PROTEIN
Znhit3	ZINC FINGER, HIT TYPE 3
Oxct1	3-OXOACID COA TRANSFERASE 1
Ccbl2	CYSTEINE CONJUGATE-BETA LYASE 2
Adsl	ADENYLOSUCCINATE LYASE
Immp2l	IMP2 INNER MITOCHONDRIAL MEMBRANE PEPTIDASE-LIKE (S. CEREVISIAE)
Stra13	STIMULATED BY RETINOIC ACID 13
Sra1	STEROID RECEPTOR RNA ACTIVATOR 1
Sirt5	SIRTUIN 5 (SILENT MATING TYPE INFORMATION REGULATION 2

	HOMOLOG) 5 (S. CEREVISIAE)
Bola3	BOLA-LIKE 3 (E. COLI)
Rala	V-RAL SIMIAN LEUKEMIA VIRAL ONCOGENE HOMOLOG A (RAS RELATED)
Psmb7	PROTEASOME (PROSOME, MACROPAIN) SUBUNIT, BETA TYPE 7
Bcat2	BRANCHED CHAIN AMINOTRANSFERASE 2, MITOCHONDRIAL
Rdh14	RIKEN CDNA 3110030G19 GENE
Psmd8	PROTEASOME (PROSOME, MACROPAIN) 26S SUBUNIT, NON-ATPASE, 8
Tnfrsf10b	TUMOR NECROSIS FACTOR RECEPTOR SUPERFAMILY, MEMBER 10B
Kbtbd4	KELCH REPEAT AND BTB (POZ) DOMAIN CONTAINING 4
Art5	ADP-RIBOSYLTRANSFERASE 5
Pdcd5	PROGRAMMED CELL DEATH 5
Uros	UROPORPHYRINOGEN III SYNTHASE
Suv39h1	SUPPRESSOR OF VARIEGATION 3-9 HOMOLOG 1 (DROSOPHILA)
Myoc	MYOCILIN
Lcmt1	LEUCINE CARBOXYL METHYLTRANSFERASE 1
Gm561	GENE MODEL 561, (NCBI)
Mllt3	DNA SEGMENT, CHR 4, ERATO DOI 321, EXPRESSED
Cdc34	CELL DIVISION CYCLE 34 HOMOLOG (S. CEREVISIAE)

Appendix VI

A.6.1 Functional tables from DAVID

The following colours represent mutual changes across comparison groups:

terms in: P1 K/O EXT *vs*. WT EXT, P1 K/O EXT *vs*. P1 K/O, P1 K/O EXT *vs*. P3 K/O

terms in: WT EXT *vs.* WT, P1 K/O EXT *vs.* P1

terms in: P1 K/O EXT *vs.* P3 K/O

terms in: WT EXT *vs.* WT, P1 K/O EXT *vs.* P1

terms in: P1 K/O EXT *vs.* P1 K/OP1 K/O EXT *vs.* WT

A.6.1.1 WT EXT *vs.* WT

Using standard criteria (described) was inadequate for differentiating up and downregulated genes in this group as the *P*-value across all genes was insignificant, i.e. >0.05. Instead, genes were distinguished on the basis of fold change only, classified on greater or less than 1 fold. Based on this, 56 genes were up and 26 downregulated, as obtained by DAVID analysis. Table A.6.1 illustrates functional clusters upregulated (FDR < 10). Only the immune response and immune system processes were down regulated in WT mice with EXT when compared to WT alone.

TERM	No. of genes
cytoskeletal protein binding	7
actin binding	6
protein binding	28
response to wounding	6
cytokinesis	3
chemokine activity	3
inflammatory response	5

Table A.6.1 Functional annotation charts for upregulated genes in WT EXT when compared to WT (colours described 7.3.1.2)

A.6.1.2 PHD1 K/O *vs.* WT

Using the standard criteria, 129 genes were up (A.6.2) and 53 genes were downregulated, though as with the above, none were clustered into groups based on function, from the DAVID output. None of the upregulated function terms in were common amongst any of the other comparisons. 'Response to endogenous stimulus' was the only downregulated term.

Term	Count
G-protein coupled receptor protein signaling pathway	31
G-protein coupled receptor activity	29
rhodopsin-like receptor activity	27
neurological system process	27
system process	28
sensory perception	24
transmembrane receptor activity	30
sensory perception of smell	21
olfactory receptor activity	21
sensory perception of chemical stimulus	21
cell surface receptor linked signal transduction	33
signal transduction	41
cell communication	41
receptor activity	31

Table A.6.2 Functional annotation charts for upregulated genes in PHD1 K/O when compared to WT (no colours indicates no similarity between other comparison groups)

A.6.1.3 PHD1 K/O EXT *vs.* PHD1 K/O

Using a *P*-value of 0.001 and a fold change of ± 0 showed an upregulation of 219 genes (A.6.3) and a downregulation of 11. Using $P<0.05$ gave a list encompassing a number of genes too large to be used in the DAVID analysis. Table illustrates the large range of functional terms upregulated in PHD1 K/O EXT mice when compared to PHD1 K/O alone. Many of these terms were common amongst other groups, as indicated by colour labelling. None of the downregulated genes could be clustered into terms.

Term	Count
immune response	29
immune system process	35
protein binding	104
inflammatory response	17
response to wounding	19
response to external stimulus	22
defense response	26
innate immune response	10
cytoskeletal protein binding	17
actin binding	14
ceramide metabolic process	6
sphingoid metabolic process	6
immunoglobulin mediated immune response	8
B cell mediated immunity	8
chemokine activity	6
chemokine receptor binding	6
immune effector process	10
response to stress	24
adaptive immune response	8
lymphocyte mediated immunity	8
positive regulation of biological process	27
leukocyte mediated immunity	8
sphingolipid metabolic process	6
membrane invagination	10
endocytosis	10
positive regulation of immune system process	8
mitosis	10
activation of immune response	7
M phase of mitotic cell cycle	10
binding	147
G-protein-coupled receptor binding	6
humoral immune response mediated by immunoglobulin	5
regulation of immune system process	8
positive regulation of multicellular organismal process	8
regulation of multicellular organismal process	12
membrane organization and biogenesis	11
positive regulation of immune response	7
acute inflammatory response	6
M phase	10
regulation of immune response	7
mitotic cell cycle	10
complement activation, classical pathway	4
positive regulation of cellular process	21
proteolysis	19
lipid metabolic process	17
lipid binding	12

Table A.6.3 Functional annotation charts for upregulated genes in PHD1 K/O EXT when compared to PHD1 K/O (colours described 6.3.1.2)

A.6.1.4 PHD1 K/O EXT *vs.* WT EXT

A fold change of ±0 was used as few genes had a *P*-value <0.05: 164 genes were upregulated and 59 genes downregulated in PHD1 K/O EXT mice. Table A.6.4 illustrates upregulated functions in PHD1 K/O mice with extirpation when compared with WT EXT mice (FDR < 10). Only one function fitted the criteria in downregulated genes: cofactor metabolic processes.

TERM	No. of genes
immune response	29
immune system process	34
response to wounding	20
inflammatory response	17
response to external stimulus	23
defense response	27
chemotaxis	9
taxis	9
carbohydrate binding	13
innate immune response	8
response to stress	21
response to other organism	9
G-protein-coupled receptor binding	6
chemokine activity	5
chemokine receptor binding	5
multi-organism process	10
inorganic anion transport	8
locomotory behavior	9
phosphate transport	6
acute inflammatory response	6
lipid binding	12
polysaccharide binding	6
protein binding	69
anion transport	8
pattern binding	6
response to biotic stimulus	9
cell adhesion	15
biological adhesion	15
sugar binding	8
response to stimulus	45
actin binding	9
behavior	10
binding	116
phospholipid binding	8
immunoglobulin mediated immune response	5
B cell mediated immunity	5

Table A.6.4 Functional annotation charts for upregulated genes in PHD1 K/O EXT when compared to WT EXT. (colours described 6.3.1.2)

A.6.1.6 PHD1 EXT K/O *vs.* PHD3 EXT K/O

Using the standard criteria, 151 genes were up and 188 genes were downregulated. Table A.6.6 indicates functional terms upregulated and table A.6.7 downregulated, in PHD1 K/O EXT when compared to PHD3 K/O EXT mice.

Term	Count
immune response	26
immune system process	31
response to wounding	17
inflammatory response	14
defense response	23
response to external stimulus	18
response to stress	20
antigen processing and presentation of exogenous peptide	5
antigen processing and presentation of exogenous antigen	5
adaptive immune response	7
lymphocyte mediated immunity	7
leukocyte mediated immunity	7
multi-organism process	10
response to stimulus	46
antigen processing and presentation of peptide antigen	5
response to other organism	8
beta-N-acetylhexosaminidase activity	3
antigen processing and presentation of peptide antigen	4
antigen processing and presentation of exogenous peptide	4
immune effector process	7
innate immune response	6
positive regulation of immune response	6
positive regulation of immune system process	6
antigen processing and presentation of peptide antigen	4
immunoglobulin mediated immune response	5
regulation of immune response	6
B cell mediated immunity	5
regulation of immune system process	6
protein binding	62
catabolic process	13
positive regulation of multicellular organismal process	6
acute inflammatory response	5
lipid binding	10
response to biotic stimulus	8

Table A.6.6 Functional annotation charts for upregulated genes in PHD1 K/O when compared to PHD3 K/O EXT. (colours described 6.3.1.2)

Term	Count
cofactor metabolic process	9
coenzyme metabolic process	8
metabolic process	75
catalytic activity	56
cofactor biosynthetic process	6
identical protein binding	8
chromatin assembly	5
pyrophosphatase activity	11

Table A.6.7 Functional annotation charts for downregulated genes in PHD1 K/O when compared to PHD3 K/O EXT. (colours described 6.3.1.2)

Appendix VII

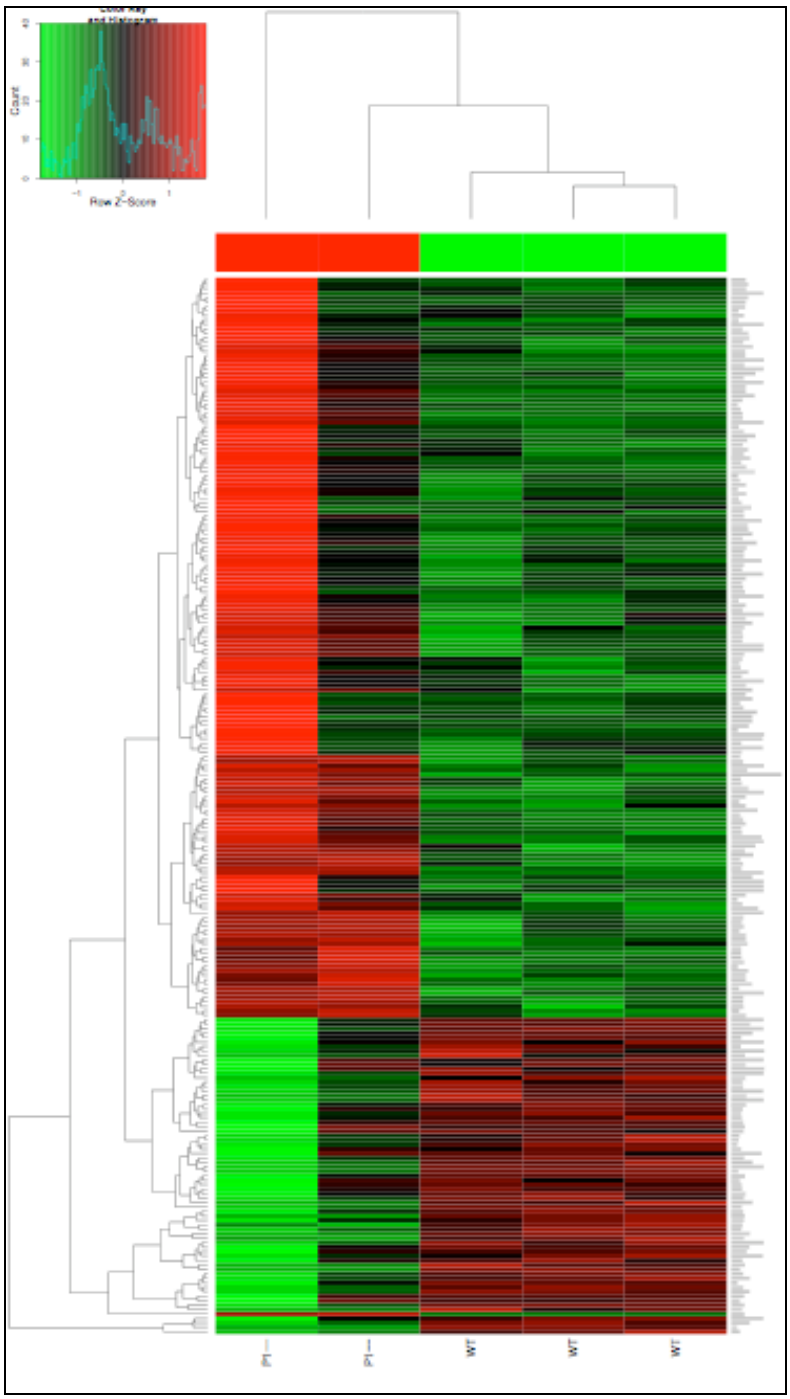

A heat map illustrating genes up- (red) and downregulated (green) in PHD1 K/O mice (colums 1-2) *vs.*WT (columns 3-5) using a *P*-value of 0.05 and ± 0 FC

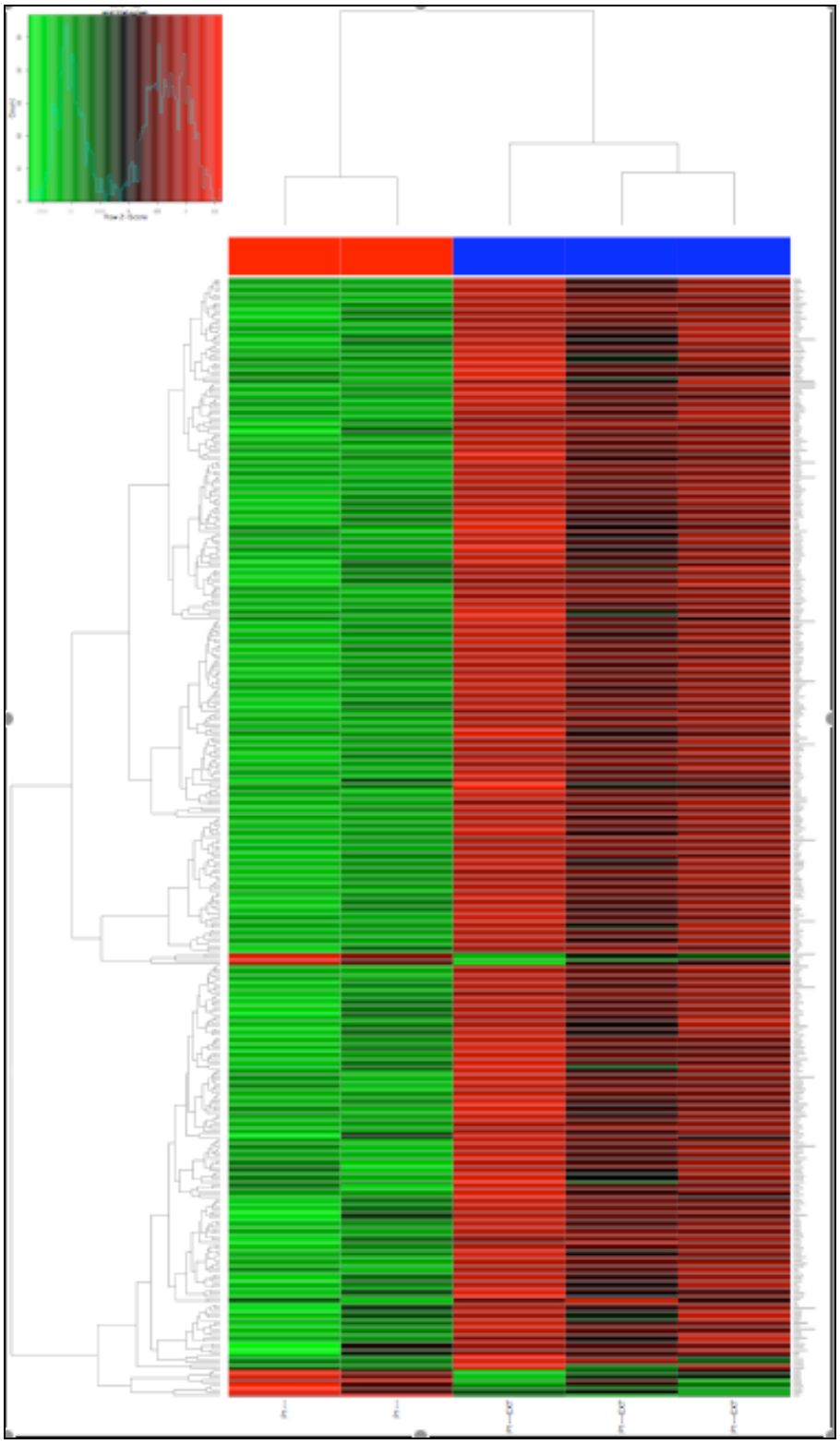

A heat map illustrating genes up- (red) and downregulated (green) in PHD1 K/O EXT (columns 3-5) *vs.* PHD1 K/O mice (columns 1 and 2) using a *P*-value of 0.05 and ± 0 FC

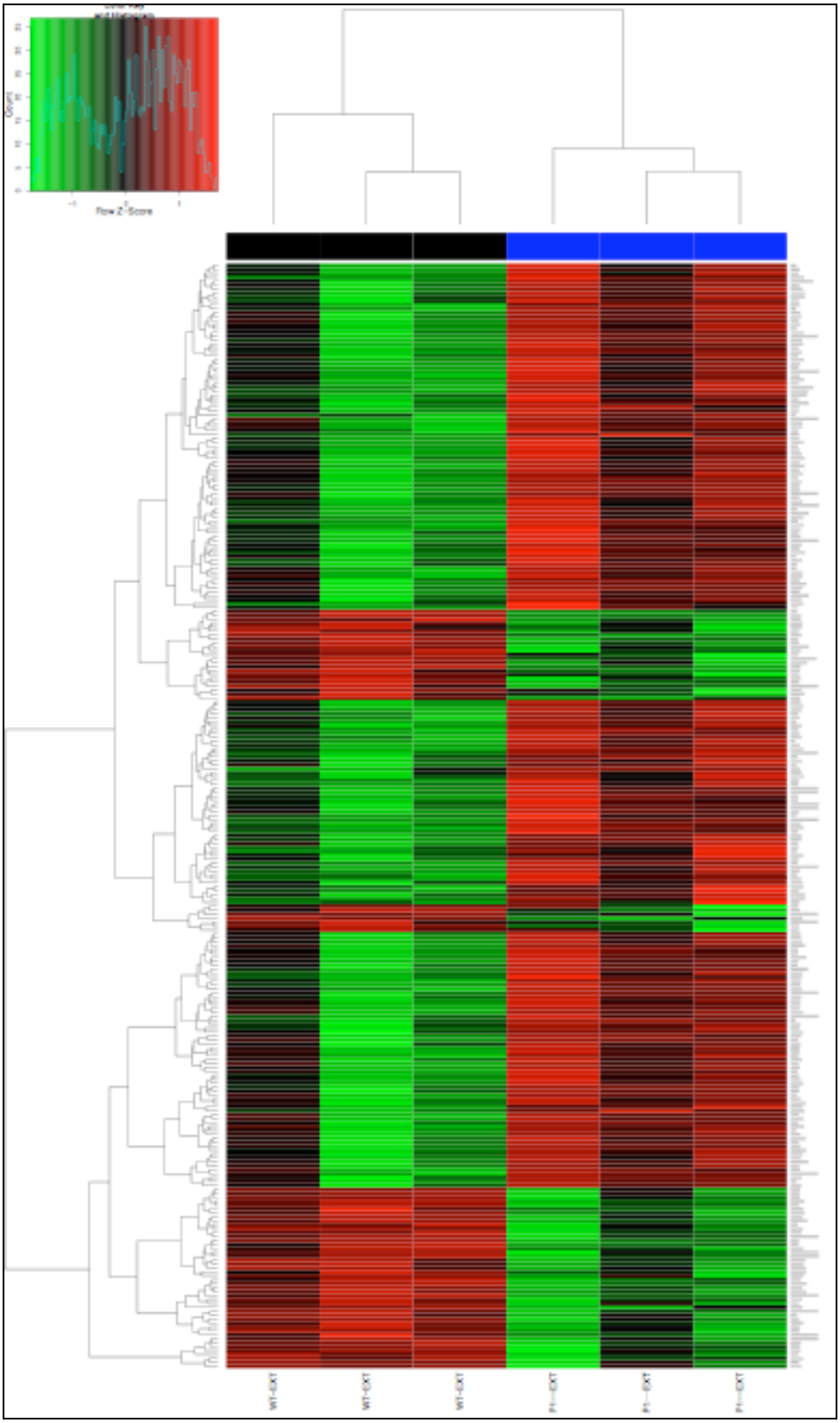

A heat map illustrating genes up- (red) and downregulated (green) in PHD1 K/O EXT (columns 4-6) vs. WT EXT (columns 1-3) using a *P*-value of 0.001 and a FC of ± 2

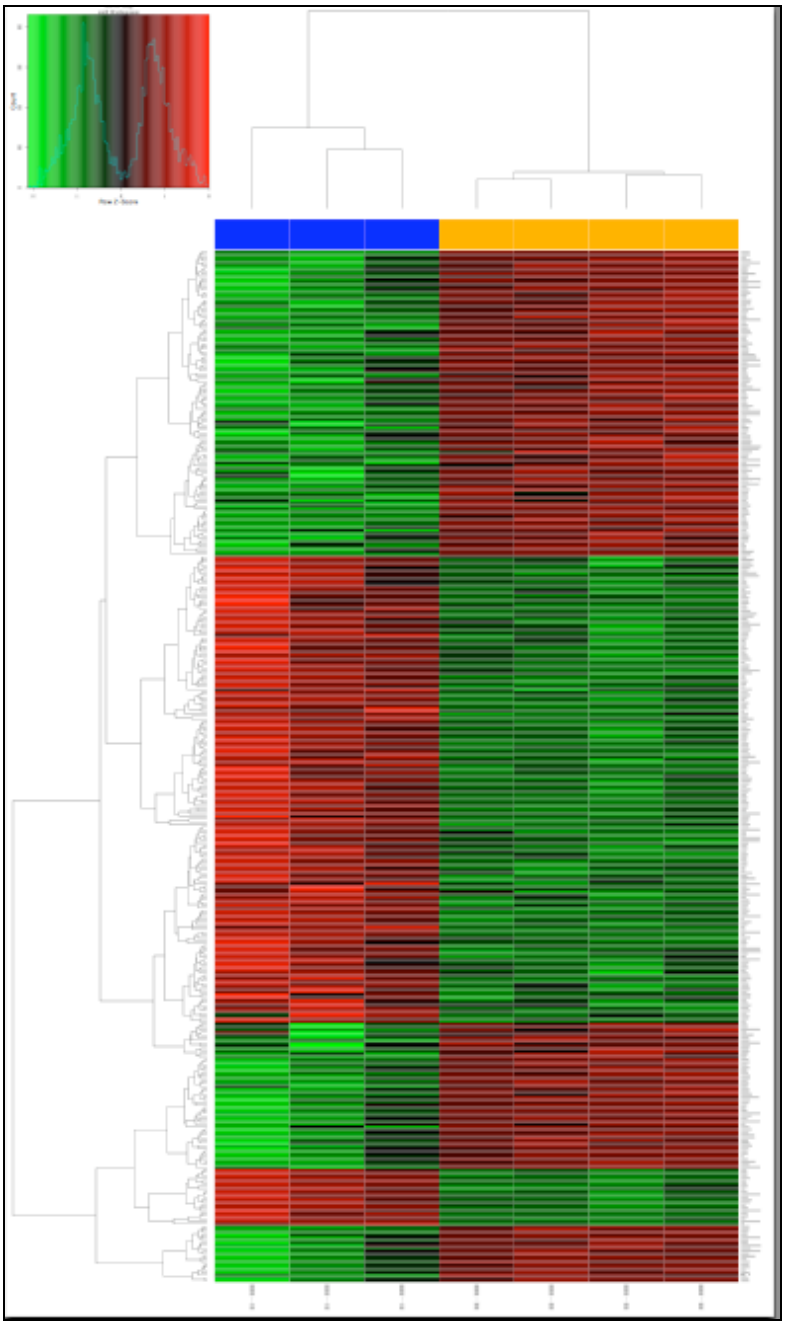

A heat map illustrating genes up- (red) and downregulated (green) in PHD1 K/O EXT (columns 1-3) vs. PHD3 K/O EXT (columns 4-7) using a *P*-value of 0.001 and a FC of ± 2